Genome-wide cDNA and RNAi screening to identify modulators of responses to a novel Wnt signalling inhibitor

Felicity L. E. Rudge

Supervisor: Professor Trevor Dale

Cardiff University

School of Biosciences

Ph.D. Thesis

Submission date: September 2013

Acknowledgements

This Ph.D. project has been made possible thanks to the unwavering support of an incredible group of family, friends and colleagues, for which I will be forever grateful.

I am indebted to my supervisor, Professor Trevor Dale, for his invaluable guidance and input in to my research, and for his continuing encouragement and faith especially during the tricky times.

I would like to thank all members, past and present, of 'Third Floor East' for five years of support and fun! In particular, I would like to thank Beth Lloyd-Lewis, Jamie Freeman and Ken Ewan for their advice and useful discussions, Gui Jie Feng for her guidance, help and constant care ('When you need it…chocolate!'), Claudia for helping me set the world to rights and spurring me on, and Pete Watson for his encouragement and humour.

Ein herzlicher Dank geht auch an das unglaubliche Team TA Oncology, Biomolecular Pharmacology Lead Discovery, NCE Technologies, MedChem und Compound Distribution von Merck Serono in Darmstadt. Ich bin sehr dankbar für eure Gastfreundschaft, Unterstützung und Geduld während meines Aufenthalts. Ein besonderer Dank gilt vor allem Eike Straub für seine Hilfe und Ratschläge bei der Datenanalyse, Andree Blaukat, der es mir ermoeglicht hat ein weiteres Mal nach Deutschland zu kommen und ausserdem vielen Dank an Dirk Wenke (und sein Team) für seine unbezahlbaren Ratschlaege und Ermutigungen. Very special thanks must also go to Dirk, Sharon, Maddy and Tom for being so welcoming and providing me with a 'home-from-home' during my time in Darmstadt.

Finally, a resounding 'thank you' goes to my friends and family. Massive thanks to my friends for always being there with buckets of moral support (even after being subjected to hours of science talk). To Mum and Dad, I don't know where I would be without you, you're always amazing. And to Elliott, for having very big shoulders and reminding me that tea (and gin) make everything better.

Abstract

Wnt/β-catenin signalling plays a central role in the regulation of multicelluar organism development and in the maintenance of tissue homeostasis in adults. Dysregulation of Wnt signalling resulting in aberrant pathway activation is a key initiating step in the development of a diverse range of cancers, including colorectal cancer, and as such is an important target for therapeutic intervention. A novel Wnt pathway inhibitor, 'MSC', has been identified as blocking activated Wnt signalling, specifically through inhibiting the ability of CDK8 and CDK19 to activate nuclear β-catenin/TCF-dependent transcription. However, despite potently inhibiting Wnt-dependent transcription, the ability of MSC to reduce cellular viability was limited. This study aimed to determine genes that whose loss operated with MSC to reduce cell survival.

A whole-genome RNAi chemical sensitisation screen identified 3 genes whose depletion in combination with MSC treatment conditionally reduced the viability of HCT116 cells *in vitro*. The outstanding hit of this screen was Histidyl Aminoacyl tRNA Synthetase (HARS). The identification of this enzyme as an MSC 'interactor' suggested links between Wnt signalling and the regulation of translation. BRAF and MED11 RNAi also conferred conditional sensitivity to MSC. Interestingly, MED11 is a component of the Mediator complex, a multiprotein transcription regulatory complex in which CDK8 functions to regulate β-catenin/TCF-dependent transcription, suggesting that mediator complex may be a key target of MSC action.

A parallel overexpression screen was initiated to identify novel Wnt pathway activators, and subsequently used to map MSC resistance. Expression of the transcription factors GBX1 and HMGB2, determined to be novel regulators of TCF-dependent transcription, blocked MSC-mediated disruption of Wnt signalling. Overexpression of either gene in a clinical context might therefore be regarded as a contra-indication for MSC-class therapies.

These studies have highlighted potential avenues for broadening the scope of MSC activity through the determination of survival and resistance mechanisms, thus the rational design of MSC-combination therapies could be of huge clinical benefit for the treatment of colorectal cancer.

Table of Contents

Abbreviations

A

AD	Alzheimer's Disease
ADP	Adenosine Diphosphase
ANOVA	Analysis of Variance
APC	Adenomatous Polyposis Coli
ATP	Adenosine Triphosphate

B

β–TrCP	Beta-Transducin Repeat Containing E3 Ubiquitin Protein Ligase
Bcl9	B-cell Lymphoma 9 Protein
BLAST	Basic Local Alignment Search Tool
BRAF	V-Raf Murine Sarcoma Viral Oncogene Homologue B
BRCA1	Breast Cancer 1, Early Onset

C

CAMKII	Calcium/Calmodulin-Dependent Protein Kinase II
CAS	Chemical Abstracts Service
CBP	cAMP response element-binding protein (CREB) binding protein
CDK	Cyclin Dependent Kinase
cDNA	Complementary Deoxyribonucleic Acid
ChEMBL	Chemical database of European Molecular Biology Laboratory
CK1	Casein Kinase 1
CMV	Cytomegalovirus
Cn	Calcineurin
CNS	Central Nervous System
COX	Cyclooxygenase
CRAF	V-Raf Murine Sarcoma Viral Oncogene Homologue C
CRC	Colorectal Cancer
CRD	Cysteine Rich Domain
CRHR2	Corticotropin Releasing Hormone Receptor 2
Cyc	Cyclin

D

DAVID	Database for Annotation, Visualization and Integrated Discovery
DAX	Axin-Axin homodimerisation domain
DEP	Dishevelled, Egl-10, Pleckstrin
DIX	Dishevelled-Axin dimerisation domain
Dkk	Dickkopf
DMEM	Dulbecco's Modified Eagle's Medium
DMRTA2	Doublesex- and Mab-3-Related Transcription Factor A2
DMSO	Dimethyl Sulphoxide
DNA	Deoxyribonucleic Acid
ΔNLRP	Delta Amino-Terminus Low Density Lipoprotein Receptor-Related Protein
Dvl	Dishevelled

E

E2F1	E2F transcription factor 1
EC50	50% Effective Concentration
EG5	Kinesin family member 11
eGFP	Enhanced Green Fluorescent Protein
EGFR	Epidermal Growth Factor Receptor
EMBL	European Molecular Biology Laboratory
EP2	Prostaglandin E Receptor 2 (Subtype EP2)
ER	Oestrogen Receptor
esiRNA	Endoribonuclease-synthesised Short Interfering Ribonucleic Acid

F

FAP	Familial Adenomatous Polyposis
FBS	Foetal Bovine Serum
FDA	US Food and Drug Administration
Fz	Frizzled

G

GAPDH	Glyceraldehyde-3-Phosphate Dehydrogenase
GBX	Gastrulation Brain Homeobox
GI_{50}	50% Growth Inhibition
GO	Gene Ontology
GPCR	G-protein Coupled Receptor
Gro	Groucho
GSK	Glycogen Synthase Kinase

H

HARS	Histidyl Aminoacyl tRNA Synthetase
HDAC	Histone Deacetylase
HEK293	Human Embryonic Kidney 293 cells
Hh	Hedgehog
HMGB2	High-Mobility Group Box 2
HPD	4-Hydroxyphenylpyruvate Dioxygenase
HRAS	Homologue
HRP	Horseradish Peroxidase

I

IC_{50}	50% Inhibitory Concentration
ICR	Institute of Cancer Research
IKZF1	Ikaros Family Zinc Finger Protein 1

J

JAK	Janus Kinase
JNK	Jun-N-terminal Kinase

K

KEGG	Kyoto Encyclopaedia of Genes and Genomes
Ki	Inhibitor Constant
KIT	Karlsruhe Institute of Technology
KRAS	Kirsten Rat Sarcoma Viral Oncogene Homologue

L

LB	Lysogeny Broth
LEF	Lymphoid Enhancer Factor
Lgr5	Leucine-Rich Repeat Containing G Protein-Coupled Receptor 5
LOH	Loss Of Heterozygosity
LRP	Low Density Lipoprotein Receptor-Related Protein

M

MAPK	Mitogen-Activated Protein Kinase
Med	Mediator Complex Subunit
MEM	Minimal Essential Medium
mTOR	Mammalian Target Of Rapamycin

N

NFAT	Nuclear Factor of Activated T-cells
NLK	Nemo-Like Kinase
NSAID	Non-Steroidal Anti-Inflammatory Drug
NTR	Netrin-Related Domain

P

Parp1	Poly (ADP-Ribose) Polymerase 1
PCP	Planar Cell Polarity
PCR	Polymerase Chain Reaction
PDE6B	Phosphodiesterase 6B
PDZ	Postsynaptic Density 95, Discs Large, Zona Occludens-1 Domain
PGE2	Prostaglandin E2
PHD	Plant Homeodomain
PI3K	Phosphoinositide-3-Kinase
PITX1	Paired-Like Homeodomain 1
PKA	Protein Kinase A
PKC	Protein Kinase C
PLC	Phospholipase C
PLK1	Polo-Like Kinase 1
PNS	Periperal Nervous System
PORCN	Porcupine
PP2A	Protein Phosphatase 2A
PPAR	Peroxisome Proliferator Activated Receptor
PTEN	Phosphatase And Tensin Homolog
PTP	Protein Tyrosine Phosphatase
Pygo	Pygopus

R

R-Luc	Renilla Luciferase
RARS	Arginyl-tRNA Synthetase
RGS	Regulator of G-protein Signalling
RIPA	Radioimmunoprecipitation Assay
RLU	Relative Luminescence Units
RNAi	Ribonucleic Acid Inhibition
RNA Pol	Ribonucleic Acid Polymerase
ROK	Rho Kinase
RPMI	Roswell Park Memorial Institute
RTK	Receptor Tyrosine Kinase
RTN2	Reticulon 2

S

SCF	Skp, Cullin, F-box
SD	Standard Deviation
SezL2	Seizure Related 6 Homologue (Mouse)-Like 2
sFRP	Secreted Frizzled-Related Protein
shRNA	Short Hairpin Ribonucleic Acid
siRNA	Short Interfering Ribonucleic Acid
SLC	Solute Carrier
SoC	Standard of Care
Src	V-Src Avian Sarcoma (Schmidt-Ruppin A-2) Viral Oncogene Homolog
STAT	Signal Transducer and Activator of Transcription

T

TA	Transit Amplifying
TAF4	TATA Box Binding Protein (TBP)-Associated Factor 4
TBST	Tris-Buffered Saline with Tween 20
TCF	T-cell Factor
TE	Tris Ethylenediaminetetraacetic acid
TGF-β	Transforming Growth Factor-Beta
TGIF	TGFB-Induced Factor Homeobox 1
THRA	Thyroid Hormone Receptor, Alpha
TK	Thymidine Kinase
TLE	Transducin-Like Enhancer of Split
TLIG	TCF-Luciferase-IRES-GFP
TNIK	TRAF2 and NCK-Interacting Protein Kinase
TNKS	Tankyrase

U

UGP2	Uridyl Diphosphate Glucose Pyrophosphorylase 2

V

VEGFR2	Vascular Endothelial Growth Factor Receptor 2
VP16	Activator protein from herpes simplex virus

W

Wg	Wingless
WIF	Wnt Inhibitory Factor
Wnt	Wingless-type MMTV integration site family
WRE	Wnt Response Element

X

Xnr	Xenopus Nodal-Related

Numbers

2D	Two Dimensional
3D	Three Dimensional

Chapter 1. Introduction

1.1 Signalling Pathways

Cell fate during the development of multicellular organisms is widely regulated by cell-cell signalling events. This signal transduction was first shown by Spemann and Mangold who demonstrated that transplantation of selected regions of newt embryonic tissue (termed 'organisers') into a host embryo resulted in the induction of secondary embryonic primordia, suggesting that cell-cell communication could be achieved by secreted signals (Spemann and Mangold, 1924; 2001). These secreted signals, or ligands, transduce signalling pathways that are pivotal in the organisation of embryonic development. Interestingly, in animal systems this cell fate determination is controlled (in the most part) by seven key signalling pathways; wingless related (Wnt), hedgehog (Hh), janus kinase (JAK)/signal transducer and activator of transcription (STAT), transforming growth factor-β (TGF-β), receptor tyrosine kinase (RTK), Notch, and nuclear hormone pathways (Barolo and Posakony, 2002; Pires-daSilva and Sommer, 2003). Despite their multiplicity of signal transduction mechanisms and the downstream components involved, these seven pathways elicit many of their effects through the transcriptional regulation of target genes via conditional (i.e. signal-dependent) transcription factors and are employed repeatedly during development (Barolo and Posakony, 2002; Pires-daSilva and Sommer, 2003).

1.1.1 The Wnt signalling pathways

The Wnt ligand family, which comprises 19 secreted Wnt glycoproteins in higher vertebrates (Papkoff et al., 1987), act through several extracellular receptors to activate discrete intracellular signalling cascades. As well as having critical roles in the early development of an organism, Wnt signalling is also essential to adult tissue homeostasis, with its importance in stem-cell self renewal more recently identified (Angers and Moon, 2009; Barker et al., 2009; Clevers, 2006).

The ability of a subset of Wnt ligands to induce an increase in cytoplasmic beta-catenin (β-catenin) levels initially lead to their division in to two subgroups: the 'canonical' Wnt/β-catenin (or 'Wnt-1') signalling class, and the 'non-canonical' β-catenin independent (or 'Wnt-5a') class (McMahon and Moon, 1989; Shimizu et al., 1997; Wong et al., 1994). It has subsequently been determined that although several Wnt proteins preferentially activate either Wnt/β-catenin dependent or independent signalling, Wnt ligands themselves are not inherently canonical or non-canonical, rather that the diverse signalling cascades that these ligands trigger are defined by the ligand-receptor complex formed under a given cellular context (He et al., 1997; Liu et al., 2005; Tamai et al., 2004). Frequently Wnt signalling is activated by multireceptor complexes including members of the Fz family of 7 transmembrane receptors. In total, there are greater than 15 Wnt receptors and co-receptors in vertebrates, including 12 Frizzled receptors (Fz) (van Amerongen et al., 2008), low-density lipoprotein receptor-related proteins 5/6 co-receptors (LRP5/6) (He et al., 2004), receptor tyrosine kinase-like orphan receptors Ror1/2 (Paganoni et al., 2010) and the receptor tyrosine kinase Ryk (Lu et al., 2004). The number of possible combinations of ligand-receptor complexes provides an early indication of the intricacy of this signalling mechanism (Kikuchi et al., 2009). Of the multiple Wnt-signalling cascades 'encoded' by these combinations there are three that are most well understood (Figure 1):

1. *The canonical Wnt/β-catenin pathway*

   This is the best-characterised pathway, and as the focus of this investigation it will be described in more detail later. Briefly, under steady-state 'Wnt-off' conditions β-catenin is phosphorylated within a multi-protein destruction complex by glycogen synthase kinase 3 beta (GSK3β), targetting it for proteosomal degradation. In the presence of Wnt, a Wnt-Fz-LRP5/6 receptor complex is formed which recruits and inhibits the destruction complex, stabilising β-catenin which translocates to the nucleus and activates the T-cell factor/lymphoid

enhancer factor (TCF/LEF)-dependent transcription of Wnt-target genes. Physiologically, this pathway is involved in regulating cell fate determination and proliferation (Kühl and Kühl, 2012; Rudloff and Kemler, 2012).

- Figure 1b and Figure 2

2. *The planar cell polarity (PCP) pathway*

Wnt-5a and Wnt-11 have been shown to activate the Rac1 and RhoA GTPases downstream of dishevelled (mammalian homologues are termed Dvl1-3), which subsequently activate mediators Jun-N-terminal kinase (JNK) and Rho kinase (ROK) (Fanto and McNeill, 2004). This pathway regulates the alignment of cells within the plane of a tissue and is evident in, for example, the uniform arrangement of hairs on the fly wing and the coordinated polarisation of hair cells in the mammalian ear. This alignment is also exhibited in larger structures including mammalian epidermis hair follicle orientation (Devenport and Fuchs, 2008).

Significantly, the PCP and Wnt/β-catenin pathways are often antagonists of one another, which (in part) occurs through cross-talk at the Wnt-receptor level. For example, the PCP-activating Wnt-5a ligand competes with Wnt-3a's binding to Fz2, inhibiting the formation of a Fz/LRP5 ligand-receptor complex thus maintaining Wnt/β-catenin signalling in the off state (Sato et al., 2010).

- Figure 1a

3. *The Wnt/Ca^{2+} pathway*

Binding of selected Wnt ligands (including Wnt-4, Wnt-5a and Wnt-11) to Fz2, 3, 4, 5 and 6, and Ror1/2 receptors triggers the activation of heterotrimeric G-proteins, which activate phospholipase C (PLC) and leads to the release of intracellularly stored calcium (Blumenthal et al., 2006; Kuhl et al., 2000; Nishita et al., 2010). Calcium sensitive

enzymes such as Ca^{2+} and calmodulin-dependent kinase II (CAMKII) and protein kinase C (PKC) and the phosphatase calcineurin (Cn) are activated, and subsequently activate the transcription factor nuclear factor of activated T-cells (NFAT) (De, 2011; Saneyoshi et al., 2002). NFAT transcriptionally regulates genes involved in cell fate and cell migration (De, 2011).

Wnt/Ca^{2+} signalling is also capable of antagonising the Wnt/β-catenin response through the phosphorylation of TCF transcription factors by Wnt/Ca^{2+} activated nemo-like kinase (NLK) (Ishitani et al., 2003).

- Figure 1c

However, it is currently unclear precisely how many non-canonical Wnt responses exist due to the limited molecular characterisation of β-catenin independent molecular endpoints. Hence, our incomplete understanding of the multiple effects elicited by the multiple combinations of ligand-receptor complexes means that robust endpoint read-outs, such as TCF-reporter assays that are used to characterise the canonical pathway, are lacking (van Amerongen, 2012).

Figure 1 placement.

Figure 1. Overview of multiple Wnt signalling pathways

A. The Planar Cell Polarity Pathway. Signalling via the elements shown alters levels of c-Jun dependent transcription. However, non-transcriptional readouts including alterations to actin polymerisation drive many of the physiological effects.
B. The 'canonical' Wnt β-catenin signalling pathway (see later for details)
C. The Wnt-Ca2+ pathway. Signalling via the elements shown regulates NFAT dependent transcription, but other endpoints likely play a major role in physiological responses.
D. Receptor combinations at the plasma membrane that (in the case of LRP5/6 and Fz) simultaneously bind to different surfaces of a Wnt ligands leading to the formation of a multi-receptor complex. The exact combinations of receptors present in the complex are thought to specify the activation of distinct downstream pathways (adapted from (Niehrs, 2012)).

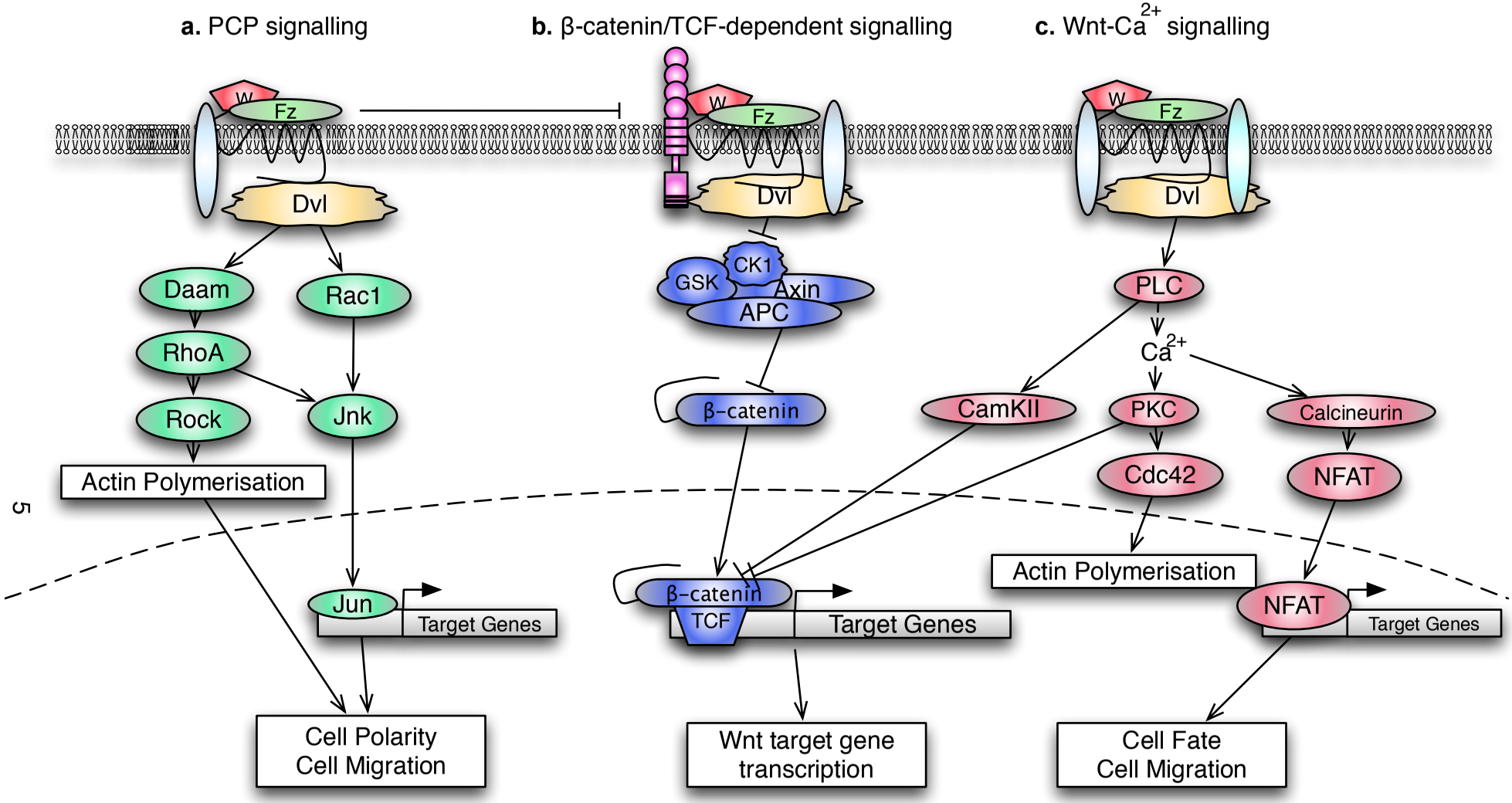

Figure 1. Overview of multiple Wnt signalling pathways

a. The Planar Cell Polarity Pathway. Signalling via the elements shown alters levels of c-Jun dependent transcription. However, non-transcriptional readouts including alterations to actin polymerisation drive many of the physiological effects.
b. The 'canonical' Wnt/β-catenin signalling pathway (see later for details).
c. The Wnt-Ca^{2+} pathway. Signalling via the elements shown regulates NFAT dependent transcription, but other endpoints likely play a major role in physiological responses (adapted from (Niehrs, 2012)).

1.1.1.1 The canonical Wnt/β-catenin pathway

The focus of this research is the Wnt/β-catenin cascade, and henceforth will simply be referred to as the Wnt signalling pathway. The pathway is comprised of proteins whose function in Wnt signalling is conserved across cell types and organisms, and form the basis of a 'core' minimal pathway required for the transcription of Wnt-target genes (Logan and Nusse, 2004).

At its simplest, Wnt signalling via the interaction of these core components can be considered as having two states: 'Off' (in the absence of Wnt ligand) and 'On' (in the presence of Wnt ligand; Figure 2). In the 'Off' state, the TCF-transcriptional co-activator β-catenin is recruited to a multiprotein 'destruction' complex by the multidomain scaffold proteins Axin and Adenomatous Polyposis Coli (APC). This facilitates the sequential phosphorylation of essential serine/threonine residues by two further destruction complex constituents, Casein Kinase 1α (CK1α) and Glycogen Synthase Kinase 3β (GSK3β), targetting the phosphorylated β-catenin for degradation by the proteasome (Liu et al., 2002; Orford et al., 1997).

In the 'On' state, signalling is initiated by the binding of Wnt ligand to the transmembrane receptors LRP5/6 (single-pass receptor) and Fz (seven-transmembrane receptor). Dishevelled (Dvl) and Axin bind to the intracellular domains of these receptors, preventing the formation of the destruction complex and allowing for the accumulation of β-catenin. β-catenin subsequently translocates to the nucleus and binds the transcription factor TCF/LEF to activate the transcription of Wnt-target genes (reviewed in (Cadigan and Waterman, 2012)).

Placement for Figure 2.

Figure 2. The canonical Wnt/β-catenin Signalling Pathway

OFF: In the absence of Wnt ligand, Axin forms a scaffold, binding Adenomatous Polyposis Coli (APC) protein, Casein Kinase Iα (CK1α), Glycogen Synthase Kinase 3β (GSK3β), and β-catenin. β-catenin is phosphorylated by CK1α and GSK3β at the N-terminus, ubiquitinated by β-TrCP (an E3 ubiquitin ligase) and targeted for degradation by the proteosome, suppressing transcription.

ON: In the presence of Wnt ligand, Frizzled (Fz) and LDL-like receptor protein (LRP)5/6 form a co-receptor complex. LRP5/6 is phosphorylated by CK1γ. Subsequent phosphorylation of LRP5/6 by GSK3β is mediated through the recruitment of Dishevelled (Dvl) to the plasma membrane by Fz, which also recruits Axin to LRP5/6. The destruction complex is inactivated, β-catenin stabilises and translocates to the nucleus. Through the displacement of Groucho from Lymphoid Enhancer Factor (LEF)/T-cell factor (TCF), a transcriptionally active complex is formed and target genes (e.g. *Myc* and *Axin*2) are transcribed (reproduced with kind permission from (Ewan and Dale, 2008)).

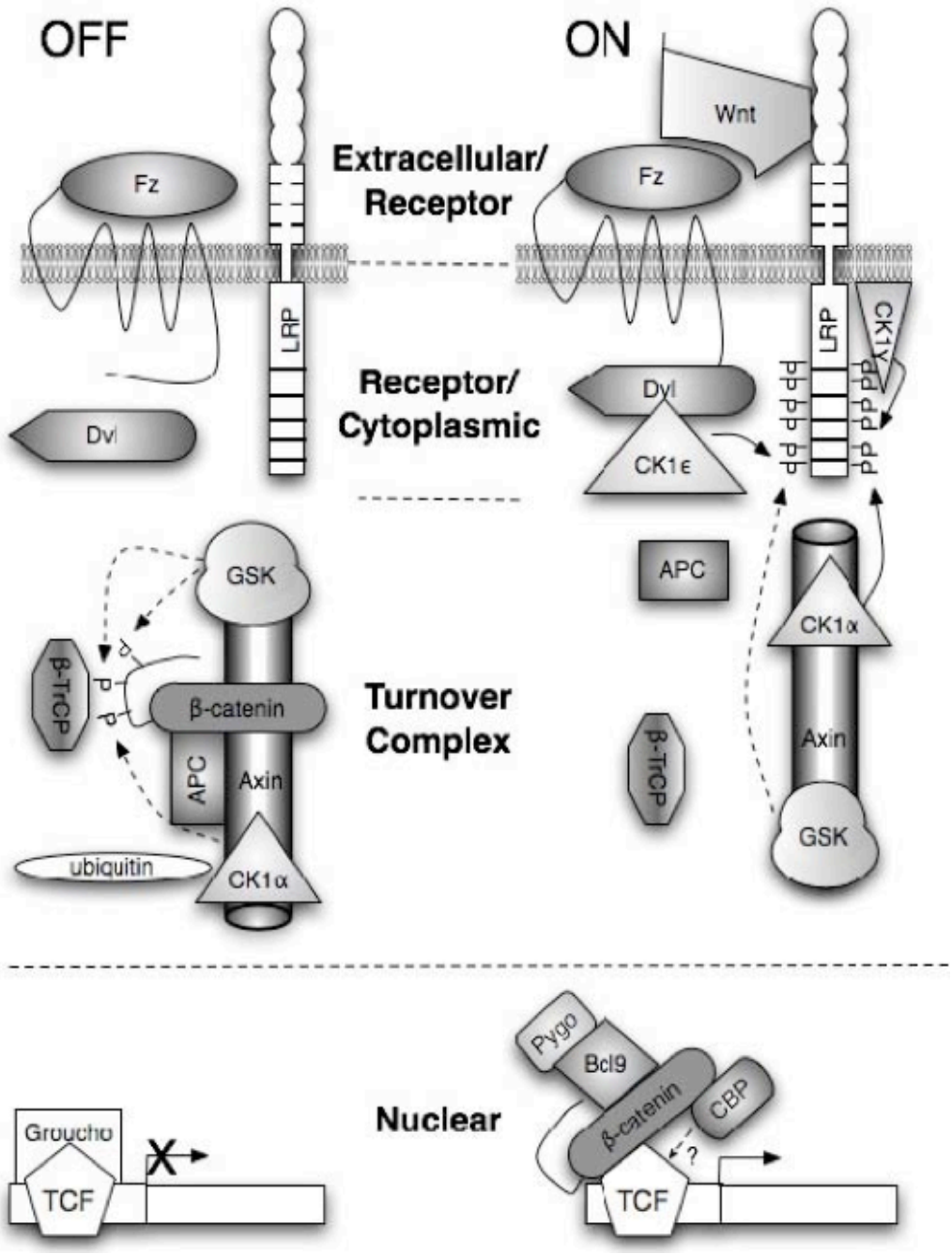

Figure 2. The canonical Wnt/β-catenin signalling pathway

OFF: In the absence of Wnt ligand, Axin forms a scaffold, binding Adenomatous Polyposis Coli (APC) protein, Casein Kinase Iα (CKIα), Glycogen Synthase Kinase 3β (GSK3β), and β-catenin. β-catenin is phosphorylated by CKIα and GSK3β at the N-terminus, ubiquitinated by β-TrCP (an E3 ubiquitin ligase) and targeted for degradation by the proteosome, suppressing transcription.

ON: In the presence of Wnt ligand, Frizzled (Fz) and LDL-like receptor protein (LRP)5/6 form a co-receptor complex. LRP5/6 is phosphorylated by CKIγ. Subsequent phosphorylation of LRP5/6 by GSK3β is mediated through the recruitment of Dishevelled (Dvl) to the plasma membrane by Fz, which also recruits Axin to LRP5/6. The destruction complex is inactivated, β-catenin stabilises and translocates to the nucleus. Through the displacement of Groucho from Lymphoid Enhancer Factor (LEF)/T-cell factor (TCF), a transcriptionally active complex is formed and target genes (e.g. *Myc* and *Axin*2) are transcribed (reproduced with kind permission from (Ewan and Dale, 2008)).

This simple overview provides a framework that allows the pathway to be considered in four stages:

i. Extracellular Wnt-receptor interactions
ii. Intracellular receptor signal transduction
iii. The β-catenin destruction complex
iv. TCF/LEF-mediated transcription

1.1.1.1.1 Extracellular Wnt-receptor interactions

A defining feature of canonical Wnt signalling is the requirement for the presence of both Fz and LRP5/6 receptors (or 'co-receptors') in order for TCF-dependent transcription to occur. *In vitro* it has been demonstrated that a trimeric Wnt-Fz-LRP5/6 complex forms in the presence of both Wnt-1 and Wnt-3a (using the extracellular domains of Fz8 and LRP6 (Bourhis et al., 2011; Tamai et al., 2000)). This indicates that Wnt ligands bind to both receptors simultaneously in order to form the complex. In an important advance, Janda *et al*. (Janda et al., 2012), recently determined the structure of XWnt8 in complex with the Wnt binding domain (CRD) of Fz. Interestingly it has also been shown *in vitro* that LRP6 is able to bind two different Wnt proteins concurrently, suggesting that multiple combinations within a trimeric or possibly multimeric complex may occur *in vivo* (Chen et al., 2011; Ettenberg et al., 2010; Gong et al., 2010).

In vivo, levels of Wnt-Fz-LRP5/6 complexes are enhanced by the concentration of Wnt ligand at the cell surface by proteoglycans such as Syndecan 1 and Dally (Lin and Perrimon, 1999; Perrimon and Bernfield, 2000). The ligand then binds to the cysteine-rich domain (CRD) of Fz and to one of two PE domains of LRP6 (Ettenberg et al., 2010; Gong et al., 2010; Mao et al., 2001b). Levels of Fz receptor have recently been shown to be regulated by the Lgr5 receptor in complex with the ligand R-spondin, thereby altering the level of Wnt pathway activation in response to the same level of Wnt ligand (Macdonald and He, 2012).

As well as being modulated by activators, Wnt signalling is further regulated by evolutionarily conserved inhibitors. Antagonism at the extracellular receptor level is a common feature, with small protein inhibitors often preventing ligand-receptor interaction. Secreted antagonists include Wnt-inhibitory factor 1 (WIF 1), secreted Frizzled-related proteins (sFRPs) and Dickkopf (Dkk) proteins. WIF 1 has been shown to bind both canonical and non-canonical Wnts via a 'WIF domain' (Hsieh et al., 1999), however although this is believed to sequester the signal, the precise mechanism of WIF 1-Wnt regulation is not entirely understood (Cruciat and Niehrs, 2012). Similarly, sFRPs prevent binding of Wnt – receptor interaction, for which two mechanisms have been proposed. sFRPs contain a CRD which has been suggested to recruit Wnts away from the co-receptors (Lin et al., 1997). A second domain, Netrin-related domain (NTR), was shown to be required for optimal Wnt inhibition (using a Wnt reporter assay; (Bhat et al., 2007)), whilst it has since been shown that the NTR domain alone is capable of binding Wnt8 and inhibiting signalling (Lopez-Rios et al., 2008). A further model of sFRP-mediated inhibition via direct binding to Fz should also be considered. sFRPs and Fz proteins are able to dimerise through the CRD, hence have the potential to inhibit signalling through the formation of non-functional complexes (Bafico et al., 1999; Dann et al., 2001; Rodriguez et al., 2005). Dkks specifically inhibit canonical Wnt signalling through high-affinity binding to LRP5/6, forming a tertiary complex with a second receptor Kremen1/2 (Mao et al., 2002; 2001a). These interactions are mediated through the colipase fold of Dkk, with the inhibitory effect imparted by the DKK_N domain (Brott and Sokol, 2002). Interestingly, and in contrast to Dkk1 which solely inhibits Wnt signalling, Dkk2 can act as either an inhibitor or activator of signalling (Brott and Sokol, 2002; Mao and Niehrs, 2003). This cellular-context dependent dual-activity may be determined by the presence or absence of the Kremen2 receptor; in its absence Dkk2 activates signalling (Mao and Niehrs, 2003). Together, these demonstrate that the tight regulation of the Wnt/β-catenin cascade is first evident at the extracellular level.

1.1.1.1.2 Intracellular receptor signal transduction

Extracellular cues are translated intracellularly by means of receptor phosphorylation events and subsequently the engagement of cytoplasmic components, of which Dvl and Axin have key roles in controlling downstream signal transduction.

Present within the cytoplasmic region of LRP5/6 are five conserved PPPSPxS motifs. These motifs are dually phosphorylated by GSK3β in the presence of Wnt, providing the docking site for Axin (Tamai et al., 2004; Zeng et al., 2005). Significantly it has been demonstrated that only a single motif is sufficient for signal transduction, and mutation of the S residue in all motifs results in total signal ablation (Swiatek et al., 2006; Tamai et al., 2004).

The LRP5/6 PPPSP motif is initially phosphorylated by GSK3β, priming the xS residue for phosphorylation by membrane-associated CK1γ (Davidson et al., 2005; Zeng et al., 2005). Phosphorylation by GSK3 is dependent on Fz-LRP5/6 interaction, and conditionally occurs following Wnt-induced Dvl recruitment to the membrane by Fz. Dvl binds to the cytoplasmic portion of Fz via its PDZ (Postsynaptic density 95, discs large, zona occludens-1 domain (Wong et al., 2003)), with recent evidence suggesting that this is further facilitated by the binding of the DEP (Dishevelled, Egl-10, Pleckstrin) domain to both Fz and potentially phospholipids within the plasma membrane (Simons et al., 2009; Tauriello et al., 2012). It has been postulated that this in turn directly recruits Axin to the membrane (through the oligomerisation of Dvl-Axin at their DIX/DAX domains), initiating the phosphorylation of LRP5/6 by the Axin-tethered GSK3 (Zeng et al., 2008).

Three models have been proposed regarding the mechanism of signal transduction from this point. The first is the 'Initiation-Amplification model', whereby the priming of LRP5/6 for Axin binding in this way may create a 'feed-forward loop' that promotes and enhances further Axin recruitment (MacDonald et al., 2008; Zeng et al., 2008). Evidence that LRP5/6 minimally requires four

phosphorylated PPPSPxS motifs to produce a semi-transduction competent receptor suggests that the phosphorylation of these motifs is dependent on having functional neighbour motifs, and that this phosphorylation is essential for achieving maximal Axin recruitment (MacDonald et al., 2008; Zeng et al., 2008). A second hypothesis generated from similar evidence is that 'LRP5/6 Signalosomes' form. Based on the observation that Wnt ligands induce LRP6 aggregation and that Dvl DIX-DIX polymerisation is required for adequate phosphorylation of these large aggregates, this large complex could then recruit high levels of Axin (leading the inactivation of β-catenin turnover) through DIX-DAX interaction, hence potentiating the Wnt signal (Bilic et al., 2007; Schwarz-Romond et al., 2007). The third model proposes that 'Endosomal Signalling' vesicles are formed as a consequence of Wnt-driven caveolin recruitment to LRP6 (Yamamoto et al., 2006). Caveolin-LRP6 binding enables phosphorylated LRP6 to recruit Axin, and subsequently 'signalosomes' are formed by caveolin-mediated endocytosis. Regardless of which of these models is determined to be correct, the ultimate outcome is that Axin membrane-recruitment occurs and that β-catenin turnover activity is suppressed and/or β-catenin turnover complex components are targeted for degradation (Macdonald and He, 2012; Mao et al., 2001a; Tolwinski et al., 2003). This prevents destruction complex formation and allows for the accumulation of β-catenin.

1.1.1.1.3 The β-catenin destruction complex

In order to understand Wnt-initiated β-catenin accumulation in the cytoplasm, it is important to first consider how β-catenin is regulated in the absence of Wnt ligand. When Wnt stimulation is lacking cytoplasmic β-catenin is phosphorylated and subsequently targetted for degradation by a large multi-protein complex; the 'β-catenin destruction complex'. This complex consists of several core components (in addition to β-catenin); scaffold proteins Axin and APC, serine/threonine kinases GSK3β and CK1α, and upon β-catenin phosphorylation the F-box containing E3-ubiquitin ligase β-TrCP is recruited. The complex is

likely to involve additional proteins that are dynamically recruited/engaged, however complete understanding of the intricacy of the machinery remains elusive (Stamos and Weis, 2013).

In the absence of Wnt signalling, free Axin is able to act as a central scaffold for the assembly of the destruction complex components. CK1α, GSK3β and β-catenin bind to sites in the centre of Axin, such that the kinases are in close proximity to their β-catenin substrate. The stability provided by this scaffold greatly enhances CK1α phosphorylation of β-catenin at Serine45 (Amit, 2002; Dajani et al., 2003; Liu et al., 2002), priming it for further phosphorylation by GSK3β at conserved N-terminal Ser33 and Ser37 residues (Hagen et al., 2002; Liu et al., 2002). This creates the conserved β-TrCP binding site, which in a complex with Skp1/Cullin forms the SCF that ubiquitinates and targets β-catenin to the proteosome, triggering its proteolytic degradation (Hart et al., 1999; Orford et al., 1997). Additionally, the scaffold APC binds to Axin's RGS (regulator of G-protein signalling homology) domain where it is phosphorylated by CK1α and GSK3β at seven 20-mer repeats, resulting in a ~1500 fold increase in its affinity for β-catenin (Ha et al., 2004; Liu et al., 2006). Not only does this act to further stabilise the complex, it is also postulated to shield β-catenin from dephosphorylation by Protein Phosphatase 2A (PP2A), ensuring that Wnt/β-catenin signalling remains sequestered (Su et al., 2008).

What is also not entirely clear is how Wnt-dependent LRP6 phosphorylation prevents β-catenin phosphorylation. As briefly discussed in the previous section, it is thought that Dvl recruits Axin away from the destruction complex. It was originally proposed that this resulted in dissociation of β-catenin and GSK3β from Axin, causing Axin hypophosphorylation and hence removing the β-catenin binding sites (Kimelman and Xu, 2006). Axin inactivation (or degradation) may also be enhanced by the Wnt-induced dissociation of APC from the destruction complex causing subsequent inhibition of GSK3β activity (Valvezan et al., 2012). However, the decrease in Axin activity and/or levels has been shown to lag

behind that of β-catenin accumulation, hence other mechanisms of destruction complex disruption must also be required for this process (Willert et al., 1999; Yamamoto, 1999). More recently it has been discovered that LRP6 phosphorylation (at the PPPSPxS motifs) results in the direct binding to and inhibition of GSK3β catalytic activity. This suggests that that Axin recruitment to the plasma membrane via Dvl leads to the phosphor-dependent PPPSP-inactivation of GSK3β activity and therefore β-catenin degradation (Cselenyi et al., 2008; Wu et al., 2009; Zeng et al., 2005).

Despite the uncertainty surrounding the mechanism of destruction complex disruption, it is evident that Wnt-receptor complex formation inhibits β-catenin phosphorylation, allowing it to accumulate. The raised levels of β-catenin associate with binding partners throughout the cell and accumulate in the nucleus in a process that is thought to be primarily driven by the concentration of binding partners in the nucleus (Lloyd-Lewis, 2011).

1.1.1.1.4 TCF/LEF-mediated transcription

Following translocation to the nucleus, β-catenin associates with the TCF/LEF transcription factor family, activating transcription of Wnt-target genes. Target genes contain a binding sequence called the Wnt Response Element (WRE) which is recognised and bound by the High Mobility Group (HMG) domain of TCF/LEF (van Beest et al., 2000; van de Wetering and Clevers, 1992).

In the absence of β-catenin, TCF/LEFs repress gene transcription by forming a complex with co-repressors including hydrogen peroxide-inducible clone (HIC5; (Ghogomu et al., 2006)) and myeloid translocation gene families (MTG; (Moore et al., 2008)), however the most well characterised is the Groucho/Transducin-like enhancer of split (Gro/TLE) family (Cavallo et al., 1998; Roose et al., 1998). Gro/TLE binds to the central region of TCF/LEF (Groucho binding sequence; GBS) and co-represses target genes in part by regulating histone modifications through the binding of histone deacetylases (HDACs; (Chen et al., 1999)).

β-catenin-TCF/LEF transcription activation is thought to occur in two ways. The simplest model is that following stabilisation and nuclear translocation of β-catenin, it displaces the Grouch/TLE co-repressor and recruits other proteins to form a transcriptionally active complex (Daniels and Weis, 2005). Alternatively, a 'transcriptional switch' may mediate transcriptional activation. In vertebrates four TCF/LEF isoforms exist: TCF1, LEF1, TCF3, TCF4. In the absence of Wnt signals it has been shown that TCF3 acts as a repressor (in most cases), which can be phosphorylated following Wnt signalling (e.g. by homeodomain-interacting protein kinase 2; HIPK2), causing TCF3 to dissociate from the WRE (Cole et al., 2008; Kim et al., 2000; Merrill et al., 2004). TCF3 is then replaced by one of the alternative TCF/LEF isoforms (bound to β-catenin), hence a switch occurs from an inactive to active complex. Interestingly it has been demonstrated that LEF1 most commonly activates genes upon recruitment (Kratochwil et al., 2002; Reya et al., 2000), whereas TCF1 and TCF4 can apparently serves as both co-activators and co-inhibitors dependent on the cellular context in which they are involved (Galceran et al., 1999; Korinek et al., 1998; Roose et al., 1999; Tang et al., 2008).

In either case, β-catenin's N-terminal transactivation domain binds Bcl9, which in turn recruits Pygopus (Pygo1/2, (Kramps et al., 2002)). The plant homeodomain (PHD) of Pygo binds methylated Histone 3, bridging the Wnt target gene's WRE with the proximal promoter (Fiedler et al., 2008). Interestingly, Pygo has also been demonstrated to interact with RNA polymerase II transcriptional regulatory complexes including Mediator via the Med12/13 and the TFIID subunit TAF4, again linking the β-catenin-TCF/LEF complex directly to transcriptional activation (Carrera et al., 2008; Wright and Tjian, 2009).

It is clear that Wnt/β-catenin signalling actually extends far beyond the simplicity of the 'core' signalling pathway components. In fact, Wnt-transcriptional regulation is dependent on many proteins interacting in a vast range of complexes, with these interactions varying in their nature depending on the cellular/system context. In many ways, the pathway may best be regarded as a

network; a concept that has important implication for the design of therapeutic inhibitors (see later; (Kestler and Kuhl, 2008)).

1.1.1.2 Wnt signalling in development, homeostasis and tumourigenesis

Over the last 30 years Wnt signalling has been highlighted as a key pathway across all animal species studied, with its activity ranging from the regulation of cell fate and the establishment of tissue polarity in embryonic development, to the maintenance of stem cell populations and the control of cell proliferation in adult tissues (Clevers, 2006; van Amerongen and Nusse, 2009).

Dissection of the Wnt pathway in 'model organisms' has provided much of our understanding of its activity. In *Drosophila melanogaster* Wnt/Wg (Wingless; the *Drosophila* Wnt equivalent) signalling is required for the patterning of the embryonic wing epidermis (Bejsovec and Arias, 1991), whilst in the wing imaginal disc it functions as a morphogen, determining cell fate in a concentration-dependent manner (Neumann and Cohen, 1996; Zecca et al., 1996). Its role in vertebrate axis specification was first identified in *Xenopus laevis* (McMahon and Moon, 1989), and genetically engineered murine systems continue to provide a wealth of knowledge spanning mammalian embryogenesis, development and adult tissue homeostasis (Wang et al., 2012).

Having such vast developmental and homeostatic implications means that hyper- or hypo-activation of Wnt signalling can have detrimental effects. Increased Wnt signalling is implicated in the progression of multiple cancers (Figure 3), whilst decreased signalling has been linked to Alzheimer's Disease (AD) and bone formation disorders (De Ferrari and Moon, 2006; Hoeppner et al., 2009). In the case of cancer, activation of Wnt signalling in the absence of ligand is the principal mechanism of that drives disease progression. In the early stages of Wnt research it was discovered that the *Apc* gene harbours an inactivating mutation in ~85% of colorectal cancers, constitutively activating Wnt-target gene transcription (Kinzler et al., 1991; Nishisho et al., 1991; Su et al., 1993).

Although dysregulation frequently occurs when a ‘core’ member of the pathway is mutated and causes constitutive activation of the pathway (as with *Apc*), epigenetic silencing of genes encoding Wnt inhibitors also potentiates cancer progression, for example Dkk1 and sFRP1 have both been shown to be inactivated in colorectal cancer (Aguilera et al., 2006; Caldwell et al., 2004). The tumourigenic effect of this aberrant signalling has been a driving force behind much of the research conducted on the Wnt cascade, with a significant focus on the identification of pathway-targeted therapeutics for the treatment of cancer. As this project principally focuses on the effects of Wnt inhibitors on colorectal cancers, the role of Wnt signalling in the intestine will now be discussed.

Figure 3 placement

Figure 3. Wnt signalling is dysregulated in multiple cancers

The incidence of the 20 most common cancers diagnosed in 2010 (UK only; excluding non-melanoma skin cancer). * indicates cancers with known links to Wnt signalling (adapted from (CRUK)).

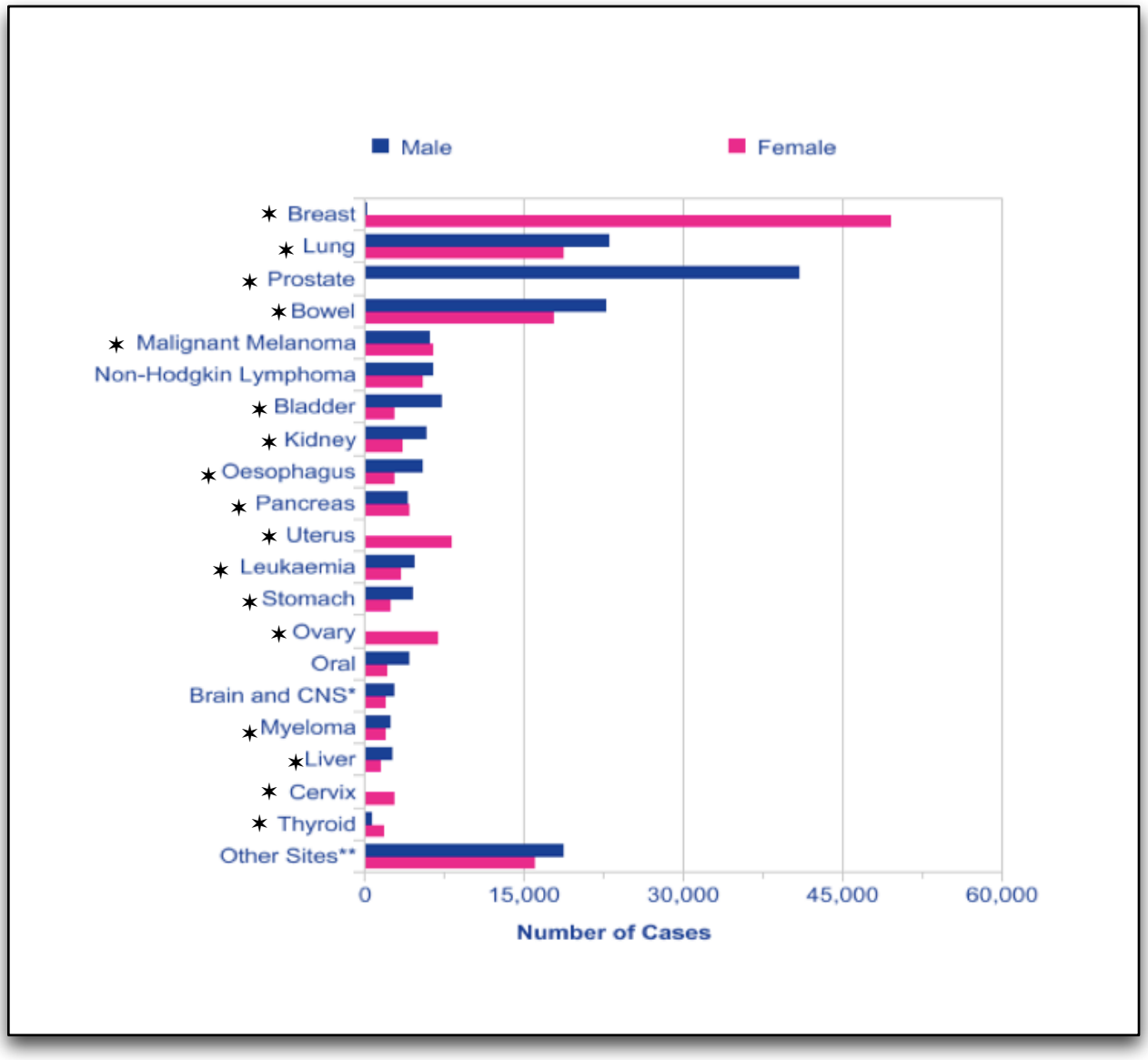

Figure 3. Wnt signalling is dysregulated in multiple cancers

The incidence of the 20 most common cancers diagnosed in 2010 (UK only; excluding non-melanoma skin cancer. Adapted from (CRUK)). * indicates cancers with known links to Wnt signalling.

1.1.1.2.1 Wnt signalling in the intestine

1.1.1.2.1.1 Intestinal homeostasis

The mammalian intestinal wall comprises three layers; an outer layer of smooth muscle cells, a middle layer of connective tissue containing lymphatic vasculature, and an inner lining of a single-cell thick epithelium. The small intestine is responsible for nutrient absorption, and hence the epithelium is arranged into two functionally distinct structures in order to maximise its absorbance efficiency; the absorbing villus and proliferative crypt. The finger-like luminal villi protrusions are composed of multiple differentiated cells (enterocytes, goblet, enteroendocrine and tuft cells (Gerbe et al., 2011; Pinto and Clevers, 2005a)), whilst the glandular crypt invaginations contain undifferentiated stem and progenitor cell populations (Pinto and Clevers, 2005a). The large intestine (or colon) also contains sub-mucosal crypts, however as this predominantly functions to absorb water it has a flat luminal epithelium as opposed to villi (Schepers and Clevers, 2012).

Intestinal epithelium undergoes rapid renewal, with proliferative cells in the crypt driving differentiated cell turnover in the villus. Multipotent intestinal stem cells anchored at the base of the crypt divide approximately once per day, which generates a population of transit-amplifying (TA) cells (Barker et al., 2007). The TA cells divide rapidly (every 12-16 hours), and the non-proliferative daughter cells migrate up the villus where they differentiate into the functional cell subtypes and continue their migration towards the villus' apex (Figure 4). These cells themselves are eventually lost, undergoing apoptosis before being shed into the lumen (Pinto and Clevers, 2005a). Interestingly, within this daughter population in the small intestine a subset of cells differentiate into Paneth cells (Pinto and Clevers, 2005b). Paneth cells migrate towards the bottom of the crypt where they actively secrete Wnt ligands that help to maintain neighbouring intestinal stem cells. They are also thought to moderate microbial ecology through the secretion of lysozyme and antimicrobial peptides (Bjerknes and

Cheng, 1981a; 1981b; Pinto and Clevers, 2005b). Less is known about the source of Wnt ligands in the colon crypt.

Figure 4 Placement

Figure 4a&b. Wnt signalling in the intestinal crypt/villus

Intestinal epithelial stem cells (pink) are located at the bottom of the crypt and are maintained in part by Wnt signalling from neighbouring Paneth cells (orange). Once the progeny of the stem cells migrate beyond the high concentration of Wnt ligand at the base of the crypt, they continue to proliferate as transit amplifying cells (TA cells; blue), before differentiating to cell types including absorbative enterocytes and secretory goblet cells (yellow). Adapted from (Radtke and Clevers, 2005).

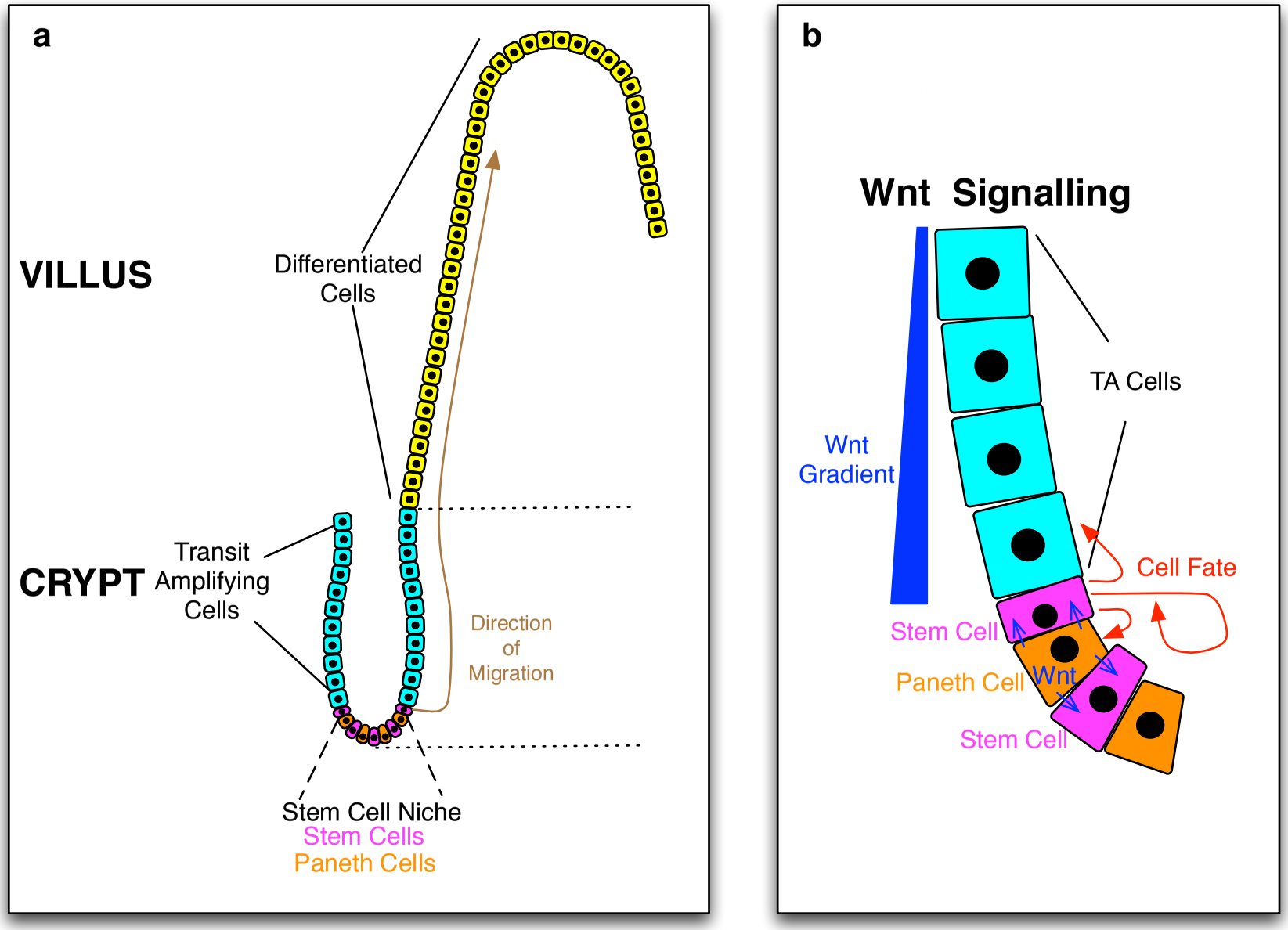

Figure 4a&b. Wnt signalling in the intestinal crypt/villus

Intestinal epithelial stem cells (pink) are located at the bottom of the crypt and are maintained in part by Wnt signalling from neighbouring Paneth cells (orange). Once the progeny of the stem cells migrate beyond the high concentration of Wnt ligand at the base of the crypt, they continue to proliferate as transit amplifying cells (TA cells; blue), before differentiating to cell types including absorbative enterocytes and secretory goblet cells (yellow). Adapted from (Radtke and Clevers, 2005).

Wnt signalling is critical for the maintenance of this homeostasis within the self-renewing crypt. This was first discovered in TCF4 knockout mice where there was an absence of inter-villi crypts in the small intestine, identifying a key role for Wnt signalling in the maintenance of the crypt progenitor regions (Korinek et al., 1998). However it is evident that cell-fate determination is also Wnt signal-dependent. The $TCF4^{-/-}$ mice lacked enterendocrine cells, whilst the villi of mice with inactivated APC became repopulated by crypt-like cells that were unable to migrate or differentiate (Korinek et al., 1998; Sansom et al., 2004). Significantly, nuclear β-catenin levels were highest in cells at the bottom of the crypt, with a gradient in signalling (inferred though the gradual decrease in expression of Wnt target genes) towards the lumen (Batlle et al., 2002; Kongkanuntn et al., 1999; Kosinski et al., 2007; van de Wetering et al., 2002). More recent studies have suggested that high levels of Wnt signalling in the intestine specify a stem cell fate, as identified by a well characterised panel of stem cell markers and a relatively low rate of proliferation. By contrast, lower levels of Wnt signalling were shown to drive the proliferation of transit amplifying cells (TA cells); cells that express c-Myc and cycle rapidly (Hirata et al., 2013). These findings highlight the essential role of Wnt/β-catenin signalling for the maintenance of cells in an undifferentiated and proliferative state in intestinal homeostasis.

1.1.1.2.1.2 Colorectal cancer

One of the earliest links between Wnt signalling and colorectal cancer was identified in patients with familial adenomatous polyposis (FAP) who harbour hereditary loss-of-function mutations in one *Apc* allele, with polyps developing by loss of heterozygosity (LOH) (Groden et al., 1991; Joslyn et al., 1991; Kinzler et al., 1991; Nishisho et al., 1991). It was subsequently shown that APC bound to β-catenin and regulated β-catenin degradation (Rubinfeld et al., 1993). FAP patient colon polyps are benign however progression into adenocarcinoma occurs with the accumulation of further mutations such as activation of Ras or inactivation of the tumour suppressors PTEN and p53 (Fodde et al., 2001;

Janssen et al., 2006; Marsh et al., 2008). It has since been identified that the majority of sporadic colorectal cancers carry somatic mutations in *Apc* with the remainder of tumours often carrying activating mutations in *β-catenin* or *Axin2* (Kinzler and Vogelstein, 1996; Liu et al., 2000; Morin et al., 1997), though it is evident that the neoplastic transformation of tissue induced by this overactive signalling event is insufficient to drive tumour progression.

Colorectal cancer has been studied in several mouse models, with the first created and now most widely used being the Apc^{Min} (Multiple intestinal neoplasia) mouse (Moser et al., 1990). Generated using random mutagenesis, the Apc^{Min} mice harbour a nonsense mutation in an allele of *Apc*. Similarly to patients with FAP the mice develop multiple polyps which become tumourigenic following LOH, although conversely to the colon polyps and tumours of FAP patients these predominantly arise in the small intestine. Other models have since been generated using gene targetting, with the aim of phenotypically recapitulating colorectal cancers more closely. Of particular interest are the adult systems in which conditional bi-allelic truncation or deletion of *Apc* can be induced in colorectal epithelium (Sansom et al., 2004; Shibata et al., 1997). Within days all cells of the epithelium acquire a progenitor-like phenotype. Interestingly *c-Myc* (a Wnt target gene (He et al., 1998)) must be intact for tumourigenesis to occur, and its knockdown is able to rescue the targeted *Apc* phenotype (Sansom et al., 2007). Together these results suggest that not only is Wnt signalling critical for the regulation of intestinal homeostasis, it's dysregulation and resulting constitutive activation drives polyp formation, ultimately prolonging the transcription of Wnt target genes that in turn drive polyp transformation into adenomas.

1.1.1.3 Colorectal cancer therapeutics

Over the past few years Wnt signalling has become a major focus for drug discovery as mechanisms leading to its dysregulation have been uncovered.

Although aberrant Wnt signalling in colorectal cancer would appear to be an ideal target for therapeutic intervention, the complexity of the pathway (e.g. numerous ligand-receptor combinations), its normal function in tissue homeostasis, and the lack of easily 'druggable' targets (i.e. a suitable Wnt-specific enzyme), means that the development of Wnt-inhibiting therapeutics has proved difficult. This picture is further complicated by the fact that 'core' Wnt components often have other roles outside Wnt signalling (e.g. β-catenin is involved in cell-cell adhesion junctions) and that dysregulation of the pathway (both up and down regulation) is also involved in the progression of a panel of diseases. Together these limitations mean that it is difficult to predict potential side-effects of Wnt inhibitors. Despite this, novel information regarding the mechanistic details of Wnt signalling is driving the development of new targetted therapeutic agents (Lian et al., 2012; Merrill, 2012). The role of some of these inhibitors under development for the treatment of colorectal cancer will now be discussed (see Appendix 1 for comprehensive list of canonical Wnt pathway inhibitors).

1.1.1.3.1 Wnt-targetting colorectal cancer therapeutics

A key point to emphasise before discussing the details of anti-colorectal cancer therapeutics is that inhibitors that block Wnt signalling upstream of mutated APC or β-catenin can be considered as potential anti-colorectal cancer therapeutics since the pathway does not behave as a digital switch in which the pathway is either ON or OFF (despite the simple version illustrated in Figure 2). In reality, the activated levels of β-catenin/TCF-dependent transcription can be modulated by the expression of multiple other components. For example, the extracellular Wnt inhibitor Dkk1 is one of the most commonly inactivated molecules linked to Wnt signalling (Aguilera et al., 2006), but functions at the level of Wnt ligand binding. For ease of discussion, therapeutics are considered below as if they target distinct 'levels' of the pathway (where this has been demonstrated). A unified consideration of how therapeutics can be used to 'target a Wnt network' follows.

1.1.1.3.1.1 Extracellular-targetted therapies

The most upstream approach to the inhibition of Wnt signalling has been the prevention of Wnt ligand secretion and receptor binding. Anti-Wnt antibodies and Wnt binding proteins titrate Wnt ligands and have been used as biological therapeutics (Cruciat and Niehrs, 2012). One of the most advanced 'Wnt-titration' therapeutics is a soluble Fz8 CRD fused to a humanized immunoglobulin Fc domain (F8CRDhFc). This reagent was initially shown to be effective against teratocarcinomas and MMTV-Wnt-1 driven breast cancer (DeAlmeida et al., 2007; Liu et al., 2012) and has now been developed (as OMP-54F28) for phase 1 clinical trials against a range of solid tumours.

A number of biological agents have been developed that inhibit Wnts binding to Frizzled and LRP5/6 receptors. One of the furthest developed is an antibody (OMP-18R5) that binds 5/10 Fz receptors (Fz-1,2,5,7,8) and is active as a single agent against a subset of colon, breast, pancreatic and lung cancers (Gurney et al., 2012). This antibody, now known as Vantictumab, entered phase 1 clinical trials in 2011.

There is huge potential for the further development of extracellular biological Wnt pathway modulators that could be guided by the recent structural characterisation of Wnt, LRP and Frizzled interactions. Definition of the ligand binding specificity of further Wnt receptors (e.g. LRP5, Ror, Ryk) and inhibitor binding domains (e.g. sFRP, WIF and Dkk) should offer additional opportunities to target distinct Wnt subsets and explain some currently unpredictable effects of reagents, such as the enhancement of Wnt signalling by Dkk2 and sFRP2 in a subset of cellular contexts (Cruciat and Niehrs, 2012; Marschall and Fisher, 2010).

1.1.1.3.1.2 Cytoplasm-targetted therapies

The antihelmitic compound niclosamide was identified as a Wnt signalling inhibitor in a cell imaging-based assay for Fz1 endocytosis (Chen et al., 2009), and was shown to reduce Fz and LRP6 levels together with TCF-dependent transcription (Lu et al., 2011). Niclosamide inhibited the growth of colorectal and ovarian tumours in both preventative and therapeutic settings *in vivo* (Osada et al., 2011; Yo et al., 2012).

By binding β−catenin, CK1α and GSK3β, Axin acts as a scaffold that enhances β−catenin phosphorylation and ubiquitin-dependent degradation (Clevers and Nusse, 2012). An inhibitor of tankyrase, XAV939, was identified in a cell-based screen for repressors of TCF-dependent transcription (Huang et al., 2009b). TNKS1 and TNKS2 ADP-ribosylate Axin, marking it for ubiquitylation by the RNF146 E3 ubiquitin-ligase. The increased Axin levels resulting from tankyrase inhibition enhance β−catenin degradation (Riffell et al., 2012). XAV939 reduced colorectal (and breast cancer) cell growth under conditions of low serum, and reduced rates of adenoma formation in the mouse intestine following APC deletion (Casas-Selves et al., 2012).

In a biochemical screen for regulators of β−catenin stability another antihelmitic compound, pyrvinium, was identified as a pan-CK1 binding molecule that showed selective allosteric activation of purified CK1α (Thorne et al., 2010). However, recent biochemical studies have suggested that pyrvinium may not function by binding CK1, but instead functions through an AKT-dependent mechanism leading to GSK3 activation (Venerando et al., 2013). In addition to promoting β−catenin turnover, pyrvinium promoted Axin stability and the degradation of Pygo. Significantly it has been shown that pyrvinium inhibits the growth of colon cancer cells *in vitro*, demonstrating its potential as a colorectal cancer therapeutic (Saraswati et al., 2010).

1.1.1.3.1.3 Nuclear-targetted therapies

One of the most direct approaches to interfere with β−catenin/TCF-dependent transcription is to block the interaction between β−catenin and TCF-transcription factors. Lepourcelet *et al.*, identified natural products that blocked β−catenin's binding to TCF in biochemical assays and colon cancer cell proliferation *in vitro* (Lepourcelet et al., 2004). *In silico* virtual screening for compounds that bound the TCF-binding surface of β−catenin identified two small molecules, NU-74654 and BC21 (Tian et al., 2012; Trosset et al., 2006). BC21 prevented TCF binding, TCF-dependent transcription and colorectal cancer growth in cell culture. Structure-based modeling was also central to the design of 'stapled' alpha helical peptides that blocked β−catenin's interactions with TCF4 or Bcl9, a transcriptional co-activator (Grossmann et al., 2012; Kawamoto et al., 2012). In this technically challenging approach, cross-linking 'staples' were used to stabilize and increase the β−catenin affinity of short alpha-helical peptides derived from Axin (fStAx-35) and Bcl9. fStAx-35 blocked TCF-dependent transcription without altering levels of β−catenin and inhibited proliferation of colorectal cancer cells at 10-20μM concentrations.

Cell-based screening for inhibitors of TCF-dependent transcription (induced by siRNA mediated depletion of Axin) identified a series of oxazole ligands (iCRT3, 5,14) that bound β−catenin, blocking its interaction with TCF4. These compounds increased colorectal cancer cell cycle arrest in the G1/S phase (Gonsalves et al., 2011). The natural product carnosic acid was identified in a biochemical screen for inhibitors of the β−catenin/Bcl9 interaction and was shown to inhibit Wnt-target gene expression in colorectal cancer cells (la Roche et al., 2012).

Once β−catenin has formed a complex with DNA-bound TCF factors, it activates transcription through the recruitment of a range of co-activating factors (reviewed in (Cadigan and Waterman, 2012)). The C-terminal transactivation domain of β−catenin interacts with the histone acetyl-transferase CBP, contributing to changes in histone H3 and H4 modification and chromatin structure. In a cell

based screen, Emami *et al.* identified ICG-001 as an inhibitor of β–catenin/TCF-dependent transcription and showed it bound CBP and blocked the β–catenin:CBP interaction (Emami et al., 2004). Two related inhibitors (PRI-724 and CWP232291) have entered phase I clinical studies for the treatment of advanced solid tumours and AML (Garber, 2009). In addition to inhibiting the growth of intestinal tumours in APC-mutant min mice, ICG-001 reduced idiopathic pulmonary fibrosis (Henderson et al., 2010).

One of the key links between the β–catenin/TCF/DNA complex and transcriptional initiation/extension by RNA polymerase II is the multiprotein mediator complex (Xu and Ji, 2011). β–catenin binds to Med12 within the mediator 'kinase module' that comprises CDK8, cyclin C, Med12 and Med13. β–catenin is also linked to the kinase module via the β–catenin co-activators, Bcl9 and Pygo which in turn bind Med12 and Med13 (Carrera et al., 2008). CDK8 is amplified in a subset of colorectal, ovarian and breast and has been shown to be required for colorectal tumour growth *in vivo* and for the maintenance of an undifferentiated state (Adler et al., 2012; Firestein et al., 2008). CDK8 phosphorylates a number of nuclear targets including the C-terminus of RNA polymerase II. CDK8 also activates TCF-dependent transcription through the inhibitory phosphorylation of E2F1, interfering with E2F1's ability to repress β–catenin/TCF-dependent transcription (Morris et al., 2008; Zhao et al., 2012). Compounds that target CDK8 are under development by Selvita (Sel-120) and were identified indirectly in a cell-based screen for inhibitors of p21-induced transcription (Senexin A; (Porter et al., 2012)). Senexin A blocked β–catenin/TCF-dependent transcription in colon cancer cells and co-operated with the chemotherapeutic doxorubicin in preventing lung cancer growth.

1.1.1.3.1.4 Multi-level / undefined mechanisms

Cell-based screening for small molecule regulators of β–catenin/TCF-dependent transcription identified a number of additional pathway regulators without characterizing their molecular targets. Two groups identified inhibitors, CCT031374 and KY02111, which reduced levels of β–catenin and TCF-dependent transcription, even in the presence of inhibitors of GSK3 (Ewan et al., 2010; Minami et al., 2012). The therapeutic potential of targetting alternative β-catenin degradation pathways was further supported by the finding that Hexachlorophene promoted β-catenin degradation through a Siah1/APC dependent, but GSK3–independent pathway (Park et al., 2006). A series of diaminoquinazolines inhibited transcription at an undefined level in colon cancer cells (Mao et al., 2012). Furthermore, both the diterpenoid NC043 and the Fe^{2+} binding compound HQBA blocked signalling downstream of β–catenin accumulation and inhibited tumour growth *in vivo* (Coombs et al., 2011; Wang et al., 2011). Interestingly, reducing luminal iron levels in the gut was also shown to lower rates of tumourigenesis in an APC mutant mouse model (Radulescu et al., 2012).

Many small molecule inhibitors of non-Wnt pathway components have been shown to interfere with β-catenin/TCF-dependent transcription in specific cellular contexts (e.g. Src, PKA, PI3K; reviewed in (Voronkov and Krauss, 2012)). On a conceptual level, this raises a question as to what should be considered a 'Wnt-inhibitor'; particularly as some responses may be secondary to cellular transcription changes induced by primary alterations to the function of 'non-Wnt' pathways. Nonetheless, mechanistic details support direct action on the Wnt pathway for some compound classes.

1.1.1.3.1.4.1 Non-steroidal anti-inflammatory drugs (NSAIDS)

NSAIDS including sulindac, aspirin and celecoxib have been used in the clinic to prevent colon cancer and are thought to act in part by inhibiting cyclooxygenase enzymes (COX) leading to a reduction in the levels of the bioactive lipid prostaglandin E2 (PGE2; (Elder and Paraskeva, 1998; Smalley and DuBois, 1997)). Raised levels of PGE2 in cancer bind the G-protein coupled receptor (GPCR) EP2 and activate β−catenin/TCF-dependent transcription (Castellone et al., 2005), while celecoxib lowers PGE2 levels and blocks β−catenin/TCF-dependent transcription (Takahashi-Yanaga et al., 2008). However, celecoxib also acts through COX-independent pathways (Grosch et al., 2001). Some NSAIDs including indomethacin bind to peroxisome proliferator activated receptor gamma (PPARγ) nuclear receptors and, by acting as partial agonists, block the action of strong agonists (Bishop-Bailey and Warner, 2003). As PPARγ forms a ligand-dependent complex with β−catenin/TCF this offers an alternative route for NSAID action against Wnt signalling. Interestingly, the PPARγ/PPARδ antagonist FH535 was isolated in a screen for inhibitors of β−catenin/TCF-dependent transcription and was shown to interfere with the PPARγ:β−catenin interaction (Handeli and Simon, 2008). Surprisingly, the NSAID sulindac bound the Dvl PDZ domain with a K_i of 10μM and inhibited β-catenin/TCF-dependent target gene expression in *Xenopus* embryos (Lee et al., 2009). Although NSAIDS have clear effects *in vivo* and have been linked to multiple mechanisms, careful studies will be required to link effect to mechanism since many NSAIDS don't achieve the concentrations and exposures *in vivo* that are frequently studied *in vitro* (Ettarh et al., 2010).

1.1.1.3.1.4.2 Flavonoids

Flavonoids are a broad family of polyphenolic plant compounds that target a range of cellular pathways and processes (reviewed in (Havsteen, 2002)). Several flavonoids are active against Wnt signalling, including; genistein, quercetin, isoquercitrin and curcumin (reviewed in (Amado et al., 2011)). With the exception of flavone activity against tankyrase (Yashiroda et al., 2010), little evidence has so far identified a direct Wnt molecular target that could account for the array of biochemical changes observed, including reductions in β−catenin and Dvl protein levels and the prevention of DNA binding by β−catenin:TCF protein complexes. Part of the difficulty in identifying a direct mechanism may be due to the effects many flavonoids have on pathways including PI3K, MAPK and Notch that may indirectly modulate the Wnt pathway activity.

1.1.1.3.2 Drugging a Wnt network

The conventional, linear view of Wnt signalling underemphasizes key aspects of the pathway. Firstly, signalling is not either 'on' or 'off'; key outputs such as the level of β−catenin/TCF-dependent transcription can be modulated over 4 orders of magnitude and the level of activity determines biological outcomes (Buchert et al., 2010; Luis et al., 2011). Secondly hundreds of context-specific 'Wnt pathway regulators' have been identified, particularly in the last few years with the onset of high-throughput RNAi and proteomic screens (Major et al., 2008; Tang et al., 2008). Thirdly, the absolute level of pathway activity likely reflects the integrated output of multiple regulators in patterns that are not simply additive. For example, R-spondin, which binds to the Lgr5 receptor, does not itself signal but alters the output from a fixed level of Wnt ligand by altering Fz receptor degradation (Macdonald and He, 2012). Lastly, non-Wnt signals such as EGF can directly modulate the activity of β−catenin/TCF-dependent transcription independent of upstream Wnt pathway components (Yang et al., 2011). The range of potential functional interactions, when fully described, may best be represented as a graph network (Kestler and Kuhl, 2008). The network view can be used to highlight

aspects of therapeutic targetting including compound dosing, dynamics and the use of compound combinations that target a distinct pathways a subset of which are alluded to in the ‘theoretical pathway’ structure diagram in Figure 5. The network view is also a useful tool with which to discuss the approach and results in this thesis, thus is considered in more detail below in relation to the use of therapeutics targetting the pathway.

Figure 5. A schematic representation of the Wnt network

Network nodes represent functional units (proteins or protein complexes; see inset) and vertices represent functional interactions (+ve or –ve). While the total network is complex, individual cell contexts express a simpler subset of nodes, each of which would contribute toward total pathway activity. Targetting highly connected core components of pathways that are expressed in all cell types (coloured nodes; e.g. Wnt, MAPK, Notch etc.) would be most effective at blocking the corresponding pathway, but would be predicted to maximise toxicity. Targetting non-core nodes or individual vertices (e.g. a signal-transducing protein-protein interaction) might lack single-agent efficacy due to a partial effect on Wnt pathway activity but would minimise toxicity. By contrast, inhibiting molecules such as CBP (e.g. ICG-001) or CK1α (e.g. pyrvinium) that can be represented as highly connected nodes or as components of multiple nodes would enhance the probability of single agent efficacy, but would increase the probability of toxicity via action at unintended nodes. Combinations of single node-specific inhibitors should maximise the cell context specificity. Drug resistance to single agent inhibitors may develop through mutation to target nodes or by expression of nodes from outside the cell context.

Figure 5

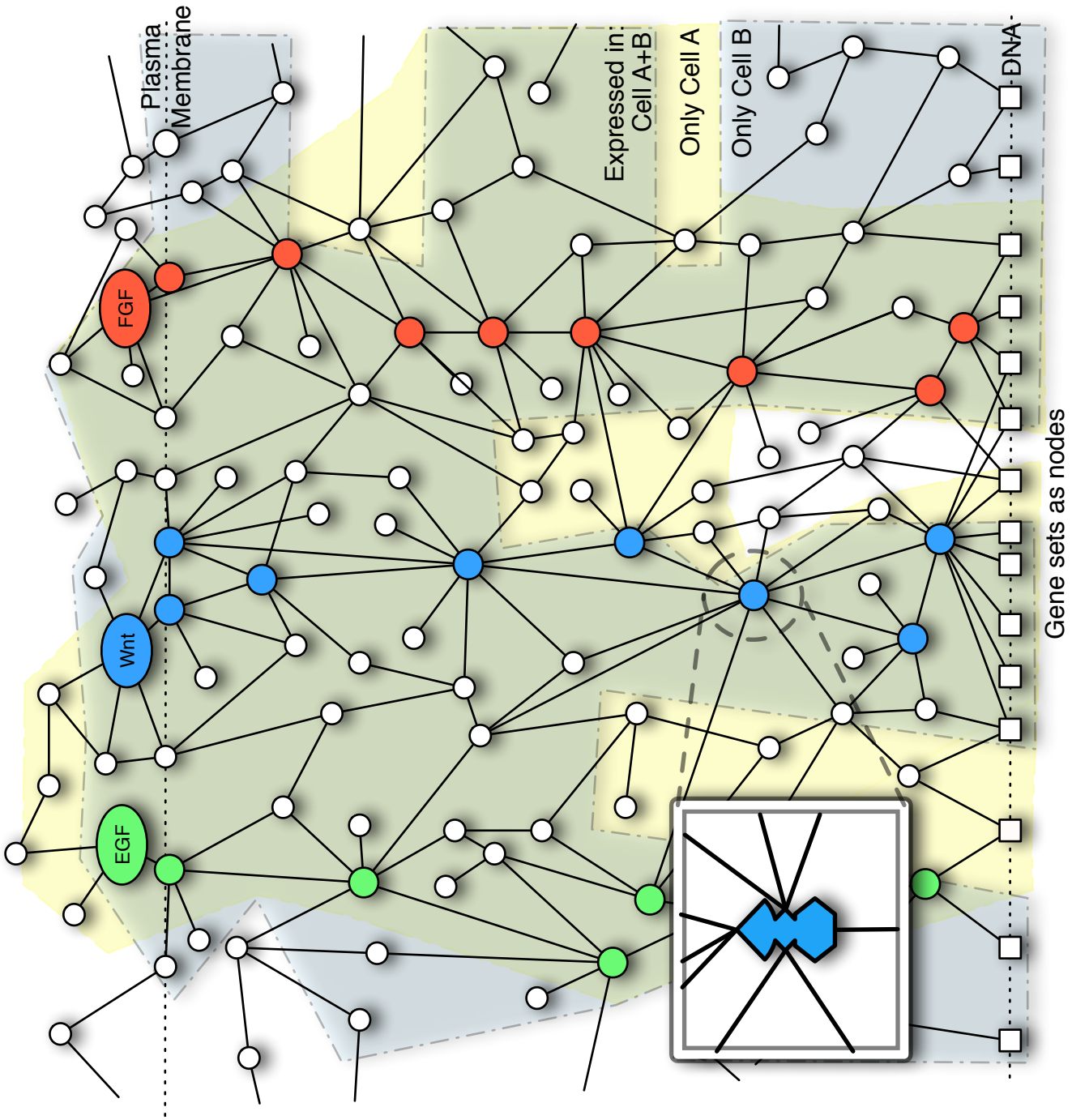
Plasma Membrane
Expressed in: Cell A+B
Only Cell A
Only Cell B
DNA
FGF
Wnt
EGF
Gene sets as nodes

1.1.1.3.2.1 The Wnt signalling network, drug doses and dynamics

'Just right' levels of Wnt signalling are required for homeostasis within normal and, at altered levels, diseased tissue. For example, liver and melanoma oncogenesis is associated with lower levels of β–catenin/TCF-dependent transcription than intestinal tumourigenesis (Buchert et al., 2010; Lucero et al., 2010). Therapeutic molecules that partially alter signalling levels may therefore reach an efficacy threshold in one tissue but may be ineffective in another, even if the molecular target is equally expressed. Partial efficacy may result from the partial inhibition of a strong pathway regulator (e.g. a well-connected network node in Figure 5) or full inhibition of a molecule that contributes a smaller effect on total pathway activity (e.g. a peripheral node in Figure 5). For example, the partial inhibition of GSK3β (a well connected node) by lithium may be needed to generate a 'just right' level of β–catenin/TCF-dependent transcription for the treatment of bipolar patients (Klein, 2012). Surprisingly, a therapeutic level of Wnt signalling may be either lower or higher than that that characterizes the disease state, even in cancer. An example of this was identified in the case of riluzole, an FDA-approved drug that was originally approved for treating amyotrophic lateral sclerosis, which was subsequently found to be an effective melanoma-specific therapeutic (possibly) functioning by super-activating the pathway above a 'just right' level (Biechele et al., 2010)

Different levels of pathway activity distinguish stem and 'transit amplifying' cells within one tissue. As discussed earlier, in the intestinal epithelium high levels of mutant β–catenin induced supernumerary stem cell formation and was accompanied by low levels of proliferation, while a lower levels led to fewer stem cells, but increased progenitor cell proliferation (Hirata et al., 2013). Within individual tumours, heterogeneous levels of nuclear β–catenin and TCF-dependent transcription are driven by microenvironmental factors that in turn couple to distinct cell phenotypes including stem cell, migratory and proliferative (de Sousa et al., 2011). Each tumour cell subpopulation (e.g. stem or progenitor) will likely have cellular networks that respond differentially to therapeutics.

Inhibitors such as the anti-Fz antibody OMP18-R5 have been shown to be active against tumour-initiating/cancer stem cells (Gurney et al., 2012), but it is not currently clear whether they are directly active against the Wnt-driven proliferative compartment. These hidden details of therapeutic mechanism may make the use of biomarkers of drug response difficult using techniques such as western blotting, if the target cell subpopulation is not first purified.

On a longer timescale, immediate-early responses to Wnt inhibitors will feed through to changes in target gene expression, including alterations to cell differentiation. Analysis of the timing of 'Wnt-off' responses in an intestinal hyperplasia model showed that responses (changes in apoptosis/differentiation) were complete within only 48 hours (Jarde et al., 2013). By contrast, tumour-regression frequently took 2-4 weeks for therapeutics described earlier. Although this time difference may be explained by the details of the therapeutic, its access to the tumour or a unique feature of a particular tumour model, it is interesting to speculate that initial treatments induce a rapid response from tumour subpopulations with a sensitive Wnt network and that unresponsive cells later convert into responsive cells as their microenvironment changes during therapy. This interpretation would predict that short pulses of Wnt pathway inhibitor combinations that target distinct cell(s) with a discrete network structure would induce very rapid responses and could minimize long-exposure associated toxicity. Interestingly, short-period pulses of Wnt signalling have been suggested to be optimal during tissue regeneration (Zimmerman et al., 2012), and for the efficient differentiation of human pluripotent stem cells into cardiomyocytes *in vitro* (Lian et al., 2012; Minami et al., 2012).

1.1.1.3.2.2 The Wnt signalling network and cellular toxicity

One common concern for the use Wnt pathway therapeutics is the potential for acute toxicity in adult tissues that are maintained by stem cells, based on the central role for Wnts in stem cell biology (Wend et al., 2010). Additional side effects may include metabolic changes, based for example, on the role of Wnt

signalling in the maintenance of liver zonation; and the potential for neurological effects, based on the action of Wnts on synapse formation in the CNS and PNS (Benhamouche et al., 2006; Harrison-Uy and Pleasure, 2012; Klein, 2012; Koles and Budnik, 2012; Liu et al., 2011; Wend et al., 2010; Zarnescu and Zinsmaier, 2009). Toxicity may also be associated with off-target effects of inhibitors. For example, pyrvinium has been suggested to have alkylating activity in addition to its effects on CK1α (Saraswati et al., 2010). Longer-term treatment with Wnt-inhibitor therapeutics might be expected to promote the onset of diseases for which Wnt activators are being developed and vice-versa. This could include ageing-related diseases (Naito et al., 2012). Nonetheless an understanding of the 'Wnt network' in diseased tissue may be able to maximize on-target specificity by exploiting unique dependencies/network structures that are not likely to be present within other adult tissues.

1.1.1.3.2.3 The Wnt network and combinatorial therapies

Standard of Care (SoC) chemotherapy in cancer

Combinatorial therapy can be divided into two types: combinations in which compounds target distinct tumour cell types and combinations that target distinct processes within one cell. Targetting Fz receptors in solid tumours with OMP-18R5 synergized with chemotherapeutic agents including taxol, irinotecan and gemcitabine, at least in part by reducing the slow-growing, tumour-initiating/cancer stem cell compartment, whilst SoC chemotherapeutics agents 'debulked' tumours by targetting rapidly proliferating cells (Curtin and Lorenzi, 2010; de Sousa et al., 2011; Gurney et al., 2012; Malanchi et al., 2011). Providing further evidence for this hypothesis, the CK1α inhibitor pyrvinium and sFRP7 potentiated the activity of doxorubicin against prostate and HCC tumours respectively (Wang et al., 2011; Yu et al., 2008). Additionally, salinomycin and gemcitabine combined to repress pancreatic tumour growth (Zhang et al., 2011). *In vitro*, PKF115-584, quercetin and an anti-Wnt-1 antibody increased the chemosensitivity of colon and melanoma cells towards 5FU, temozolomide,

cisplatin, doxorubicin and docetaxel respectively (He et al., 2005; Sinnberg et al., 2011; Wang et al., 2011; Xavier et al., 2011; Yu et al., 2008), while GDK100017 enhanced lung cancer radiosensitivity (Lee et al., 2013). By contrast, the tankyrase inhibitor XAV-939 failed to synergise with 5FU or oxaliplatin in the killing of primary colorectal cancer spheroid cultures (Tenbaum et al., 2012). *In vivo,* Wnt inhibitors may also work indirectly by reducing a side effect of standard chemotherapy – the ability to promote tumour relapse. The CDK8 inhibitor Senexin A and pyrvinium were shown to prevent doxorubicin-induced stromal phenotypes that supported tumour progression, while pyrvinium also enhanced SoC efficacy by reducing the Wnt ligand-dependent expression of the drug export protein, mdr-1 (Basu et al., 2012; Porter et al., 2012). The tankyrase inhibitor, XAV939 reduced paracrine stromal Wnt signalling to tumour cells and synergized with araC to increase survival in acute lymphoblastic leukemia (Yang et al., 2013). Similarly, DNA-damage induced Wnt-16 expression in fibroblasts promoted prostate cancer resistance to chemotherapeutics through a pathway that was inhibited by XAV939 (Sun et al., 2012).

Far less explored are the mechanisms by which chemotherapeutic agents synergise with Wnt inhibitors within a single cell type. Studies in embryonic stem cells showed that the DNA damaging agent cisplatin induced β-catenin/TCF-dependent transcription, which in turn blocked apoptosis, suggesting that the inhibition of Wnt signalling may enhance the cell-killing efficacy of DNA-damaging SoC agents (Carreras Puigvert et al., 2013).

Wnt:non-Wnt inhibitor combinations

In the context of a network, the definition of which components are 'Wnt-specific' is somewhat unclear. Components of pathways such as PI3K, Ras/MAPK and Notch interact to affect the levels of β−catenin/TCF-dependent transcription as well affecting well-studied non-Wnt outcomes (reviewed in (Bertrand et al., 2012; Hu and Li, 2010; Itasaki and Hoppler, 2009; Voronkov and Krauss, 2012)). For example, activation of Ras or PI3K signalling increased β−catenin nuclear accumulation, tumour initiation and progression in the intestine (He et al., 2007;

Marsh et al., 2008; Phelps et al., 2009; Sansom et al., 2006). Unexpectedly however, reduction of PI3K signalling through treatment of colorectal cancers with PI3K inhibitors did not revert cancers to a less advanced tumour phenotype as might have been predicted, but instead led to the activation of a metastatic phenotype that was dependent on high levels of nuclear β–catenin (Tenbaum et al., 2012). Encouragingly though, treatment of primary colorectal cancers expressing high levels of nuclear β–catenin in spheroid culture with the tankyrase inhibitor XAV-939 reduced β–catenin levels, redirecting cell the cellular program such that PI3K-inhibition induced apoptosis rather than promoting metastasis (Tenbaum et al., 2012). More in line with expectation, combinations of the Wnt inhibitors pyrvinium and PKF115-584 with a Ras inhibitor (FTS) were found to synergise in the *in vitro* killing of colorectal cancer cell lines with mutant KRAS and APC or β–catenin (Mologni et al., 2012). The Wnt inhibitors XAV939 and pyrvinium also synergistically inhibited non small cell lung cancer cell line growth in combination with the EGFR receptor inhibitor gefitinib (Casas-Selves et al., 2012).

Wnt:Wnt inhibitor combinations

Although combinations involving different Wnt inhibitors have not yet been described, they should offer therapeutic advantages. Firstly, they should allow greater control over the absolute level of pathway activity than single agents. Secondly, they should allow the tailoring of inhibitor combinations (and therefore maximal effect) to Wnt pathway branches that are selectively active in the disease setting, thereby reducing toxicity. Finally, in the cancer context, they should reduce the chances of resistance developing through the activation of alternative branches of the network (Figure 5). A useful initial combination would likely involve both extracellular and intracellular Wnt pathway inhibitors in colorectal cancer since APC/β–catenin mutations are frequently accompanied by reduced expression of extracellular Wnt repressors such as Dkk1 (Ying and Tao, 2009). In addition, combinations should allow a greater range of disease-associated phenotypes to be targeted since activation at the Wnt ligand level can

induce a greater range of cancer hallmark changes than downstream changes induced by, for example, mutant β-catenin alone (Collu et al., 2009).

A major future task will be the identification of efficacious therapeutic combinations and corresponding susceptible patient populations from the huge numbers of potential drug combinations and genotypes. One approach to this would require the systematic mapping of functional dependencies amongst 'Wnt pathway regulators' combined with mutation and expression analyses of diseased tissues to allow the definition of 'patient-stratified functional networks' that would represent each cell type within the diseased tissue (Figure 5). A second more empirical approach would be to identify efficacious combinations through direct experiment using patient tissues (Tenbaum et al., 2012). Here, the recent identification of R-spondin dependent organoid growth conditions for normal and diseased tissues has been a major advance (Schuijers and Clevers, 2012), since this may in future allow inhibitor combinations to be directly tested *in vitro* on tumour material, prior to the use of efficacious agent combinations in the patients from which the tumours were isolated. However, high-throughput implementation of *in vitro* organoid growth and treatment technologies would be needed to maximize their potential in drug combination studies. A third empirical approach is to use 'synthetic lethal' genome-scale screens to identify disease-specific, druggable molecular targets that synergise with single-agent therapeutics to induce cell killing. This approach was taken as part of the work in this thesis. A key starting point for these studies would be the identification of cell systems/single agent therapeutic combinations that have a low background of cell killing, against which alterations in gene expression during the screen would be predicted to result in robust conditional changes in cell viability. Suitable combinations for a screen that could be suggested based on the existing literature would include the combination of a tankyrase inhibitor and breast cancer cells since tankyrase inhibition was able to reduce β–catenin/TCF-dependent transcription but was unable to induce cell death under normal cell growth conditions (Bao et al., 2012).

1.2 Contextualisation of the cDNA studies conducted

The foundation for the cDNA screen undertaken in this research was established in the Dale laboratory. Experimental support for the 'network' nature of Wnt signalling resulted from studies within the Dale laboratory that are described in Jamie Freeman's thesis (Freeman, 2008). In this work, a cell-based cDNA over-expression screen of 9000 *Xenopus tropicalis* cDNAs was carried out for novel regulators of the TCF-dependent transcription. This led to the identification of ~50 novel pathway activators through the co-expression of cDNAs a mutant Wnt co-receptor, ΔNLRP (shown to induce a 'mid-level' of Wnt pathway activity, Figure 6 (Brennan et al., 2004)). Surprisingly, it was subsequently found that 47/50 'activating' cDNAs did not activate TCF-dependent transcription when expressed alone in the HEK293-based 7df3 reporter cell line, suggesting that their function was dependent on the activity of ΔNLRP.

Figure 6 placement

Figure 6. Schematic representation of the dynamic range of Wnt/TCF-dependent transcription

Constitutive activation of basal Wnt signalling by ΔNLRP is anticipated to provide a platform for the identification of 'super-activators' and 'inhibitors' of TCF-dependent transcription (adapted from (DasGupta et al., 2005)).

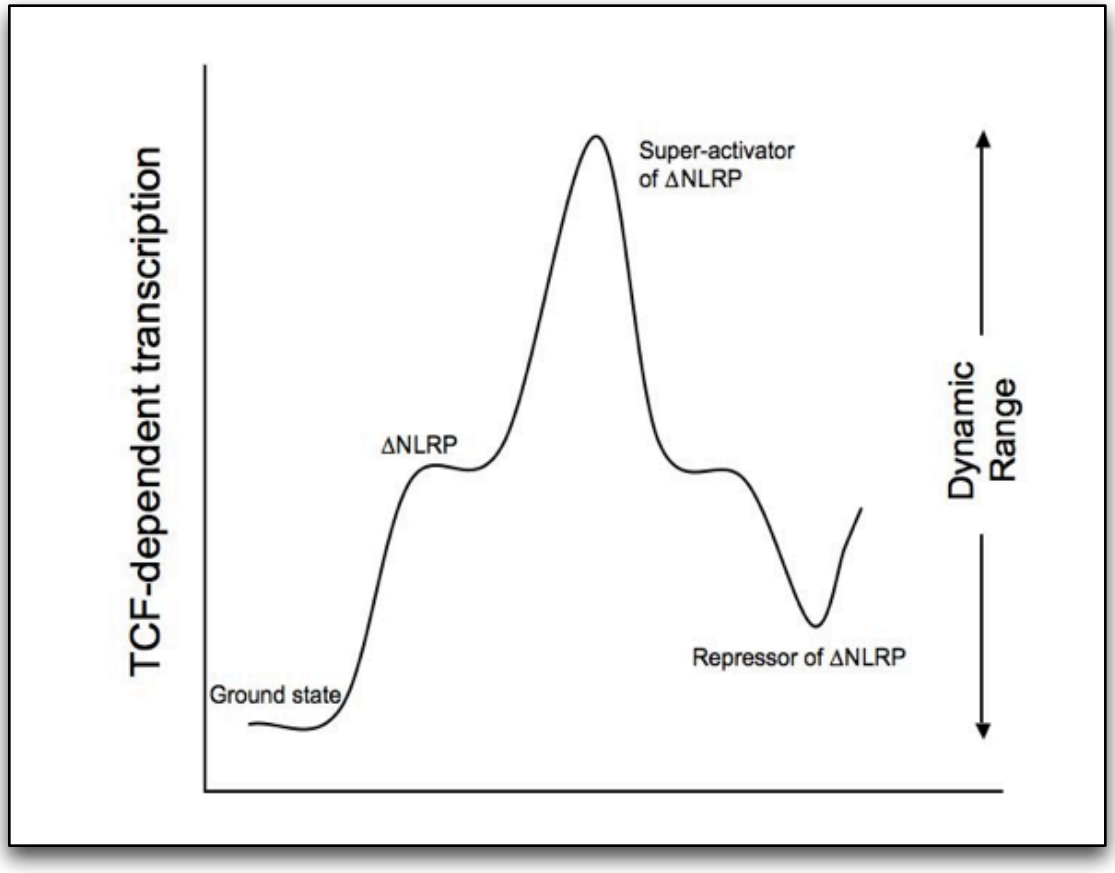

Figure 6. Schematic representation of the dynamic range of Wnt/TCF-dependent transcription

Constitutive activation of basal Wnt signalling by ΔNLRP is anticipated to provide a platform for the identification of 'super-activators' and 'inhibitors' of TCF-dependent transcription (adapted from (DasGupta et al., 2005)).

A key observation in this work was that when each of the 50 activating cDNAs was expressed in the presence of each other (50 x 50), a unique pattern of functional co-operativity was observed. Many cDNA pairs would only functionally co-operate to induce transcription in combination with a selected subset of other cDNAs. A network of functional co-operation was constructed that usefully informed other studies of the pathway. Firstly, it was observed that functional co-operativity was more often observed between components of different protein complexes (as highlighted by the overlap with protein interaction networks). Secondly, it was determined that 'core' Wnt pathway components appeared to be highly connected nodes in the functional connectome. Thirdly, it was noted that cDNA pairs showed distinct patterns of sensitivity to small molecule inhibitors of TCF-dependent transcription, suggesting that the functional connectome could be used to 'place' the action of drugs with unknown molecular targets in a functional context.

1.3 Background to the 'MSC' compound used in this report

The Dale laboratory previously published the results of a cell-based screen for inhibitors of the Wnt signalling pathway (Ewan et al., 2010). In the Ewan study, a HEK293 based cell line (7df3) containing an integrated, Dvl-ER fusion protein and a TCF-luciferase reporter was used to screen for small molecule inhibitors of TCF-dependent transcription (see Methods; Figure 7). The Wnt pathway was induced in the cell line by addition of estradiol, leading to the refolding of the Dvl-ER fusion partner and the activation of TCF-dependent transcription. The Ewan study (Ewan et al., 2010) described the screen of a 63,000 compound library that was added (1 well per compound) simultaneously with estradiol, and levels of TCF-dependent transcription were assessed 24 hours later (Figure 7). The 306 'hit' compounds that reproducibly reduced TCF-dependent transcription were processed through a series of 'deconvolution' assays that were designed to:

1. Remove non-specific 'toxic' compounds. 7df3 cells could be cultured in the absence of estradiol and had very low levels of background TCF-dependent transcription, suggesting that any compounds that simply killed 7df3 cells *and* reduced TCF-dependent transcription, were doing so through non-Wnt 'toxic' pathways.
2. Identify compounds that had activity against tumour cell lines in 2D growth including HCT116, SW480 and HT29 cells. This step was based on the observation that growth in these lines could be suppressed through the reduction of TCF-dependent transcription as engineered through siRNA depletion of Wnt regulators such as β-catenin or through the re-expression of Wnt pathway inhibitors such as APC or transcriptionally-inactive forms of TCF factors.
3. Remove compounds that blocked 'non-specific' TK-luciferase (i.e. non-Wnt) promoter activity. The aim here was to remove 'off-target' inhibitors of transcription.
4. Deconvolve the 'level' at which the compound worked within the pathway by testing whether the pathway could be blocked when it was activated at multiple levels through the expression of various Wnt pathway activators (e.g. ΔNLRP, Dvl-2, Axin-GSK3 binding domain, ΔN-β-catenin, VP16-TCF).

Based on these criteria and following an assessment of their chemical tractability (e.g. size, reactivity, stability, patent position etc.), a subset of 10 compounds were selected for additional studies. Nine of the ten compounds were described by Ewan *et al.* and were not subsequently developed as therapeutic candidates based on a further assessment of their chemical tractability and the robustness of their biological responses (Ewan et al., 2010). One of the compounds not described in the paper (CCT071459) had an IC_{50} of 1μM in the 7df3 TCF-luciferase reporter assay and was selected for further development in a major collaboration between Cardiff University, The Institute of Cancer Research (ICR) and Merck Serono.

Continued development of the CCT071459 compound series took place during the course of the work described in this thesis, and subsequently the activity of the more developed 'daughter compound' termed MSC was assessed in these studies. Reference to unpublished studies carried out by other individuals within the Cardiff / ICR / Merck Serono collaboration will be made at appropriate places throughout this work where the data affected the direction of the work undertaken.

1.3.1 The molecular target of MSC

Following extensive collaboration-wide target identification studies (including cellular reporter assays, stable isotope labelling by amino acids in cell culture followed by mass spectrometry and enzyme activity confirmation assays), the molecular targets of MSC were determined as being CDK8 and CDK19. CDK8 and CDK19 are members of the cyclin-dependent family of serine/threonine kinases, whose function is regulated by the conditional presence of a cyclin subunit. The CDK family is crucial in controlling cellular proliferation in mammalian systems through the regulation of the cell cycle (Malumbres and Barbacid, 2005). The cell cycle is a tightly controlled series of events essential for the precise, error-free replication of eukaryotic cells. The transition from one cell cycle phase to the next is controlled, in part, by specific CDK-cyclin complexes. The expression of cyclin D (CycD) is triggered by mitogenic signals. CycD preferentially binds and activates CDK4 and CDK6, which then phosphorylate 'pocket proteins' including retinoblastoma protein (RB) and partially inhibit its anti-proliferative effect, allowing expression of the E-type cyclins and thus priming the cells to initiate DNA synthesis. Late in the G1 phase and immediately prior to the DNA replication S phase, CDK2 interacts with CycE which drives G1/S phase transition through additional phosphorylation of pocket proteins (resulting in their complete inhibition and maximising CycE availability). Subsequently a CDK2-CycA complex is formed which pushes the cell cycle from S phase to the G2 phase. During the G2 phase CDK1 is bound to CycA which facilitates the onset of mitosis, with cells driven through the final mitosis (M) phase by the binding to and activation of CDK1 by CycB, forming the 'M phase

promoting factor' (Malumbres and Barbacid, 2009; Pitts et al., 2013). The formation of the correct CDK-cyclin complexes is achieved through the synthesis at degradation of each cyclin at defined points during the cell cycle, providing an additional level of control over its progression (Malumbres and Barbacid, 2009).

As briefly described, RB and p53 play crucial roles in the regulation of the cell cycle by preventing aberrant cellular proliferation and genome mutation respectively (Cox and Lane, 1995; Hernando et al., 2004). Loss of function of these proteins reduces cell cycle regulation, thus uncontrolled cellular proliferation and/or loss of genome stability occurs. For this reason they are described as tumour suppressors, with their corresponding *RB1* and *TP53* genes classified as tumour suppressor genes.

It is evident that not all of the >20 CDKs presently identified are key players in cell cycle regulation; many possess diverse roles outside of cell cycle control (reviewed in (Lim and Kaldis, 2013)). The targets of MSC, CDK8 and CDK19, are two examples of such 'non-cell cycle associated' CDKs. CDK8 is a ubiquitously expressed nuclear protein whose best characterised function is as a regulator of transcription as part of the Mediator complex, and is hence described as a 'transcriptional CDK' (Galbraith et al., 2010). In complex with CycC (also ubiquitously expressed) and the mediator proteins Med12 and Med13, the CDK8:CycC kinase core forms the regulatory module of the multi-protein Mediator complex which plays a central role in the control of both basal and regulated transcription (Firestein and Hahn, 2009; Malik and Roeder, 2010). Interestingly it has also been identified that CDK8 is an essential regulator of nuclear β-catenin activity, which in turn provides a link between the basal transcription components and the enhancement of β-catenin-TCF/LEF dependent transcription (Firestein and Hahn, 2009).

CDK19 (also known as CDK11) is a paralogue of CDK8, with the human CDK19 protein sharing 77% sequence homology with its CDK8 counterpart. Less is known about the activity of CDK19, although it has been shown that CDK19 is able to interact with the same Mediator complex kinase module components as

CDK8 (Conaway et al., 2005; Knuesel et al., 2009), suggesting that these kinases are functionally redundant (to an as yet unknown degree). This is supported by in-house studies that have shown that a reduction in HCT116 colorectal cancer cell number is dependent on the dual knockdown of CDK8 and CDK19 genes (with no effect on cell number observed when each gene was knocked-down independently; data not shown).

Significantly, CDK8 has been determined to be a colorectal cancer oncogene (Firestein and Hahn, 2009). The observation that CDK8 is amplified in a range of colon cancers combined with its role in the regulation of both transcription and β-catenin nuclear activity indicates that CDK8 may super-activate β-catenin, and serve to potentiate malignancies driven by aberrant Wnt/β-catenin signalling (Firestein et al., 2008; Firestein and Hahn, 2009). Therapeutic reduction of this activity is therefore a desirable target for the treatment of colorectal cancers.

1.4 Aims and objectives

The work described in this thesis can be divided into two parts. In the first, a cDNA screen for novel regulators of Wnt signalling was undertaken. The rationale for this study was an extension of the deconvolution studies (point 4 on page 42). Data from the drug discovery collaboration determined that MSC acted at the level of the TCF-complex, in that it blocked transcription driven by a VP16-TCF fusion protein – a strong activator that drives ligand- and β-catenin-independent TCF-dependent transcription. Following a whole genome cDNA screen for the identification of Wnt signalling regulators (using a cDNA library provided by Dr. Gary Davidson from Karlsuhe Institute of Technology), the objective was to determine whether transcription induced by any novel pathway regulators identified would be sensitive or resistant to inhibition by MSC. The underlying hypothesis was that a large-scale 'map' of inhibitor sensitivity in relation to novel and existing cDNA regulators would help identify the probable molecular target of MSC and would identify genes whose function might alter MSC compound resistance and sensitivity in a clinical context.

The second major part of the work described in this thesis was initiated after the Cardiff / ICR / Merck Serono collaboration identified the molecular target of the MSC compound as the CDK8 and CDK19 serine/threonine kinases. It is important to note that CDK8 has been shown to play a central role in the coupling of β-catenin/TCF to RNA polymerase II at Wnt target genes (in addition to other roles; see discussion). By this stage in the drug development programme, work including my studies had shown that the more advanced CCT071459 daughter compound MSC had nanomolar activity against TCF-dependent transcription, yet had little efficacy against colorectal cancer cell growth in 2D culture (unlike the CCT071459 parent compound).

In the second major part of the work here described, a synthetic lethality screen using an esiRNA library was carried out to identify genes whose function was conditionally required for cell growth in 2D culture in the presence of the

CDK8/19 inhibitor, MSC. The rationale for the synthetic lethality screen was based on the analogous observation that siRNA depletion of Parp1 in BRCA1 mutant cells uncovered a synthetic dependence of Parp1 function conditionally in cells lacking BRCA1 function, and that Parp1 small molecule inhibitors could be used to selectively kill BRCA1 deficient cells (Farmer et al., 2005). The underlying hypothesis for the synthetic lethality study was that novel gene functions functionally co-operate with CDK8/19 to drive growth in 2D cell culture. This hypothesis was based (at least in part) on the observation that HCT116 colorectal cancer cells in which Wnt/β-catenin driven transcription was reduced (by loss of β-catenin and reduction in Wnt ligand levels), *did* show reduced levels of *in vivo* cell proliferation (HCT116 cell xenografts; (Bafico et al., 2004)), suggesting that loss of TCF-dependent transcription may not be sufficient for growth inhibition in 2D culture.

In summary, the cDNA overexpression study identified a number of novel Wnt pathway regulators, two of which were resistant to MSC inhibition. Furthermore, the esiRNA synthetic lethality screen identified a small number of genes whose loss led to MSC-dependent inhibition of 2D colorectal cancer cell growth.

Chapter 2. Materials and Methods

2.1 Routine cell culture and cell line details

Unless otherwise stated, cells were passaged when they approached 70% confluence and were routinely tested (monthly) for mycoplasma contamination by PCR analysis. Details of the mutation status of colorectal cell lines used can be found in Appendix 2.

2.1.1 The 7df3 TCF-Luciferase (TLIG) reporter cell line

The Wnt-pathway reporter cell line was generated by Dr. Helen Wildish, as described by Ewan *et al*. (Ewan et al., 2010). Briefly, HEK293T cells expressing a haemagglutanin tagged-dishevelled 2-oestrogen receptor fusion protein (HA-Dvl2-ER) that allowed for oestrogen-dependent Wnt signalling induction were co-transfected with a Wnt-responsive bicistonic luciferase/green fluorescent protein (GFP) reporter plasmid ('TLIG' vector; Figure 7a). The integrated TLIG reporter construct comprises a Wnt responsive element (WRE) from the *Xenopus* Xnr3 promoter upstream of four repeats of a short TCF binding sequence and the basal TK-promoter TATA box and transcriptional initiation site. Clone '7df3' (stably expressing the reporter construct under 3µg/ml blasticidin and 200µg/ml hygromycin selection (Life Technologies and Roche respectively)) was chosen based on its high signal:noise luminescence ratio following lithium induction (Figure 7bi&ii).

7df3 cells were cultured in Dulbecco's Modified Essential Medium (DMEM; Life Technologies) supplemented with 10% foetal bovine serum (FBS; Life Technologies), 2mM L-glutamine (Life Technologies) and 50units/ml penicillin, 50µg/ml streptomycin (Life Technologies) at 37°C and 5% CO_2. The cells were maintained under 3µg/ml blasticidin and 200µg/ml hygromycin selection.

Figure 7 placement

Figure 7. Schematic representation of the TCF-luciferase reporter cell line

a. The TLIG reporter construct was generated to contain four multimerised TCF binding sites downstream from the Xnr3 promoter, driving the transcription of luciferase and GFP reporter genes in the presence of Wnt pathway stimulation (taken from (Ewan et al., 2010)).

bi and ii. HEK293 cells were stably transfected with a Dvl (labelled Dsh here) and the TLIG reporter construct. The clones were induced with lithium and the most responsive clone (with highest induction:lowest background ratio) was selected (figure reproduced with the kind permission of Dr. Jamie Freeman (Freeman, 2008)).

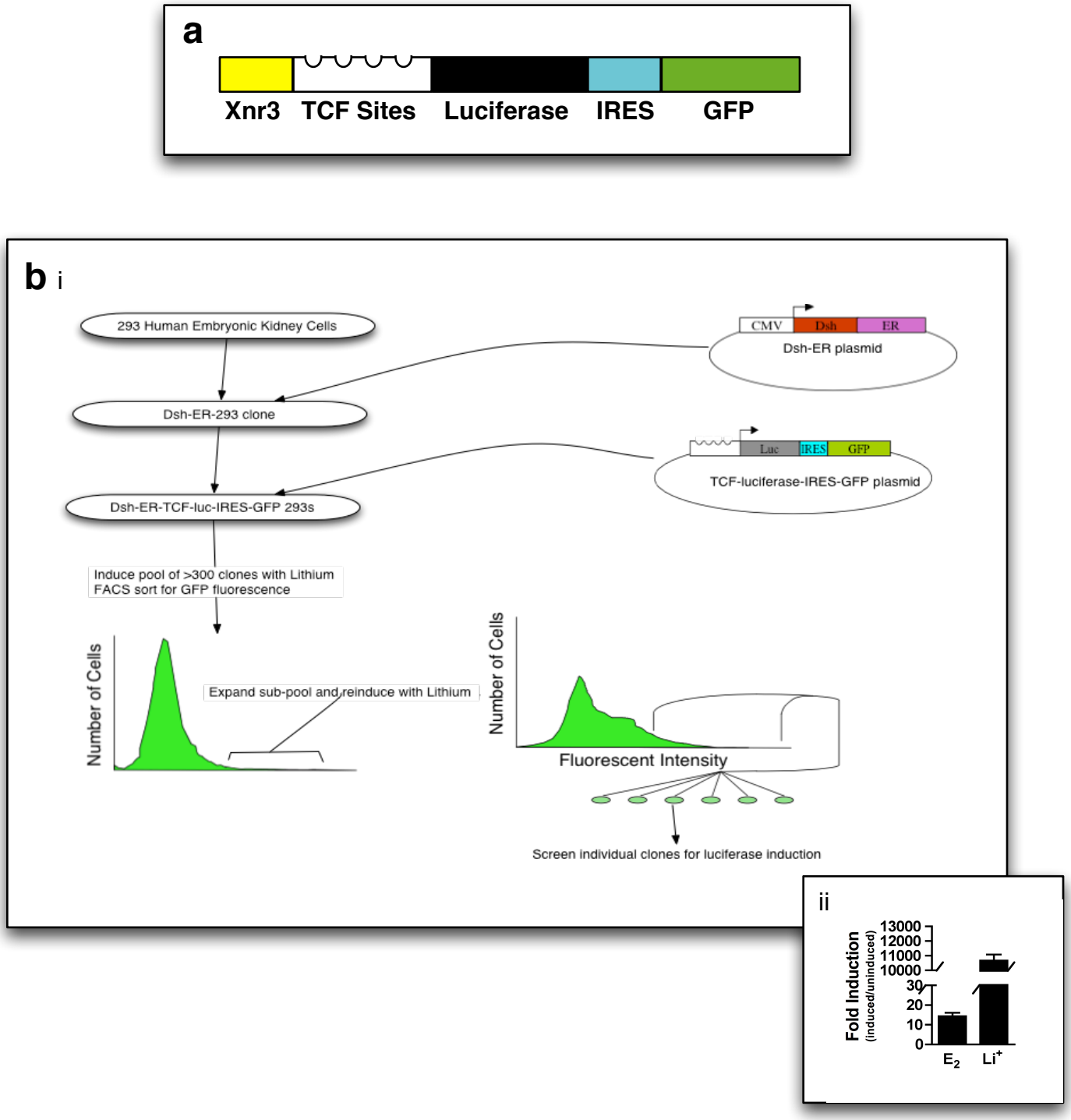

Figure 7. Schematic representation of the TCF-luciferase reporter cell line

a. The TLIG reporter construct was generated to contain four multimerised TCF binding sites downstream from the Xnr3 promoter, driving the transcription of luciferase and GFP reporter genes in the presence of Wnt pathway stimulation (taken from (Ewan et al., 2010)).

bi and ii. HEK293 cells were stably transfected with a Dvl (labelled Dsh here) and the TLIG reporter construct. The clones were induced with lithium and the most responsive clone (with highest induction:lowest background ratio) was selected (figure reproduced with the kind permission of Dr. Jamie Freeman (Freeman)).

2.1.2 Wild type and AT506.C2 reporter HCT116 colorectal cancer cells

AT506.C2 is a HCT116 cell line stably transfected (using GeneJuice) with the super8-TOPflash luciferase TCF-reporter ((Veeman et al., 2003). Cell line created by Dr. Christa Burger, Merck Serono). AT506.C2 and HCT116 wild type cells were cultured in Minimal Essential Medium (MEM) Eagle (Sigma) supplemented with 10% FBS (PAA) and 2mM L-glutamine at 37°C and 5% CO_2.

2.1.3 SW480 colorectal cancer cells

The cells were cultured in Lebovitz's L-15 Medium (Life Technologies) supplemented with 10% FBS (Life Technologies) at 37°C and 5% CO_2.

2.1.4 SW620 colorectal cancer cells

The cells were cultured in DMEM/F-12 (Life Technologies) supplemented with 10% FBS (Life Technologies) and 2mM L-glutamine at 37°C and 5% CO_2.

2.1.5 Colo205 colorectal cancer cells

The cells were cultured in DMEM supplemented with 10% FBS (Life Technologies) at 37°C and 5% CO_2.

2.1.6 Colo320 and DLD-1 colorectal cancer cells

The cells were cultured in RPMI 1640 (Life Technologies) supplemented with 10% FBS (Life Technologies), 2mM L-glutamine and 1mM sodium pyruvate at 37°C and 5% CO_2.

2.1.7 Ls174T colorectal cancer cells

The cells were cultured in Minimal Essential Medium (MEM) Eagle (Sigma) supplemented with 10% FBS (Life Technologies) at 37°C and 5% CO_2.

2.1.8 Cell banking

A critical requirement for the high-throughput assays was the availability of large batches of identical cells. These were prepared and frozen prior to use. To ensure that assays were carried out using cells from the same passage, cells

were bulked up under normal culture conditions, trypsinised, counted and frozen in 70% appropriate antibiotic free culture media, 20% FBS and 10% DMSO.

2.2 cDNA expression

2.2.1 The cDNA library

The Medaka (*Oryzias latipes*) cDNA library was kindly provided by Dr. Gary Davidson (Karlsruhe Institute of Technology, Karlsruhe; see Appendix 3 for Ensembl IDs). In brief, the master library was prepared from full-length enriched and subtracted cDNA taken from 3 different developmental stages, including unfertilized eggs (each driven by a CMV promoter of their pCMV-Sport6 vector (Lickert et al., 2004)). Sequencing was then performed and full-length, unique clones selected (18,000; originally from Jochen Wittbrodt, EMBL, Heidelberg). The library contained 18,000 individual genes, but was provided as multiple pools of 24 cDNAs. Each pool was supplied as 1μg plasmid DNA in a 50μl volume (20μg/ml) in 8 x 96 well plates. Representative pools from the library were quantified by absorbance to ensure that DNA was present prior to analysis.

2.2.2 ΔNLRP, CMV-LacZ, pcDNA.

ΔNLRP is a constitutively active form of the Wnt co-receptor LRP6 lacking the N-terminal extracellular domain ((Brennan et al., 2004)). A plasmid expressing a CMV-driven myc-tagged ΔNLRP6 was used to activate TCF-dependent transcription to a 'mid' level. CMV-LacZ (cytomegalovirus-driven constitutively active LacZ expression plasmid; Life Technologies) was used as a transfection control. pcDNA3.1 (Life Technologies), a plasmid with a CMV-promoter, but no insert, was frequently used as a control or as 'filler' DNA to equalise levels of CMV-promoter-containing plasmid DNA in transfections.

2.2.3 Constitutive activator/control stock plasmid replenishment

XL-1 Blue subcloning-grade competent cells (Stratagene) were transformed with desired plasmid according to the manufacturer's manual, plated onto selective lysogeny broth (LB) agar plates (plasmid antibiotic selection marker dependent) and incubated overnight at 37°C. Individual colonies were picked and grown in 250ml LB broth (containing appropriate antibiotic) at 37°C overnight (with shaking). Plasmids were purified using the QIAfilter Plasmid Maxi Kit (Qiagen) according to manufacturer's protocol and DNA concentrations measured using the ND-1000 Spectrophotometer (NanoDrop Technologies).

2.3 cDNA library screening

2.3.1 The primary screen

7df3 cells were transfected with a combination of 100ng of DNA comprising 70ng of each pooled cDNA (24 clones/pool) in a 96 well format together with 20ng constitutively active ΔNLRP6 plasmid to induce a mid-level of TCF-reporter activity, and 10ng/well CMV-LacZ transfection control plasmid as an internal control to allow results to be normalised to β-galactosidase expression as a marker of transfection efficacy. Twenty-four hours prior to transfection, 7df3 cells were cultured to ~80% confluency and seeded into 96-well, black walled, clear bottom plates (Nunc) at a density of $3X10^5$ cells/ml in 100μl antibiotic free DMEM. A total of 100ng DNA/well was prepared in Optimem (serum free media; Life Technologies) in a final volume of 25μl, followed by the addition of 0.3 μl/well of Transfectin (BioRad) diluted in 25μl Optimem. Subsequent medium changes were completed according to the manufacturer's guidelines. Luciferase and β-galactosidase reporter assays were carried out 48 hours after transfection (see 2.4.1). The screen was performed twice (with two repeats on each occasion) before selecting wells for deconvolution. See 'Results' for details on hit selection.

To control for the 'inducibility' of the 7df3 cells (as compared to their 'transfectability'), a subset of wells in each experiment was treated with β-estradiol to determine whether the TCF-luciferase reporter could be activated. For this, a final concentration of 4μM β-estradiol was added to untransfected cells for 24 hours prior to assay. This approach helped to monitor cell responsiveness from passage to passage.

2.3.2 Deconvolution of cDNA 'hit' pools

Hits identified in the primary screen as either activating or inhibiting the Wnt reporter were pools of multiple cDNAs containing 24 plasmids. To identify the activating/inhibiting cDNA(s) within each pool, each plasmid present within the pools that were identified as 'hits' were individually prepared. Briefly, plasmids were grown from glycerol stock in 5ml of LB broth with 100μg/ml carbenicillin (37°C, overnight incubation). Plasmids were then purified using the SV Wizard Plus Miniprep DNA Purification System (Promega). DNA concentration was measured as detailed in 2.2.3. To assess the function of each member of each pool, cells prepared as with the primary screen were co-transfected with 70ng of each plasmid, 30ng ΔNLRP6 and 10ng LacZ, in individual wells on three replicate plates. Three independent repeats were conducted. Activation relative to 36 ΔNLRP controls was determined. Putative hits were then reconfirmed both in the presence and absence of ΔNLRP6 co-activation and hit samples sequenced by Dundee Sequencing Service (using the SP6 and T7 primers provided). Sequences were analysed using BLAST analysis to determine hit identity.

2.3.3 cDNA MSC interference studies

Cells transfected as described in the previous section (both in presence and absence of ΔNLRP6 co-activation) were treated with 125nM MSC (10 x 7df3 IC_{50}) in antibiotic and serum free media (or 0.1% DMSO for untreated controls) 24 hours post-transfection. TCF-luciferase reporter activity was measured (see

2.5.1) 72 hours post-MSC treatment. Three independent repeats were conducted.

2.4 esiRNA screening

2.4.1 esiRNA production and sequences

A genome-wide enzymatically-synthesized small interfering RNA library (esiRNA) representing 17,188 human genes was kindly donated by Professor Frank Buchholz (Max Planck Institute of Molecular Cell Biology and Genetics, Dresden (Buchholz et al., 2006; Kittler et al., 2004; Theis and Buchholz, 2011). The library was supplied as 47 x 384-well plates containing individual esiRNAs. The library was used at a final concentration of 20ng per well in the primary and secondary screening experiments. The library was sequentially diluted in TE buffer (Promega) and dispensed in to 384 well white test plates (Greiner Bio-One) using the Biomek FX (Beckman Coulter) from a stock concentration of 200ng/μl to a final concentration of 4ng/μl esiRNA/well aliquotted at 5μl/well (thus 20ng esiRNA/well). Appendix 4 and 5 provides information regarding well IDs and sequences of the primary library.

A secondary, non-overlapping sub-library of 57 esiRNAs was selected from the primary screen for hit reconfirmation. These non-overlapping esiRNAs were designed and synthesised by Eupheria Biotech (Sigma). Sequences for these non-overlapping esiRNAs can also be found in Appendix 6.

Non-targetting siRNA negative controls; enhanced green fluorescent protein (eGFP) and renilla luciferase (R-Luc), and gene targetting positive controls; polo-like kinase 1 (PLK1) and kinesin family member 11 (EG5) were purchased from Eupheria Biotech (Sigma) and plated into the 12 empty wells of each 'master dilution' plate at 20ng/well (4 repeats of each control/plate).

2.4.2 Assay optimisation

Multiple different parameters were extensively assessed in order to establish the optimal final screening conditions. These included determination of appropriate cell seeding density and frozen batch testing, HiPerFect transfection concentration, test compound concentration, assay time course, and assay miniaturisation. Of the conditions that were systematically varied in the assay optimisation studies, the final conditions that were determined to be optimal were as follows: plating of 2000 cells/well ($1.3x10^5$ cells/ml, 15μl/well), 5μl/ml HiPerFect (in final assay volume containing cells), with 10μM test compound (in final assay volume) or DMSO control, and assay read points at 72 hours and 120 hours post-transfection.

2.4.3 The primary screen protocol

esiRNA and siRNA transfections were carried out in 'reverse format'. For this, cells were plated onto esiRNA:HiPerFect complexes since this was found to reduce assay variability. The esiRNA library and siRNA controls were pre-dispensed at 20ng/well (5ul/well) in white 384 well assay plates and stored at -80˚C. Assay plates were defrosted overnight at 4˚C and centrifuged for 1 minute pre-assay. The HiPerFect transfection mix was freshly prepared to give a final 'concentration' of 5ul/ml in the presence of the cells. Prior to cell addition, this equated to 7ul/well containing 0.14μl HiPerFect and 6.86μl of serum-free medium Thus the total volume prior to transfection, 15 minutes prior to use was 12μl. Fresh HCT116 cells (from the same batch on every occasion) were thawed and seeded 72 hours prior to use. On the day of transfection, they were trypsinised and seeded at 2000 cells/well in 384 well format plates in serum-containing MEM Eagle.

48 hours post-transfection, compound was added to achieve a final concentration of 10μM, with the equivalent percentage of DMSO vehicle (0.1%) added where compound treatment was not required. At either 72 hours or 120 hours post-transfection cells were lysed (see 2.5.2) and frozen at -80˚C until all screening

had been completed. Lysates were then defrosted at 4˚C overnight and equilibrated room temperature on the day of reading, and cell numbers (i.e. cellular viability) measured according to subsection 2.5.2. Screening was performed in batches of 47 test plates, with 3 repeats of each condition conducted on different days.

All liquid handling steps throughout the course of optimisation were performed manually, however these processes were semi-automated during the final screen using the Multidrop Combi (Thermo Scientific). Furthermore, cells were manually counted using a haemocytometer during small-scale assays, whilst during screen bulk-cell preparation the Vi-CELL® (Beckman Coulter) was used to determine cell counts and viability. A final measure to increase through-put was the switch from the Varioskan Flash Multimode Reader (Thermo Scientific) used during optimisation, to the LEADseeker Multimodality Imaging System (GE Healthcare). All parameters (including final reagent batches) were tested under screen assay conditions in a pilot experiment.

Reverse transfection is a method of transfecting cells in suspension commonly used for high-throughput screens involving multiple multi-well plates (e.g. 384 well plates in this instance). Cells were cultured to ~80% confluency in preparation for transfection and diluted to the required cell number. HiPerFect (Qiagen) diluted to the desired concentration in serum-free MEM Eagle was dispensed into pre-prepared 384well white assay plates containing test esiRNA (as described in 2.4.1). After 20mins incubation cells were seeded on to the esiRNA:lipid complexes at the required density.

Several different conditions were tested during optimisation assays, which are detailed in the figure legends of the corresponding data. Final screening conditions are described in Results 3.2.1.

2.4.4 'Hit' esiRNA reconfirmation in HCT116 cells

93 selected hit esiRNAs (as identified using data analysis methods detailed in 2.6.2.1) were narrowed to 45 hits were selected for bespoke generation of non-overlapping esiRNAs; see Appendix 6 for sequences.

2.4.5 'Hit' Western blot assays

'Hit targets' were assayed for the effects of esiRNA depletion of the expression of their cognate protein. This assay had a different transfection format because of the scale of the assay required to prepare sufficient cell extract for analysis. Where possible, transfection conditions were matched as closely as possible to those determined in the primary and secondary hit identification studies described above (using 24 well plate set-up to obtain enough protein; 19 times greater surface area than 384 well). Briefly, HCT116 cells were reverse transfected (26,700 cells/well) with 380ng esiRNA in complex with HiPerFect transfection reagent (both original and non-overlapping samples were assessed). 48, 72 and 120 hours post transfection, cells were harvested in RIPA buffer with a Complete Protease inhibitor (Roche), and proteins denatured at 95°C for 5 minutes in Laemmli loading buffer (Life Technologies). Following protein concentration determination using the Bradford assay, 3μg of each sample was run on 4% - 12% polyacrylamide and run at 100V. Protein was then transferred to a nitrocellulose membrane using the Life Technologies iBlot system according to manufacturer's protocol. Membranes were washed in TBST before being blocked using 10% milk powder in TBST at room temperature for 1 hour. The blot was simultaneously probed with the HARS (AbCam) and GAPDH (Merck Millipore) primary antibodies (in 5% milk-TBST) overnight at 4°C, and protein detected using the secondary horseradish peroxidase (HRP)-conjugated α-mouse antibody (Sigma) for 1 hour at room temperature. Pierce SuperSignal chemiluminscent substrate was used to determine HARS (and GAPDH) protein levels.

2.4.6 Compound combination assays

HCT116 cells were seeded at 4500 cells/well in 96 well plates (using previously described culture conditions). In the primary assay, cells were treated 24 hours post-seeding (with 10μM MSC + 1μM, 5μM or 25μM test compound, both individually and in combination, along side untreated DMSO controls), and viability measured using the ATPlite assay 24, 48 and 72 hours post-treatment (n=5). Compounds deemed to be effective in a combination-dependent manner (determined by one-way ANOVA and Tukey test) were selected and further assessment by 'chequerboard' titration analysis. HCT116 cells (seeded as previously described) were treated with a 'chequerboard' titration of 'hit' inhibitor concentrations (20nM – 25μM) in the presence and absence of MSC titration (40nM - 25μM; both individually and in combination, along side untreated DMSO controls). Cell viability was measured as previously at 24, 48 and 72 hours (n = 3).

'Hit' combinations were tested in multiple cell lines according to the established HCT116 assay set-up. Test compound was titrated (at a narrower range of 200nM, 1μM and 5μM) was tested against 10μM MSC (both individually and in combination, along side untreated DMSO controls). Cell viability was measured as previously at 24, 48 and 72 hours (n = 3).

2.5 Luminescence assays

2.5.1 Wnt reporter assay

Luciferase reporter activity assays were performed using the Bright-Glo and Beta Glo assay systems (Promega). 48 hours post-transfection cells were lysed by the addition of Glo-lysis buffer (Promega) and shaken at room temperature for 20mins. Lysate was split for two assays: 30μl for firefly luciferase assay, and 25μl for analysing β-galactosidase activity. To assay luciferase activity, 30μl

Bright-Glo reagent was added to the cell lysate, and assayed immediately for luminescence using the FLUOstar Optima plate reader (BMG Labtech). To assess β-galactosidase control activity, 20μl Beta-Glo reagent was added to the cell lysate and shaken for a further 20mins at room temperature before the luminescence read-out was measured using the FLUOstar Optima.

TCF-luciferase counts were normalised to β-galactosidase reporter activity to control for variations in transfection efficiency. To allow for direct comparisons to be made between experiments, β-galactosidase-normalised luciferase values were subsequently normalised to the entire plate mean activity of ΔNLRP6.

2.5.2 Viability assay

Viability assays were performed using the ATPlite Luminescence Assay System (Perkin Elmer). As ATP is present in all metabolically active cells it can be used as a marker of cell viability. ATP levels cells rapidly decline under conditions that induce necrosis or apoptosis, hence the luminescence read-out is reduced. This reduced signal (relative to untreated controls) is henceforth reported as a reduction in cellular viability.

Cells were lysed at the required time-point by the addition of ATPlite lysis buffer and shaken at room temperature for 5 minutes. Lysate was frozen at -80˚C until the completion of all time-points. ATPlite substrate was added to all wells and shaken for 5 minutes according to the manufacturer's protocol. The luminometer used to measure cell viability in each case is detailed in 2.4.3.

2.6 Data analysis and statistical methods

2.6.1 cDNA screen data analysis

Each of the wells were normalised to their corresponding β-galactosidase control activity to account for variations in transfection efficiency. The normalised values

were then expressed as a fold of whole plate ΔNLRP induction (without controls). This 'non-controls-based normalisation', allowed for data to be normalised relative to the over-all distribution of values as opposed to being exclusively reliant on the performance of the controls. Fold data from 4 independent repeats was combined into a single mean value and ranked in order of affect on ΔNLRP induction. Each well was expressed as both a fold of the plate mean, and as the number of standard deviations away from the plate mean. Results were cross-checked against their raw data to eliminate false positive hit selection.

Due to capacity of the deconvolution process (as each well contained 24 individual cDNAs), only 20 of the top activating pools (and 16 of the most inhibitory pools – not deconvolved at this time) were selected for subsequent deconvolution. Activating cDNAs were deconvolved (see 2.3.2) based on their ability to activate TCF-dependent transcription in the presence and absence of ΔNLRP co-activation. Initial deconvolution of the putative activator from the pool of 24 cDNAs was conducted by expressing the mean luciferase value of the samples (n=3) relative to 36 ΔNLRP control wells. A student's two-tailed t-test was used to determine significance of activation. The tentatively deconvolved activator from each pool was isolated and its activating ability reconfirmed, both in the presence and absence of ΔNLRP. Where ΔNLRP stimulation was absent, cDNA activation was measured relative to the pcDNA3.1 control wells (n=6).

2.6.2 esiRNA screen data analysis

2.6.2.1 Screen optimisation

Statistical analyses were conducted using Prism5 (GraphPad Software, Inc.). Targetting and non-targetting esiRNA controls were expressed as a percentage of untreated cell data.

2.6.2.2 Primary screen quality control

To determine whether a plate had passed or failed during screening, internal controls that had been placed on each plate (eGFP, R-Luc, PLK1 and EG5

esiRNAs) were assessed on a per-plate basis to determine whether any plates had failed based on the dynamic range of the controls. The following selection criteria were employed:

72 hours: eGFP + R-Luc ('non-targetting') > 30,000 counts

PLK1 + EG5 ('targetting') < 15,000 counts

120 hours: eGFP + R-Luc ('non-targetting') > 50,000 counts

PLK1 + EG5 ('targetting') < 25,000 counts

Plates whose controls did not reach the cut-offs were flagged for further manual scrutiny, following which a subset of plates was selected for repetition.

2.6.2.3 Global data analysis using cellHTS2

All screen data sets were normalised using the cellHTS2 software package implemented in R (Boutros et al., 2006). This publicly available software has been specifically developed by the Boutros Laboratory for the analysis of high-throughput (384 well microtitre plate), cell-based RNAi screens.

The data was normalised using a two-step procedure. The assumption was made that the majority of samples would have no effect on viability and hence can act as their own controls (whether in combination with compound or not). This first step, termed 'non-controls-based normalisation', allowed for data to be normalised relative to the over-all distribution of values as opposed to being exclusively reliant on the performance of the controls (Birmingham et al., 2009). In this sense, the data sets were first normalised to the median value of each corresponding plate. This often provides a more accurate representation of the true value of 'inactive' genes that define the measure of central tendency (especially due to the high number of values per plate in this instance), as opposed to the arithmetic mean which can be affected by outliers (Brideau et al., 2003). These median-normalised values were then further normalised using the B-score method (Brideau et al., 2003), which was used to explicitly correct for

spatial effects caused by temperature and CO_2 differences, for example (a well-documented phenomenon known as plate edge effect; (Lundholt et al., 2003)). Although this analysis is similar to that achieved by Z scoring in that it is a "ratio of an adjusted raw value in the numerator to a measure of variability in the denominator" (Brideau et al., 2003), the complex algorithm used in this instance more extensively adjusts for variability in the numerator and allows for a greater measure of variability in the denominator. Each individual replicate was assigned a B-score (a 'variance' score of each point in relation to its corresponding plate), which allowed for direct comparison of the strength of effect of all esiRNAs within a defined condition through rank ordering of these B-scores.

2.6.2.4 Linear modelling

As would be expected from a large-scale whole genome screen, many synthetic interactions were uncovered between individual esiRNAs and MSC treatment. In order to robustly identify samples whose inhibition resulted in lethality only in the presence of MSC, a statistical model was used that could account for distinct classes of interaction. A 'Linear Model Interaction Test' was developed by Dr. Eike Staub at Merck Serono for this purpose.

In brief, with the linear model, the dependence of viability on presence of drug, esiRNA, or especially the combination of both, can be assessed by model coefficients and significance calls (p values for which the null hypothesis is that the coefficients are zero, i.e. there would be no effect). Based on these parameters, a selection strategy was developed to filter out the hits using the screening approach. Finally, the siRNA hits were assessed for their absolute ability to reduce viability, i.e. how strongly they can reduce viability compared to the positive controls (e.g. PLK).

The relationship of the dependent variable; synthetic lethality ('y'), and the two independent variables; esiRNA knockdown – yes/no (a), and compound treatment – yes/no (b) were modeled as described below; firstly in a simplified

example to illustrate the principle and then using values that include scaling parameters that were used to process real data.

- Example:

  y = 20*a + 40*b - 1000*(a:b)

  - **y**(**a**=0;**b**=0) = 0
  - **y**(**a**=1;**b**=0) = 20
  - **y**(**a**=0;**b**=1) = 40
  - **y**(**a**=1;**b**=1) = -940

In this scenario, 20, 40 and -1000 are hypothetical examples of model coefficients that would be derived from the B-scores resulting from the three 'treatment conditions'. The model functions as follows: in the absence of both esiRNA (**a** = 0) and compound (**b** = 0) treatment there is no effect on cell viability, thus the synthetic lethality score (**y**), or 'interaction score' (as subsequently described), is 0. When cells are subject to RNAi (**a** = 1) in the absence of compound (**b** = 0), the interaction score **y** = 20. When the cells are treated with compound (**b** = 1) in the absence of RNAi (**a** = 0), the interaction score **y** = 40. However, when cells are subjected to both RNAi (**a** = 1) and compound treatment (**b**=1), interaction score **y** = -940, thus *only* when **a** and **b** are 1 is the synthetic lethality interaction effect evident. The 'Linear Model Interaction Test' is an extension of this example model and is able to scale for the real world values observed in this screen (coefficients in this instance represent B-score values more likely to be seen), whereby:

  - **y**(**a**=0;**b**=0) = 30000
  - **y**(**a**=1;**b**=0) = 30000
  - **y**(**a**=0;**b**=1) = 30000

- **y**(**a**=1;**b**=1) = 5000

Again, an interaction effect is only seen in the presence of both RNAi and compound treatment, however in this instance the advanced model has to account for the fact that 30,000 represents a zero value in actual terms, thus in the above example y = 5000 describes the literal value, rather than the true interaction value of -25,000.

An 'interaction value' was determined for each sample that statistically summarised synergy (including the interaction significance) between compound and RNAi, whilst taking the effect of esiRNA knockdown alone on cellular viability into consideration.

Different thresholds were set for prioritising and defining primary hits, which are described in the Results section. These included:

- Interaction value < -1000
- esiRNA p value > 0.1
- Ratio (interaction p value / esiRNA p value) < $1x10^{-2}$

2.6.2.4 esiRNA non-overlapping reconfirmation analysis

This non-overlapping esiRNA assay was performed as with the primary screen. These hits were analysed 'manually' (as Dr. Staub was engaged with high-priority analyses), with reduction in viability (the 'equivalent' in this instance of the 'interaction' value previously described) calculated using the raw data (as whole-plate normalisation was not appropriate since the hits had been specifically selected based on their ability to reduce viability) by determining the interaction based on the percentage reduction in viability compared to the 'high' control (R-Luc; with EG5 used as the baseline) and significance of interaction determined using a two-way ANOVA, and a subset of genes reconfirmed that were deemed to have 'synthetic lethal' activity.

Chapter 3. Results

3.1 cDNA screen

Previous studies in the laboratory identified that overexpression of cDNAs (or cDNA pairs) that regulated Wnt pathway activity could be used to characterise the mechanism of action of novel small molecule pathway inhibitors whose targets were unknown (Ewan et al., 2010; Freeman, 2008). However, these studies used a library of 9000 cDNAs, raising the possibility that additional regulators, and hence additional interactions that could facilitate the analysis of drug action, could be identified from a whole-genome scale screen.

In order identify further cDNA regulators of TCF-dependent transcription, a whole genome Medaka cDNA library was screened in the 7df3 cell line according to the cascade shown in Figure 8. The aim of the screen was to identify genes whose overexpression in the presence of ΔNLRP6 (a constitutively active form of LRP6; stimulating Wnt signalling at the top of the pathway) stimulation resulted in 'super-activation' or inhibition of TCF-dependent transcription. Following the identification of novel signalling activators and the elucidation of the activator's dependence on pathway co-stimulation by ΔNLRP, MSC-interference assays were conducted to determine the ability of the compound to disrupt this Wnt signalling (super-)activation. In parallel with 'conventional' deconvolution assays being conducted in the laboratory, it was postulated that this would help to narrow the mechanism of action of the compound by mapping its activity onto a 'network' of Wnt activator interactions.

An overview of the assay cascade is illustrated in Figure 8. A Medaka library of 17,526 genes in pools of 24 cDNAs/well (in 96 well plate format) was kindly provided by Gary Davidson (KIT). In brief, 7df3 reporter cells were co-transfected with the 70ng of each cDNA pool and 20ng of constitutively active ΔNLRP using forward transfection techniques previously established in-house. Cells were also transfected with 10ng of LacZ as a control for transfection

efficiency. Luciferase and β-galactosidase reporter activities were measured 48 hours after transfection. Following normalisation, pools were ranked according to their ability to activate or inhibit TCF-dependent transcription relative to ΔNLRP activation alone, and the top 20 activating and 16 inhibiting pools were selected for deconvolution.

Figure 8 placement

Figure 8. cDNA screening cascade

Flow diagram indicating the overall approach taken to characterise Wnt-regulatory genes within the Medaka cDNA library using the 7df3 reporter cell line. The screen was designed to identify super-activators and inhibitors of TCF-dependent transcription that was driven by the activated Wnt co-receptor ΔNLRP, an activator that functions near the 'top' of the linear representation of the Wnt pathway. Due to assay prioritisation, the individual inhibitory cDNAs that had been prepared from the inhibitory pools were not further characterised.

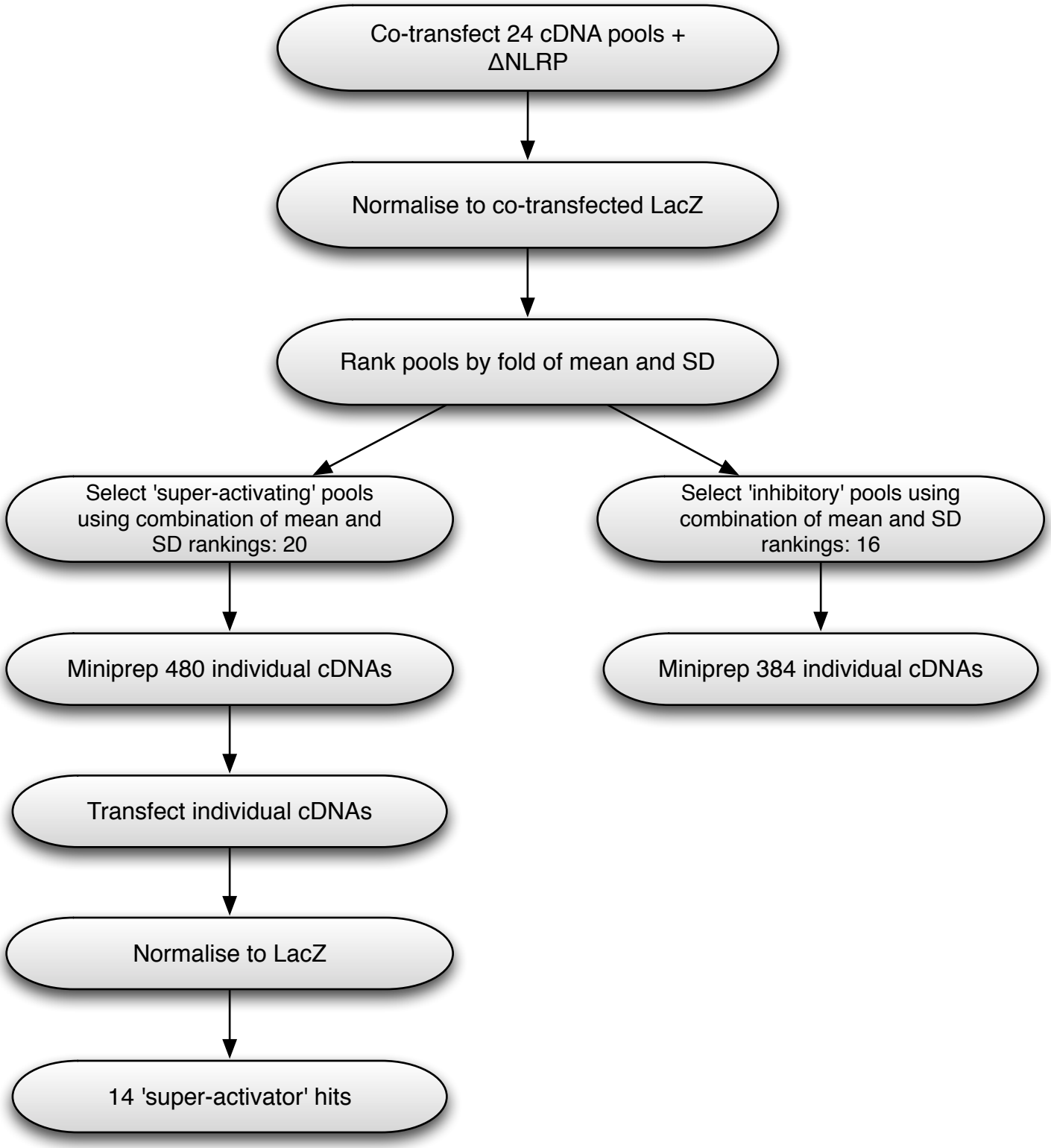

Figure 8. cDNA screening cascade

Flow diagram indicating the overall approach taken to characterise Wnt-regulatory genes within the Medaka cDNA library using the 7df3 reporter cell line. The screen was designed to identify super-activators and inhibitors of TCF-dependent transcription that was driven by the activated Wnt co-receptor ΔNLRP, an activator that functions near the 'top' of the linear representation of the Wnt pathway. Due to assay prioritisation, the individual inhibitory cDNAs that had been prepared from the inhibitory pools were not further characterised.

An overview of the primary screen data analysis can be seen in Figure 9. Each of the 786 wells (8 plates x 96 well plate format) were normalised to their corresponding β-galactosidase control activity to account for variations in transfection efficiency. The normalised values were then expressed as a fold of whole plate ΔNLRP induction (without controls), based on the assumption that the majority of pools would have no effect on basal ΔNLRP activity. This normalisation allowed for cross-plate comparisons of the whole screen to be made, as it had previously been observed that plate to plate variation could lead to an inappropriate focus on hits from one plate if absolute luciferase expression values were used to select hit pools for further analyses. Fold data from 4 independent repeats (conducted on different days) was combined into a single mean value and ranked in order of affect on ΔNLRP induction. Each well was expressed as both a fold of the plate mean, and as the number of standard deviations away from the plate mean. To ensure that false positive hits were not selected as a consequence of the normalisation process, β-galactosidase control data was cross-checked (for each individual selected pool). Final hit pools showed normal levels of β-galactosidase expression suggesting that the 'effects' of cDNA expression on TCF-luciferase expression were not due to effects on the expression of CMV-driven β-galactosidase. Due to capacity of the deconvolution process, only 20 of the top activating pools and 16 of the most inhibitory pools were selected. More hits were selected for the activating pools as these were thought to offer the greater opportunity in the analysis of MSC compound action. The selection scores were arbitrary as they were based on a maximum number of hits that could be processed, but equated to selection cut-offs of 2.52 and 0.315 for reporter activity fold of plate mean, and 1.03 and -0.635 for reporter activity standard deviations away from plate mean (see Figures 10a&b). The primary data from the selected pools was also manually checked to ensure that the 'Fold of ΔNLRP' values were not inappropriately skewed by outlier values.

Figure 9 placement

Figure 9. Data analysis protocol for cDNA pool selection

Flow diagram indicating the overall approach taken to select cDNA pools with Wnt-regulatory activity within the Medaka cDNA library using the 7df3 reporter cell line. Luciferase reporter activity was first normalised (on a well-by well basis) to β-galactosidase expression from the co-transfected control plasmid. Each of the 4 repeat cDNA pool values were expressed as fold of corresponding plate ΔNLRP mean and the number of standard deviations from dataset mean, and the highest ranking (and most overlapping) hit pools selected. Following the cross-check of β-galactosidase activity to minimise false hit selection, 20 'super-activating' and 16 'inhibitory' pools were selected and their individual cDNA components prepared by DNA miniprep. 864 individual cDNAs were prepared in total.

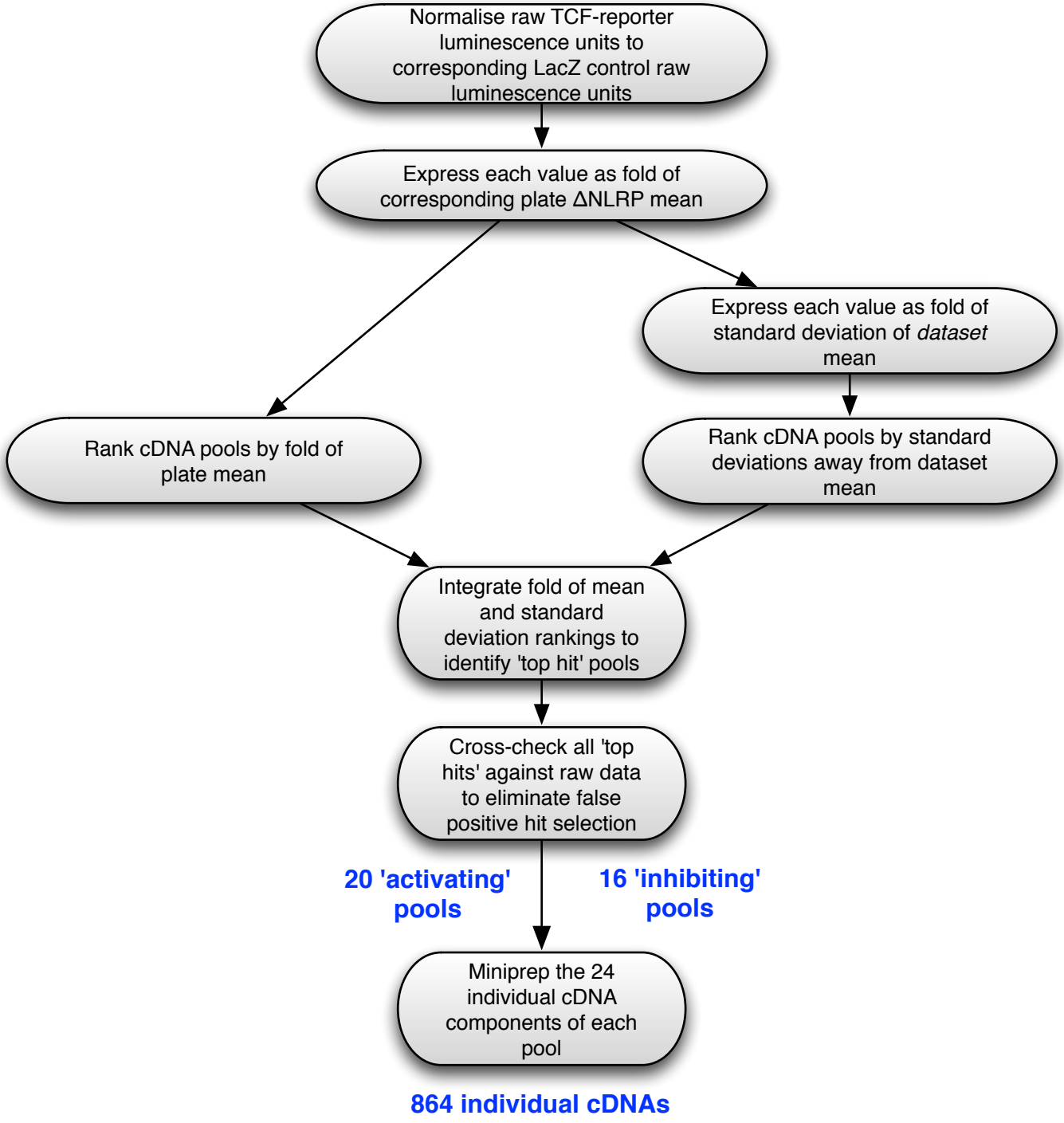

Figure 9. Data analysis protocol for cDNA pool selection

Flow diagram indicating the overall approach taken to select cDNA pools with Wnt-regulatory activity within the Medaka cDNA library using the 7df3 reporter cell line. Luciferase reporter activity was first normalised (on a well-by well basis) to β-galactosidase expression from the co-transfected control plasmid. Each of the 4 repeat cDNA pool values were expressed as fold of corresponding plate ΔNLRP mean and the number of standard deviations from dataset mean, and the highest ranking (and most overlapping) hit pools selected. Following the cross-check of β-galactosidase activity to minimise false hit selection, 20 ‘super-activating’ and 16 ‘inhibitory’ pools were selected and their individual cDNA components prepared by DNA miniprep. 864 individual cDNAs were prepared in total.

Figure 10a&b. Primary cDNA screen hit distribution

Luciferase reporter activity was first normalised (on a well-by well basis) to β-galactosidase expression from the co-transfected control plasmid. Each cDNA pool was assayed 4 times. Each of the 96-well plates are individually coloured above. Any point greater than 5 fold of plate mean or 5 standard deviations above the mean was represented as 5 to allow the spread of the majority of the data to be visualised.

a. Normalised luciferase reporter activity was expressed as a fold of the plate mean for each of the 8 x 96 well plates (as coloured; each point = 1 well) that were assayed. Lines indicating cut-offs of 2.52 and 0.315 the plate mean are illustrated as used for hit selection.

b. Normalised luciferase reporter activity for wells in each plate (as coloured; each point = 1 well) were expressed as the number of standard deviations away from the dataset mean. Selection cut-offs indicate 1.03 and -0.635 standard deviations from plate mean.

Figure 10a

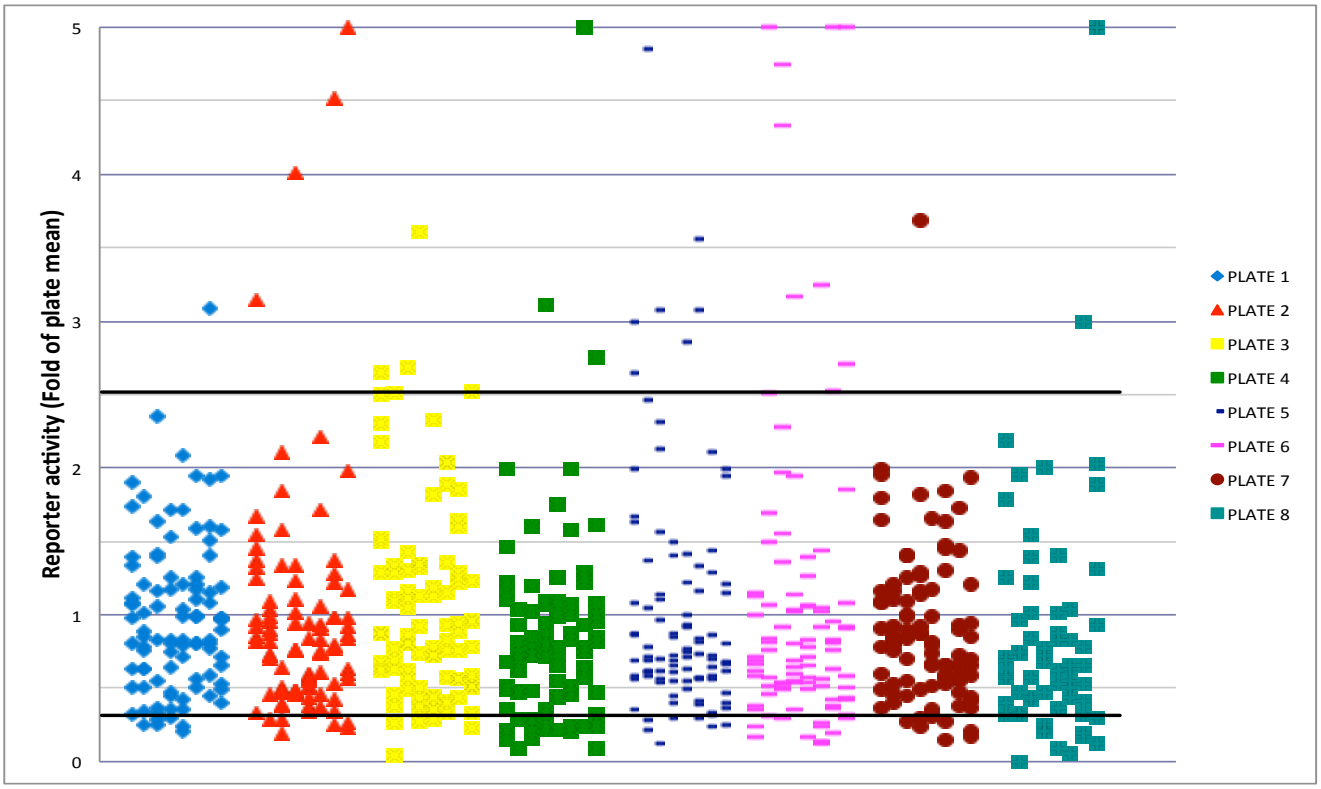

Figure 10b

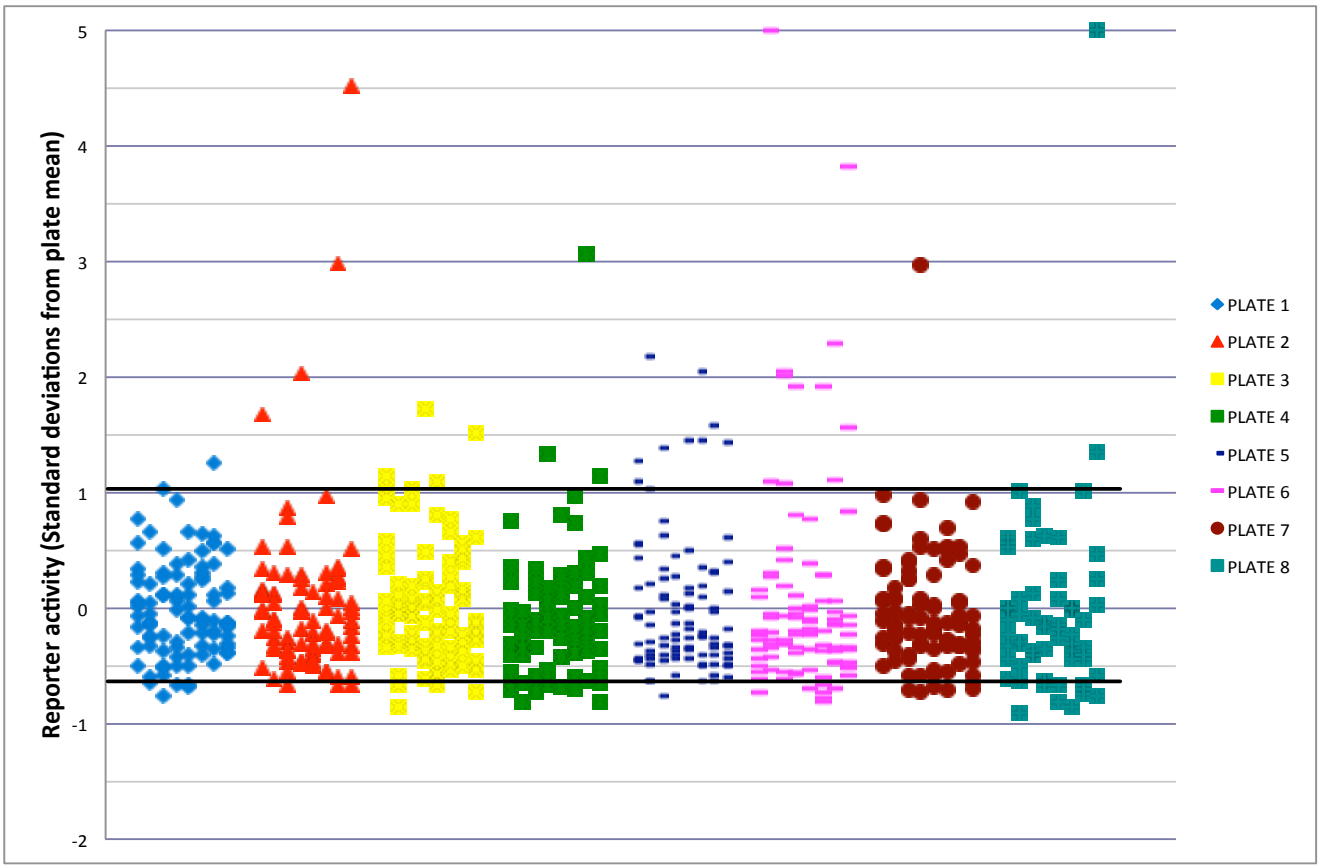

As the principal aim of the study was to identify genes whose overexpression resulted in upregulation of TCF-dependent transcription and to subsequently 'map' the ability of MSC to disrupt this interaction, the activator pools were prioritised for deconvolution. Each of the 24 cDNAs comprising the pool was prepared individually and co-transfected into 7df3 cells in accordance with the primary screen format (see Figure 11 for a hit pool deconvolution flowchart). Following three independent repeats the activating cDNA from each pool was determined. As previously, TCF-dependent luciferase units were normalised to their corresponding β-galactosidase transfection control. Because the cDNAs had been specifically selected based on their ability to induce TCF-dependent transcription, each of the three repeats was expressed as a fold of ΔNLRP control wells (n=12; on the same plate) and the mean activity of the three repeats tested for significance against the ΔNLRP controls (n=36; from all three repeats) using a student's two-tailed t-test.

Figure 11 placement

Figure 11. Activator cDNA pool deconvolution approach

Flow diagram demonstrating the approach taken to deconvolve Wnt-regulatory genes from the 20 most activating cDNA pools selected from the primary screen of the Medaka cDNA library using the 7df3 reporter cell line. Following co-expression of the activators with the activated Wnt co-receptor ΔNLRP, data was normalised to the β-galactosidase control to account for variations in transfection efficiency. The mean of three repeats was calculated and the significance of any activation (relative to 36 ΔNLRP control wells) was determined, with 17 activators putatively determined. Following further reconfirmation 14 activating cDNAs were fully validated and taken forward for further investigation.

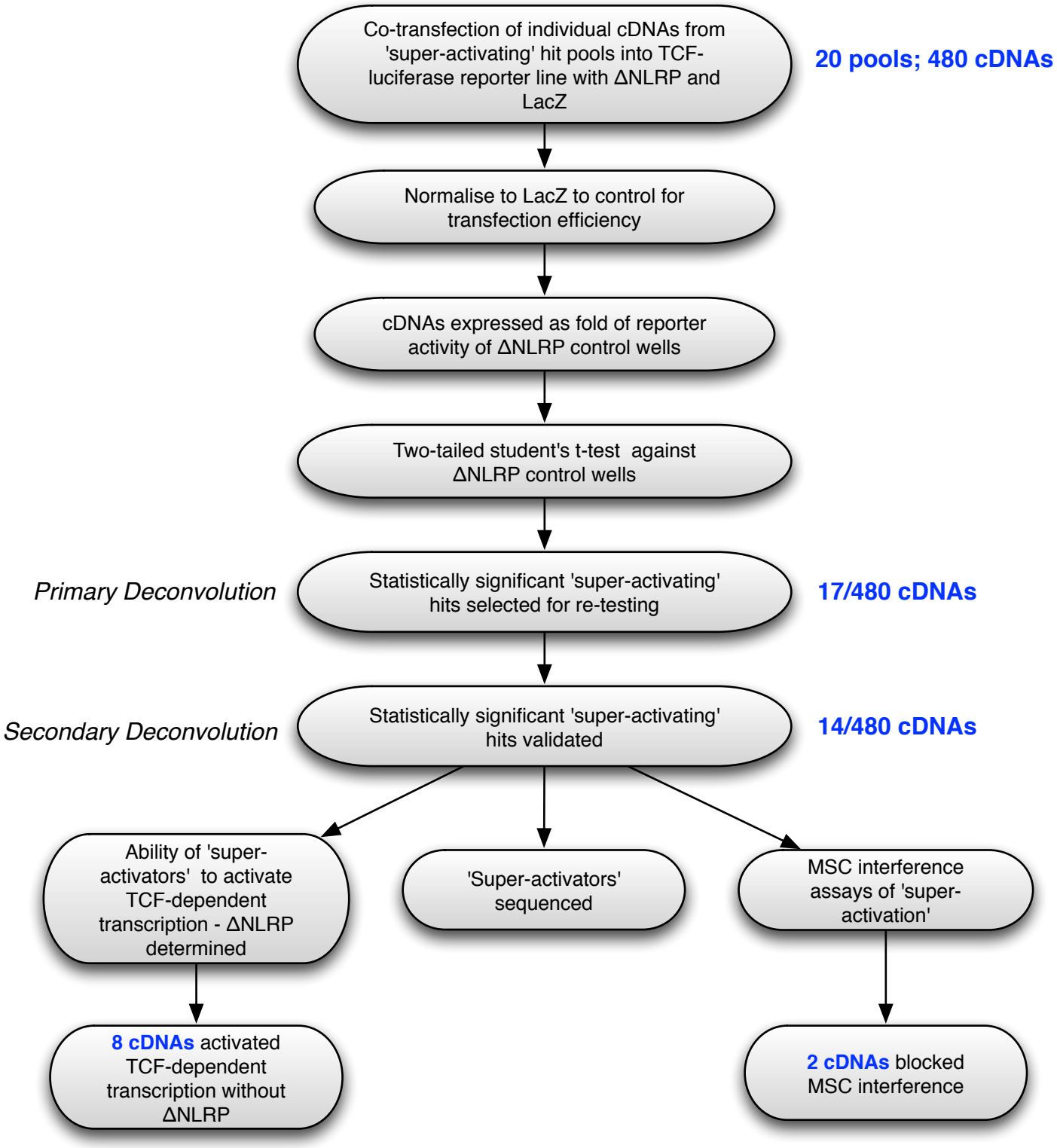

Figure 11. Activator cDNA pool deconvolution approach

Flow diagram demonstrating the approach taken to deconvolve Wnt-regulatory genes from the 20 most activating cDNA pools selected from the primary screen of the Medaka cDNA library using the 7df3 reporter cell line. Following co-expression of the activators with the activated Wnt co-receptor ΔNLRP, data was normalised to the β-galactosidase control to account for variations in transfection efficiency. The mean of three repeats was calculated and the significance of any activation (relative to 36 ΔNLRP control wells) was determined, with 17 activators putatively determined. Following further reconfirmation 14 activating cDNAs were fully validated and taken forward for further investigation.

Fourteen out of the 480 cDNAs isolated from the 20 pools were fully validated as being ‘super-activators’ based on activation >1.5X ‘basal’ ΔNLRP TCF-dependent transcription and a t-test p value <0.01. The putative Wnt pathway activators are listed in Table 1.

Library Ensembl ID	Proposed Gene ID	BlastX Description [Homo sapiens]	Accession Number	BLAST Expect (E) value
ENSORLG00000011147	SEZ6L2	Seizure 6-like protein 2 isoform 5 precursor	NP_001230261.1	1.00E-56
ENSORLG00000003634	β-catenin	Catenin beta-1	NP_001895.1	0
ENSORLG00000017521	GBX1	Homeobox protein GBX-1	NP_001092304.1	3.00E-114
ENSORLG00000020562	IKZF1	DNA-binding protein Ikaros isoform 1	NP_006051.1	1.00E-141
No ENSEMBL IDi	-	B-cell lymphoma 6 protein isoform 2	NP_001128210.1	1.00E-108
No ENSEMBL IDii	-	High mobility group protein B2	NP_002120.1	4.00E-61
ENSORLG00000007641	WNT-1	Proto-oncogene Wnt-1 precursor	NP_005421.1	2.00E-170
ENSORLG00000015359	HMGXB4	HMG domain-containing protein 4	NP_001003681.1	4.00E-87
ENSORLG00000011432	KRAS	GTPase KRas isoform b precursor	NP_004976.2	7.00E-106
ENSORLG00000000858	PITX1	Doublesex- and mab-3-related transcription factor A2	NP_115486.1	2.00E-56
ENSORLG00000018912	HRAS	GTPase HRas isoform 1	NP_005334.1	3.00E-116
ENSORLG00000006877	RTN2	High mobility group protein B2	NP_002120.1	2.00E-70
ENSORLG00000000668	OCLN	Occludin isoform a	NP_002529.1	9.00E-63
ENSORLG00000010346	TGIF1	Homeobox protein TGIF1 isoform b	NP_775299.1	5.00E-57

Table 1. Validated cDNA activator hit list

The identity of the 14 reconfirmed super-activators of TCF-dependent transcription. 'Library Ensembl ID' and 'Proposed Gene ID' columns indicate the preliminary identity of the gene according its well location (as determined by deconvolution) as detailed in the parent gene-by-gene cDNA library. The cDNA hits were sequenced and the translated nucleotide sequences analysed using BLAST against the *Homo sapiens* genome to confirm this identity (both protein description and accession number are detailed). BLAST E value indicates the significance of the match; the lower the E value the more significant the alignment. cDNAs whose identity differs to the hypothesised gene ID are underlined.

The success of the screen was validated by the identification of known Wnt signalling activators in the presence of ΔNLRP; these included Wnt 1 and β-catenin, whose identities were confirmed by sequence analysis (Figure 12a; Table 1). In this context, it is clear that both Wnt 1 and β-catenin are able to super-stimulate TCF-dependent transcription driven by limiting levels of ΔNLRP. Although the 14 hits had been allocated a proposed gene ID using the available library Ensembl IDs, each hit was re-sequenced and its identify compared to the *Homo sapiens* homologue by protein BLAST analysis of their translated nucleotide sequences. Ten of the activators were confirmed to be the same as their library annotation, whilst two hits without an associated Ensembl ID (annotated 'No Ensembl IDi' and 'No Ensemble IDii') were identified as being Bcl-6 and HMGB2. Finally, two genes originally annotated as PITX1 and RTN2 were subsequently identified as DMRTA2 and HMGB2 respectively (annotated as HMGB2* to prevent confusion). Interestingly, HMGB2 from a different cDNA pool had been confirmed as matching its proposed identity, suggesting that contamination may have occurred during individual cDNA hit preparation. Further work is required to establish the cause of this and determine the true effect (if any) of RTN2. Additional Wnt pathway regulators including KRAS, HRAS and HMGB2 were confirmed, with these hits overlapping with those identified in the precursor cDNA screen conducted by Jamie Freeman (Freeman, 2008). Interestingly for one of the pools, both IKZF1 and Bcl-6 were identified as significantly super-activating TCF-dependent transcription although at the lower end of activation. Further experiments will be required to determine whether there is synergistic activity between the these and ΔNLRP or whether their effect on TCF-dependent transcription was 'additive'.

For several of the original hit pools there was no single activator of TCF-dependent transcription evident. The simplest reason why these hits failed to reconfirm may be due to the identification of false positive hits. However one additional explanation for this observation is that more than one of the 24 cDNAs within the pool co-operated to drive TCF-dependent transcription. The hit

identification rate from the analogous screen of 9,000 *Xenopus tropicalis* cDNAs (in 3000 pools of 3 clones) 54 primary activating hits/139 pools suggested that there was a distinct possibility that pools of 24 clones may contain more than two clones with the ability to synergise with each other without requiring any functional interaction with ΔNLRP (Freeman, 2008).

Figure 12a&b. Reconfirmation analysis of activator cDNAs

Putatively active cDNAs identified from initial 'whole pool deconvolutions' were selected re-analysed for super-activation activation activity in the presence (**a**) and absence (**b**) of the constitutively active ΔNLRP in 7df3 cells. Hits annotated according to sequence analysis where available, or their original library annotation where not. The blue dashed line indicates the level of ΔNLRP control activation, and the red line indicates the level of pcDNA3.1 activation, to aid comparison.

a. cDNA activation (n=3) in the presence of ΔNLRP expressed as fold of ΔNLRP activation control (n=12). The standard deviation of each condition is shown. Significance of activation relative to ΔNLRP control wells was determined using students' two tailed t-test; ***** = p value<0.01.

b. cDNA activation (n=3) in the absence of ΔNLRP expressed as fold of pcDNA3.1 control (n=6). The standard deviation of each condition is shown. Significance of activation relative to pcDNA3.1 control wells was determined using student's two tailed t-test; ***** = p value<0.01.

Figure 12a

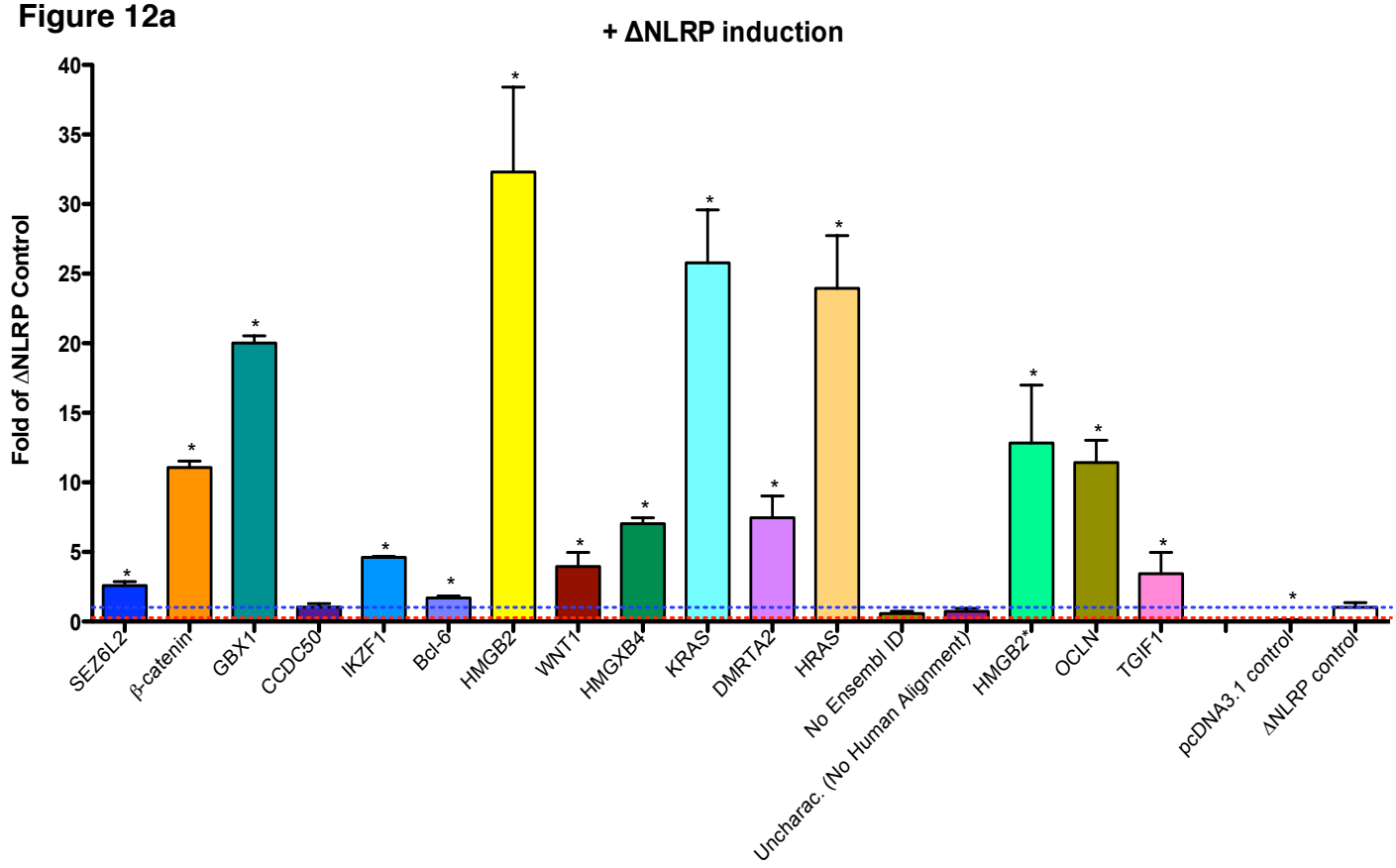

Figure 12b

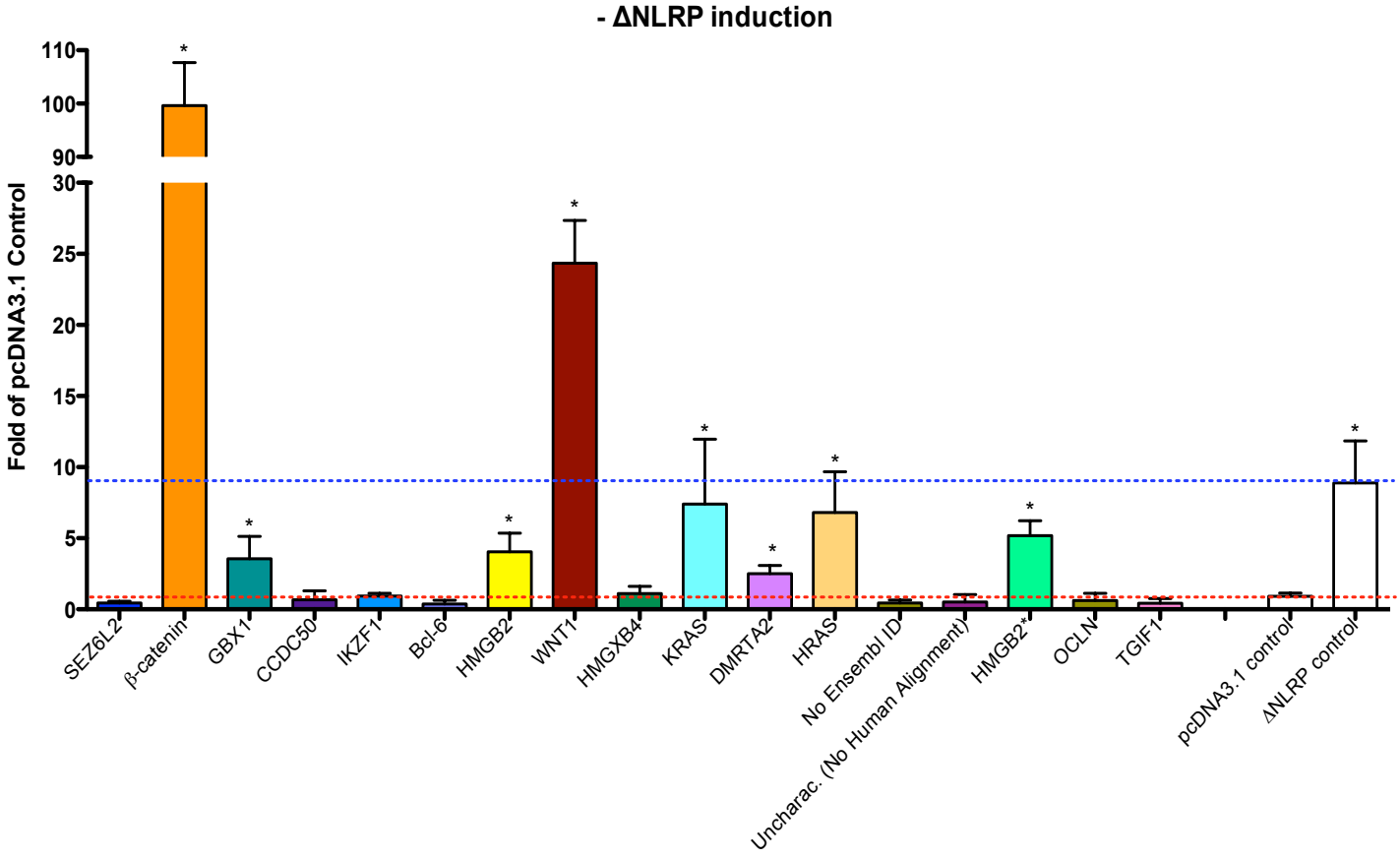

The fourteen super-activating cDNAs were also tested for activity in the absence of ΔNLRP co-stimulation (Figure 12b). Of the fourteen cDNAs assayed, eight significantly activated TCF-dependent transcription independently of pathway co-activation. Five of the hits were known Wnt signalling activators with three, the transcription factors DMRTA2, GBX1 and HMGB2 having little known association with Wnt signalling. Interestingly, only β-catenin and Wnt 1 activated TCF-dependent transcription to a greater level than the ΔNLRP control.

Using the online resource GeneCodis (Carmona-Saez et al., 2007; Nogales-Cadenas et al., 2009; Tabas-Madrid et al., 2012), the gene products were analysed for over-representation of annotations (relative to the whole genome) in several key areas. Annotation of the genes with a Gene Ontology (GO) identifier meant that the hit genes could be compared for enrichment in the categories of biological process, molecular function and cellular component. The genes were also compared to the Kyoto Encyclopaedia of Genes and Genomes (KEGG) collection of pathway maps to determine any enrichment of specific pathway features. However, no significant enrichment was identified, likely due to the very small set of genes being analysed. In future experiments, it is probable that this set of genes could be increased through the analysis of more pools or through the analysis of cDNAs on an individual basis, given the greater expression level of single cDNAs (if the expense can be justified).

The super-activators were further investigated In order to determine whether their stimulation of TCF-dependent transcription could be disrupted by MSC. Previous studies by J. Freeman (Freeman, 2008), showed that many cDNAs and cDNA pairs differed in their sensitivity to inhibition by putative Wnt pathway small molecule inhibitors. Hence mapping compound sensitivity was predicted to provide insight into MSC's mechanism of action.

Figure 13a&b. MSC-compound interference of 'super-activator'-induced TCF-dependent transcription

The ability of 10μM MSC to disrupt hit super-activation in 7df3 cells was determined.

a. The percentage effect of MSC treatment on the ability of the 14 'super-activators' to activate TCF-dependent in the presence of ΔNLRP was determined relative to their DMSO treated control (n=3). The standard deviation of each condition is shown.

b. The percentage effect of MSC treatment on the ability of the 8 'super-activators' capable of activating TCF-dependent *independently* of ΔNLRP co-activation was determined relative to DMSO treated comparisons (n=3). The standard deviation of each condition is shown.

Figure 13a

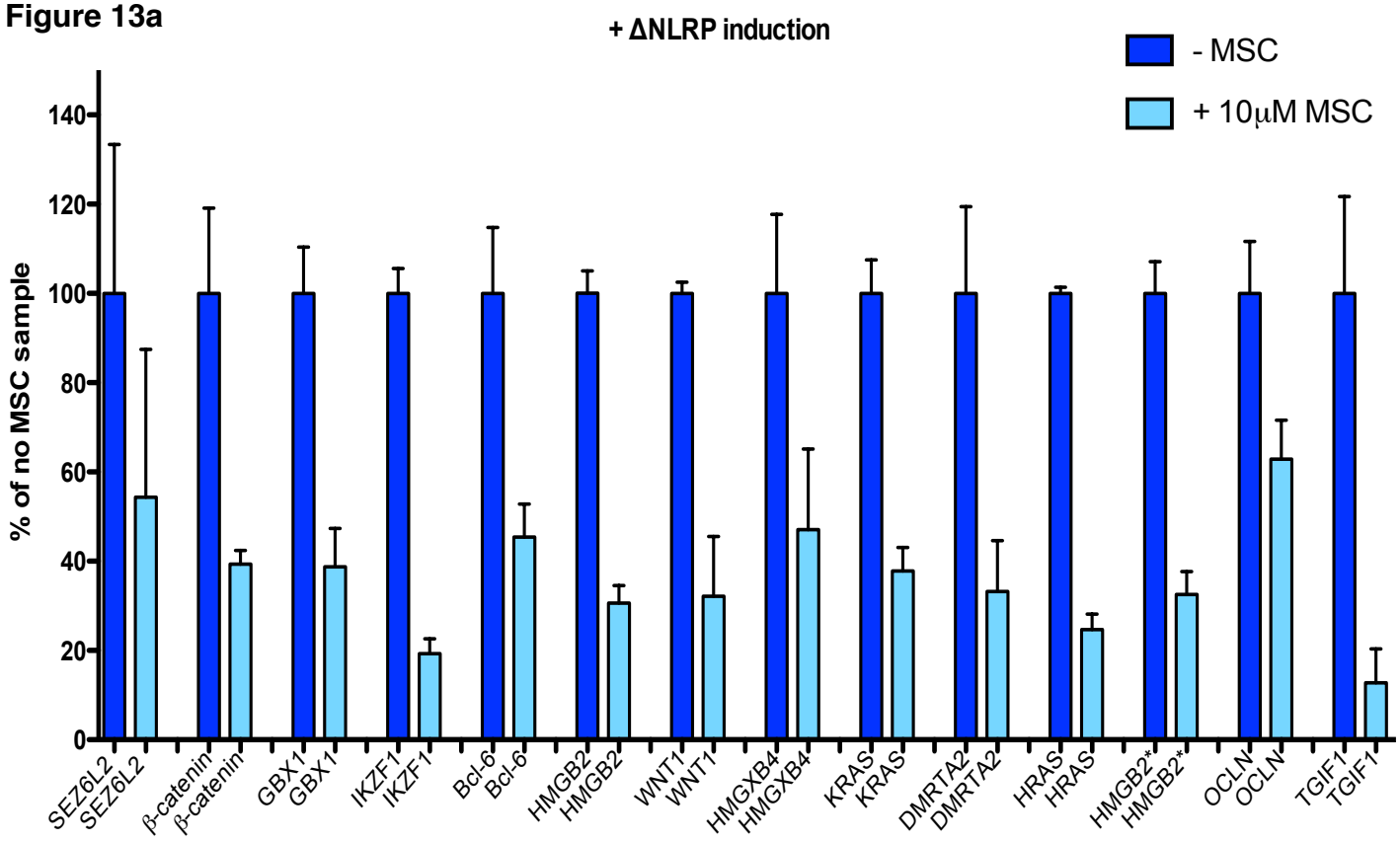

Figure 13b

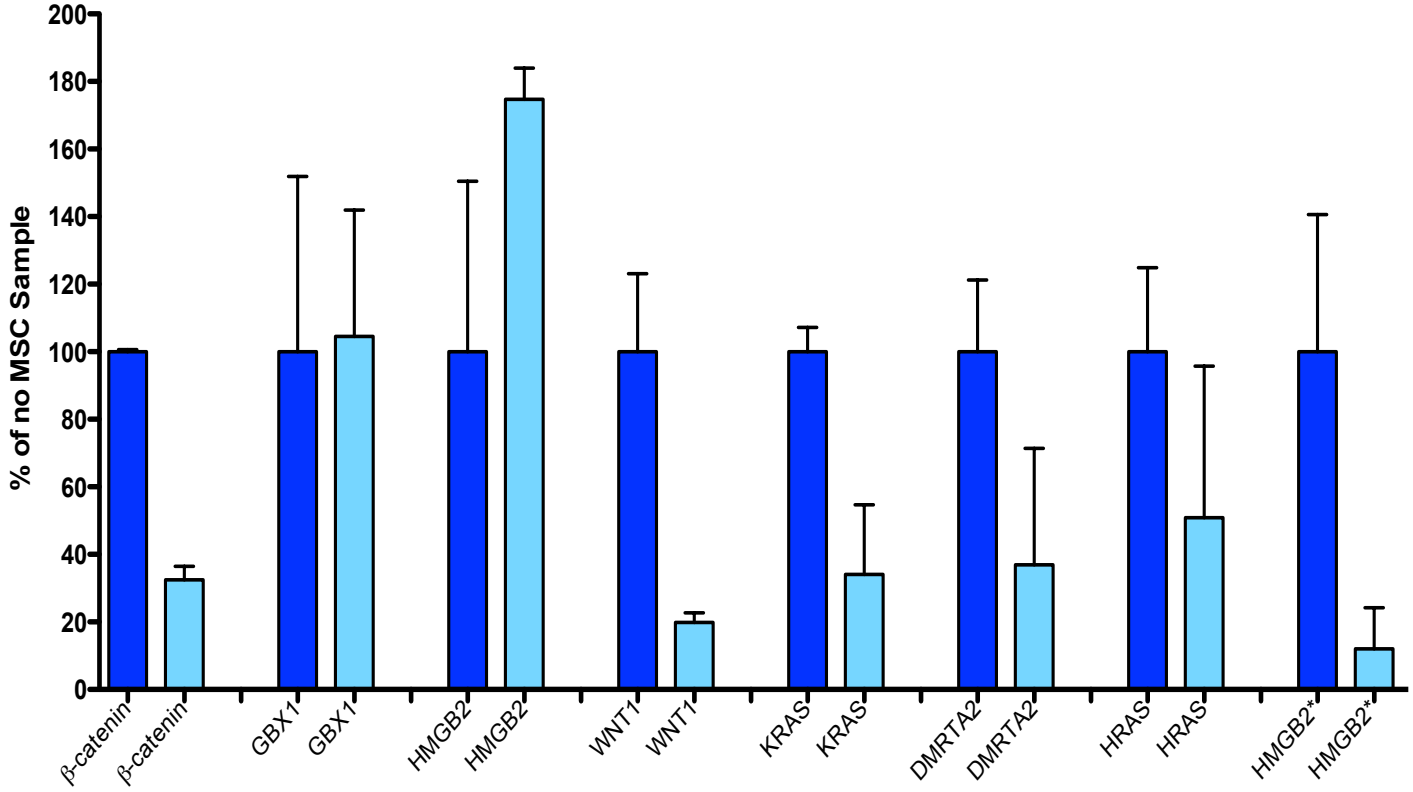

Ten micromolar MSC was added to 7df3 cells 24 hours after transfection and 24 hours prior to analysis. As can be seen in Figure 13a, the activity of all the cDNAs in combination with ΔNLRP was inhibited by MSC treatment in relation to DMSO control treatment. It is unclear whether the level of inhibition was significantly different between each combination as this would need reconfirmation with additional experiments and a greater number of repeats. Interestingly in the absence of ΔNLRP co-stimulation (Figure 13b), GBX1 and HMGB2 maintained their activation phenotype following MSC treatment, but again this requires repetition to confirm the compound resistance seen.

As MSC's target had been determined as being the serine/threonine kinases CDK8 and CDK19 by this point in the study, it was unsurprising that MSC was able to interfere with those hits dependent on ΔNLRP co-expression in order to mediate their super-activating effects. This was because CDK8 acts at the transcriptional level of the complex, playing a central role in the coupling of β-catenin/TCF to RNA polymerase II at Wnt target genes, meaning any processes synergising with the upstream constitutively active ΔNLRP would be disrupted by MSC. The more interesting hits for consideration at this point were those able to activate TCF-dependent transcription in the absence of ΔNLRP. Again as expected MSC was able to reduce β-catenin, Wnt 1, KRAS and HRAS activated TCF-dependent transcription. Interestingly however, MSC was unable to interfere with GBX1 and HMGB2 induced TCF-dependent transcription. It is interesting to note that GBX1 and HMGB2 are transcription factors and it is possible that they mediate their effects at TCF-dependent promoters without a requirement for CDK8/Mediator complex activation (see discussion for further consideration of this point). Further studies into this effect would be required since a difference in response was observed between HMGB2 and the alternative clone that was sequenced (HMGB2*). This raises the possibility that as yet uncharacterised sequence differences may be present between the 2 clones or that the HMGB2 MSC response is not highly reproducible. However,

due to a change in project focus as a result of the identification of CDK8/CDK19 as MSC's molecular target, this issue was not pursued further.

In summary, these studies have identified potential novel super-activators of Wnt signalling in a conditional setting, and were consistent with previous studies that suggested the activity of MSC was located at the transcriptional regulation level.

3.2 esiRNA screen

This section describes a synthetic lethality screen for genes whose function in colorectal cancer cell 2D cell growth was required only in the presence of the MSC CDK8/19 inhibitor.

Before discussing the details of the screen, it is important to describe a result that was surprising in the context of the literature that was known at the time (Figure 14). Bafico *et al*. (Bafico et al., 2004) showed that HCT116 cells, in which Wnt/β-catenin driven transcription was reduced (by loss of β-catenin and reduction in Wnt ligand levels) had reduced levels of 3D cell proliferation (Bafico et al., 2004). This suggested that if MSC reduced TCF-dependent transcription, it should reduce 2D cell proliferation. In addition, Firestein *et al*. (Firestein et al., 2008), showed that shRNA-depletion of CDK8 expression reduced HCT116 cell growth in 2D culture. Based on these results reports, it was predicted that a highly active CDK8/19 inhibitor with 12.4nM activity against 7df3 TCF-dependent transcription would inhibit HCT116 cell proliferation.

To test this prediction, HCT116 cells were treated with a titration of MSC (from 4.5nM – 30μM) for 48 and 72 hours and cell proliferation was measured using an ATPlite assay. Surprisingly, it can be seen in Figure 14a that there was no effect of compound on proliferation even at 2000 times the 7df3 TCF-reporter IC_{50} of MSC (12.5nM) at either 48 or 72 hours. This result further suggested that the growth-inhibitory activity that had previously been observed using the initial 'hit' compound from the same series (CCT071459) may have been due to 'off target' effects of the initial compound that were unrelated to its ability to inhibit TCF-dependent transcription or to bind CDK8/19. Interestingly, MSC was shown to have some anti-proliferative activity in 3D culture and in vivo anti-tumour studies (Figure 33 and data not shown; see Discussion).

To examine whether the lack of a 2D growth response was due to the inactivity of the MSC compound in HCT116 cells against TCF-dependent transcription, a variant of the HCT116 line with a TCF-reporter HCT116 line (AT506; stably

transfected with the TOPflash TCF-reporter construct) was tested (Figure 14b). MSC exhibited a dose-dependent inhibition of TCF-reporter activity in the AT506 cells with the 48 hour IC_{50} (154nM) being 12 times that observed in the 7df3 cells. Inhibition of TCF-dependent transcription was also observed in other TCF-reporter cell lines studied in the collaboration, including colorectal cancer cells (e.g. Ls174T cells). However, a particular point of note from this study was the observation that TCF-reporter activity was only inhibited to ~45% of maximum; by contrast inhibition of TCF-reporter activity in 7df3 cells was >90% in most assays (data not shown). Similar 'partial efficacy' responses to compound treatment were observed in other colorectal cancer cell lines with integrated TCF-reporters (e.g. ~40% in SW480 cells; Merck Serono data not shown).

There are several reasons that could explain the lack of growth inhibition in the HCT116 cells following MSC compound treatment. These include one or more of:

1. Partial efficacy. It is possible that the final level of Wnt reporter activity remained sufficient to maintain cell proliferation. i.e. There is a minimum threshold level of Wnt reporter activity that is required for cell proliferation and the MSC compound failed to reduce activity below this level.
2. 2D versus 3D (*in vivo*). 2D cell models don't reveal a cell growth dependence on TCF-reporter levels. In Merck Serono studies, it was observed that MSC partially inhibited tumour growth in vivo (data not shown), suggesting that in vivo studies may maintain this dependence.
3. MSC compound treatment is NOT equivalent to a simple reduction in β-catenin levels or a reduction in TCF-reporter activity. Since the time the project was started, the identity of the MSC target has been determined as the kinases CDK8 and CDK19. Loss of function of these kinases affects TCF-reporter activity in ways that are not yet fully understood.

Each of these possible explanations is consistent with the idea that MSC compound activity effects in 2D culture may be masked by contributions from

other pathways or gene products. Many of these pathways may also function *in vivo* and could act to reduce the potential clinical activity of MSC.

It is thus possible to view the lack of response to MSC compound as an opportunity to identify gene products whose activity co-operates with MSC's target in maintaining tumour growth. This stimulated the design of a whole-genome 'chemical sensitisation' screen.

The goal of the chemical sensitisation screen was to identify genes whose function was required for 2D cell proliferation in the presence of MSC. It was predicted that genes whose inhibition had no affect on cell viability in the absence of compound but resulted in complete loss of viability in the presence of compound would be ideal starting points for the design of rational compound combination strategies for the treatment of Wnt/CDK8/19-dependent cancers.

Figure 14a&b. Effects of MSC on HCT116 cells 2D cell proliferation and TCF-dependent transcription.

a. The viability dose response of HCT116 cells to MSC at 48 and 72 hours as a percentage of DMSO control. Viability of the cells was measured using the ATPlite luminescence assay. Mean values ±S.D. of 6 replicate wells per condition are displayed.

b. The TCF-luciferase reporter dose response of (HCT116)-AT506.C2 Wnt reporter cells to MSC at 48 and 72 hours as a percentage of DMSO control. TCF-luciferase was measured using the BrightGlo luminescence assay. Mean values ±S.D. of 6 replicate wells per condition are displayed.

Figure 14a

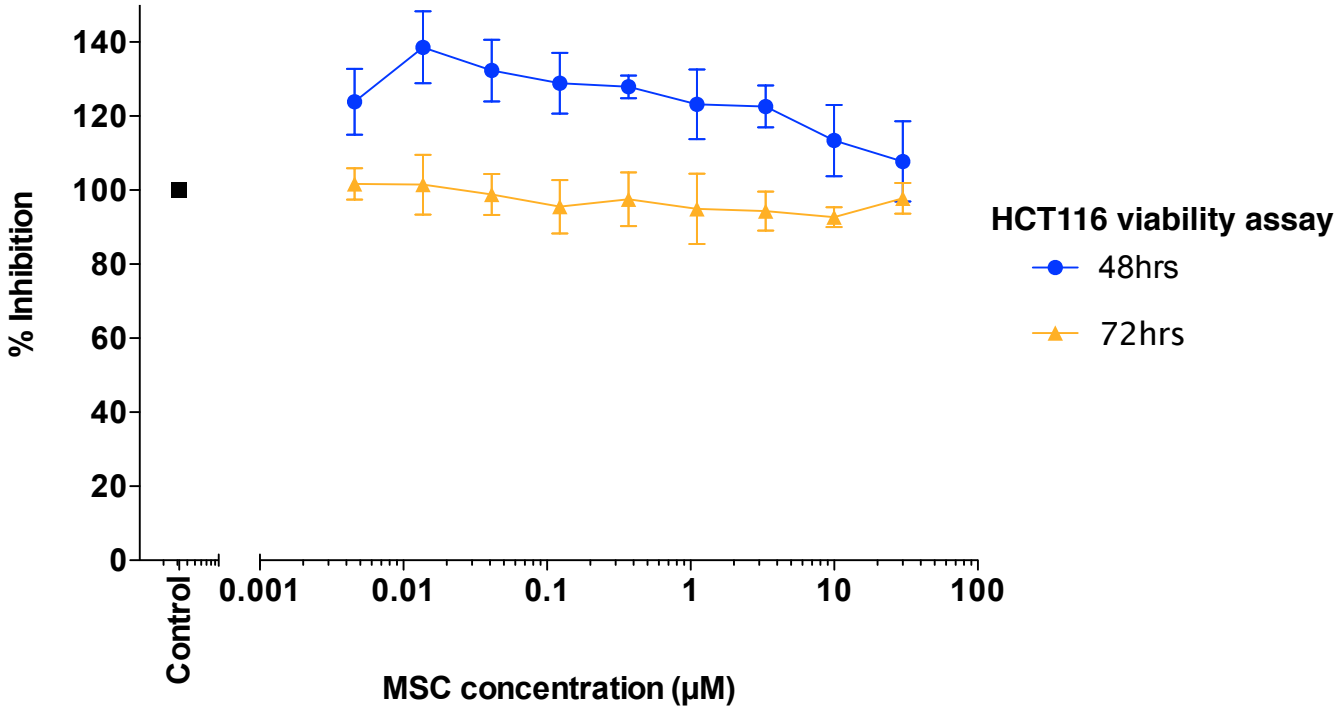

Figure 14b

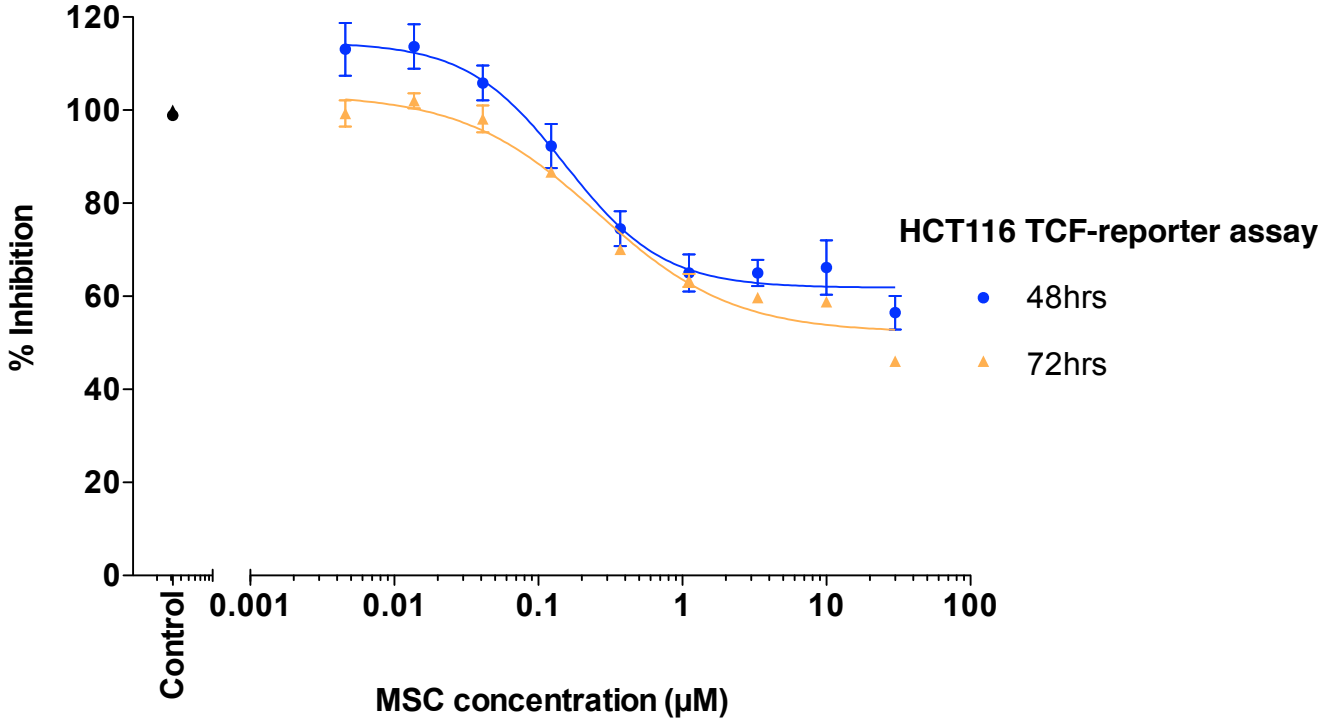

3.2.1 esiRNA assay development and optimisation

Before a synthetic lethality screen could be carried out, a major series of optimisation experiments had to be performed since the scale of the final assay (total 216,576 individual data points) would be prohibitively expensive both in cost and time to repeat. Based on published and in house data on Wnt/β-catenin/CDK8 dependence, HCT116 cells were chosen for the assays. Following the Dale group's previous success with reverse siRNA transfection approaches (Freeman, 2008; Lloyd-Lewis, 2011), cells were set up to deplete gene products by transfection with esiRNA for 48 hours followed by compound addition for a further 24 or 72 hours, resulting in total assay durations of 72 hours and 120 hours respectively. The assay readout selected was a reduction in 2D cell viability as measured using a 'simple' ATPLite luminescence assay. This assay is based on the principle that there is a decrease in ATP (and hence luminescence from exogenous supplied luciferase enzyme that is added to the lysed cell extracts) as cell viability or cell number decreases. This provided a rapid, quantitative method for determining viability.

The key reagent in this study was the 17,188 gene esiRNA library provided by Prof. Frank Buchholz. Endoribonuclease synthesised small interfering RNAs (esiRNAs) comprise a set of overlapping siRNAs that are enzymatically generated by the digestion of longer dsRNA hybrids by the Dicer/RNAse III enzyme (Buchholz et al., 2006). The advantages of this reagent by comparison with chemically synthesised siRNAs are that they more efficiently target more genes (fewer false negatives) based on their greater sequence complexity, while having fewer false positives due to the lower concentration of any particular sequence siRNA. These advantages have been extensively documented (Buchholz et al., 2006; Echeverri et al., 2006; Kittler et al., 2004; Theis and Buchholz, 2011).

The overall plan of the optimisation process is shown in Figure 15.

Figure 15 placement

Figure 15. Overview of esiRNA screen optimisation processes

Initial studies identified the optimal transfection reagent. Cells were seeded at 3,000 and 6,000 cells per 384-well compared 3 different transfection reagents using a set of control esiRNAs. The best performing reagent was then used for a more extensive optimisation of cell numbers and transfection reagent concentrations. The volume of the assays was subsequently scaled down and fine-level assay optimisation was conducted under final screen conditions. This involved tests on batches of frozen or live cells and optimisation of plate reader parameters. The work culminated in a pilot screen that was based primarily on the use of control esiRNAs.

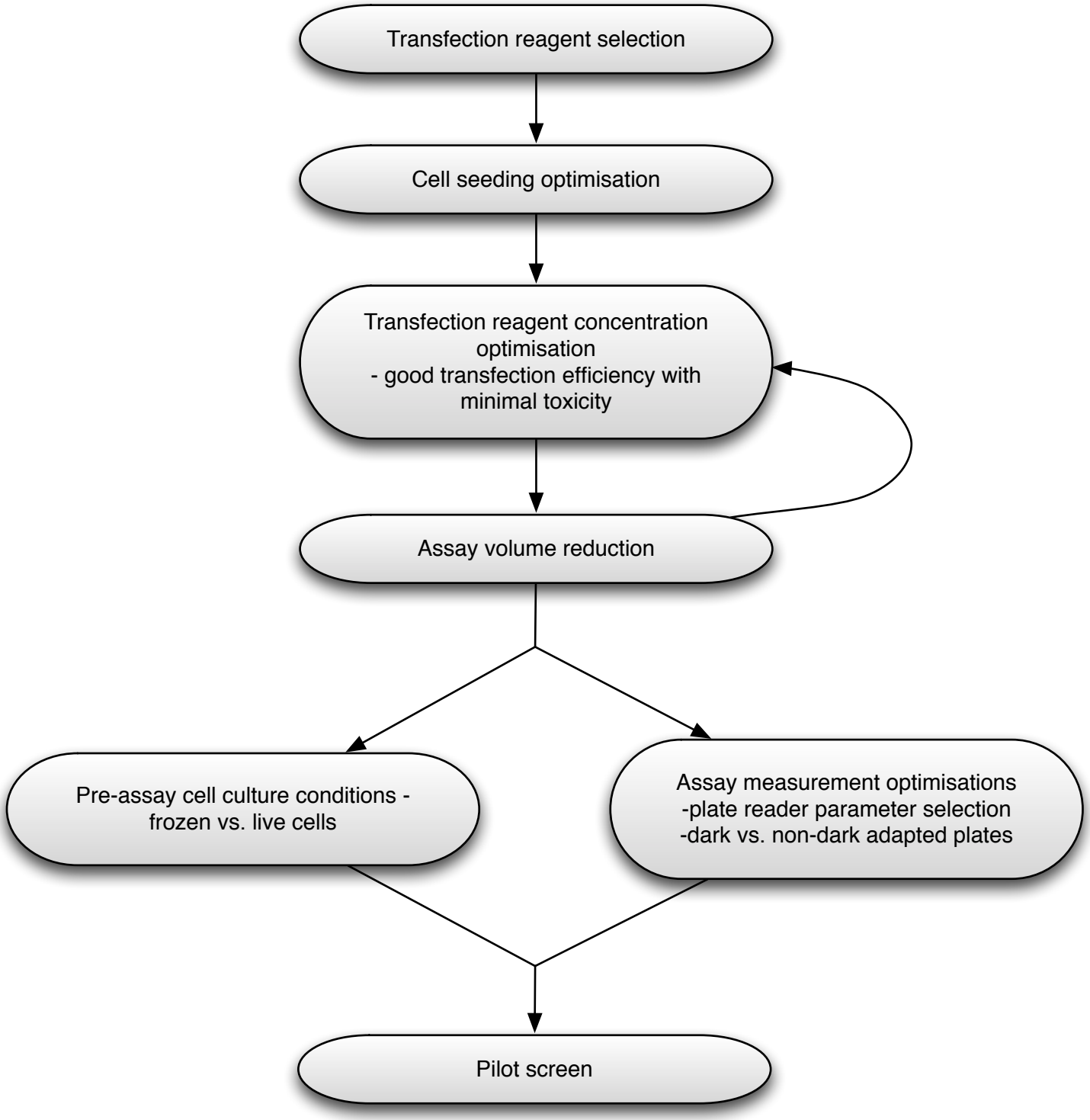

Figure 15. Overview of esiRNA screen optimisation processes

Initial studies identified the optimal transfection reagent. Cells were seeded at 3,000 and 6,000 cells per 384-well compared 3 different transfection reagents using a set of control esiRNAs. The best performing reagent was then used for a more extensive optimisation of cell numbers and transfection reagent concentrations. The volume of the assays was subsequently scaled down and fine-level assay optimisation was conducted under final screen conditions. This involved tests on batches of frozen or live cells and optimisation of plate reader parameters. The work culminated in a pilot screen that was based primarily on the use of control esiRNAs.

Transfection reagent selection

A key reagent for esiRNA transfection studies is the transfection reagent. Most optimised commercial reagents for esiRNA transfection are based on the formation of lipid-nucleic acid complexes however unfortunately the identity of the lipid/lipid mixes are normally proprietary information (hence undisclosed). Nonetheless, it has been established that key parameters for optimisation include cell number (the target being the lipids in the plasma membrane), the esiRNA and the lipid concentration (lipid delivery systems often mediate cytotoxic effects by compromising cell membranes), together with details of protocol that optimise the size and uniformity of siRNA-containing micelles. As a first step in this optimisation process, several transfection reagents were compared (Figure 16).

Figure 16a,b placement

****ON OPPOSITE PAGE****

Figure 16a
DharmaFECT

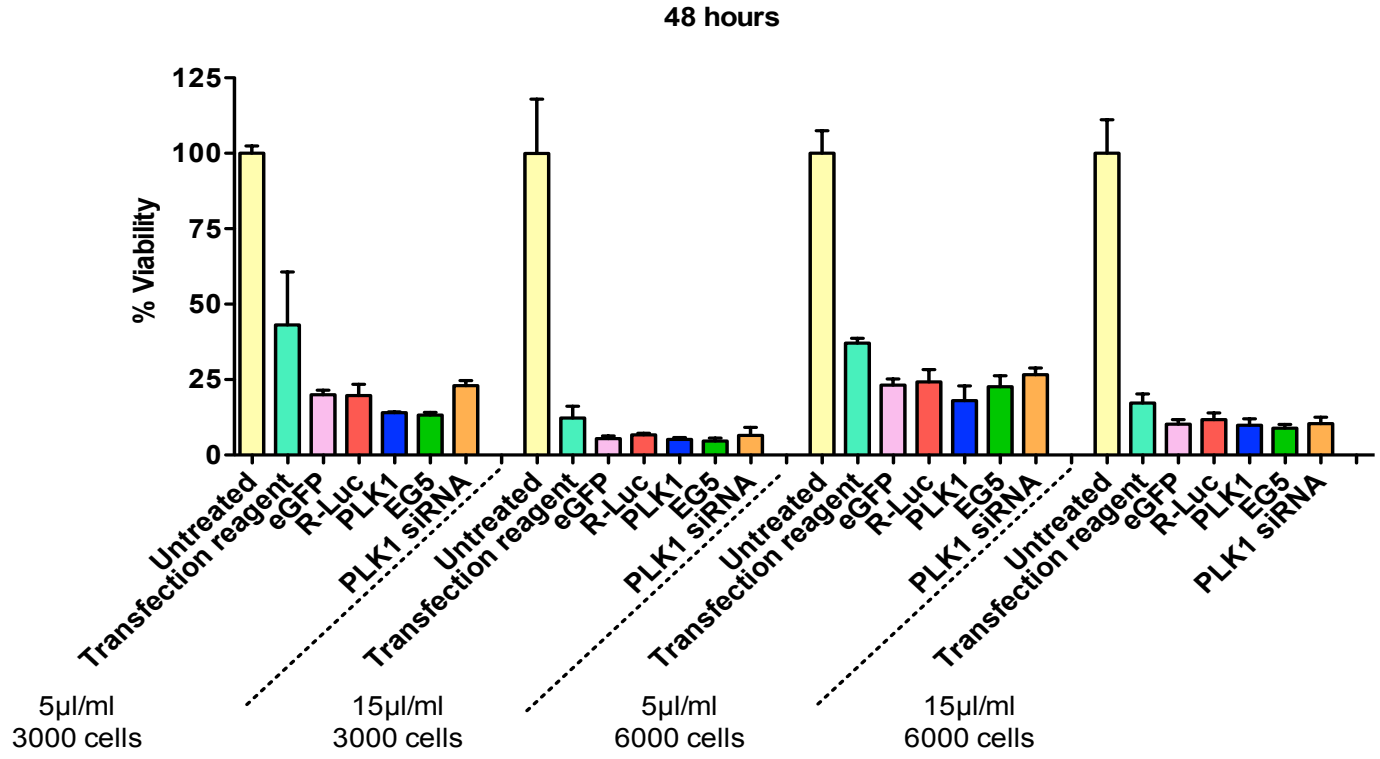

Figure 16b
DharmaFECT

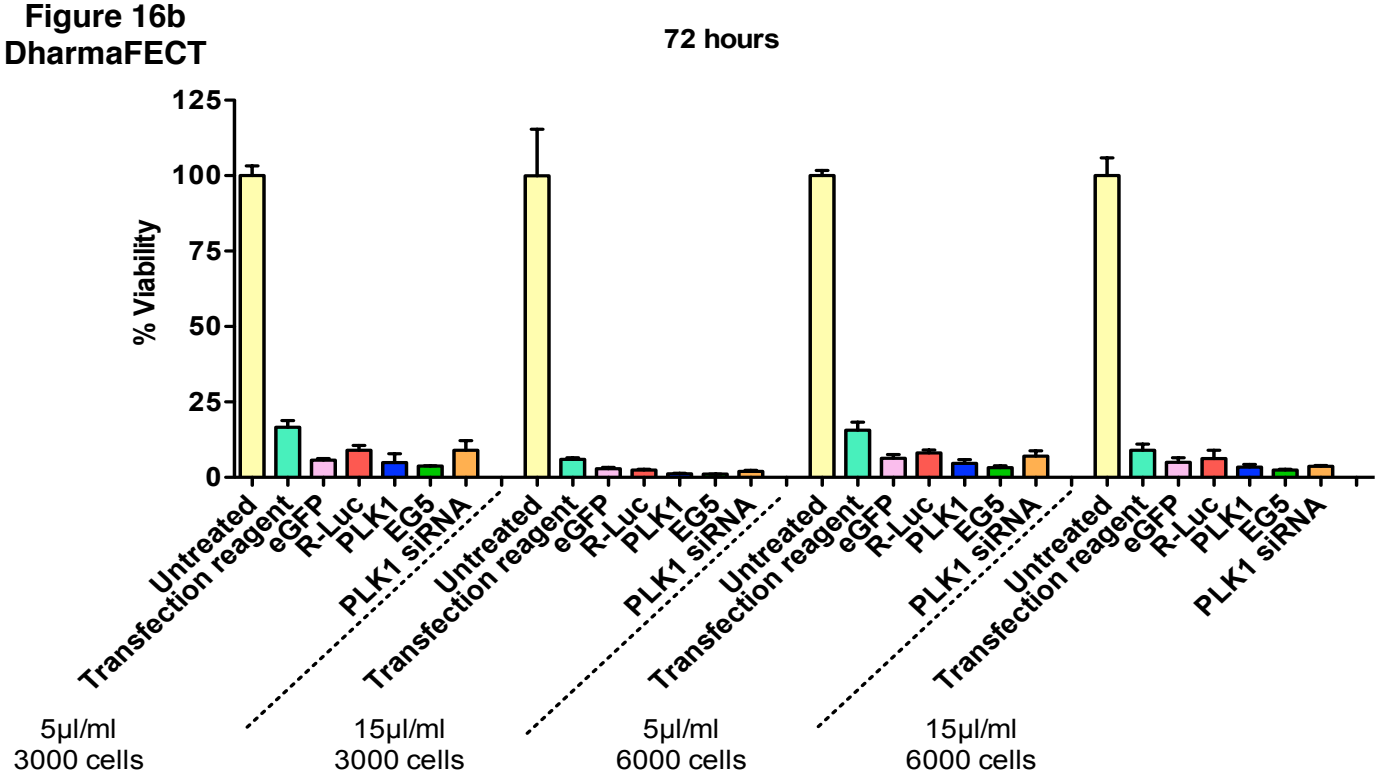

Figure 16c,d placement

****ON OPPOSITE PAGE****

Figure 16c
HiPerFect

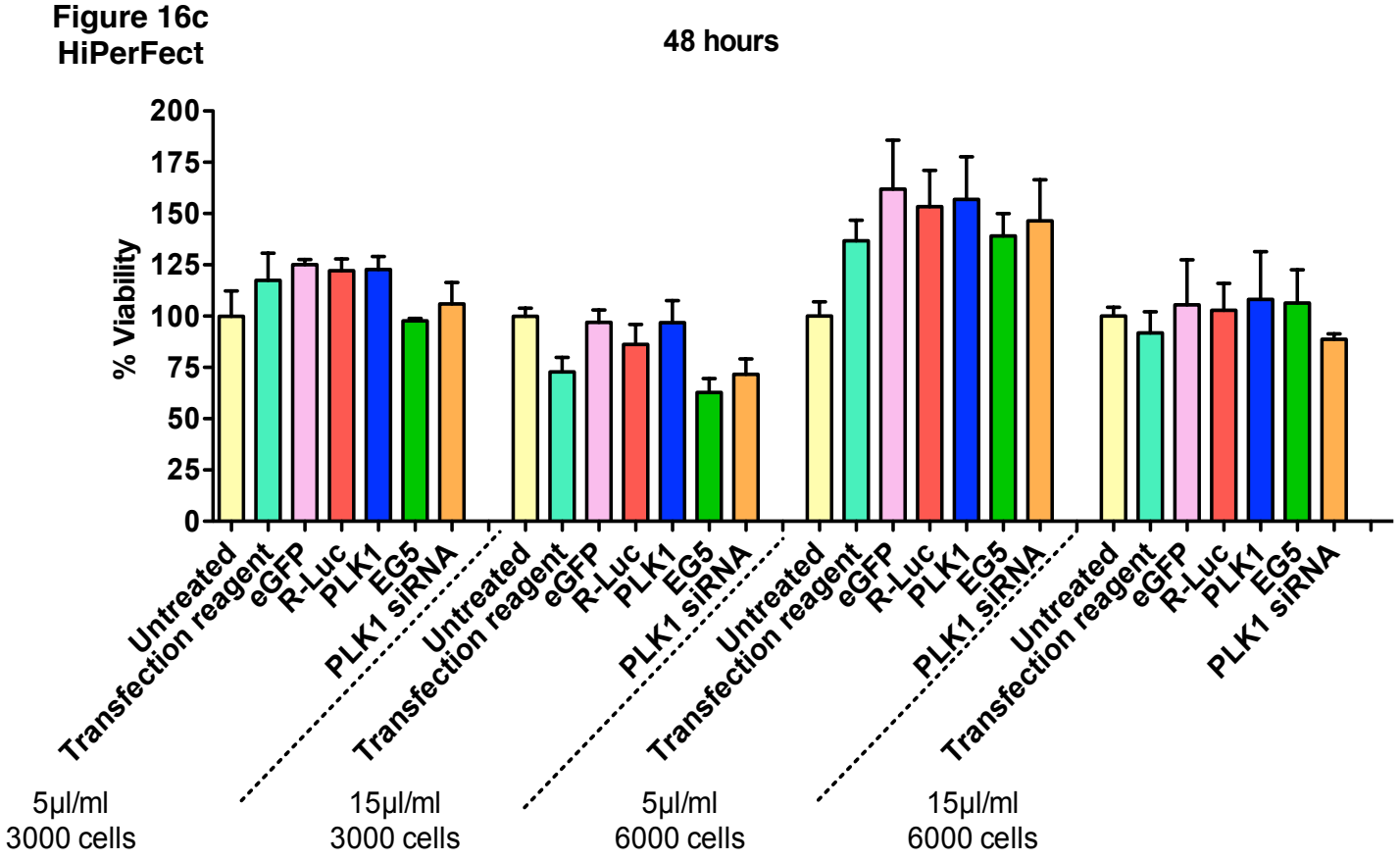

Figure 16d
HiPerFect

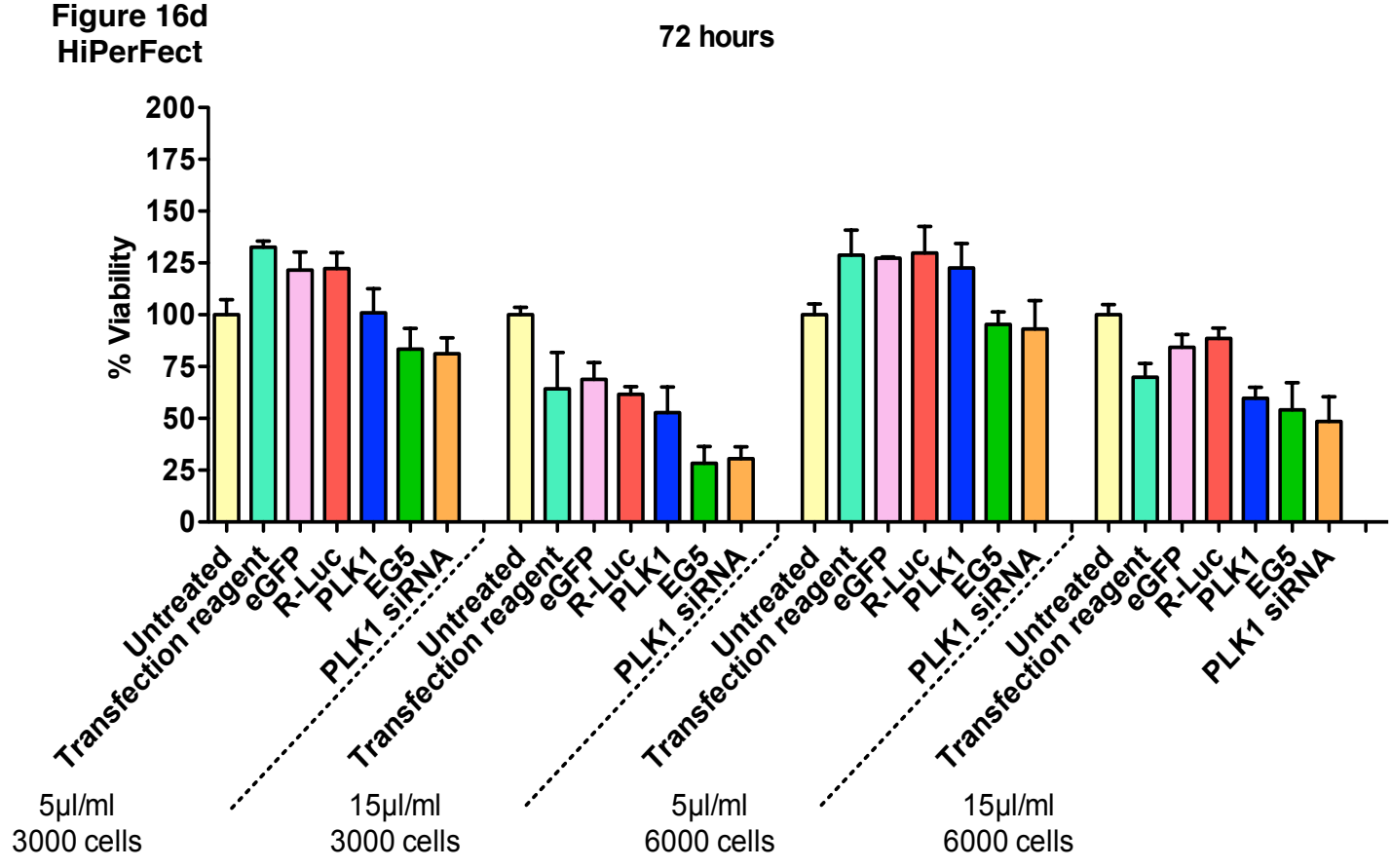

Figure 16e&f placement

Figure 16. Transfection reagent selection

The transfection efficiency and cytotoxicity of three transfection reagents; DharmaFECT (**a** & **b)**, HiPerFect (**c** & **d**) and INTERFERin (**e** & **f**) was determined at 5μl/ml and 15μl/ml transfection reagent. Cell seeding densities of 3000 cell and 6000 cells per well were reverse transfected with control esiRNA ('non-targetting' eGFP and R-Luciferase; 'targetting' PLK1 and EG5) in 384 well plates and viability assessed using the ATPlite luminescence assay at 48 and 72 hours. Mean values ±S.D. of 3 repeats are displayed as percentage of untreated control.

****ON OPPOSITE PAGE****

Figure 16e
INTERFERin

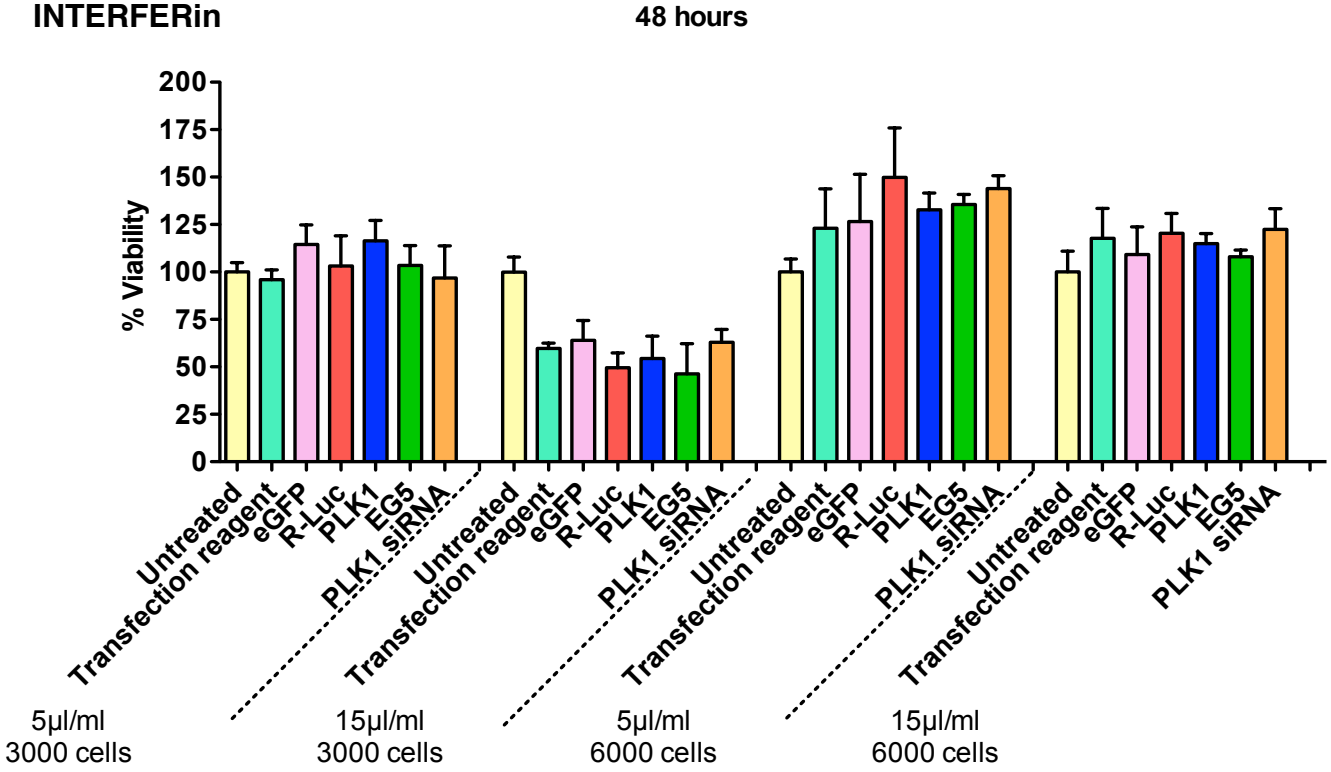

Figure 16f
INTERFERin

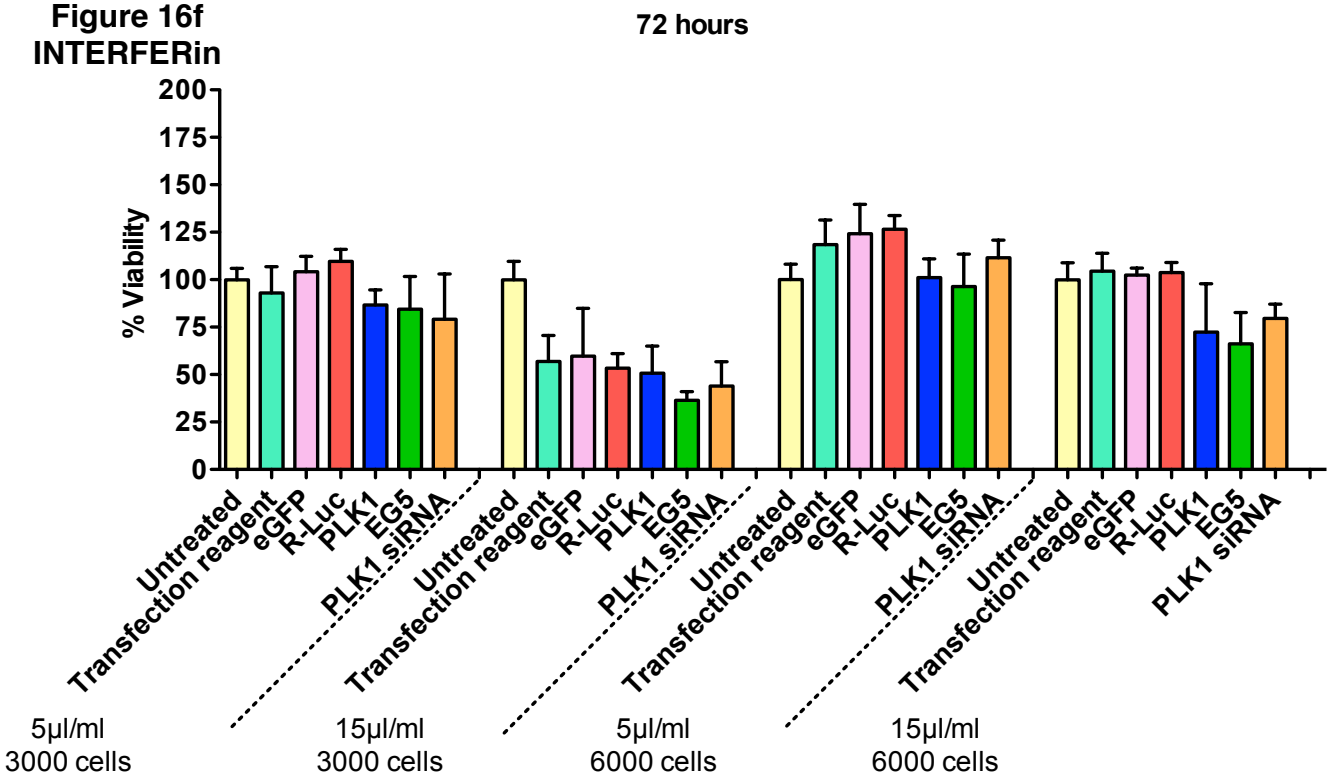

Three transfection reagents; **a** & **b**: DharmaFECT, **c** & **d**: HiPerFect; **e** & **f**: INTERFERin were compared for their ability to transduce esiRNAs against enhanced green fluorescent protein (eGFP), renilla luciferase (R-Luc), polo-like kinase 1 (PLK1) and kinesin-related motor protein 11 (EG5) esiRNAs at 48 and 72 hours post-transfection (as shown in Figure 16). PLK1 siRNA was used as an additional control. Cells were assayed for ATP levels using the ATPlite luminescence assay, with reduction of cellular ATP level being equated as loss of cell viability since ATP rapidly declines when cells undergo necrosis or apoptosis. Optimal reagents were expected to show no (or minimal) viability reduction with eGFP and R-Luc reagents but to exhibit target-related reduction in cellular viability in response to depletion of PLK1 (mitotic progression regulator, knockdown of which results in mitotic arrest) and EG5 (required for the establishment of a bipolar spindle in mitotic cells). PLK1 siRNA had previously been used at Merck Serono and was used as a 'known control' as targeted gene knockdown with this reagent was expected to result in >70% reduction in viability at 72 hours (data not shown).

Each transfection reagent was tested using the afore mentioned controls, and cellular viability measured alongside untreated cells and cells treated with transfection reagent alone in order to determine transfection reagent toxicity. 20ng esiRNA (or 5μl TE buffer for untreated/transfection media controls) was aliquotted into a 384 well plate and transfection reagent dispensed directly into the wells at 5μl/ml or 15μl/ml (final assay volume concentration). Following micelle formation, cells were dispensed onto the esiRNA:lipid complexes at 3000 or 6000 cells/well and viability measured at either 48 or 72 hours post-transfection. ATP-dependent luminescence was measured (as relative light units; RLU) using a luminometer, and the effect of each condition given as a percentage of the mean of the untreated control cells (Figure 16 a-f). As can be seen in Figure 16c, 3000 cells transfected with 15μl/ml HiPerFect (at 72 hours) showed the closest response to that expected, with ~70% reduction in cell viability with EG5 esiRNA and PLK1 siRNA knockdown. However, with ~25%

reduction in viability mediated by transfection reagent alone, and no apparent targetted-knockdown as expected with PLK1 esiRNA transfection, it was evident that further optimisation would be required from this starting point. By comparison, the use of DharmaFECT (Figure 16a and b) resulted in both transfection reagent toxicity and off-target esiRNA toxicity (as seen by further reduction in cell viability even with transfection of the eGFP and R-Luc controls), and so it was not used any further. INTERFERin (Figure 16 e and f) exhibited limited transfection efficiency and non-specific transfection reagent toxicity was evident at 3000 cells transfected with 15μl/ml (at both 48 and 72 hours), and so it was concluded that HiPerFect was the most promising reagent to take forward for assay optimisation.

Cell seeding optimisation

In order to determine ideal parameters for the high-throughput screen, cell numbers and the assay timecourse were further optimised using HiPerFect (Figure 17a-d).

Figure 17a&b placement

****ON OPPOSITE PAGE****

Figure 17a

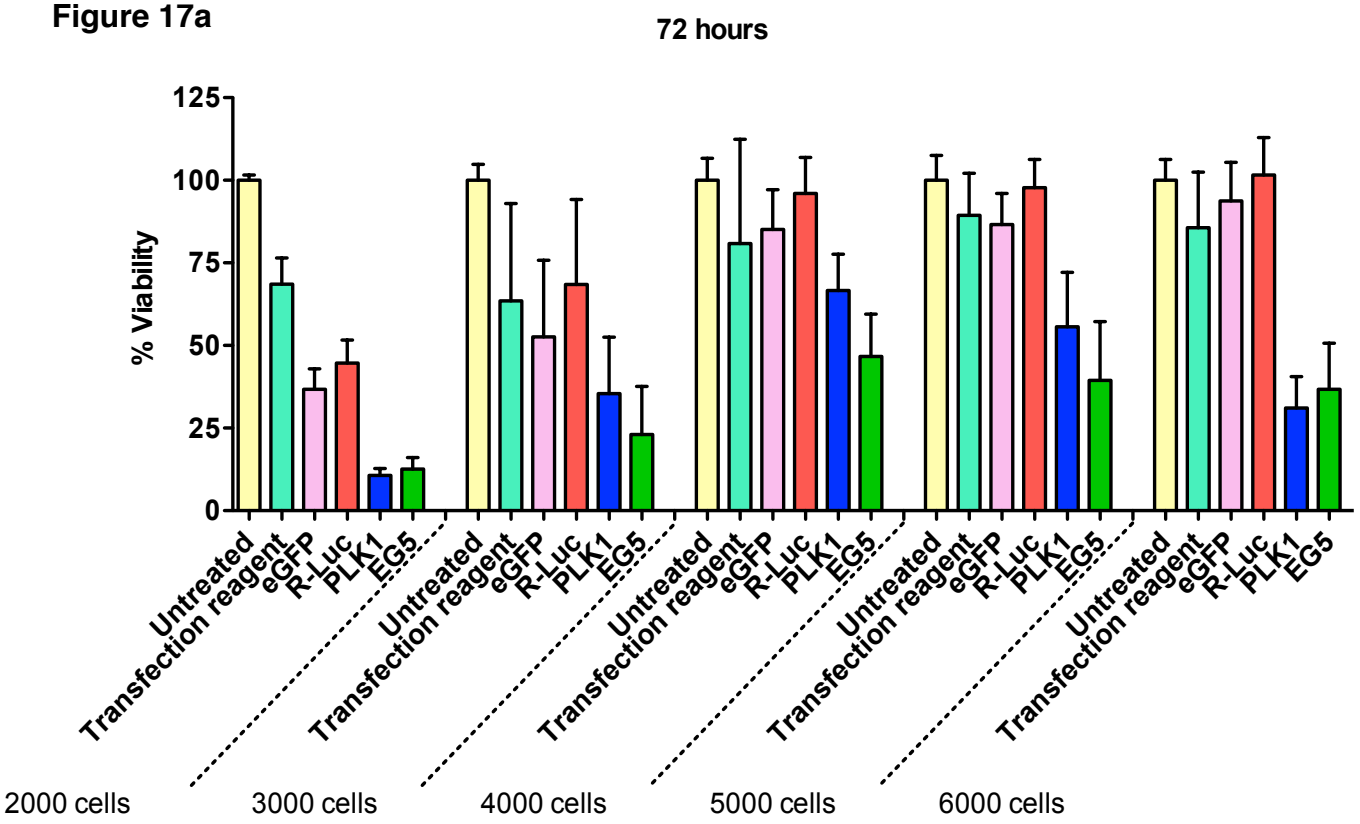

Figure 17b

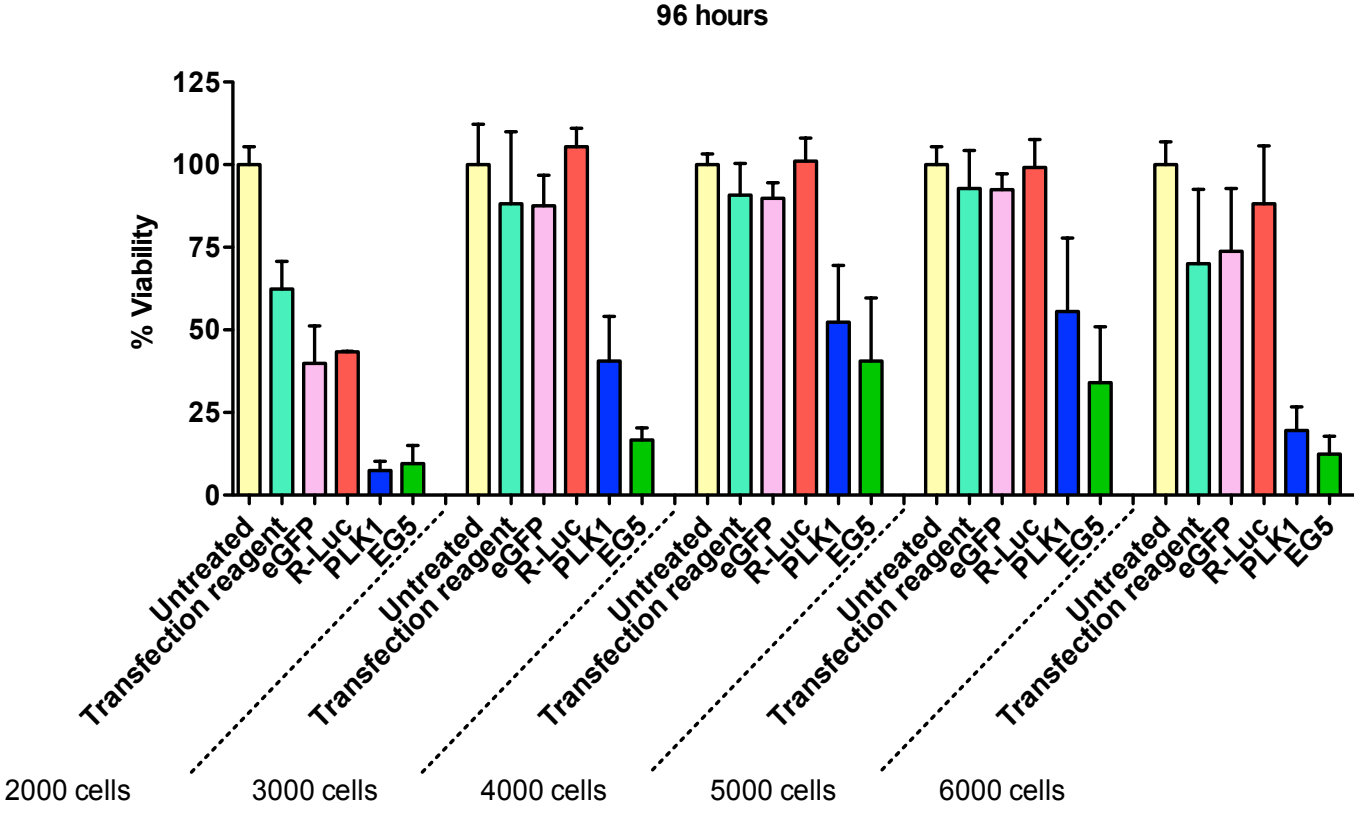

Figure 17c&d placement

Figure 17. Cell number and timecourse assessment

Cell seeding of 2000, 3000, 4000, 5000 and 6000cells/well were reverse transfected with 15μl/ml HiPerFect and cell viability mediated by the panel of control esiRNAs measured at 72, 96, 120 and 144 hours post-transfection. Cell seeding of 2000cells/well responded most effectively, with loss in viability sustained across all timepoints. Mean values ±S.D. of 3 repeats are displayed as percentage of untreated control.

****ON OPPOSITE PAGE****

Figure 17c

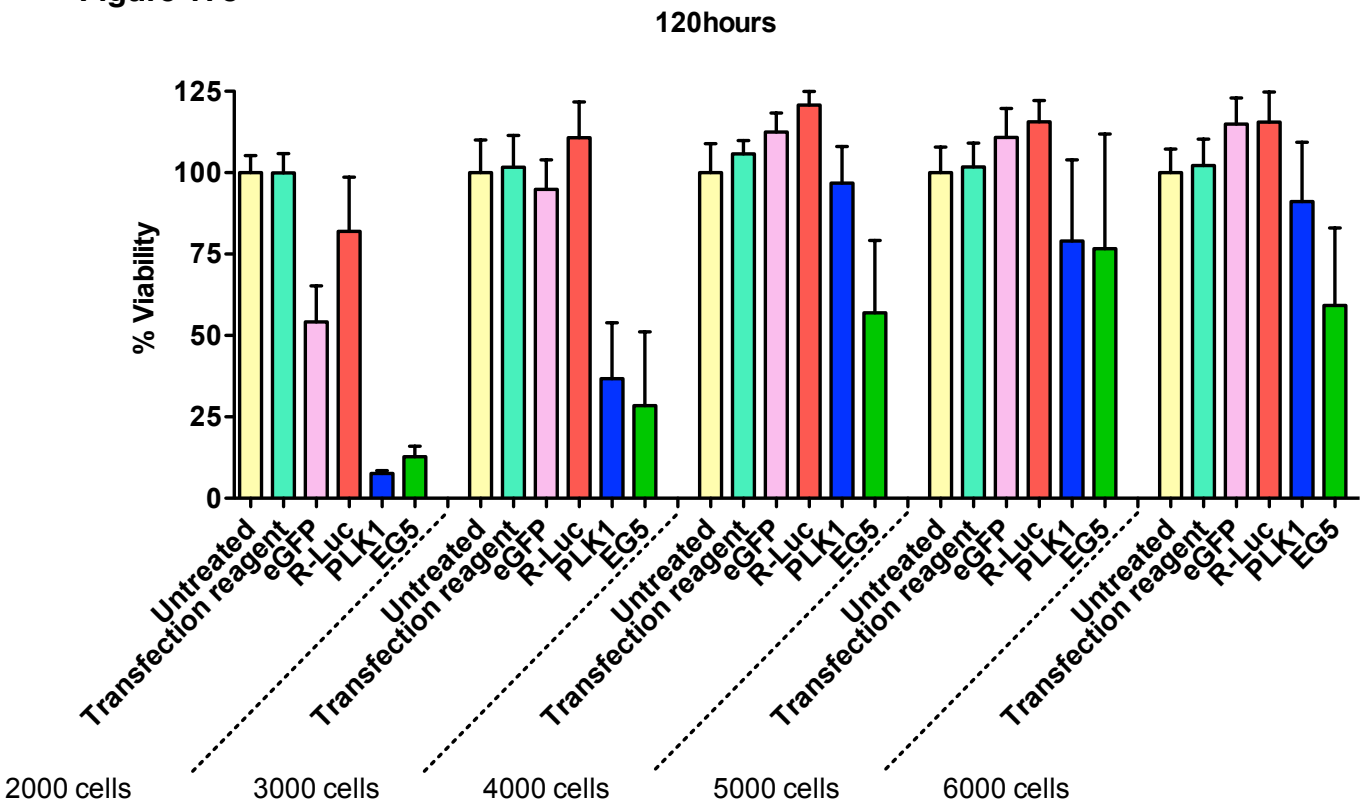

Figure 17d

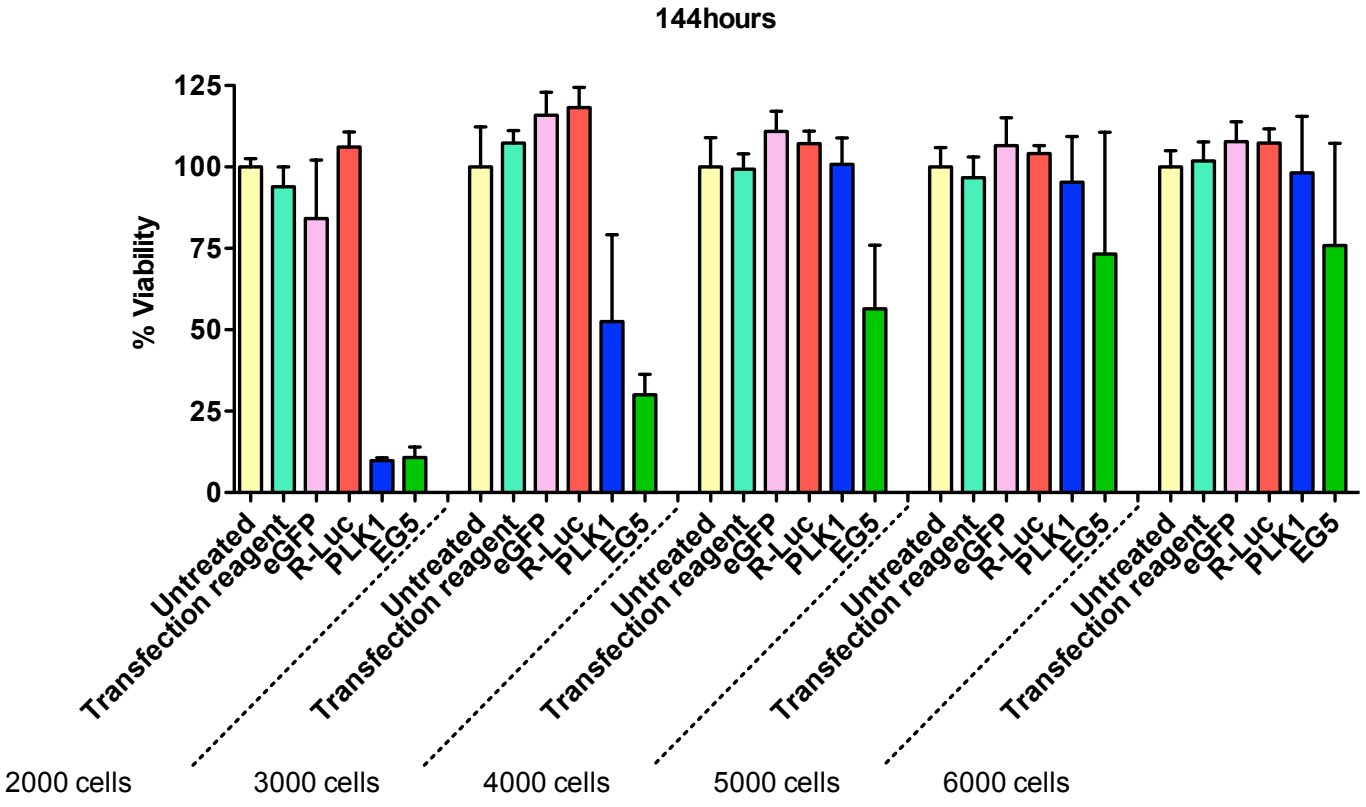

Using the reagents and assay format previously described (see previous 'Transfection reagent selection' section), 2000, 3000, 4000, 5000 and 6000 cells/well were transfected with the esiRNA panel of controls using 15μl/ml HiPerFect (Figure 17a-d). Measurements were to be taken at 72 and 120 hours post transfection, as it was anticipated that this would have given sufficient time for the various esiRNA target mRNAs to be degraded and for their existing gene products to be degraded / diluted due to cell proliferation. Measurements were also taken at 96 hours (in order to monitor assay performance between the final read parameters) and 144 hours post-transfection (to determine any cell over-growth and its potential effect on assay window).

Despite transfection reagent-mediated cytotoxicity at 72 and 96 hours, HCT116 cells seeded at 2000 cells/well recovered well and achieved >90% reduction in viability (with the 'targetting' controls) at 120 and 144 hours (Figure17c and d). Significantly, it appeared that cells seeded at greater than 3000 cells/well elicited higher signals from the 'targetting' controls at the longest timepoints (120 and 144 hours), suggesting that either the knockdown was unsustainable over an extended time or that cell overgrowth masked the RNAi effects Figure17a-d). Hence, seeding at 2000 cells/well was selected for further optimisation as sustained targetted reduction in viability was achieved across all time-points.

Transfection reagent concentration optimisation

In order to reduce the non-specific toxic effect of HiPerFect on cells seeded at 2000 cells/well it was necessary to titrate the concentration of transfection reagent down from 15μl/ml. It also became evident during the course of the optimisation assays that the primary screen plates would have to be stored as frozen samples prior to ATPlite luciferase measurements due to the number of plates involved (564 plates in total). The expansion of the reagent in each well upon freezing increased the risk of well-to-well contamination (particularly at the defrosting stage), and as a consequence the total assay volume had to be reduced.

Figure 18a&b placement

Figure 18a

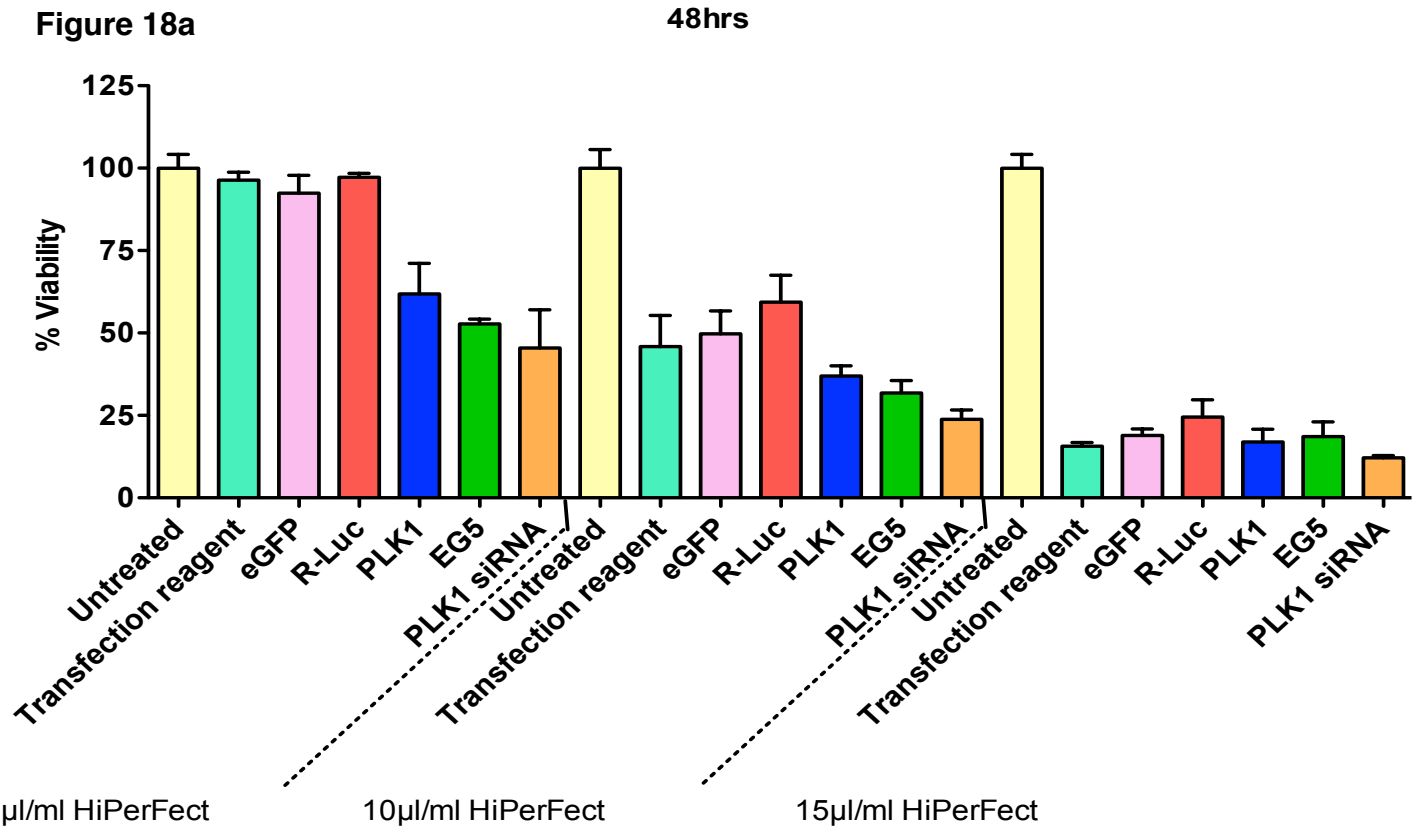

Figure 18b

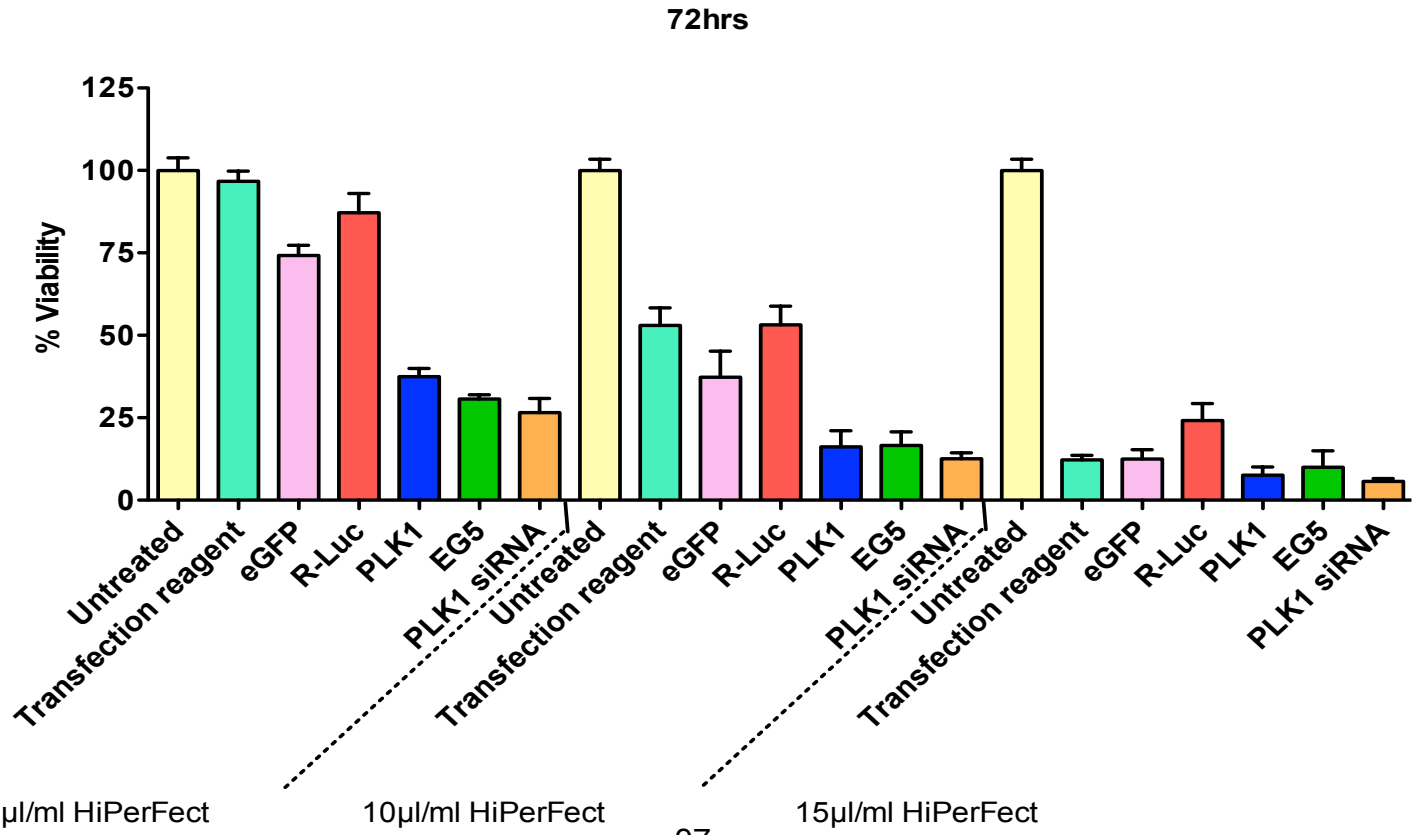

Figure 18c&d placement

Figure 18c

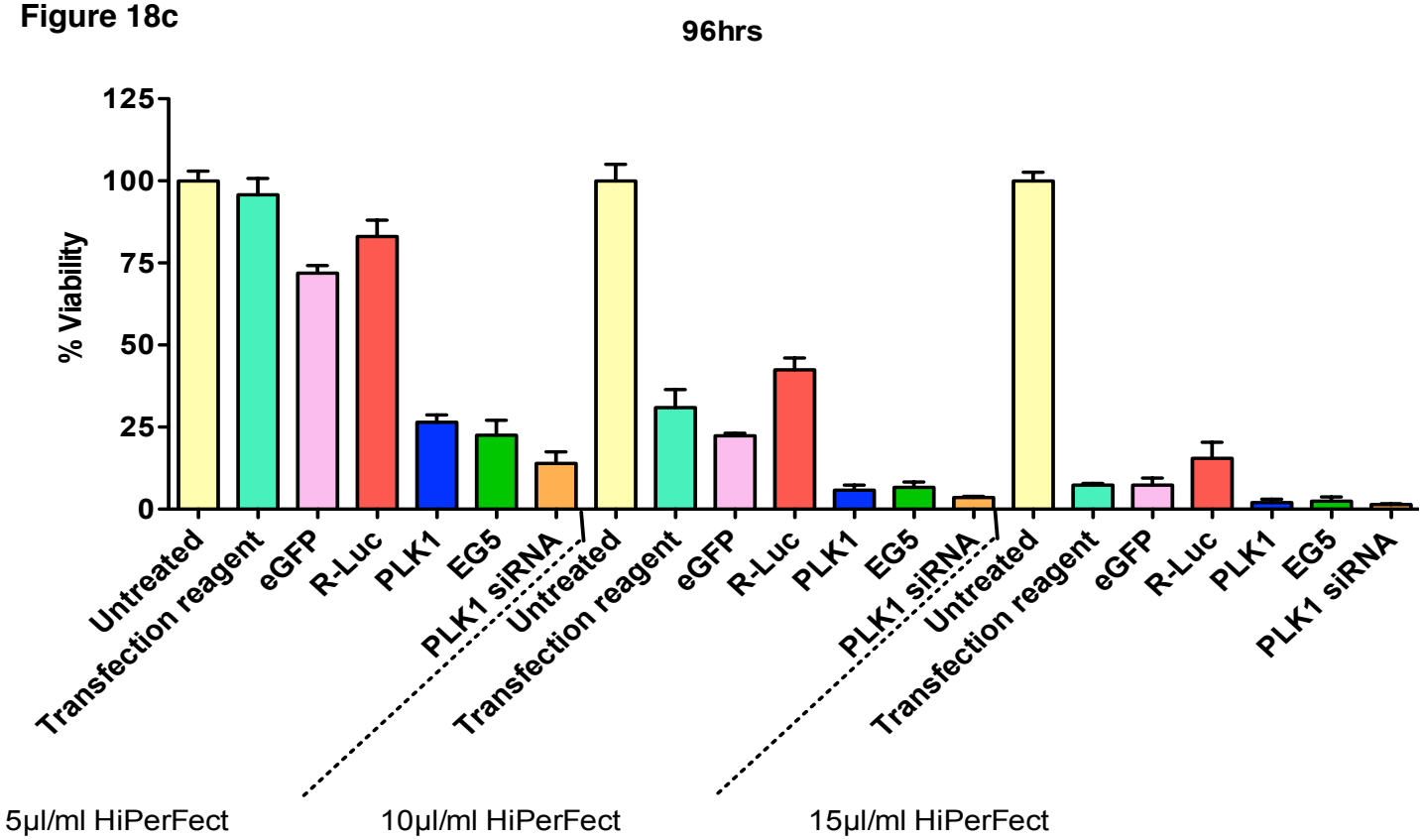

Figure 18d

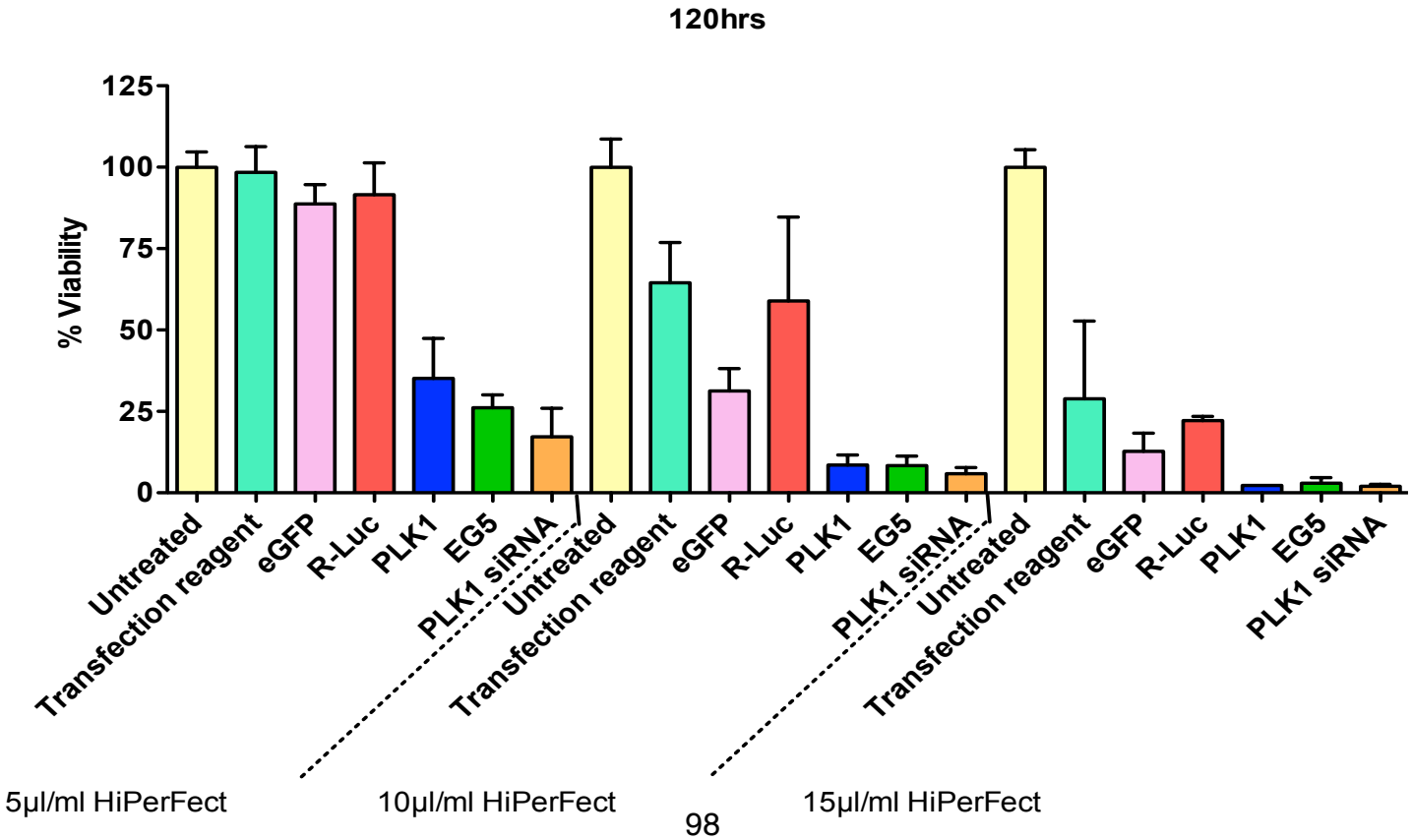

Figure 18e placement

Figure 18. Transfection reagent titration

Cells seeded at 2000cells/well were reverse transfected with 5, 10 and15μl/ml HiPerFect and cell viability mediated by the panel of control esiRNAs measured at **a.** 48, **b.** 72, **c.** 96, **d.** 120 and **e.** 144 hours post-transfection. Mean values ±S.D. of 3 repeats are displayed as percentage of untreated control.

Figure 18e

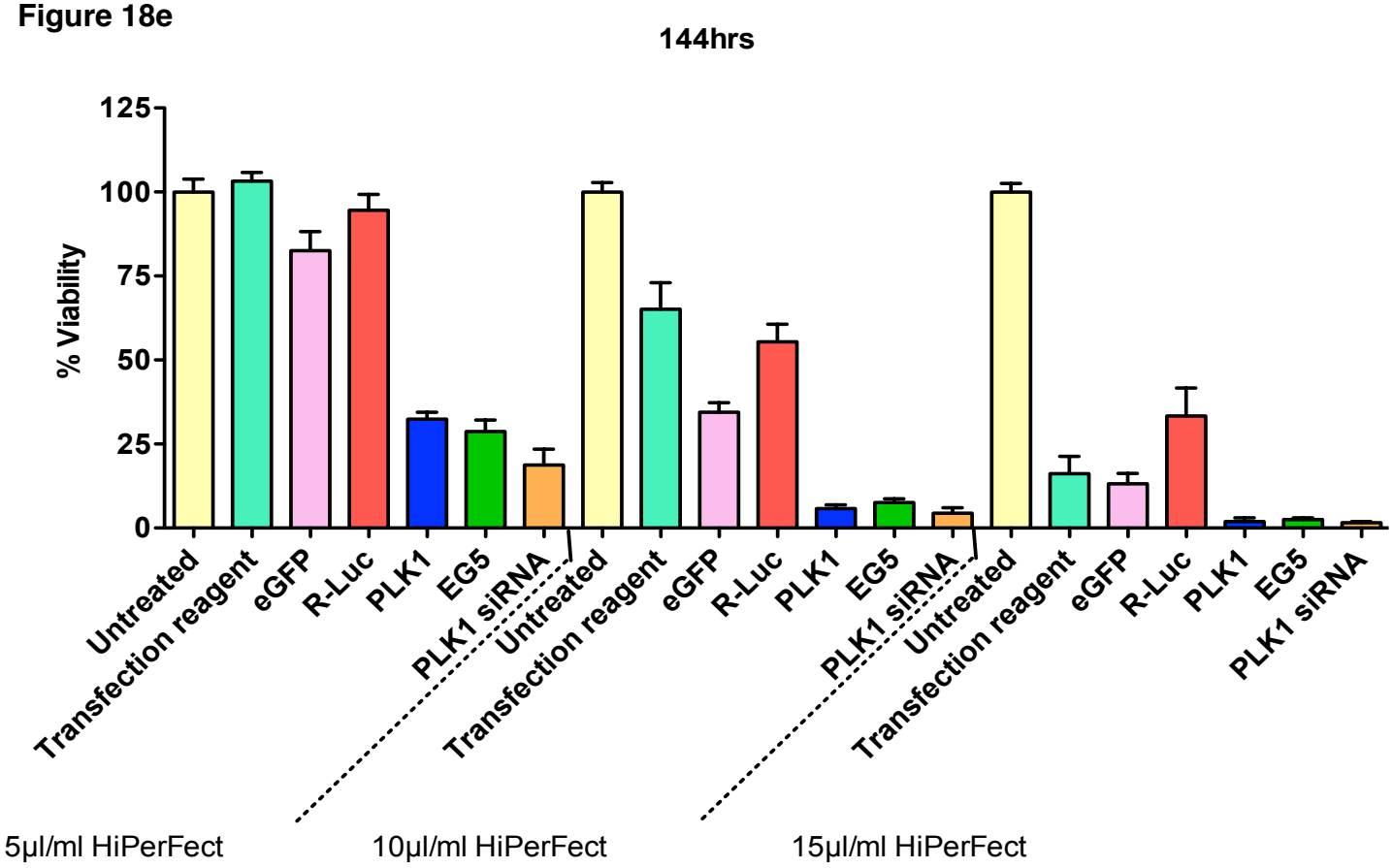

Figure 18. Transfection reagent titration

Cells seeded at 2000cells/well were reverse transfected with 5, 10 and15µl/ml HiPerFect and cell viability mediated by the panel of control esiRNAs measured at **a.** 48, **b.** 72, **c.** 96, **d.** 120 and **e.** 144 hours post-transfection. Mean values ±S.D. of 3 repeats are displayed as percentage of untreated control.

Using the previously described transfection 'control panel', 2000 cells/well were transfected using 5μl/ml, 10μl/ml and 15μl/ml HiPerFect (Figure 18a-e). The total assay volume was also reduced from 50μl to 30μl to prevent reagent overflow during the freeze-thaw process (by reducing both the cell seeding and transfection reagent mix volumes). Viability measurements were taken (using the ATPlite assay) at 48, 72, 96, 120 and 144 hours post-transfection in order to determine the complete range of RNAi effects.

As can be seen in Figure 18a-e, 2000 cells transfected with 5μl/ml HiPerFect resulted in consistent optimal non-targetted and targetted esiRNA effects (in particular from 72 hours onwards), with no non-specific transfection reagent cytotoxicity. It was evident, however, that the reduction in assay volume resulted in the previously minimally toxic HiPerFect concentration of 15μl/ml becoming highly non-specifically cytotoxic. This was likely due to the reduction in serum and nutrient-rich media concentrations, limiting the ability of the cells to recover from the transfection process. Nevertheless, transfection using the lower concentration of 5μl/ml HiPerFect prevented this effect, and was determined to be the optimal transfection reagent assay parameter.

Pre-assay cell culture conditions

To limit cross-screen variation it was essential that the HCT116 cells used were from the same batch and cultured for the same duration. Hence, cells could not maintained in continuous culture as they had been for the assay development process. As cells transfected directly from frozen were likely to require further extensive optimisation due to their post-thaw fragility, frozen cells were cultured for 72 hours prior to transfection (using the protocol described in the previous section; Figure 19a-e), and RNAi response compared to the previous assay using continually cultured cells.

Figure 19a&b placement

Figure 19a

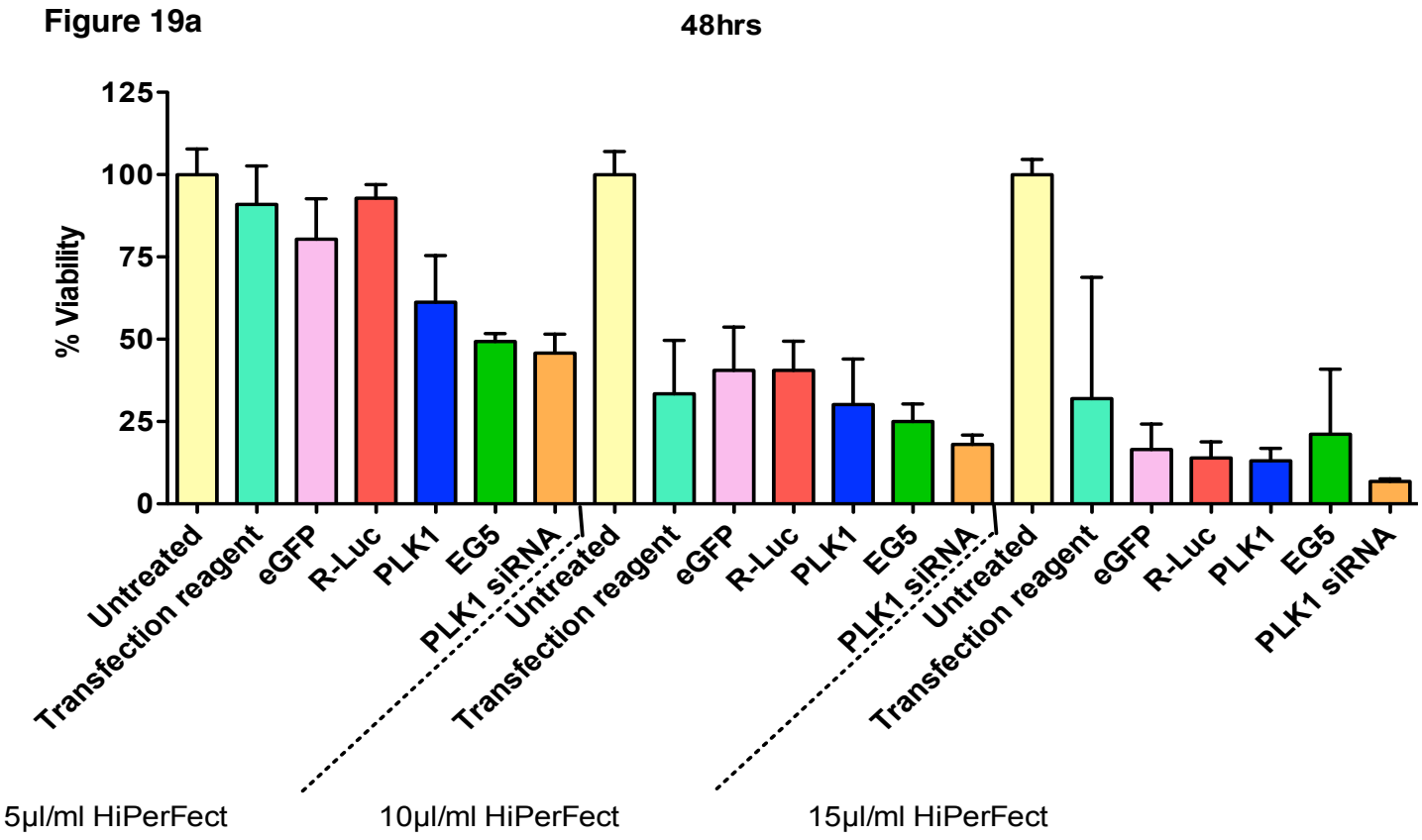

Figure 19b

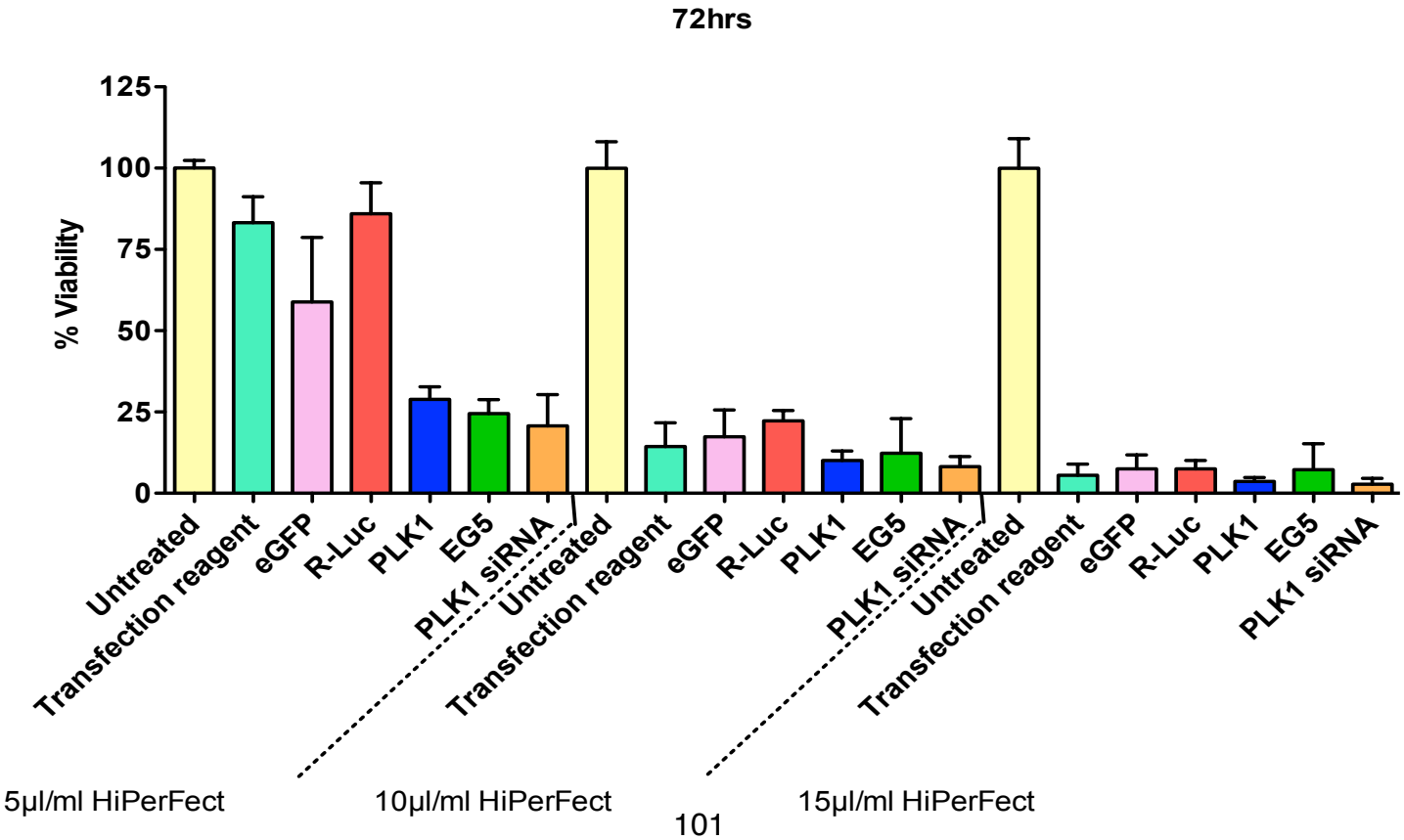

Figure 19c&d placement

Figure 19c

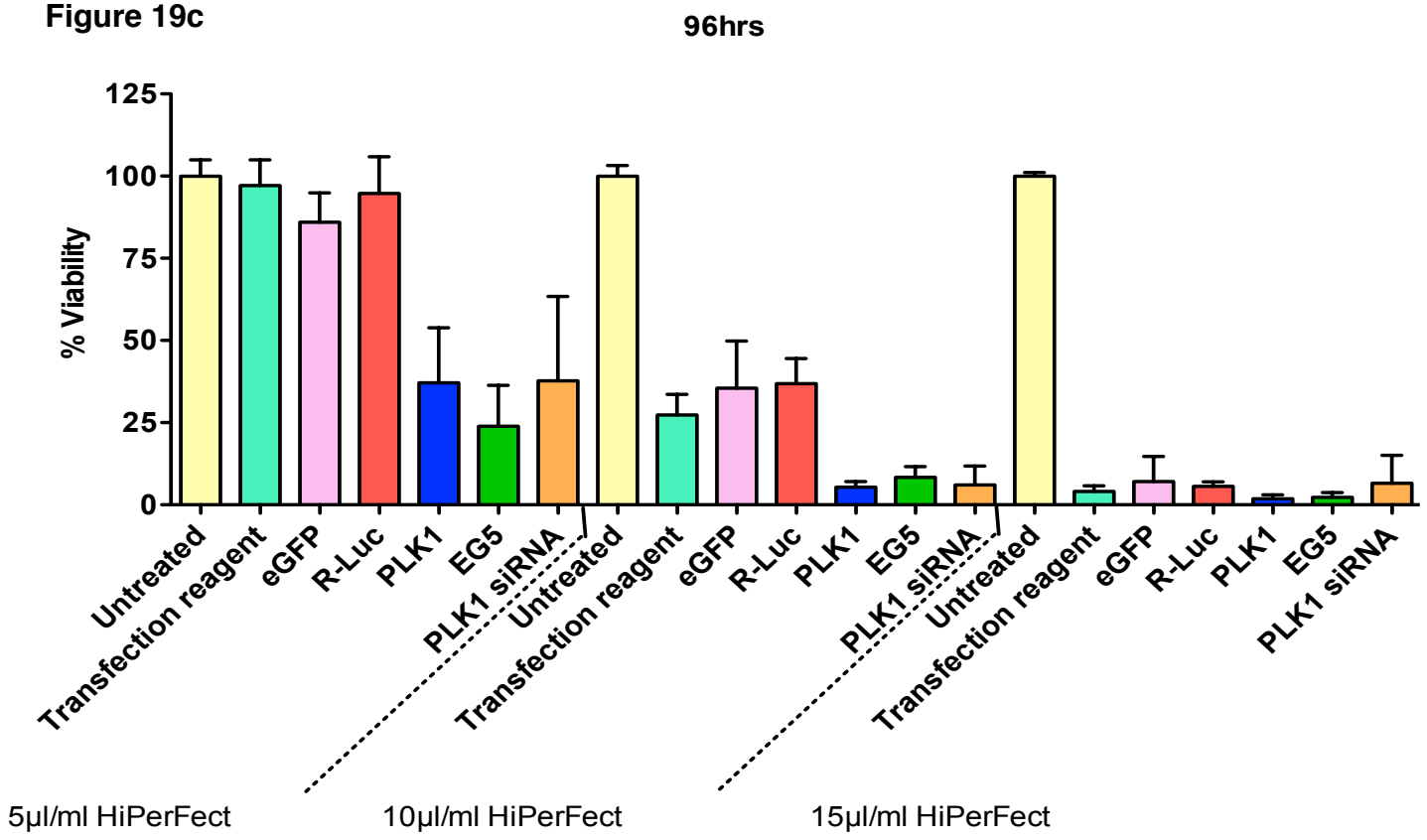

Figure 19d

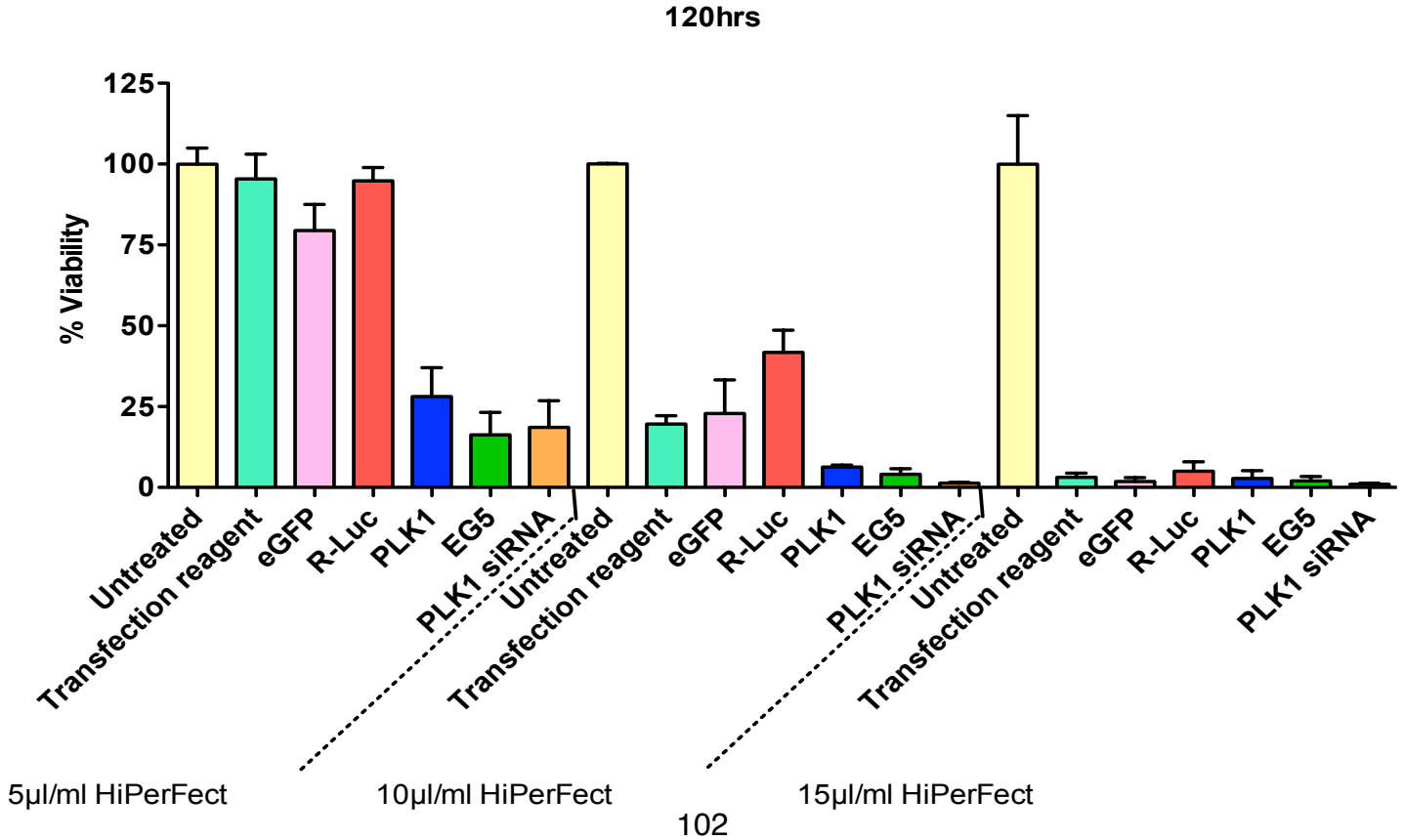

Figure 19e placement

Figure 19. Optimisation of conditions using defined-passage cells

HCT116 cells were thawed and cultured for 72 hours prior to assay seeding. Cells seeded at 2000cells/well were reverse transfected with 5, 10 and15μl/ml HiPerFect and cell viability mediated by the panel of control esiRNAs measured at **a.** 48, **b.** 72, **c.** 96, **d.** 120 and **e.** 144 hours post-transfection. 'Minimally-cultured cells' responded comparatively to long-term cultured cells, indicating that culturing cells in this method was suitable for HTS. Mean values ±S.D. of 3 repeats are displayed as percentage of untreated control.

Figure 19e

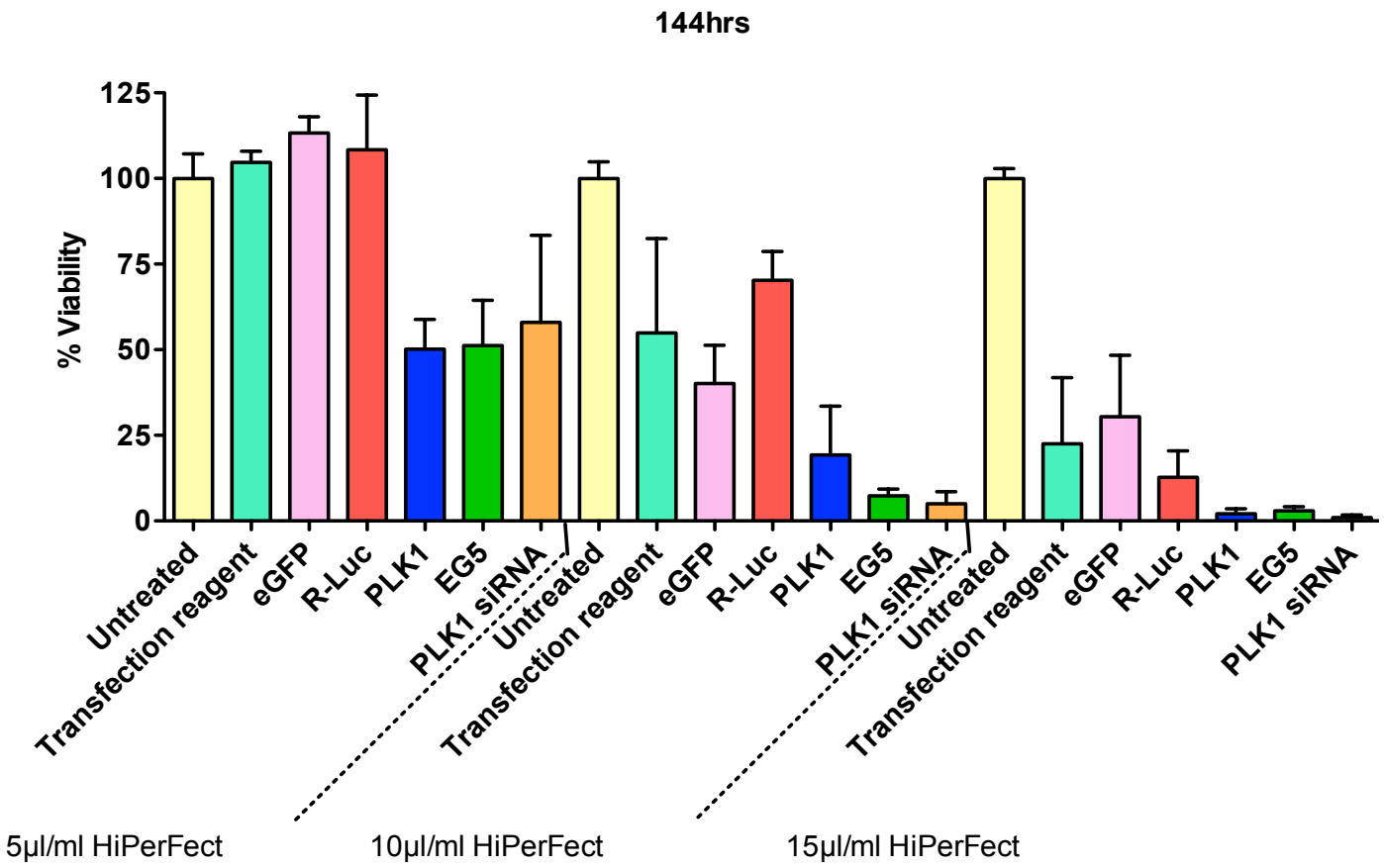

Figure 19. Optimisation of conditions using defined-passage cells

HCT116 cells were thawed and cultured for 72 hours prior to assay seeding. Cells seeded at 2000cells/well were reverse transfected with 5, 10 and15µl/ml HiPerFect and cell viability mediated by the panel of control esiRNAs measured at **a.** 48, **b.** 72, **c.** 96, **d.** 120 and **e.** 144 hours post-transfection. 'Minimally-cultured cells' responded comparatively to long-term cultured cells, indicating that culturing cells in this method was suitable for HTS. Mean values ±S.D. of 3 repeats are displayed as percentage of untreated control.

The minimally-cultured cells responded in a similar manner to the continually-cultured cells, however at 144 hours cells appeared to recover from targetted knockdown. Although this timepoint was beyond that of the final screen scope, this observation was noted and the 120 hour screen timepoint closely monitored for signs of cell overgrowth (which would mask 'true' viability reduction as cells began to suffer the effects of nutrient depletion).

Pilot screen

The optimisation process was carried out on a small scale with reagents being dispensed a single well at a time and plate ATPlite measurement times taking >5 minutes (per plate). However, this was not conducive to a high-throughput screen set-up, and as such semi-automated equipment, spacious tissue culture facilities and a rapid-reading luminometer were required. It was essential that the optimised assay was tested under the screen conditions to ensure that there were no alterations in assay performance upon transfer to the high-throughput setting.

Figure 20 placement

Figure 20. Pilot assay

Repetition of the final assay set-up (2000 cells/well, 5μl/ml HiPerFect) using high-throughput conditions (72 hour timepoint measured only) demonstrated that the assay was directly transferable and suitable for the HTS setting. Mean values ±S.D. of 3 repeats are displayed as percentage of untreated control.

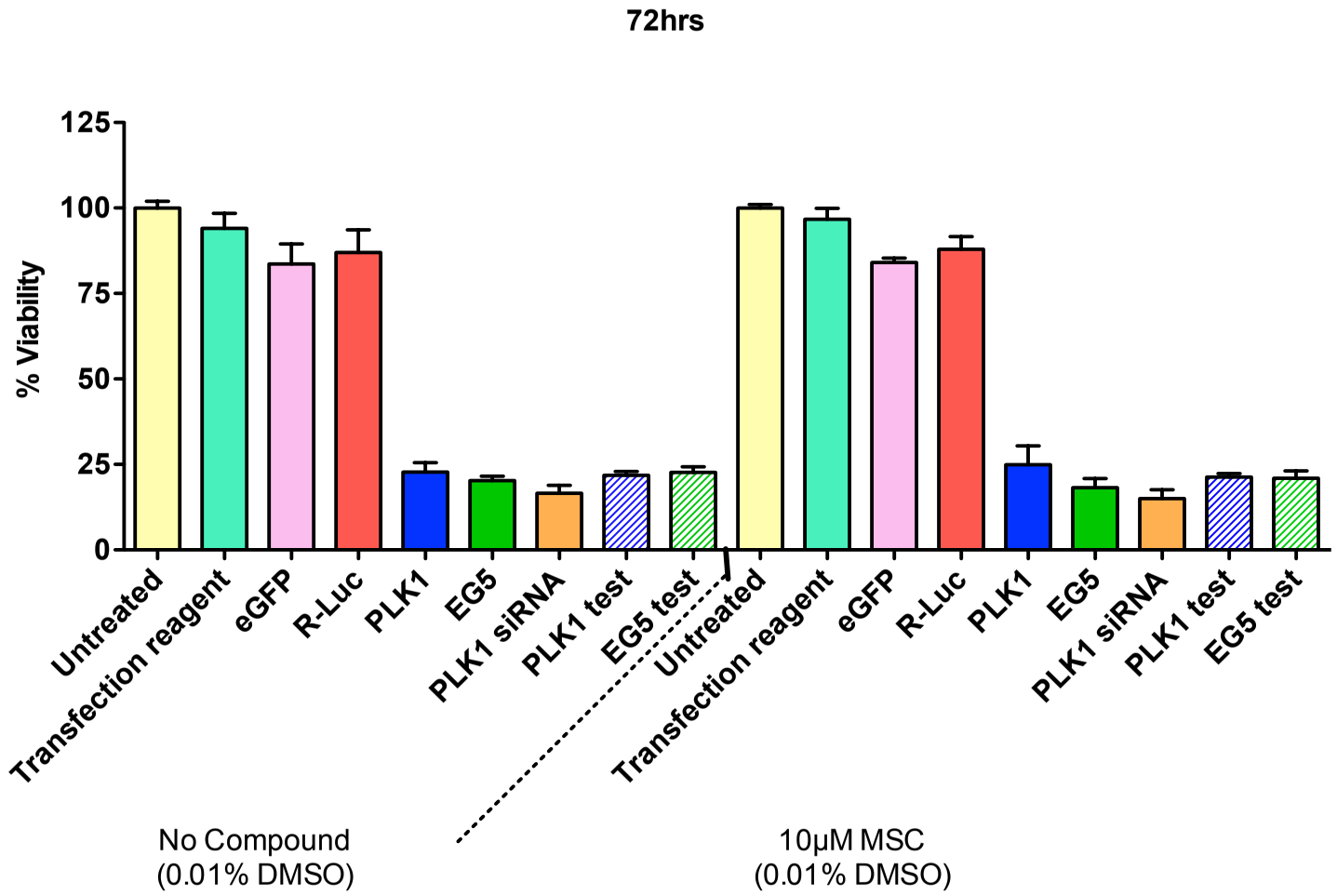

Figure 20. Pilot assay

Repetition of the final assay set-up (2000 cells/well, 5µl/ml HiPerFect) using high-throughput conditions (72 hour timepoint measured only) demonstrated that the assay was directly transferable and suitable for the HTS setting. PLK1 and EG5 from the esiRNA library were also tested. Mean values ±S.D. of 3 repeats are displayed as percentage of untreated control.

Cell response was assessed under the optimally established conditions (at the 72 hour timepoint alone for simplicity; Figure 20). In addition, PLK1 and EG5 from the esiRNA library were isolated and tested alongside the controls in order to confirm the library's viability (Figure 20; PLK1 test, EG5 test). These test esiRNAs performed comparatively to the control PLK1 and EG5, thus the library esiRNA reagents were determined to be functional and suitable for the high throughput screen.

A useful method for the determination screen of robustness (and the potential for false positive and negatives) is the calculation of the assay's Z-factor (Zhang et al., 1999). By comparing the 'high' (eGFP and R-Luc) and the 'low' (PLK1 and EG5) controls of the pilot test, the calculated Z-factor for the optimised assay was 0.55. A Z-factor of >0.5 in a cell-based screen is deemed to be excellent for high-throughput screening, and so this assay format was deemed suitable for the full-scale high-throughput screen.

Taken together the final conditions determined for the primary screen were:

- 2000 cells/well (batch-controlled)
- 5μl/ml HiPerFect
- 72 and 120 hour timepoint measurements
- LEADseeker luminometer; 3 second read

3.2.2 Primary esiRNA screen

The primary screen was conducted over a 35 day period and following cell lysis, plates were frozen down such that the ATPlite assays could be carried out in one session to enhance reproducibility. A total of 216,576 data points were acquired comprising 3 repeats of esiRNA transfections for 72 and 120 hour timepoints, in the presence and absence of MSC.

As a first step in the data analysis, internal controls that had been placed on each plate (eGFP, R-Luc, PLK1 and EG5 esiRNAs) were assessed on a per-plate basis to determine whether any plates had failed based on the dynamic range of the controls. As can be seen from the example in Figure 21, the controls on some plates failed and it was assumed that all data from the corresponding plate may have been compromised (using the criteria listed in Figure 21, a total of 62/564 plates were rejected from further analysis). Repeat esiRNA transfections were carried out for plates for which more than one of the triplicates had failed (one complete set of 72 hours + compound, and 120 hours + compound repeats required re-assessment). This ensured that at least 2 repeats existed for every plate, allowing a robust analysis to be carried out.

Figure 21 placement

Figure 21. Primary screen quality control

a. Examples of plate controls from a plate that 'passed' (1) and 'failed (2) quality control (from 72 hour timepoint). The 16 bars from each plate showing the relative luminescence units (RLU) are grouped into 4 repeats of 4 single well esiRNA control assays. From left to right, the sets are: eGFP (1-4), EG5 (5-8), R-Luc (9-12), PLK1 (13-16)). As can be seen, plate 1 showed clear effects of the EG5 and PLK1 cytotoxic esiRNAs while plate 2 showed no effect. **b**. The cut-off values used to include or exclude plates in further data analysis. Typical values indicate the approximate RLUs most commonly observed.

a

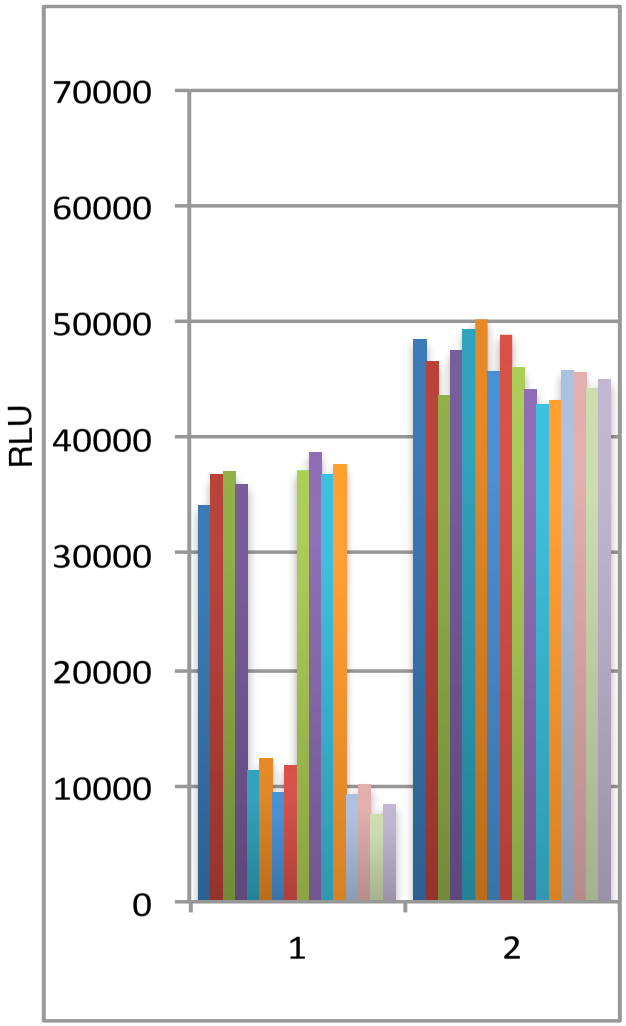

b

	72 hours	120 hours
"Non targetting" control cut-offs	>30,000	>50,000
Typical values	~40,000	~60,000
"Targetting" control cut-offs	<15,000	<25,000
Typical values	~15,000	~12,500

Figure 21. Primary screen quality control

a. Examples of plate controls from a plate that 'passed' (1) and 'failed (2) quality control (from 72 hour timepoint). The 16 bars from each plate showing the relative luminescence units (RLU) are grouped into 4 repeats of 4 single well esiRNA control assays. From left to right, the sets are: eGFP (1-4), EG5 (5-8), R-Luc (9-12), PLK1 (13-16)). As can be seen, plate 1 showed clear effects of the EG5 and PLK1 cytotoxic esiRNAs while plate 2 showed no effect. **b**. The cut-off values used to include or exclude plates in further data analysis. Typical values indicate the approximate RLUs most commonly observed.

Following the control assessment to ensure sufficient overall data quality, the primary data required pre-processing before statistical modelling and hit selection could be conducted. The R-based software package cellHTS2 was used for this purpose (see Methods 2.6.2.3 for details), which enabled relatively rapid processing of the large-scale whole-screen dataset according to selected parameters. Non-controls based normalisation of the screen dataset was conducted. Each repeat was first normalised relative to the plate median (this is less prone to being skewed by extreme outliers than the mean value). The nature of high-throughput screening means that it can be assumed that the majority of samples screened are 'inactive' providing an accurate representation of the plate's true 'central value'. As such, normalised sample values represented deviation from the whole-plate sample median. This method was used in preference to control-based normalisation, as although control-based normalisation scales data within a defined range (with the non-targetting and targetting controls acting as the upper and lower boundaries respectively in this instance) and account for plate-to-plate variations in assay window, the controls, due to their lower numbers are susceptible to greater error.

Using cellHTS2, each normalised cellular viability value (derived from ATPlite luminescence) was assigned a B-score. The B-score value was generated using an algorithm that incorporates parameters that help control for plate-based screening artefacts, for example the variation in temperature across a plate that can result in 384-well plate dependent edge effects ((Brideau et al., 2003); see Methods 2.6.2.3). The B-score is a modified measure of the data point variance from the median. At this point the B-score values were assigned to their corresponding gene identity (as detailed in the esiRNA library plate/well Ensembl ID file) and were stored as an excel file that is available on the attached data CD, Appendix 7. These gene-associated cellular viability B-scores were subsequently used for esiRNA effect modelling.

A statistical model was required that was capable of identifying hits that exhibited synergistic synthetic lethality when compound treatment was combined with gene

targetting, compared with RNA-mediated target knockdown (RNAi) or compound effects alone. This 'Linear Model Interaction Test' was developed by Dr. Eike Staub of the department of Discovery Bioinformatics, Merck Serono (and implemented using the R statistics package version 2.9.1). Details of the model are described in Methods. In brief, the relationship of the dependent variable (cellular viability B-score, resulting from previously described normalization procedures) and the two independent variables i.e. esiRNA knockdown (yes/no) and compound treatment (yes/no) were assessed using a linear model:

$$\text{Viability} \sim \text{esiRNA} + \text{MSC} + \text{esiRNA:MSC}$$

Thus, the model was developed to include the interaction between esiRNA and MSC combination treatment as the main target parameter, as we were interested primarily in effect on ATP levels that was exerted by treatment with both esiRNA and MSC in combination, but to a lesser extent by esiRNA or compound alone. Hence, an 'interaction value' was determined that statistically summarised synergy (including the interaction significance) between compound and RNAi, whilst taking the effect of esiRNA knockdown alone on cellular viability into consideration.

Two interaction values were generated for each sample; a 72 hour and a 120 hour timepoint interaction value. The interaction values for the 120 hour dataset were plotted in order to give a visual indication of whole-screen performance (Figure 22).

Figure 22 placement

Figure 22a&b. Visualisation of 120 hour primary screen interaction data

Following esiRNA transfection of HCT116 cells and treatment with MSC, an 'interaction value' of the effect of the combination was statistically determined. Negative interaction values indicate a reduction in ATP levels as a result of synthetic interactions in HCT116 cells (e.g. decreased cell proliferation, increased apoptosis or a reduction in ATP levels), whilst positive values indicate a synthetic increase in 'viability'. The combination interaction value for each sample is shown individually, and each of the plates is individually coloured. Due to the size of the screen the data has been split into two panels; **a** - plates 1 to 24, **b** - plates 25 to 47.

****ON OPPOSITE PAGE****

Figure 22a

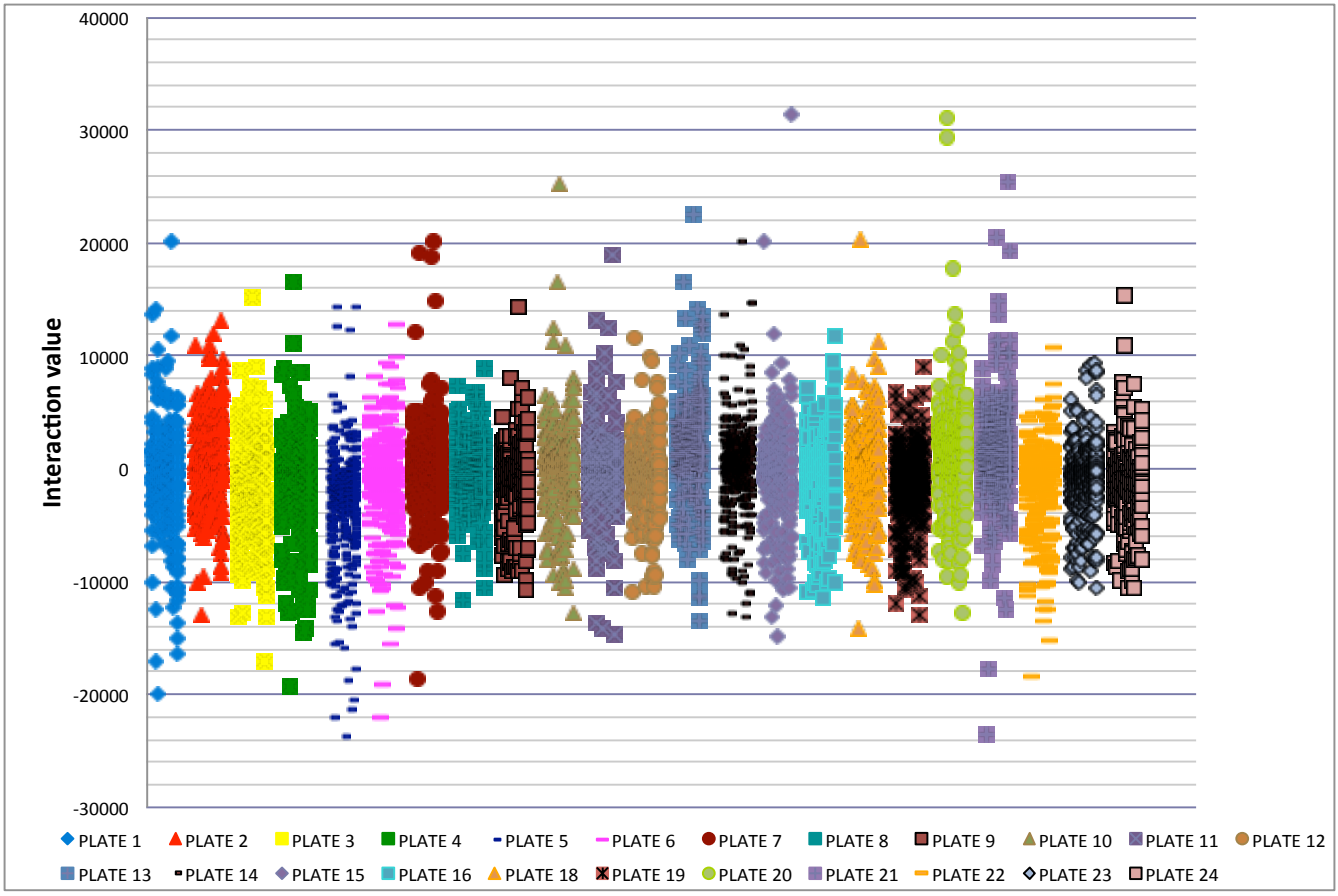

Figure 22b

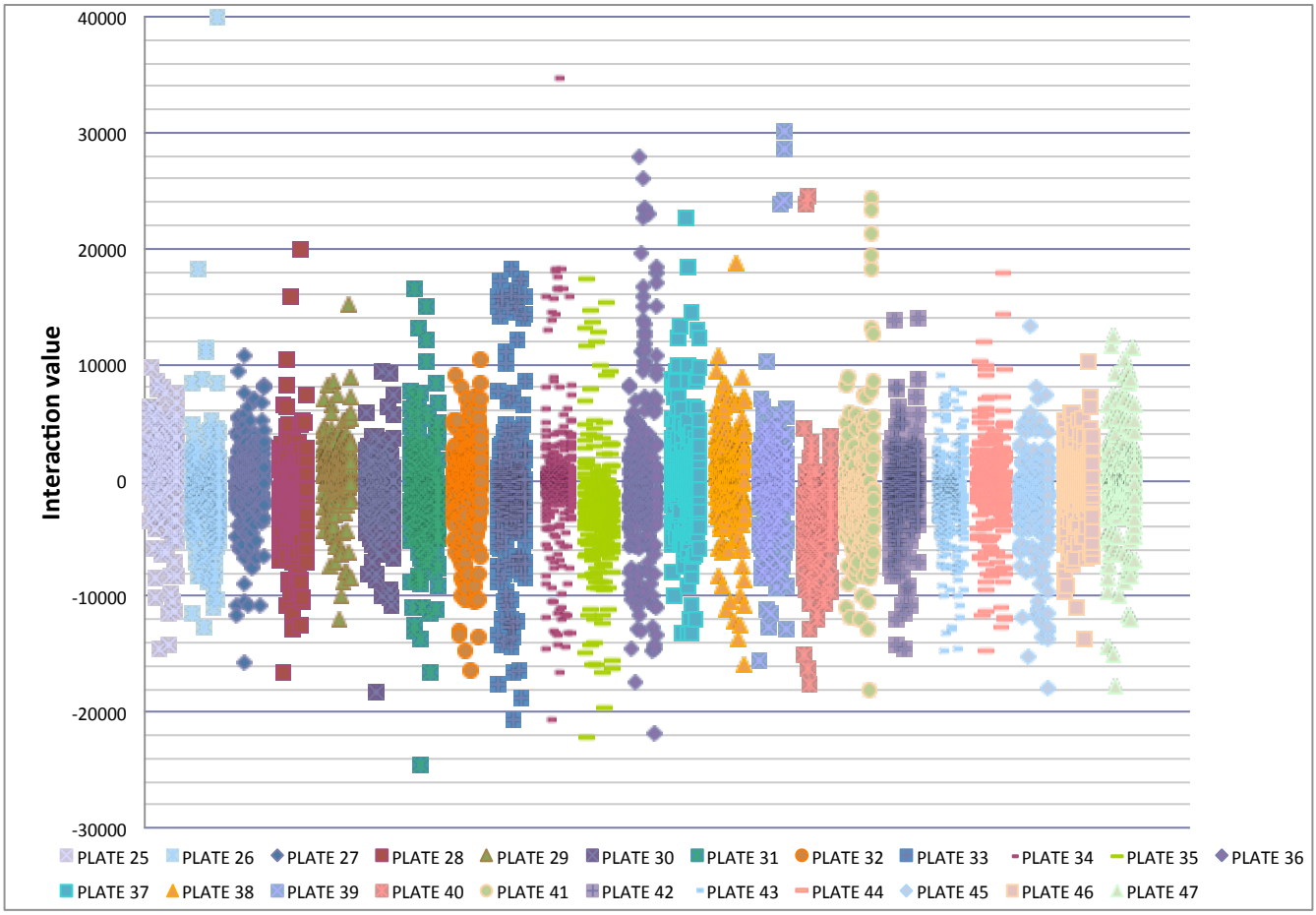

Figure 22 illustrates the spread of the RNAi-MSC interaction values on a plate-by-plate basis. The majority of the 368 samples on each plate had little or no effect, and had interaction values centred between -10,000 - +10,000. Synthetic-interactions leading to a reduction of ATP levels in the presence of esiRNA and MSC are indicated by negative values, whilst positive values indicated RNAi-MSC dependent increase in ATP levels. Negative interactions can be interpreted as an alteration in cell numbers (e.g. 'viability reduction' through reduction in cellular proliferation or an increase in cell death) or as a reduction in the ATP level per cell. For selected esiRNA:MSC combinations, it was clear that alterations to total cell numbers were responsible for synthetic interactions although this was not systematically examined. Unless specifically stated, subsequent comments on 'cell viability' as characterised in the primary and reconfirmation screens will actually refer to a reduction in ATP levels as this is the most likely interpretation.

Interestingly, some plates exhibit a greater number of hits at either end of the interaction scale than others. A possible explanation for this was that although the genes were randomly distributed across the plates, the genes that were easiest to clone (and so generate esiRNA against) were located in the earlier plates, with genes of unknown function or pseudogenes located in the later plates. Importantly, it was evident that the screening method and chosen data analysis were capable of identifying putative hits for further investigation, and these linear model interaction values were subsequently used for hit selection (discussed below).

3.2.3 Hit selection

The objective of the screen was to determine a defined hit (or hits) whose silencing in combination with MSC resulted in loss of HCT116 viability. However, there are in reality many different categories of potential interactions between an esiRNA and the MSC compound, which are important to consider prior to hit selection. These are graphically illustrated in Figures 23a and b, together with an approximation of the number of hits that were observed in each category based on the relevant interaction score. Conceptually simple synthetic interactions are shown in Figure 23a and more complex interactions in Figure 23b. Failure to discriminate these hits classes may have resulted in the selection of false positive interactions for further analysis.

Figure 23a placement

Figure 23a. Simple synthetic interactions

Schematic representation of the four 'simple' RNAi-MSC interaction outcomes. Hypothesised decrease in HCT116 viability is shown by a negative interaction value, and increase in viability is shown by a positive interaction value. MSC alone had no effect on viability across all conditions and so is only shown once for clarity.

1. MSC alone = no effect
   esiRNA alone = no effect
   esiRNA+MSC = no effect
2. esiRNA alone = no effect
   esiRNA+MSC = complete reduction in viability
3. esiRNA alone = no effect
   esiRNA+MSC = moderate reduction in viability
4. esiRNA alone = no effect
   esiRNA+MSC = increase in viability

Approximate percentage of samples (in relation to the whole screen) falling into each category is shown.

****ON OPPOSITE PAGE****

Figure 23a

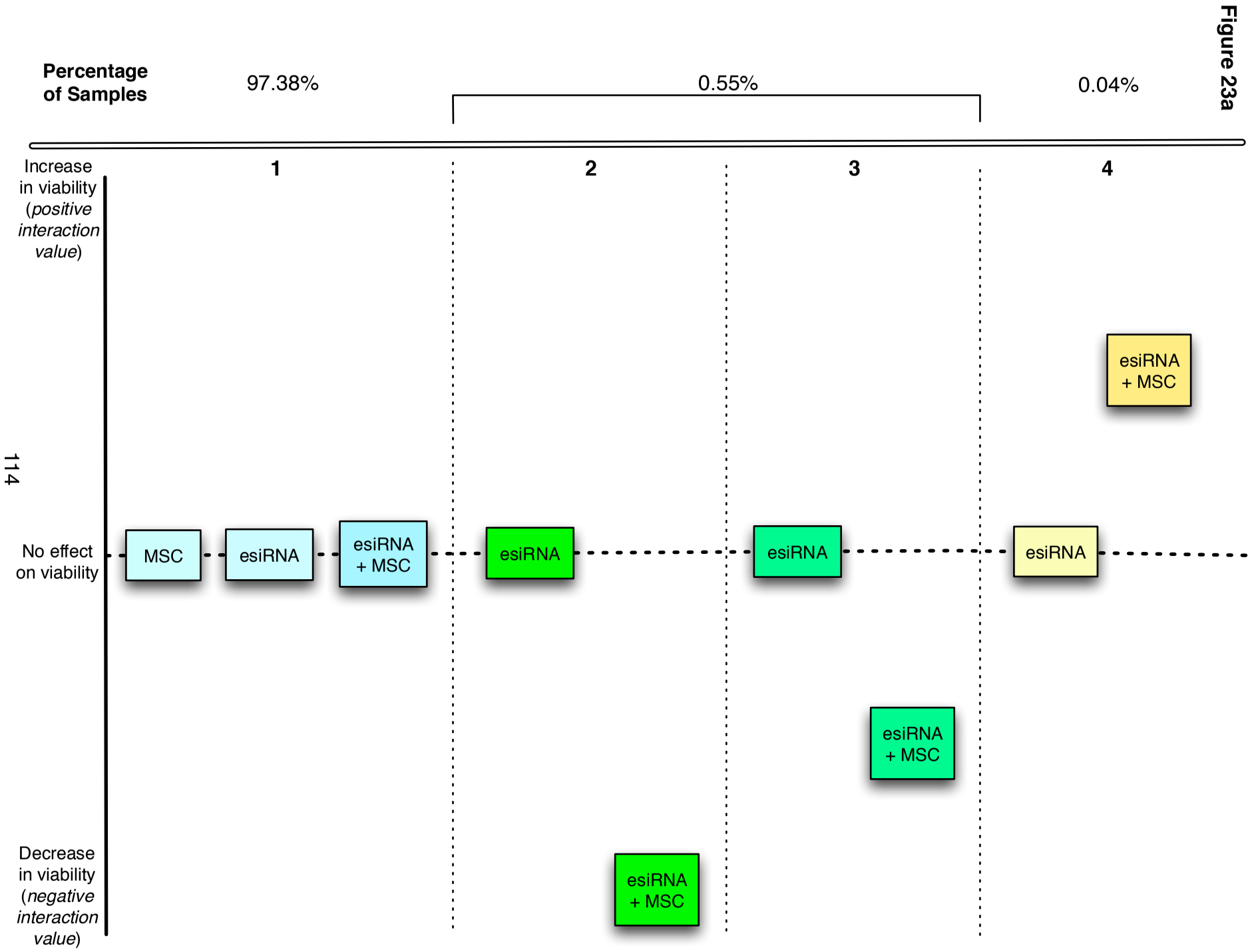
Percentage of Samples
97.38%
0.55%
0.04%
1
2
3
4
Increase in viability (positive interaction value)
No effect on viability
Decrease in viability (negative interaction value)
MSC
esiRNA
esiRNA + MSC
esiRNA
esiRNA
esiRNA
esiRNA + MSC
esiRNA + MSC
esiRNA + MSC
114

Figure 23b placement

Figure 23b. Complex synthetic interactions

Schematic representation of the hypothesised complex RNAi-MSC interaction outcomes. Decrease in HCT116 viability is shown by a negative effect value, and increase in viability is shown by a positive effect value. Scenario 1 from Figure 23a is shown for comparison.

i. esiRNA alone = marginal to moderate reduction in viability
   esiRNA+MSC = moderate to large reduction in viability
ii. esiRNA alone = moderate increase in viability
   esiRNA+MSC = no effect
iii. esiRNA alone = moderate reduction in viability
   esiRNA+MSC = no effect

Approximate percentage of samples (in relation to the whole screen) falling into each category is shown.

****ON OPPPOSITE PAGE****

Figure 23b

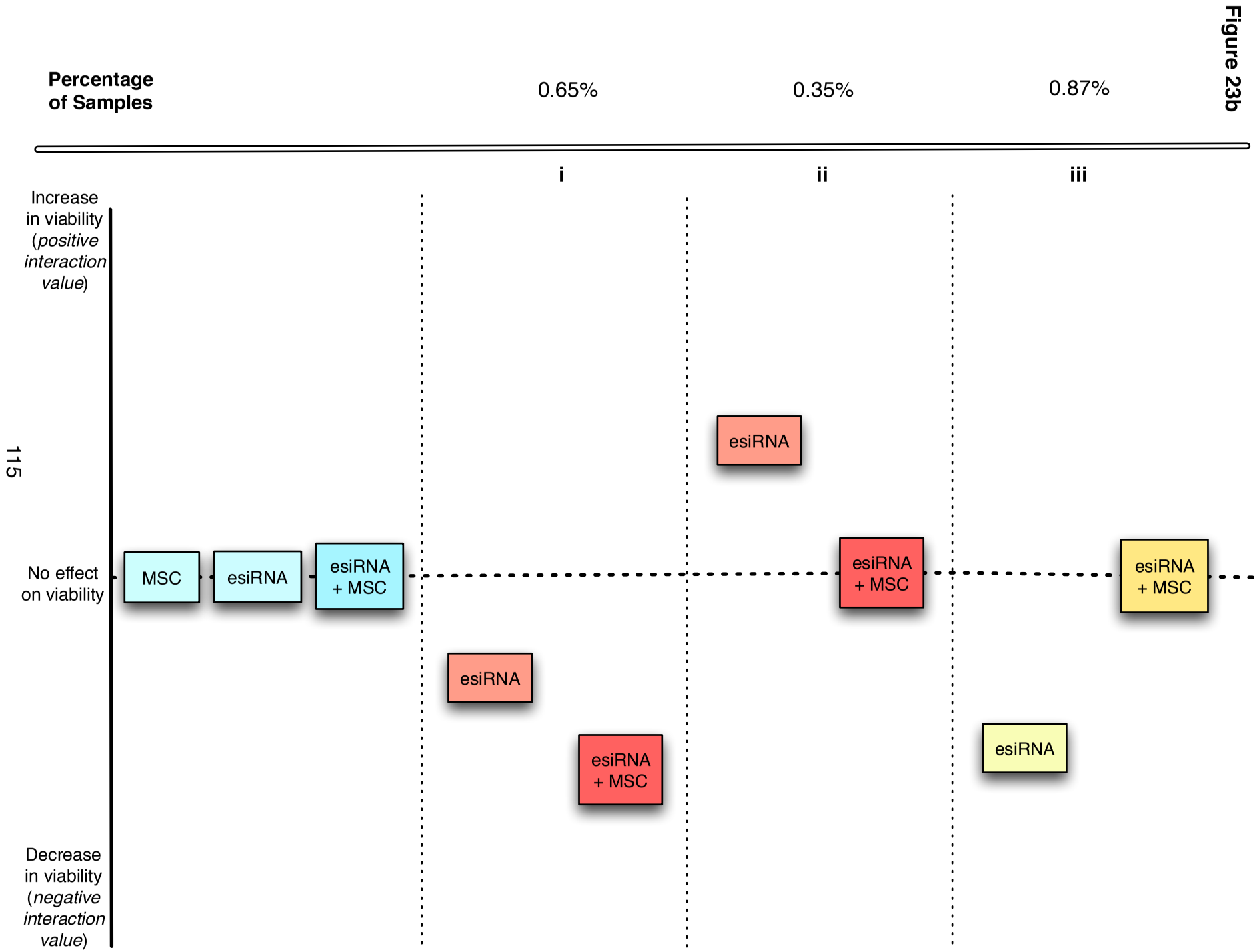
Percentage of Samples
0.65%
0.35%
0.87%
i
ii
iii
Increase in viability (positive interaction value)
No effect on viability
Decrease in viability (negative interaction value)
MSC
esiRNA
esiRNA + MSC
esiRNA
esiRNA + MSC
esiRNA
esiRNA + MSC
esiRNA + MSC
esiRNA

The interpretation of the different hit categories in Figure 23a is discussed in more detail:

Figure 23a shows simple interactions, 4 types of which can be described:

1. No interaction (blue). The vast majority of esiRNAs had no effect on cell viability and did not co-operate to alter cell viability with MSC.
2. Strongly decreased signal (dark green). These were the desired category of hits showing a strong synthetic interaction between MSC and esiRNA.
3. Moderate synthetic effect (pale green).
4. Positive effect on cell viability (yellow). The combination of MSC treatment and esiRNA knockdown had a positive effect on the ATPlite readout. The reason why ATP levels would increase following esiRNA and MSC treatment are unclear but could be because ATP synthesis or degradation rates are disturbed within target cells or because loss of the esiRNA targets increased cellular proliferation rates or decreased levels of cell death.

More complex synergies are summarised in Figure 23b. These include 3 types:

i. One where esiRNA inhibition alone moderately decreased cellular viability, while the addition of MSC further reducing it. This was a potential ‘grey area’ of the screen, as hits located within this category may have been valuable ‘true hits’, however there was also the potential risk that these were ‘false leads’ resulting from off-target toxicity of MSC in that were already suffering from an esiRNA-dependent reduction in integrity (Figure 23b, condition i).
ii. One where gene silencing increased ‘viability’ which was then reduced to normal levels in the presence of MSC (Figure 23b, condition ii); resulting in a negative interaction value.

iii. One where the esiRNA:MSC combinations increased cell proliferation when esiRNA alone reduced cell viability (Figure 23b, condition iii), again resulting in a positive interaction value.

The approximate percentage of samples within each category (in relation to the whole screen) is summarised in Figure 23. These values were generated with reference to the output of the linear interaction statistical model (see Methods for details). For the simple category 2/3 hits described above, the selection criteria that were used were:

- Interaction value < -1000
- esiRNA p value > 0.1
- Ratio (interaction p value / esiRNA p value) < $1x10^{-2}$

Using appropriately adapted parameters (see Methods), the hits in the other hit categories were identified and counted as a proportion of the total esiRNAs as shown in Figure 23:1.

Two examples of single esiRNA data outputs and the values generated by the linear interaction model analysis are illustrated in Figure 24. Figure 24a shows the interaction of HARS (histidyl-tRNA synthetase; 'PlusCmpd-sample') with MSC, in relation to HARS alone (NoCmpd-sample) and the eGFP control in the absence and presence of MSC (NoCmpd-egfp and PlusCmpd-egfp respectively). This is an example of a clear synthetic lethal interaction (*c.f.* Figure 23a:3), with a large significant interaction value, and a minimal insignificant RNAi value. A second example in the form of a 'hit' that would be selected based on its interaction value alone is demonstrated with CD79B (CD79b molecule, immunoglobulin-associated beta; Figure 24b). However, this hit could prove to be a 'false positive' if selected as RNAi alone affects viability, thus resulting in a complex esiRNA:MSC interaction (*c.f.* Figure 23b:i).

Figure 24a placement

Figure 24a

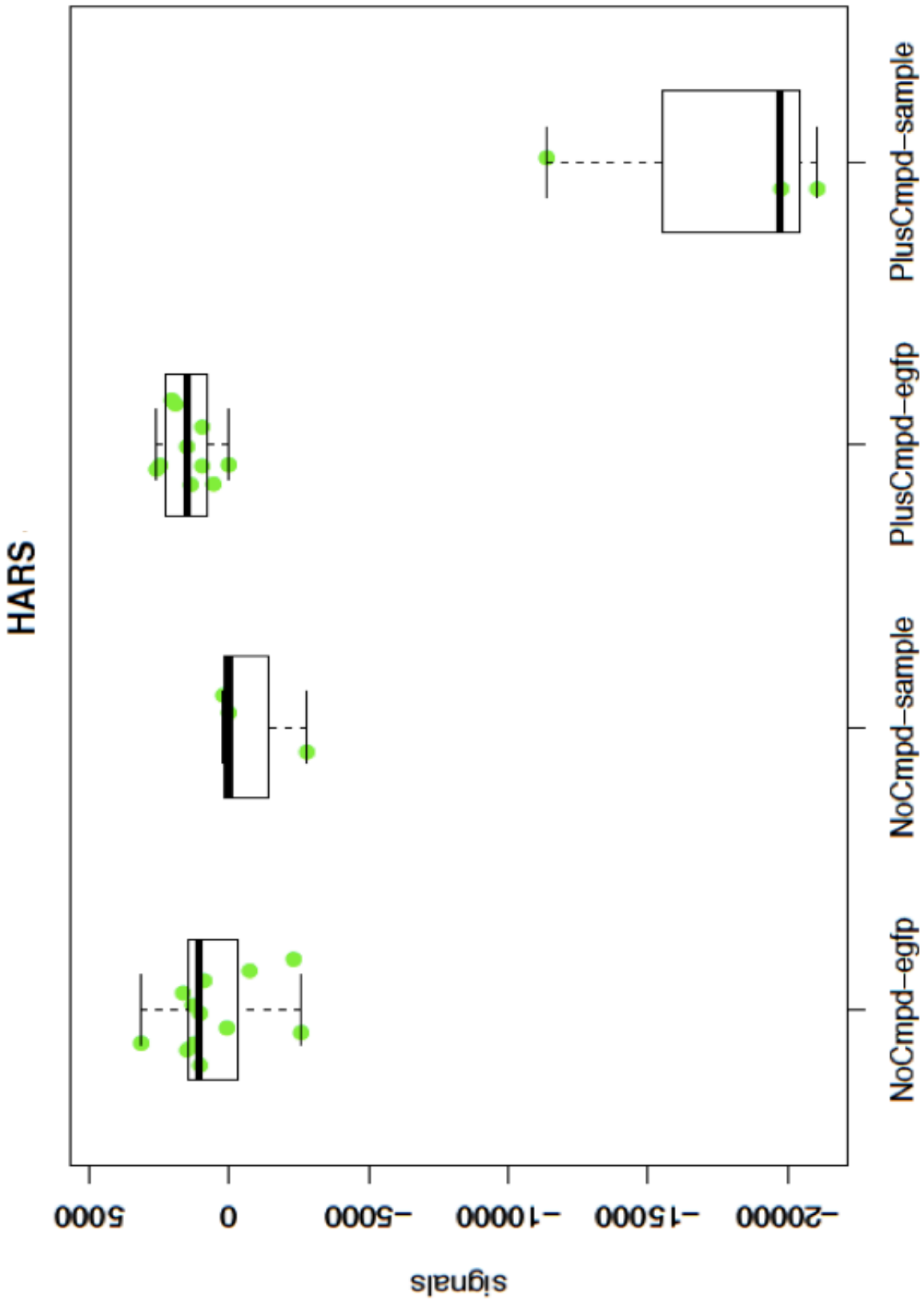
HARS
signals
5000
0
−5000
−10000
−15000
−20000
NoCmpd−egfp
NoCmpd−sample
PlusCmpd−egfp
PlusCmpd−sample

Figure 24b placement

Figure 24. Example hits from the primary esiRNA screen

Box and whisker plots for **a**. HARS, **b**. CD79B are shown. 'Signals' on the Y-axis denote the 'interaction effect' (y). On the X-axis, the eGFP -/+ compound controls are shown alongside the sample +/- compound for cells treated for 120 hours with esiRNA followed by 72 hours with compound. Individual well readings are represented as green dots while the median of the readings is shown as a thick black bar. The light box covers the interquartile range (25% and 75% quartiles) while the whiskers show the most extreme datapoints.

****ON OPPOSITE PAGE****

Figure 24b

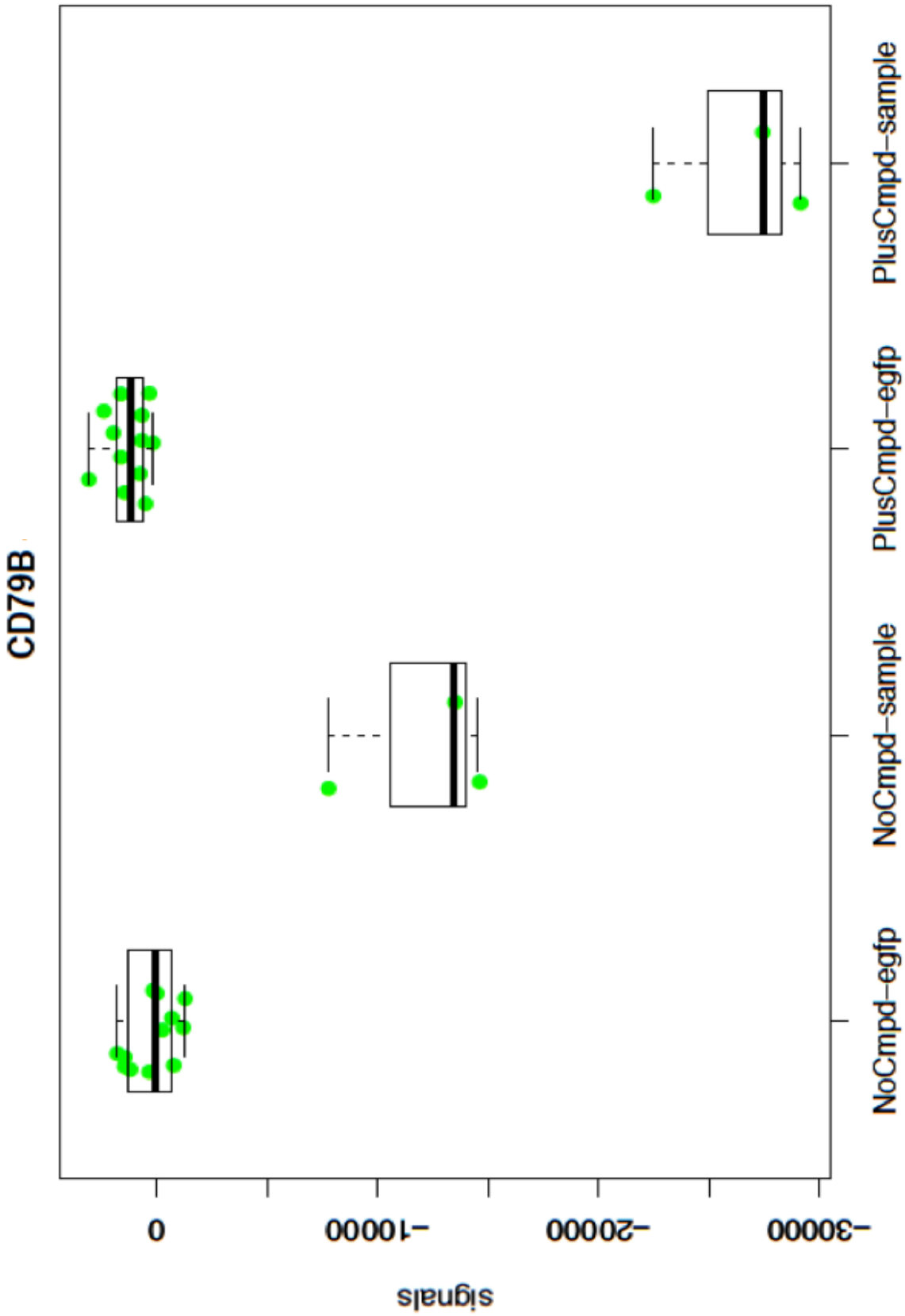
CD79B
signals
0
−10000
−20000
−30000
NoCmpd−egfp
NoCmpd−sample
PlusCmpd−egfp
PlusCmpd−sample

The aim of the screen was to focus on hit genes whose inhibition resulted in HCT116 lethality conditionally in the presence of MSC (Figure 23a:2+3, Figure 24a), In order to identify significant hits (and reduce false positive hit selection), stringent criteria were implicated to select conditionally lethal genes based on the linear model statistical output. These were:

- Interaction value < -1000
- esiRNA p value > 0.1
- Ratio (interaction p value / esiRNA p value) < $1x10^{-2}$

These parameters defined hits that had significant interaction values less than -1000 (i.e. loss of viability), with no significant effect of esiRNA alone. Furthermore, selecting hits with an interaction:esiRNA p value ratio less than $1x10^{-2}$ ensured that putative hit gene effects were genuine, and not simply on the borderline of significance. This provided a more effective way of conclusively defining hits than simply ranking hits (by interaction values, for example) as it factored in false positive elimination strategies.

Only hits that satisfied all selection criteria were chosen for reconfirmation. In total, 83 genes that elicited RNAi-MSC dependent synthetic lethality fulfilled the necessary selection requirements. Interestingly, no esiRNAs were found that induced complete cell killing in the presence of compound; the maximal effect recorded was ~45% killing. Furthermore, only samples from the 120 hour assay timepoint passed the screen quality selection criteria. The list of these primary hits (ranked according to their interaction p value) is shown in Table 2. In addition to the principal means of selection, a further 10 hits that met some but not all of the selection criteria were chosen, as they were of potentially biologically relevant or interesting. JAK3, for example, was selected due to the known ability of the activated JAK/STAT pathway to mediate cellular proliferation and tumour growth in cancer (Klampfer, 2008), and evidence that JAK/STAT signalling functions synergistically with Wnt signalling in cancer (Lin et al., 2011), and hence this was a biologically relevant hit. Conversely, Dkk2, a Wnt

signalling antagonist, would hypothetically confer a degree compound resistance when inhibited. However, a significant interaction effect of -12,700 was observed, thus this could serve to be a biologically interesting hit. This subset of manually selected hits is listed under the primary hits in Table 2 (in alphabetical order). The gene list was analysed for over-representation of annotations in the GO categories of biological process, molecular function and cellular component (as described in Results 3.1). The DAVID bioinformatics database (Huang et al., 2009a) was searched in addition to GeneCodis. The gene products were also compared to both the KEGG and Ingenuity (Ingenuity® Systems) collections for enrichment of specific pathway features. However, no significant enrichment was identified.

Hit Rank	Gene Name	Ensembl ID	Interaction p value	Interaction Value
1	HARS	ENSG00000170445	1.29E-06	-17000
2	MEN1	ENSG00000133895	3.85E-05	-12700
3	PTPN14	ENSG00000152104	4.36E-05	-10100
4	FKBP10	ENSG00000141756	5.18E-05	-13400
5	PLEKHG4B	ENSG00000153404	8.62E-05	-7460
6	LIMCH1	ENSG00000064042	1.00E-04	-7500
7	HPD	ENSG00000158104	0.000103	-13500
8	SERF1A	ENSG00000172058	0.00015	-5910
9	IL4R	ENSG00000077238	0.000161	-13200
10	DDX55	ENSG00000111364	0.000368	-8430
11	KIF27	ENSG00000165115	0.000441	-5730
12	SKA1	ENSG00000154839	0.000534	-15500
13	IL2RB	ENSG00000100385	0.000612	-8230
14	OR51E1	ENSG00000180785	0.000652	-6040
15	UGP2	ENSG00000169764	0.000673	-7650
16	GEMIN6	ENSG00000152147	0.000707	-13100
17	NOP14	ENSG00000087269	0.000863	-8400
18	FOLR3	ENSG00000110203	0.000982	-11500
19	CELA3A	ENSG00000142789	0.00109	-7390
20	TPT1	ENSG00000133112	0.00103	-10100
21	MTAP	ENSG00000099810	0.0012	-5740
22	PRSS38	ENSG00000185888	0.00134	-8370
23	C2orf69	ENSG00000178074	0.00142	-12000
24	SLC12A6	ENSG00000140199	0.00143	-24600
25	CCDC30	ENSG00000186409	0.00155	-3970
26	C2orf76	ENSG00000186132	0.00174	-9880
27	SLC25A39	ENSG00000013306	0.00185	-8970

28	PLD6	ENSG00000179598	0.0019	-12800
29	U2AF2	ENSG00000063244	0.0019	-9090
30	NHEJ1	ENSG00000187736	0.00205	-4100
31	TRIM28	ENSG00000130726	0.00223	-8110
32	THAP6	ENSG00000174796	0.00234	-13100
33	ULK1	ENSG00000177169	0.00234	-6280
34	CRHR2	ENSG00000106113	0.00247	-5510
35	FOXG1	ENSG00000176165	0.00292	-12500
36	FBF1	ENSG00000188878	0.00296	-3440
37	CCL4	ENSG00000129277	0.00332	-7790
38	LRP4	ENSG00000134569	0.00378	-10800
39	FBXO5	ENSG00000112029	0.00389	-12800
40	SLC29A1	ENSG00000112759	0.0039	-7340
41	RNGTT	ENSG00000111880	0.00416	-5820
42	BRCA1	ENSG00000012048	0.00441	-12600
43	NT5DC3	ENSG00000111696	0.00454	-8620
44	CYLD	ENSG00000083799	0.00459	-13200
45	SLC28A3	ENSG00000197506	0.00477	-12200
46	DHRS2	ENSG00000100867	0.00574	-6960
47	ENOX1	ENSG00000120658	0.00647	-12000
48	ZC3H13	ENSG00000123200	0.00723	-13000
49	SPP2	ENSG00000072080	0.00744	-22000
50	TNFRSF1A	ENSG00000067182	0.00759	-10600
51	TMEM61	ENSG00000143001	0.00766	-6400
52	BRAF	ENSG00000157764	0.00776	-12600
53	CTBP2	ENSG00000175029	0.00787	-10900
54	SNRNP48	ENSG00000168566	0.00822	-10600
55	CCDC33	ENSG00000140481	0.00846	-12800

56	C6orf162	ENSG00000111850	0.00852	-9780
57	MATN2	ENSG00000132561	0.00865	-10300
58	MSH3	ENSG00000113318	0.00924	-9660
59	CDCA2	ENSG00000184661	0.00945	-5600
60	C8orf42	ENSG00000180190	0.00954	-9100
61	PDE6B	ENSG00000133256	0.00983	-5390
62	CCDC120	ENSG00000147144	0.00984	-10400
63	SLC37A3	ENSG00000157800	0.0104	-4700
64	GPN2	ENSG00000142751	0.0116	-7500
65	COG5	ENSG00000164597	0.0118	-10400
66	ACTC1	ENSG00000159251	0.0119	-6720
67	BOLA2B	ENSG00000169627	0.0122	-8250
68	MMP20	ENSG00000137674	0.0125	-8090
69	MIER3	ENSG00000155545	0.0126	-6910
70	KCNB2	ENSG00000182674	0.0137	-10700
71	TNPO3	ENSG00000064419	0.0147	-22100
72	WDR16	ENSG00000166596	0.015	-18800
73	IER3	ENSG00000137331	0.0152	-9240
74	SART1	ENSG00000175467	0.0152	-5310
75	HS6ST1	ENSG00000136720	0.0152	-5750
76	JOSD2	ENSG00000161677	0.0162	-8770
77	PRSS21	ENSG00000007038	0.0166	-4740
78	MARCH8	ENSG00000165406	0.0169	-14200
79	SCYL1	ENSG00000142186	0.0171	-12800
80	MED11	ENSG00000161920	0.0174	-8870
81	DFNA5	ENSG00000105928	0.0175	-12800
82	NCAPG2	ENSG00000146918	0.0178	-14600
83	KCNIP2	ENSG00000120049	0.0191	-5470

N/A	ALS2	ENSG00000003393	0.00158	-11600
N/A	DKK2	ENSG00000155011	5.14E-07	-12700
N/A	JAK3	ENSG00000105639	1.57E-12	-11700
N/A	KRTCAP2	ENSG00000163463	1.26E-08	-15700
N/A	LIN54	ENSG00000189308	0.00119	-12400
N/A	PLSCR4	ENSG00000114698	3.57E-06	-14700
N/A	PTP4A3	ENSG00000184489	4.09E-05	-8890
N/A	ROGDI	ENSG00000067836	4.10E-05	-11200
N/A	SRSF1	ENSG00000136450	2.03E-06	-11300
N/A	THRA	ENSG00000126351	4.05E-05	-11200

Table 2. Primary hit selection

The top 83 hit genes selected from the primary screen data (120 hour timepoint) are ranked according to their p value. esiRNA:MSC linear interaction model values are given. 10 additional 'biologically interesting' hits are listed below the primary hits in alphabetical order.

Although the focus of the study was to identify RNAi:MSC synthetic lethal combinations, hits at the 'opposite end' of the scale were determined, i.e. combinations that were able to increase cellular proliferation or increase ATP production (Table 3). 36 genes with significant interaction values > +5000 and significant esiRNA effects (-10,000 – 0) were identified (arbitrarily selected values used to putatively determine hits in this category). The gene list was analysed for over-representation of annotations in the GO categories of biological process, molecular function and cellular component (as described in Results 3.1). Additionally the gene products were also compared to the KEGG collection for enrichment of specific pathway features. However, no significant enrichment was identified, potentially due to the small set of genes analysed.

Gene Name	Ensembl ID	Interaction p value	Interaction value
TMEM132B	ENSG00000139364	0.000753	8090
KLK6	ENSG00000167755	0.00384	9540
TTC27	ENSG00000018699	0.00413	8860
NDNF	ENSG00000173376	0.00456	6950
SPTY2D1	ENSG00000179119	0.00524	8190
CCDC42	ENSG00000161973	0.00678	7190
KDR	ENSG00000128052	0.00714	10200
C9orf139	ENSG00000180539	0.00862	13200
ERP29	ENSG00000089248	0.00889	9010
SRP72	ENSG00000174780	0.011	10300
NA	ENSG00000186841	0.0113	9570
NEDD4	ENSG00000069869	0.0122	7110
FAM47E	ENSG00000189157	0.0136	8000
TTC6	ENSG00000139865	0.0194	7180
KLF1	ENSG00000105610	0.0233	8000
PYCARD	ENSG00000103490	0.0264	7200
BMP5	ENSG00000112175	0.0277	8380
FCHO2	ENSG00000157107	0.0281	15800
C9orf43	ENSG00000157653	0.0288	9730
GXYLT1	ENSG00000151233	0.0308	7230
SCN4B	ENSG00000177098	0.0318	9570
PRLHR	ENSG00000119973	0.0331	10500
ENTPD5	ENSG00000187097	0.0339	13500
CASP9	ENSG00000132906	0.0367	23000

IGSF6	ENSG00000140749	0.0372	12300
TMEM150B	ENSG00000180061	0.0381	11000
INPP5E	ENSG00000148384	0.0391	8460
PPP6R1	ENSG00000105063	0.0418	7170
GOT1	ENSG00000120053	0.0424	6850
CCNG1	ENSG00000113328	0.0433	7020
MTL5	ENSG00000132749	0.0438	9200
NKAIN1	ENSG00000084628	0.0463	9560
PASK	ENSG00000115687	0.0472	8580
LRRC39	ENSG00000122477	0.048	7150
ZNF684	ENSG00000117010	0.0481	10200
AMN1	ENSG00000151743	0.0495	11900

Table 3. esiRNA 'activator' ranking

esiRNA:MSC combinations with positive interaction values (> +5000) and significant esiRNA effects (-10,000 – 0) were determined. Genes were ranked according to their significance (p value) of interaction.

Future detailed analysis of these hits could provide important information regarding drug resistance mechanisms, and may also identify novel Wnt pathway interactions and feedback mechanisms. However, further work in the project was restricted to genes showing synthetic lethality.

3.2.4 Reconfirmation assays

Following the identification of RNAi:MSC interactions from the primary screen, selected gene hits were further characterised (see Figure 25 for the characterisation assay cascade).

Figure 25 placement

Figure 25. Hit characterisation

Schematic representation of the hit characterisation process. Hits identified from the primary screen were reconfirmed using two methods. Non-overlapping esiRNAs against 45 of the primary hits were synthesised and RNA:MSC interactions re-verified. Simultaneously, 12 commercially available inhibitors against the 9 of the primary hits were identified and obtained. Small molecule inhibitor:MSC assays were conducted. Hit protein knockdown was subsequently ascertained. Further downstream assay plans are detailed.

****ON OPPOSITE PAGE****

Figure 25

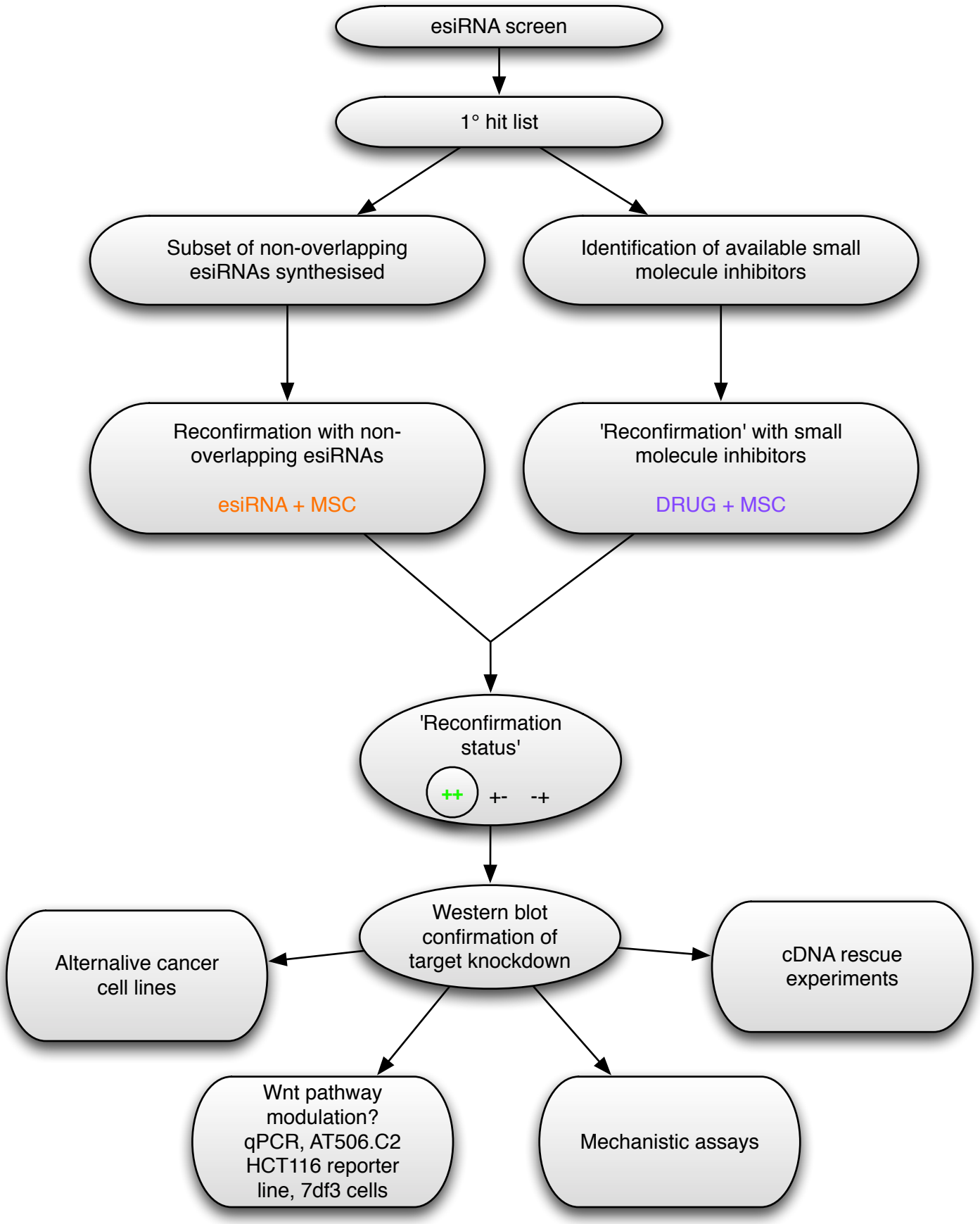
esiRNA screen
1° hit list
Subset of non-overlapping esiRNAs synthesised
Identification of available small molecule inhibitors
Reconfirmation with non-overlapping esiRNAs
esiRNA + MSC
'Reconfirmation' with small molecule inhibitors
DRUG + MSC
'Reconfirmation status'
++
+-
-+
Western blot confirmation of target knockdown
Alternalive cancer cell lines
cDNA rescue experiments
Wnt pathway modulation? qPCR, AT506.C2 HCT116 reporter line, 7df3 cells
Mechanistic assays

As hit reconfirmation assays were conducted in parallel, the left branch of the diagram (non-overlapping esiRNA reconfirmation) will first be discussed, followed by the small molecule inhibitor assays.

3.2.4.1 Non-overlapping esiRNA reconfirmation

Of the 93 hits identified in the primary hit list (Table 2), 45 genes were selected for the synthesis of a non-overlapping esiRNA. Effects mediated in the presence of non-overlapping esiRNAs (designed to target a different region of the gene away from the original esiRNA) should validate synthetic RNAi:MSC interactions (i.e. that the conditional reduction in viability was not due to off-target effects). Due to resource limitation, 45 genes were selected for revalidation based on both their rank order in the primary screen and information on their background biology. Biological insight was restricted to searches for known links to Wnt signalling or an involvement in oncogenesis. Examples within this list include HARS (the top hit), LRP4 and Dkk2 (known Wnt signalling components and antagonists (Johnson et al., 2005; Wu et al., 2000)), TPT1 (translationally-controlled tumour protein 1) and BRCA1 (breast cancer type 1 susceptibility protein (Hall et al., 1990; Miki et al., 1992)).

Interaction of the non-overlapping esiRNAs with MSC was determined using the previously established assay conditions, with the raw data analysed for evidence of interaction by determining the percentage reduction in viability compared to the ‘high’ and ‘low’ controls, and the significance of the interaction determined using two-way ANOVA. The reconfirmed genes can be seen in Table 4.

Gene Name	Ensembl ID	Percentage inhibition	p value
HARS	ENSG00000170445	32	0.0038
MED11	ENSG00000161920	9	<0.0001
BRAF	ENSG00000157764	7	0.01
FKBP10	ENSG00000141756	5	0.0057
MEN1	ENSG00000133895	Borderline – require further investigation	
U2AF2	ENSG00000063244		
JOSD2	ENSG00000161677		

Table 4. Non-overlapping hits

The seven significant hit and borderline genes determined using non-overlapping esiRNA. 'Interaction' was determined from the raw data by calculating the interaction based on the percentage reduction in viability compared to the 'high' control (R-Luc; with EG5 used as the baseline) and significance of interaction determined using a two-way ANOVA (n=3). The percentage viability reduction and p values are given for the significant hits.

Of the 45 genes tested, the interaction of 4 hits was significantly reconfirmed, with three additional hits indicating 'borderline' activity. Further repetition may be needed to validate 'borderline' hits. The reconfirmation rate of 4/45 (or 7/45 using lower stringency criteria) was low by comparison with a rate of approximately 30-40% that was observed for screens for regulators of TCF-dependent transcription and β-catenin levels and subcellular distribution (Freeman, 2008; Lloyd-Lewis, 2011). Interestingly, the previous screen conducted by B. Lloyd-Lewis used the same esiRNA library and had identified many more primary hits using non-cell killing readouts (~250 primary hits per screen; 35-40% reconfirmation). At present, we cannot be certain that the different primary and secondary hit reconfirmation rates are not related to the stringency of the hit selection in this screen. However, it is more likely that the low reconfirmation rate reflects an intrinsic aspect of the biology of cell survival in

the presence of MSC compound since ‘true hits’ that had been selected in the primary screen would have been expected to reconfirm at similar rates.

Interestingly, HARS, was again the top hit in the non-overlapping reconfirmation analysis. Both the primary and secondary esiRNAs against HARS specifically resulted in a loss of HARS protein expression (Figure 26). Importantly, in the larger-scale assays required for protein expression analysis, a significant reduction in cell number was observed only in HARS esiRNA: MSC combinations. Future studies could aim to determine whether this was driven by reductions in cell proliferation or increased apoptosis.

Interestingly the second ranked hit was MED11; a component of the multiprotein Mediator complex (involved in the activation of RNA polymerase II transcription), situated in the ‘head’ module (Taatjes, 2010; Takagi et al., 2006). The molecular target of MSC, CDK8, is central to the kinase module of this complex (Malik and Roeder, 2005), thus further disruption of the complex through interference of the head module may be required in order reduce cell viability.

The serine threonine protein kinase BRAF is a third interesting hit. With defects in BRAF linked found in a wide range of cancers (Davies et al., 2002), and notably a cause of metastasis in colorectal cancer (Tol et al., 2009), it was intriguing as to why inhibition of its functional isoform in combination with MSC should result in death of cultured colorectal cancer cells.

Figure 26. HARS western confirmation

Figure 26. HARS protein depletion

Western blot analysis for HARS expression showing depletion of HARS protein (56kDa) with both the primary screen esiRNA and the secondary reconfirmation non-overlapping esiRNA at each time point analysed. GAPDH levels are shown as controls for loading.

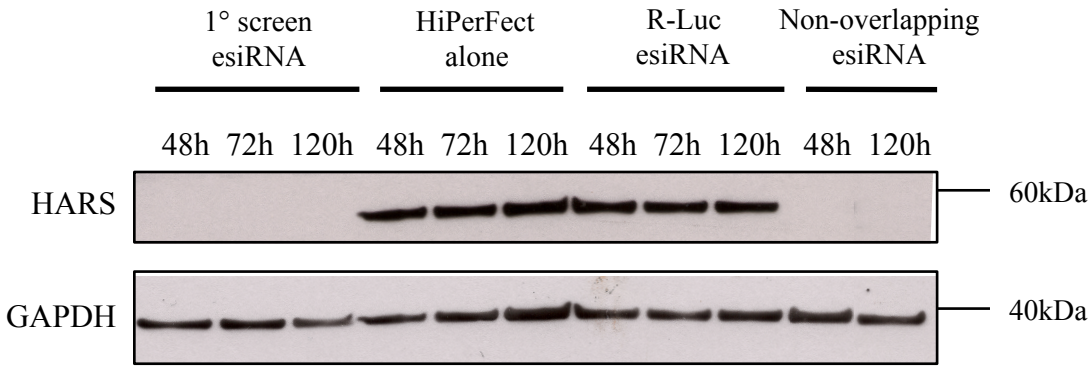

Figure 26. HARS protein depletion

Western blot analysis for HARS expression showing depletion of HARS protein (56kDa) with both the primary screen esiRNA (48, 72 and 120 hour knockdown) and the secondary reconfirmation non-overlapping esiRNA (48 and 120 hour knockdown). HiPerFect transfection media and R-Luciferase non-targetting controls are shown. GAPDH (38kDa) levels are shown as controls for loading.

3.2.4.2 Small molecule inhibitor 'reconfirmation'

In parallel with the non-overlapping esiRNA revalidation assays, attempts to replicate the conditional viability reduction with small molecule inhibitors (replacing esiRNAs) were made. The rationale for this was two fold. Firstly it was postulated that gene targetting by RNAi may not downregulate the hit targets completely (perhaps due to incomplete depletion of the gene). In this case, residual gene product activity may have prevented a strong conditional response being observed – as was observed in the esiRNA screen where no genes showed 100% synthetic lethality. Secondly, it would have been very time-consuming and costly to correlate the level of each protein reduction with response for each putative esiRNA target.

Compounds were identified that inhibited the corresponding esiRNA gene products with the rationale that they should synergise to inhibit cell growth. In the longer-run, it was anticipated that the identification of any commercially available compounds (or compounds in the clinic) would improve the potential for clinical application of MSC in chemotherapeutic combination therapies.

In order to identify commercially available compounds, an extensive *in silico* search was conducted for any inhibitors against the primary hit list (Table 2). A secondary search of the ChEMBL and DrugBank databases ((Gaulton et al., 2012; Knox et al., 2011)) was conducted by Dr. Oliver Karch (Dept. of Discovery Bioinformatics, Merck Serono). In instances where multiple compounds were available against a single molecular target, only two were obtained (due to practical and resource limitations). Apart from UGP2, all compound targets also had a corresponding non-overlapping esiRNA, thus results from the two reconfirmation assays could be used to corroborate one another. In total, twelve compounds were accessible against nine of the primary hit targets (Table 5a).

In addition, a panel of Wnt inhibitors (available 'in-house') were selected for combination testing with MSC (Table 5b; this included a second CDK8 inhibitor, Senexin A (Porter et al., 2012)). It was postulated that the partial inhibition of

Wnt signalling by MSC may have been insufficient to reduce cellular viability in response to MSC in HCT116 cells (see Figure 14b). Thus it was hypothesised that MSC might functionally synergise with other Wnt pathway inhibitors by targetting a separate 'branch' of the signalling network (see Figure 5); a suggestion that was supported by the identification of Wnt regulators in the primary esiRNA screen (Table 2).

Together this approach should allow the identification of targets that synergise with MSC via reductions in Wnt signalling and through unrelated 'interactor' mechanisms that could not have been predicted at the outset.

Hit Gene Name	Ensembl ID	Compound (with synonyms)	CAS Number
BRAF	ENSG00000157764	BAY-43-9006, Nexavar, **Sorafenib**	284461-73-0
BRAF	ENSG00000157764	**RAF265** (CHIR-265)	927880-90-8
CRHR2	ENSG00000106113	**K 41498**	434938-41-7
HPD	ENSG00000158104	**Nitisinone**	104206-65-7
JAK3	ENSG00000105639	**BX-795**	702675-74-9
JAK3	ENSG00000105639	**Tofacitinib citrate**	540737-29-9
PDE6B	ENSG00000133256	Revatio, **Sildenafil**, UK-92480, Viagra	171599-83-0
PTP4A3	ENSG00000184489	**Emodin**	518-82-1
SLC29A1	ENSG00000112759	**Lidoflazine**	3416-26-0
THRA	ENSG00000126351	**Tiratricol**, TRIAC	51-24-1
THRA	ENSG00000126351	Cytomel, Euthroid, **Liothyronine**, Rathyronine, Tertroxin, Thyrolar, Triostat	6893-02-3
UGP2	ENSG00000169764	**Iodoacetamide**	144-48-9

Table 5a. Inhibitors against primary screen hit genes

Inhibitors identified (and purchased) against genes from the primary hit list are detailed (in hit alphabetical order). Where there are 2+ inhibitors for a target, only 2 have been selected. Compound synonyms are listed, with the name in bold indicating the name used in all assays. CAS (Chemical Abstracts Service) numerical identifiers are detailed.

Target	Compound	CAS Number
PORCN	LGK-974 (derivative)	1243244-14-5
LRP6/Fz1	Niclosamide	50-65-7
LRP6	Salinomycin	53003-10-4
GSK3	BIO	667463-62-9
TNKS1&2	XAV 939	284028-89-3
PP2A	IQ-1	331001-62-8
TCF4 - β-catenin	PKF118-310	84-82-2
CBP	ICG-001	847591-62-2
CDK8	Senexin A	N/A
Multiple	Sulindac	38194-50-2

Table 5b. Inhibitors against Wnt signalling components

Wnt inhibitors are listed according to their site of action in the pathway (from extracellular to nucleus). CAS (Chemical Abstracts Service) numerical identifiers are detailed.

To investigate the interaction between the compound test list in Table 5 and MSC, an initial simple combination viability assay was conducted to rapidly ascertain any compound-compound synergy. HCT116 cells were treated (24 hours post 96-well plate seeding) with 10μM MSC in combination with 1, 5 and 25μM test compound for 24, 48 and 72 hours. The most significant effects were seen at 48 and 72 hours treatment, with 1 and 5μM test compound (Figures 27 and 28).

Figure 27a placement

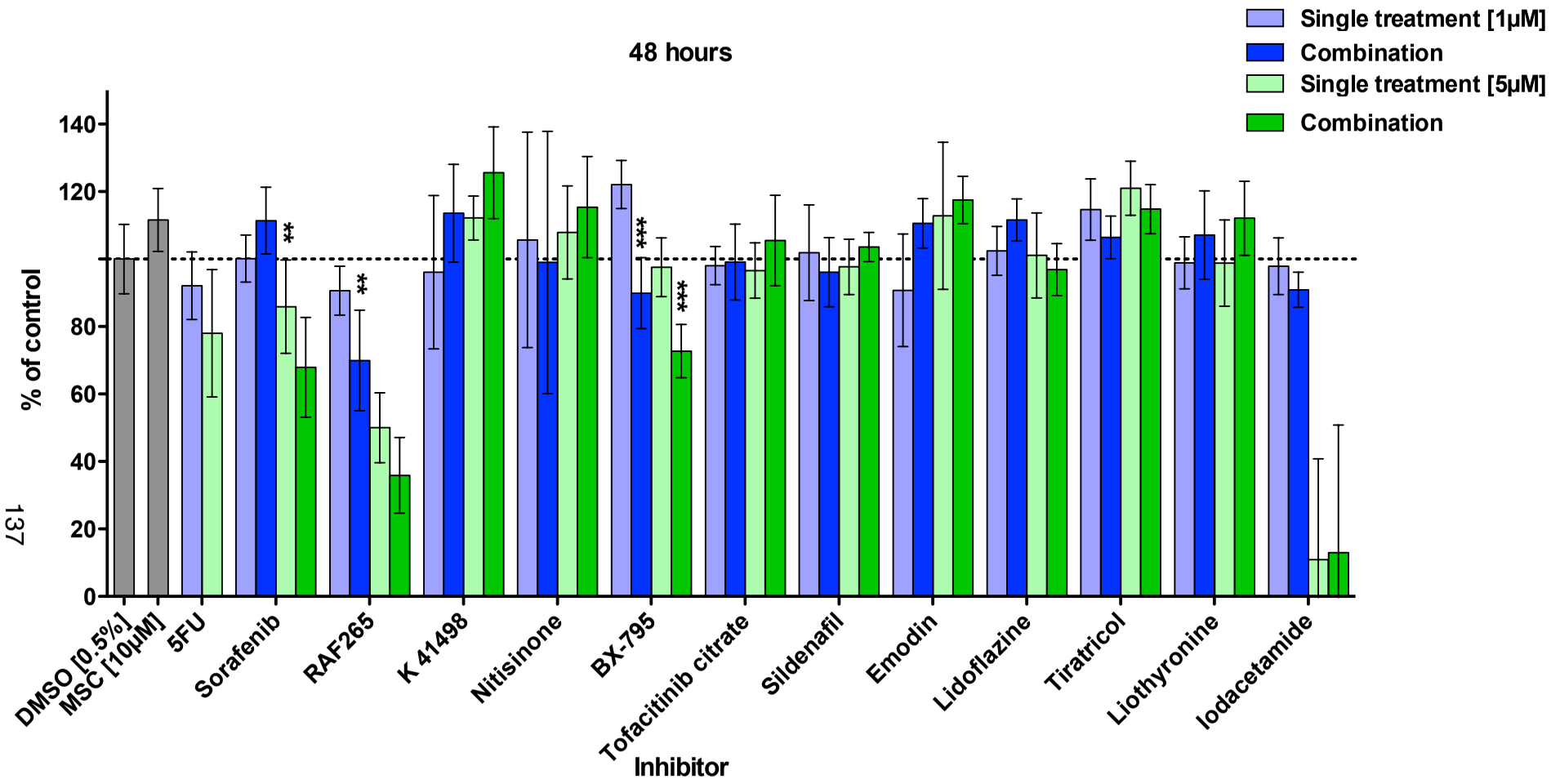

Figure 27a. esiRNA-directed inhibitor:MSC combination effect on HCT116 cell viability

HCT116 cells seeded in a 96 well plate at 4500 cells/well for 24 hours were treated with either 1µM (blue bars) or 5µM (green bars) test compound in the presence (dark bars) and absence (light bars) of 10µM MSC. Cell viability was measured at **a.** 48 and **b.** 72 hours post treatment using the ATPlite assay. All controls are normalised to DMSO treated cells (grey bar). 10µM MSC treatment alone is shown in grey. 5FU was used as a control for viability reduction. n = 5 (* = P < 0,05; ** = P < 0,01; *** = P < 0,001; 1 Way ANOVA and Tukey Test). N.B. This data was produced by Daniel Winter under my supervision during his visit to the laboratory.

Figure 27b placement

Figure 27a&b. esiRNA-directed inhibitor:MSC combination effect on HCT116 cell viability

HCT116 cells seeded in a 96 well plate at 4500 cells/well for 24 hours were treated with either 1μM (blue bars) or 5μM (green bars) test compound in the presence (dark bars) and absence (light bars) of 10μM MSC. Cell viability was measured at **a.** 48 and **b.** 72 hours post treatment using the ATPlite assay. All controls are normalised to DMSO treated cells (grey bar). 10μM MSC treatment alone is shown in grey. 5FU was used as a control for viability reduction. n = 5 (* = P < 0,05; ** = P < 0,01; *** = P < 0,001; 1 Way ANOVA and Tukey Test). N.B. This data was produced by Daniel Winter under my supervision during his visit to the laboratory.

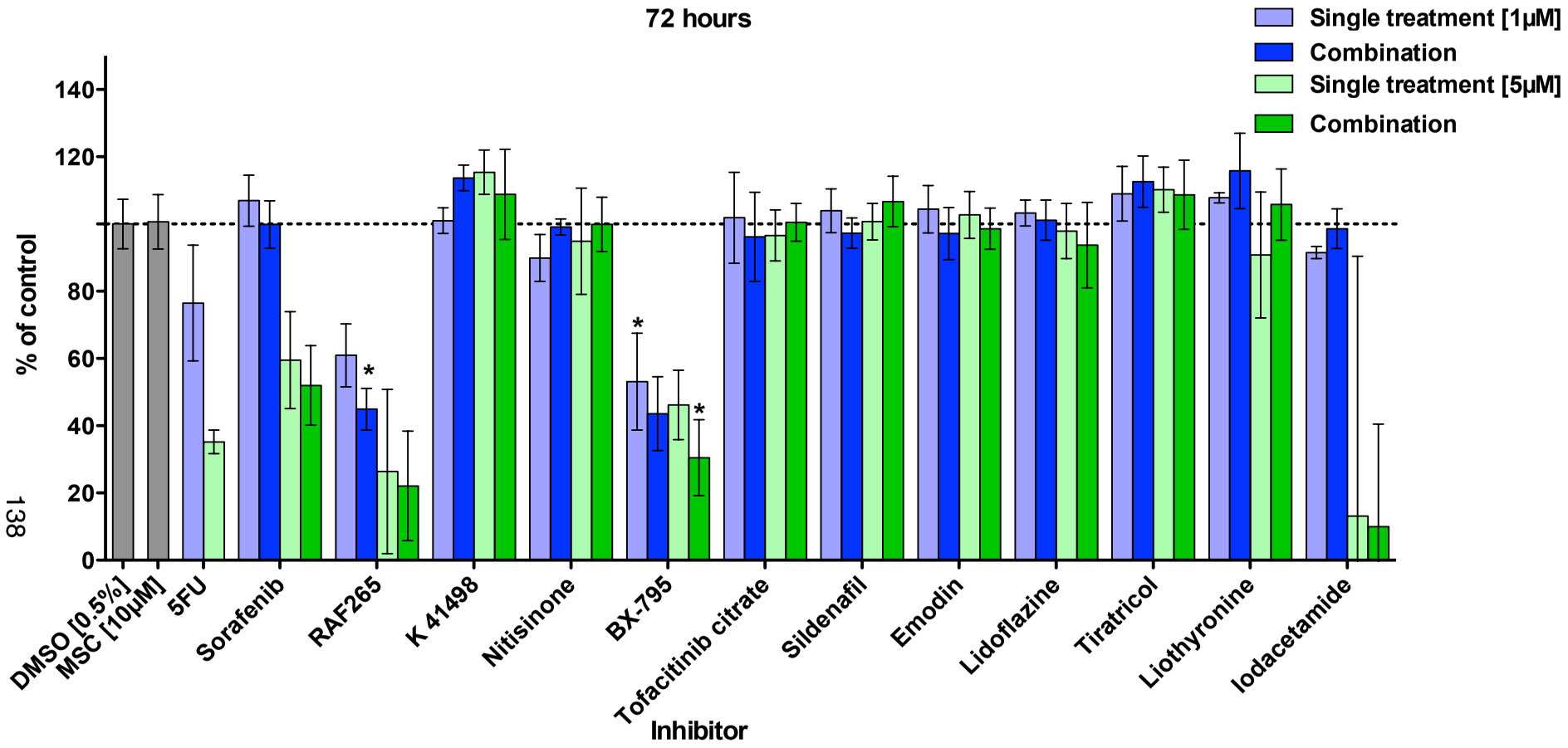

Figure 27b. esiRNA-directed inhibitor:MSC combination effect on HCT116 cell viability

HCT116 cells seeded in a 96 well plate at 4500 cells/well for 24 hours were treated with either 1µM (blue bars) or 5µM (green bars) test compound in the presence (dark bars) and absence (light bars) of 10µM MSC. Cell viability was measured at **a.** 48 and **b.** 72 hours post treatment using the ATPlite assay. All controls are normalised to DMSO treated cells (grey bar). 10µM MSC treatment alone is shown in grey. 5FU was used as a control for viability reduction. n = 5 (* = P < 0,05; ** = P < 0,01; *** = P < 0,001; 1 Way ANOVA and Tukey Test). N.B. This data was produced by Daniel Winter under my supervision during his visit to the laboratory.

Figure 28a placement

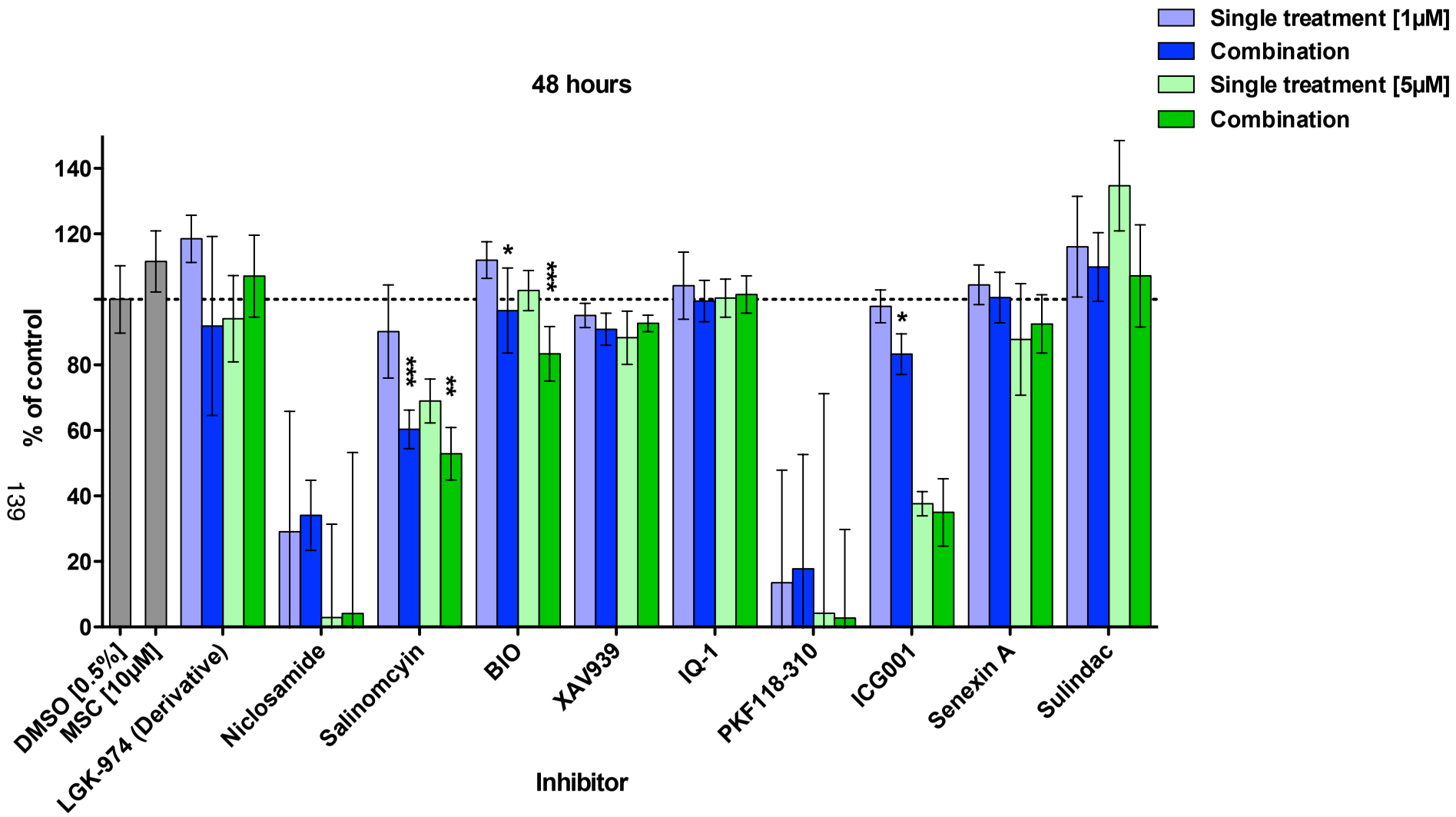

Figure 28a. Wnt-Wnt inhibitor combination effect on HCT116 cell viability

HCT116 cells seeded in a 96 well plate at 4500 cells/well for 24 hours were treated with either 1µM (blue bars) or 5µM (green bars) test compound in the presence (dark bars) and absence (light bars) of 10µM MSC. Cell viability was measured at **a.** 48 and **b.** 72 hours post treatment using the ATPlite assay. All controls are normalised to DMSO treated cells (grey bar). 10µM MSC treatment alone is shown in grey. n = 5 (* = P < 0,05; ** = P < 0,01; *** = P < 0,001; 1 Way ANOVA and Tukey Test). N.B. This data was produced by Daniel Winter under my supervision during his visit to the laboratory.

Figure 28b placement

Figure 28a&b. Wnt-Wnt inhibitor combination effect on HCT116 cell viability

HCT116 cells seeded in a 96 well plate at 4500 cells/well for 24 hours were treated with either 1μM (blue bars) or 5μM (green bars) test compound in the presence (dark bars) and absence (light bars) of 10μM MSC. Cell viability was measured at **a.** 48 and **b.** 72 hours post treatment using the ATPlite assay. All controls are normalised to DMSO treated cells (grey bar). 10μM MSC treatment alone is shown in grey. n = 5 (* = P < 0,05; ** = P < 0,01; *** = P < 0,001; 1 Way ANOVA and Tukey Test). N.B. This data was produced by Daniel Winter under my supervision during his visit to the laboratory.

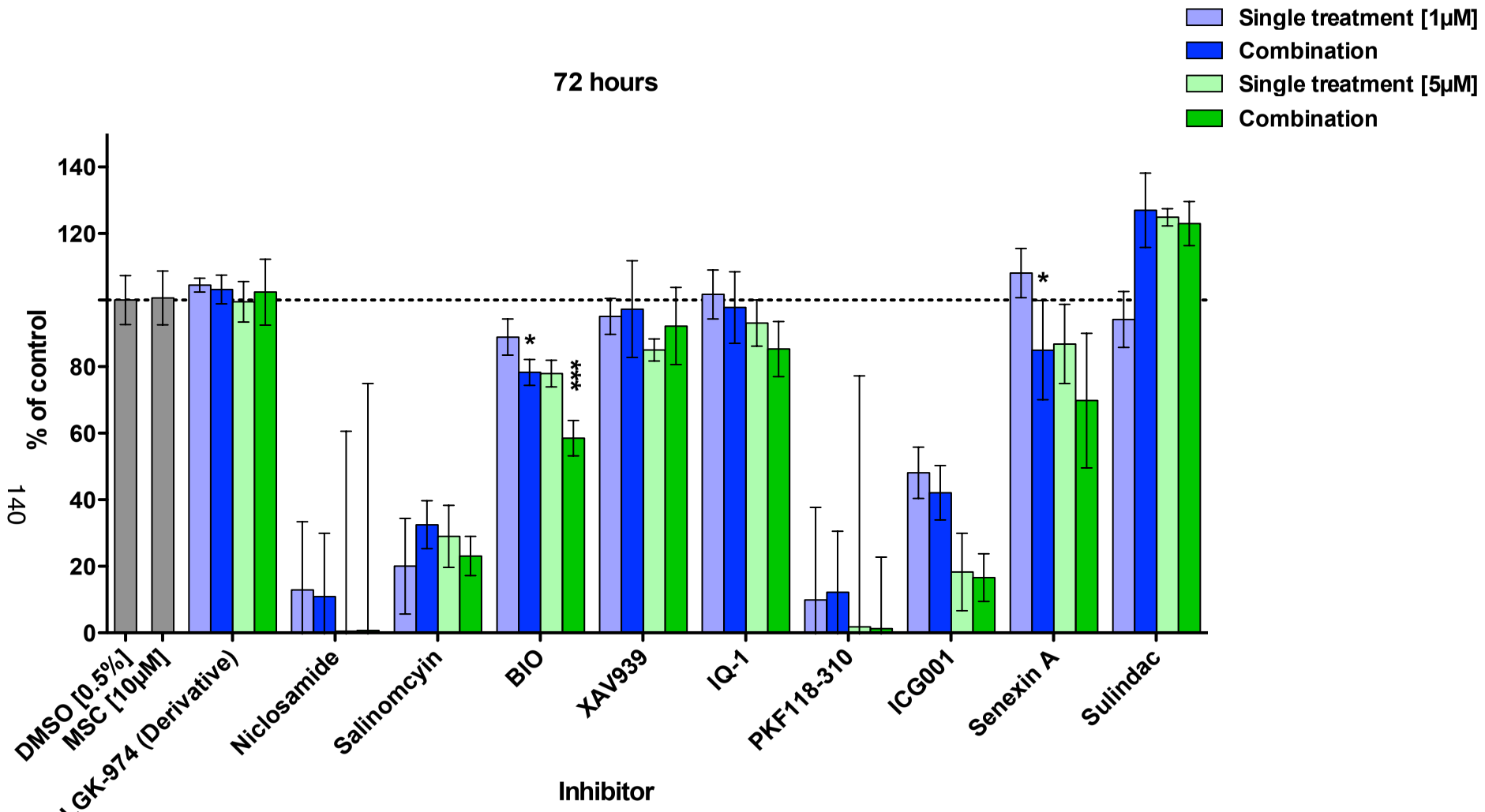

Figure 28b. Wnt-Wnt inhibitor combination effect on HCT116 cell viability

HCT116 cells seeded in a 96 well plate at 4500 cells/well for 24 hours were treated with either 1µM (blue bars) or 5µM (green bars) test compound in the presence (dark bars) and absence (light bars) of 10µM MSC. Cell viability was measured at **a.** 48 and **b.** 72 hours post treatment using the ATPlite assay. All controls are normalised to DMSO treated cells (grey bar). 10µM MSC treatment alone is shown in grey. n = 5 (* = P < 0,05; ** = P < 0,01; *** = P < 0,001; 1 Way ANOVA and Tukey Test). N.B. This data was produced by Daniel Winter under my supervision during his visit to the laboratory.

This initial compound-compound combination assay was used to determine whether compounds (if any) were able to synergise with 10μM MSC (the same concentration used in the primary screen). The plan was then to study compounds exhibiting synergy more extensively.

At the 24 hour timepoint no compounds exhibited combinatorial reduction in viability (data not shown), however this was not surprising as this treatment time was equivalent to the 72 hour esiRNA primary screen timepoint which also revealed no significant interactions. As can be seen in Figures 27 a and b (48 hour and 72 hour timepoint respectively), several compounds induced weak combination-dependent loss in viability. RAF265 (1μM) and BX-795 (1μM and 5μM) both demonstrated significant reduction in viability in combination with MSC compared with test inhibitor treatment alone at both 48 and 72 hours treatment, with 5 μM Sorafenib significantly reducing viability at 48 hours alone. Interestingly, both RAF265 and Sorafenib are BRAF inhibitors, supporting the reconfirmation of BRAF with non-overlapping esiRNA. By contrast, the interaction between the JAK3 inhibitor BX-795 and MSC was not replicated by the second JAK3 inhibitor tofacitinib citrate. Future studies with additional JAK pathway inhibitors may be able to help resolve whether the BX-795 interaction was based on an essential underlying role for the JAK pathway in the presence of MSC.

Notably, only four Wnt pathway component inhibitors exhibited any significant activity in combination with MSC (salinomycin, BIO, ICG001 and Senexin A), with BIO (6-Bromoindirubin-3′-oxime) being the only compound to significantly reduce HCT116 viability across both timepoints (Figure 28a&b). This was a somewhat surprising observation as BIO is a well-characterised inhibitor of GSK3 and powerfully activates TCF-dependent transcription in many systems.

It was also somewhat surprising that this initial assay indicated Senexin A (a CDK8 inhibitor) was able to reduce cellular viability in combination with MSC as data from the drug discovery programme had shown that MSC was a selective

and potent CDK8 inhibitor. Further investigations would be required to reconfirm this observation.

Five compounds were selected for extended studies: BIO, RAF265, BX-795, salinomycin and Senexin A. Test inhibitors were titrated (25nM to 25μM) in a 'chequerboard' assay against MSC titrations (40nM to 25μM) in order to ascertain whether combinatorial activity was evident at defined compound concentration combinations (at 24, 48 and 72 hours). Of the five compounds, only RAF265 and salinomycin demonstrated synergistic activity in these preliminary assays (see Appendix 8 for detailed BIO, BX-795 and Senexin A dose response curves). Subsequent reconfirmation studies showed that there was in fact no synergy between salinomycin and MSC (Appendix 8, however the synergy between RAF265 and MSC, although weak, was highly reproducible both in studies presented here (Figure 29a and b) and in several (n=4 total) independent repeats (data not shown).

Figure 29 placement

Figure 29. RAF265:MSC combination

HCT116 cells seeded in a 96 well plate at 4500 cells/well for 24 hours were treated with a range of RAF265 inhibitor concentrations (20nM – 25μM) in the presence (green) and absence (red) of 2.5μM MSC. Cell viability was measured at **a.** 48 hours and **b.** 72 hours post treatment using the ATPlite assay. All controls are normalised to DMSO treated cells. n = 3.

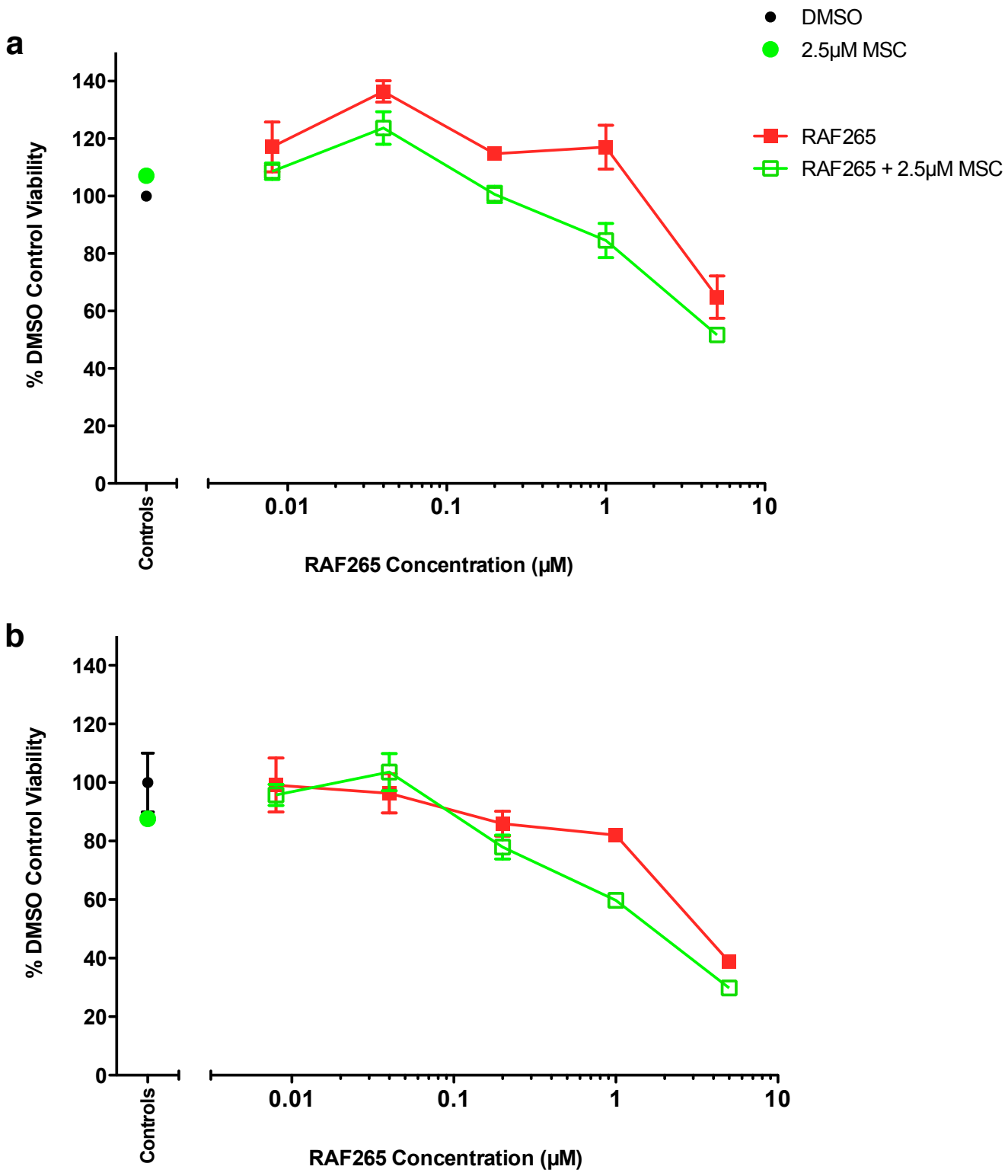

Figure 29. RAF265:MSC combination

HCT116 cells seeded in a 96 well plate at 4500 cells/well for 24 hours were treated with a range of RAF265 inhibitor concentrations (20nM – 25μM) in the presence (green) and absence (red) of 2.5μM MSC. Cell viability was measured at **a.** 48 hours and **b.** 72 hours post treatment using the ATPlite assay. All controls are normalised to DMSO treated cells. n = 3.

RAF265:MSC synergy was most evident in combination with 2.5μM MSC (Figure 29) with the most significant difference in compound effect being observed at 48 hours treatment (Figure 29a). Note also that at high concentrations, RAF265 alone showed significant toxicity that may have obscured its potential to interact with MSC. At both 48 and 72 hours (Figure 29a&b), the most significant combinatorial inhibition was seen with 1μM RAF265:2.5μM MSC treatment. Importantly, 2.5μM MSC is 200 times the 7df3 IC_{50} for MSC. At these concentrations, it is not easy to exclude the possibility that MSC synergy might be functioning through action on off-target (non-CDK8/CDK19) targets including other protein kinases.

To determine whether BRAF inhibition using alternative inhibitors would elicit the same result, Debrafenib (CAS 1195765-45-7) and SB590885 (CAS 405554-55-4) were examined in combination with MSC. The multi-kinase inhibitor, Sorafenib was also further assessed as it had shown activity in the preliminary compound assays (Figure 27a) but had not been tested in the chequerboard assays. In addition, the activity of two MEK inhibitors (acting downstream of BRAF in the MAP kinase pathway) in combination with MSC were measured in order to determine whether MAP kinase pathway inhibition in combination with Wnt signalling inhibition synergised to reduce HCT116 viability. However, neither the BRAF inhibitors nor MEK inhibitors showed any synergistic activity with MSC (data not shown), suggesting that that the RAF265 compound was the exception in its ability to synergise with MSC.

Preliminary investigations were undertaken in alternative cancer cell lines to determine whether the RAF265:MSC dependent effect in HCT116 cells was more broadly observable. At present a panel of seven CRC cell lines has been assessed (Colo205, Colo320, SW480, SW620, Ls174T and DLD1; see Methods 2.1 for cell line details) using the assay design developed for HCT116 cells. Although these assays require further optimisation (as the HCT116-optimised format is not necessarily the most suitable for other lines), Ls174T cells showed RAF265:MSC conditional lethality at 48 hours treatment (Figure 30).

Figure 30 placement

Figure 30. RAF265:MSC combination in Ls174T cells

Ls174T cells seeded in a 96 well plate at 4500 cells/well for 24 hours were treated with a titration of 200nM, 1μM and 5μM in the presence (circles) and absence (triangles) of 10μM MSC. Cell viability was measured 48 hours post treatment using the ATPlite assay. All controls are normalised to DMSO treated cells. n = 5.

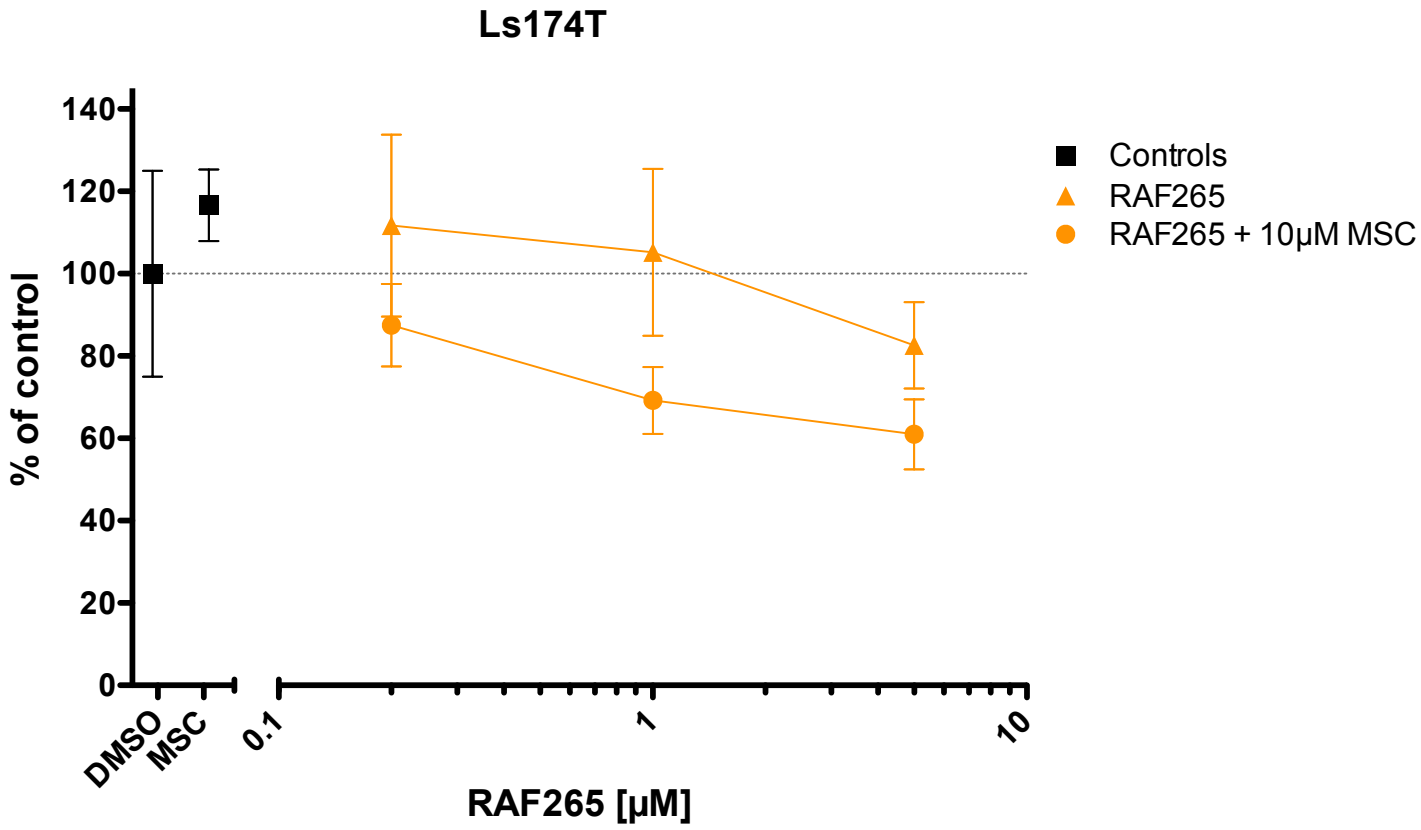

Figure 30. RAF265:MSC combination in Ls174T cells

Ls174T cells seeded in a 96 well plate at 4500 cells/well for 24 hours were treated with a titration of 200nM, 1µM and 5µM in the presence (circles) and absence (triangles) of 10µM MSC. Cell viability was measured 48 hours post treatment using the ATPlite assay. All controls are normalised to DMSO treated cells. n = 5.

Taken together, the esiRNA screen identified a small number of genes, the loss of whose gene products co-operated with MSC to reduce cellular viability. The most significant of these effects was observed with HARS. At present, no HARS-specific compounds are available to explore this interaction further. Of the other confirmed hits, BRAF appeared the most interesting since a number of small molecule inhibitors have been developed against both the wild-type and mutant protein. One of these inhibitors, RAF265, synergised with MSC in multiple assays and in at least 2 cell lines (HCT116 and Ls174T). However it is currently unclear whether the RAF265:MSC synergy operates via the Ras-MAP kinase pathway since other pathway inhibitors showed little effect.

Chapter 4. Discussion

The Wnt/β-catenin signalling cascade is critically implicated in the development of many organisms, with its dysregulation linked to several disease processes. The original aim of this study was to identify novel modulators of TCF-dependent signalling by means of cDNA and esiRNA high-throughput cell-based screens. The identity of these novel hits and their biological activity were anticipated to provide tools with which to characterise the activity and targets of a number of small molecule inhibitors of TCF-dependent transcription that had been identified from cell-based compound library screens (Ewan et al., 2010). In the early stages of this study it was not apparent which of several compound series under investigation, would ultimately be translated into a single clinical therapeutic candidate.

During the project it became clear that a member of the CCT071459 small molecule chemical series was going to become the lead compound for further drug discovery efforts. The 'daughter analogue' of this series that was studied in the work described here is referred to throughout as MSC. In the course of the first two years of the project the molecular target of the CCT071459 series was determined to be the serine threonine kinases CDK8 and CDK19 through the use of bead-conjugated analogues, affinity purification and mass spectrometry. At this point the esiRNA branch of the research changed direction to focus on the identification of genes whose function co-operated with MSC to maintain HCT116 cancer cell growth in 2D culture.

Both cDNA and esiRNA screens were successfully completed and identified fourteen cDNA regulators of TCF-dependent transcription and four genes whose function synergised with MSC to maintain HCT116 viability. To provide a context for a discussion of the identity/function of the genes from each screen, it is necessary to consider the function of the MSC target, CDK8/CDK19.

CDK8 as the MSC molecular target

CDK8 is a ubiquitously expressed cyclin-dependent serine-threonine kinase, functioning in the nucleus in a wide range of roles. However, CDK8's best characterised function is as a regulator of transcription as part of the Mediator complex (Galbraith et al., 2010). In complex with Cyclin C (CycC) and the mediator proteins Med12 and Med13, this CDK8:CycC kinase core forms the regulatory module of the multi-protein Mediator complex (Figure 31), bridging RNA polymerase II (Pol II) and DNA-binding transcription initiation factors (Malik and Roeder, 2010). Unlike cell-cycle CDKs, CDK8 is able to phosphorylate Ser2 and Ser5 of the CTD of RNA Pol II, regulating its activity (Hengartner et al., 1998; Ramanathan et al., 2001). Interestingly, a component of the core Mediator complex, MED11, was one of the four validated esiRNA hits that were identified in the whole esiRNA genome screen, suggesting that the absolute level of Mediator complex activity may be critical for cell survival in the presence of MSC.

Figure 31 placement

Figure 31. The Mediator complex

Diagrammatic plan of Mediator complex components (taken from (Malik and Roeder, 2010)). Distinct Mediator components interact and connect distinct classes of transcriptional regulators with the basal transcription apparatus including RNA polymerase II. The kinase module CDK8/19, Cyclin C, Med12 and Med13 acts as a switch to induce transcription of a subset of the 'core Mediator complex' target genes and repress others. In particular, the kinase module activates Wnt target genes, while the Med12 component has been shown to directly interact with β-catenin.

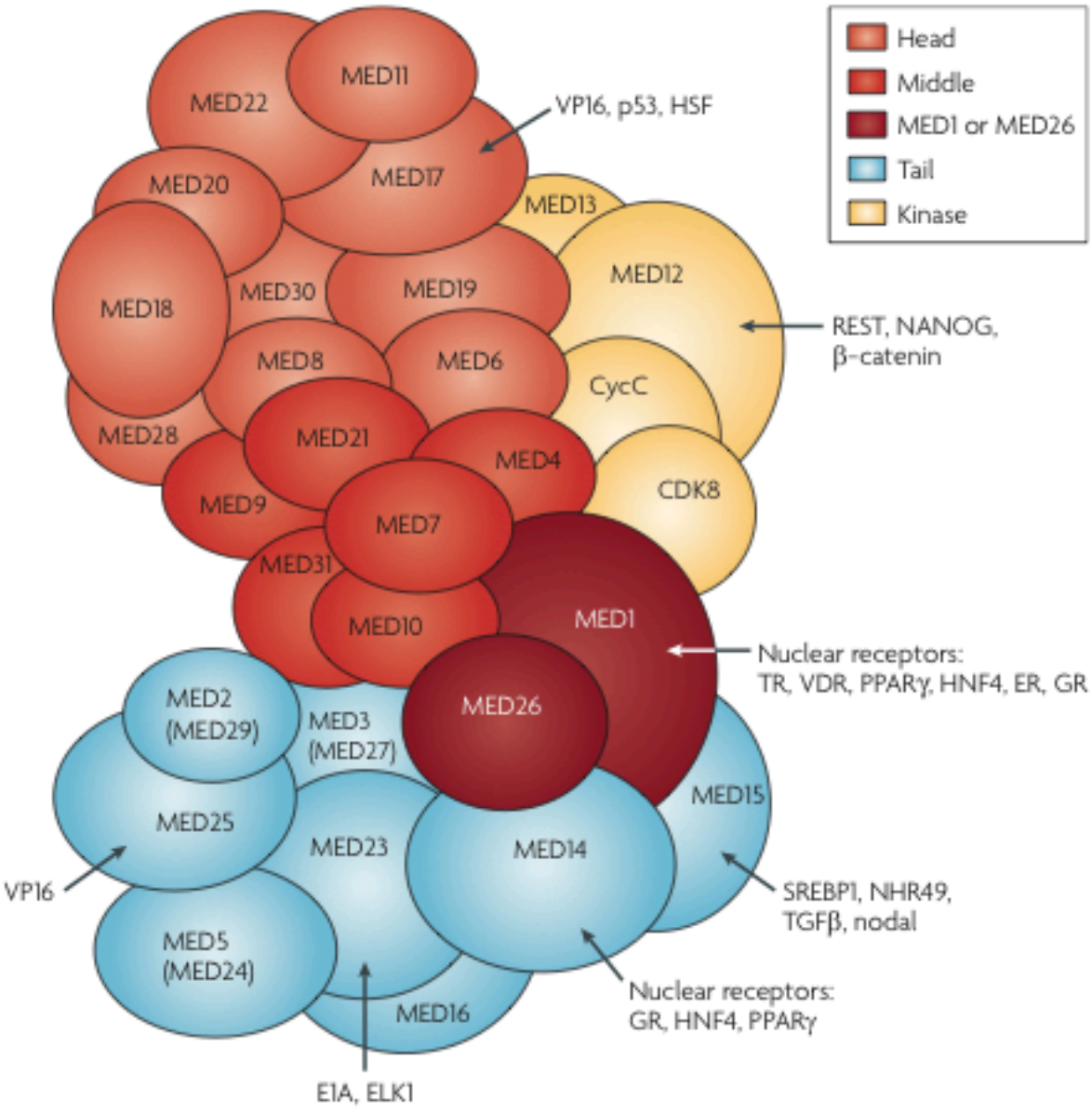

Figure 31. The Mediator complex

Diagrammatic plan of Mediator complex components (taken from (Malik and Roeder, 2010)). Distinct Mediator components interact and connect distinct classes of transcriptional regulators with the basal transcription apparatus including RNA polymerase II. The kinase module CDK8/19, Cyclin C, Med12 and Med13 acts as a switch to induce transcription of a subset of the 'core Mediator complex' target genes and repress others. In particular, the kinase module activates Wnt target genes, while the Med12 component has been shown to directly interact with β-catenin.

A manual search of the esiRNA screen 'interaction' data set also identified Med12L and Cyclin C as reducing HCT116 viability (see Appendix 7 table), however they were not selected since they narrowly missed the hit selection cutoffs. CDK8 itself (or CDK19) was not identified in the esiRNA screen, either in synergy with MSC or alone as being required for HCT116 viability. This contrasted with the study by Firestein *et al.* (Firestein et al., 2008), which showed that 2D cultured HCT116 viability was reduced by ~70% following CDK8 short hairpin RNA (shRNA) lentiviral infection after 120 hours. CDK8 function may be critical in many cell types since CDK8 null mice did not survive beyond 2.5-3.0 days of early embryogenesis as it is required for pre-implantation (Westerling et al., 2007). The contrast between the lack of response of esiRNA to CDK8 and the published studies suggests that the lack of response we observed in the screen may be due to a failure of the specific esiRNA reagent that was used. Further support for this observation has come from the demonstration that shRNAs targeted against CDK8 reduced proliferation of other colorectal cancer cell lines studied in the collaboration (data not shown).

It is important to recognise that there are two major differences between the loss of CDK8 function and treatment with a highly selective CDK8 inhibitor. Firstly, MSC inhibits the activity of both CDK8 and the closely related CDK19 paralogue (80% amino acid identity (Malumbres et al., 2009)), while siRNA-mediated loss of CDK8 does not reduce the activity of CDK19. As yet, a detailed study of CDK8, CDK19 and CDK8/CDK19 loss has not been carried out in HCT116 cells. However initial data from the drug discovery programme suggests that shRNA dependent loss of both proteins synergises in the reduction of other colorectal cancer cell types in 2D culture (data not shown). Despite this observation, it is unlikely that these kinases are completely functionally redundant, since knockdown of CDK8 alone in human cell cultures results in clear phenotypes (Donner et al., 2010; Firestein et al., 2008), and opposite roles of the kinases have been identified under certain conditions (Furumoto et al., 2007; Tsutsui et al., 2008). Thus CDK8 loss alone may be predicted to induce fewer effects than MSC due to functional compensation by CDK19.

Secondly, and by contrast, MSC treatment might have been predicted to have had less of an effect than CDK8 siRNA depletion because it only blocks CDK8's biochemical functions through ATP competition while the esiRNA removes both catalytic and structural functions. Interestingly, previous studies involving transfection of human A375 and WM165-1 cells (melanoma lines with high CDK8 protein levels) with kinase-dead mutants of CDK8 demonstrated that CDK8 structural/scaffolding functions can play a key role in cell survival (Kapoor et al., 2010; Knuesel et al., 2009).

Given the lack of growth inhibition that was observed in HCT116 cells in 2D culture following MSC treatment (Figure 14a), it is unlikely that CDK8/CDK19 catalytic activities are essential for HCT116 cell viability, although a net 'transcriptional' output of the Mediator complex may be essential for viability when kinase activity is combined with the structural loss of other Mediator components.

CDK8 and Wnt signalling

The MSC CDK8/CDK19 inhibitor was developed from the CCT series of compounds that were originally identified as being potent inhibitors of TCF-dependent transcription in the HEK293-based 7df3 reporter cell screen ((Ewan et al., 2010); unpublished data). It has been established that the CDK8 kinase core is recruited to the regulation of Wnt/β-catenin signalling through the interaction of Med12 with β-catenin's transactivation domain (Kim et al., 2006), enhancing β-catenin-TCF/LEF dependent transcription (Figure 32). This enhancer effect has been linked with the observation that CDK8 is amplified in colorectal cancer, potentiating malignancies driven by aberrant Wnt/β-catenin signalling (Firestein et al., 2008; Firestein and Hahn, 2009). CDK8 was also shown to indirectly induce TCF-dependent transcription by preventing the inhibitory action of E2F1 on β-catenin/TCF (Morris et al., 2008). Thus, it is unsurprising that the primary 'Wnt inhibitor' screen identified a compound with CDK8 antagonistic activity.

Figure 32 placement

Figure 32. CDK8 and Wnt signalling

Two pathways have been suggested to link CDK8 action to the regulation of TCF-dependent transcription. In the first, CDK8 was suggested to directly regulate the coupling of the TCF/β-catenin complex to the core RNA polymerase II complex via its role in the Mediator complex. In the second, CDK8 was shown to phosphorylate and inhibit the activity of E2F1, although it is unclear whether it does this in the context of the Mediator complex (adapted from (Galbraith et al., 2010)).

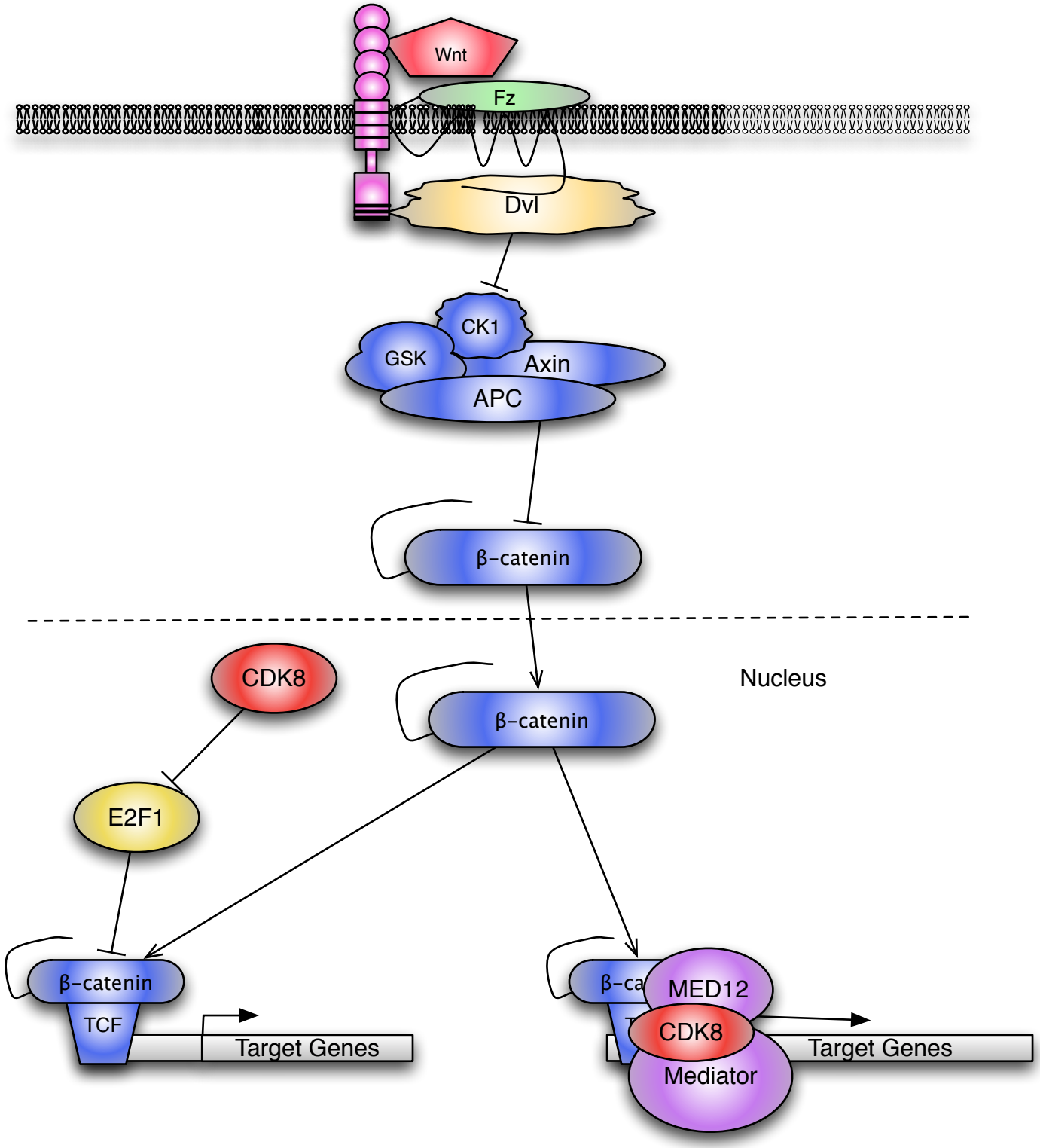

Figure 32. CDK8 and Wnt signalling

Two pathways have been suggested to link CDK8 action to the regulation of TCF-dependent transcription. In the first, CDK8 was suggested to directly regulate the coupling of the TCF/β-catenin complex to the core RNA polymerase II complex via its role in the Mediator complex. In the second, CDK8 was shown to phosphorylate and inhibit the activity of E2F1, although it is unclear whether it does this in the context of the Mediator complex (adapted from (Galbraith et al., 2010)).

Despite its potency in the original cell-based screen, TCF-reporter activity in HCT116 cells was only partially inhibited (~45%) by MSC (Figure 14b), and there was no effect of MSC on HCT116 viability (Figure 14a). Several inferences can be made from this result. Firstly, it is possible that insufficient knockdown of TCF activity was achieved. As is highlighted in Figure 5, TCF-dependent transcription can be modulated at many points along the classic 'linear' pathway, most significantly at highly connected core components. However, further 'branches' of interactions exist that may comprise MSC-resistant pathways or may function to maintain 'homeostatic' levels of Wnt signalling through feedback mechanisms. More than one mechanism of pathway activation has previously been identified in HCT116 cells, where only the simultaneous removal of both the endogenous mutant β-catenin allele and the prevention of an autocrine Wnt ligand feedback loop inhibited cell growth (Bafico et al., 2004). To explore the 'network compensation hypothesis' explanation for the lack of effect of MSC on HCT116 viability, combinations of Wnt pathway inhibitors were tested together (Figure 28). Interestingly, no strong synergy was observed between any of the ten Wnt pathway component inhibitors and MSC in reducing cellular viability, suggesting that the absolute level of TCF-dependent transcription may not be critical for the proliferative response of HCT116 cells. A demonstration that Wnt:Wnt inhibitors synergised to reduce TCF-dependent transcription levels in HCT116 reporter cells would be required to fully validate this suggestion.

A second 'stem cell' hypothesis can explain the lack of MSC effect on HCT116 viability in 2D culture (Clarke and Fuller, 2006). Wnt signalling (and CDK8) has been extensively linked to stem cell function in multiple tissues, significantly including the intestine (Adler et al., 2012; Pinto and Clevers, 2005b). The lack of a HCT116 'viability response' to MSC and the low levels of response observed with even the most efficacious RNAi:MSC combinations may be because the reduction in stem cell targets (e.g. Wnt signalling targets) is only critical for a sub-population of 'stem cell' like cells; although whether 'stem cell' like cells exist within 2D culture is a matter of debate. Nonetheless, it has been shown that in many 2D systems, subpopulations of cells may respond to pharmacological

inhibition with different responses at the same compound concentration (Fallahi-Sichani et al., 2013). Interestingly, collaborators within the CCT series research programme determined that there was a response HCT116 cells cultured in 3D soft agar to MSC treatment (albeit at ~8μM MSC; Figure 33a), suggesting that under conditions that may require 'stem cell' function growth responses may be seen. Furthermore, the more advanced daughter compound of MSC (MSCi; Figure 33b) showed a greater efficacy in 3D cultures, suggesting that larger interaction values may be achieved if this compound were to be assessed with the hits identified. In addition, the observation that other cell lines showed MSC-dependent 3D but not 2D efficacy responses at GI_{50}s close to the 7df3 IC_{50} (collaboration data, data not shown) means it remains possible that a repeat of the synthetic screen with an alternative cell line could identify targets with greater efficacy.

Figure 33 placement

Figure 33. HCT116 3D soft agar assay

The HCT116 anchorage independent growth assay in soft agar was conducted over 14 days (Stefanie Gaus, Merck Serono). The more advance 'daughter' compound (MSCi) that was developed during this study is also shown for comparison (**b**). Cells were treated with compound every 2-3 days, and cell viability measured by AlamarBlue assay (n=4).

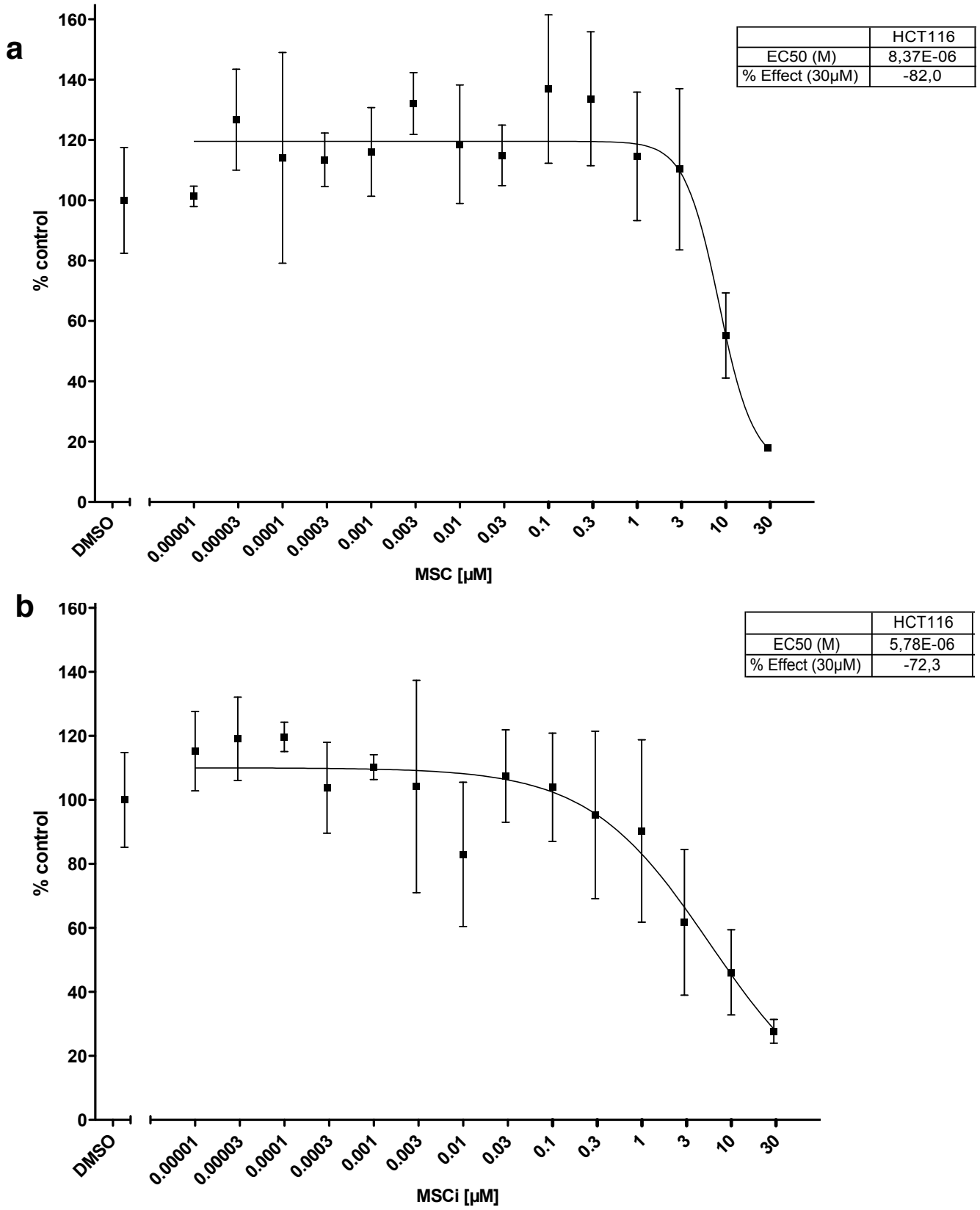

Figure 33. HCT116 3D soft agar assay

The HCT116 anchorage independent growth assay in soft agar was conducted over 14 days (Stefanie Gaus, Merck Serono). The more advance 'daughter' compound (MSCi) that was developed during this study is also shown for comparison (**b**). Cells were treated with compound every 2-3 days, and cell viability measured by AlamarBlue assay (n=4).

Other CDK8 functions

There are many additional roles for CDK8 (and CDK19) outside of their role in Wnt signalling (some of which are summarised in Figure 34). Its function in processes such as embryonic stem cell pluripotency, the positive regulation of STAT transcription factors and the promotion of growth factor dependent transcription elongation has been determined (reviewed in (Galbraith et al., 2010)). In addition, there are potentially many roles for CDK8 outside of the Mediator complex. Of note, up to 30% of this CDK8:CycC regulatory module can be purified without Mediator, suggesting that CDK8 function may extend beyond transcriptional regulation (Galbraith et al., 2010).

Not only are there many alternate roles for CDK8 other than in Wnt signalling, there are many other potential biological responses that may be relevant for the biology of CDK8 inhibitors in tumour cells in 2D culture and *in vivo.* Interestingly, Adler *et al*. suggested that the responses following inducible-shRNA-dependent CDK8 loss were particularly linked to the loss of a stem cell component ((Adler et al., 2012) and in house studies).

It is important to consider that this is a large field of research that is in its relative infancy at present and as such CDK8 is a constantly moving target, with over 2,200 studies published in the past five years (1,200 of which were published in the last two years alone) compared to 1,600 in the time prior to 2008. The responses that were seen in the cDNA and esiRNA studies here cannot yet be definitively linked to any one CDK8 function and may be due to one or a combination of CDK8 effectors or due to processes that are only indirectly linked to CDK8 pathways and are required for the far-downstream contribution of CDK8 to cell viability.

Figure 34 Placement

Figure 34. Many roles for CDK8

Schematic illustration of the known functions of CDK8.

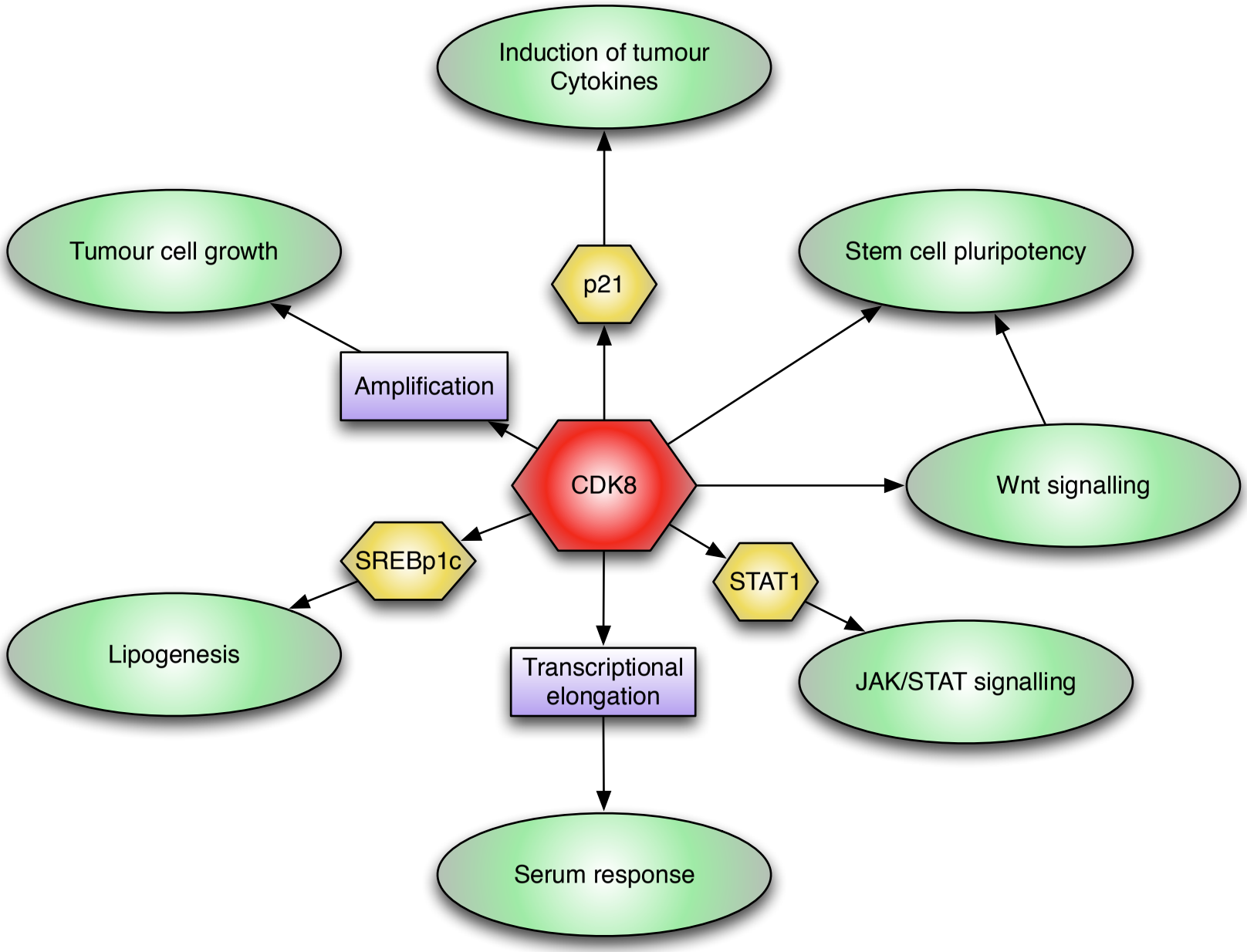

Figure 34. Many roles for CDK8

Schematic illustration of the known functions of CDK8.

In house assays have shown that CCT family compounds induce a reduction of HCT116 xenograft tumour proliferation *in vivo* (data not shown). As tumours are subject to numerous paracrine signalling events between tumour cells and between tumour cells and stromal cells (fibroblasts, endothelial cells, immune cells), CCT-series compound action *in vivo* may be indirectly mediated by effects on CDK8 action in the stromal as well as the tumour component. Supporting this suggestion, it has recently been shown that HCT116 cells were able to protect an apoptosis-sensitive fibroblast population from apoptosis in co-culture in a CDK8-dependent paracrine manner (Porter et al., 2012), suggesting that epithelial (with elevated CDK8)-stromal interactions *in vivo* are critical in mediating response to MSC. Furthermore, the majority of the surface area of cells cultured in 2D is either in contact with the plastic culture surface or nutrient media, thus cell-cell interaction and communication is limited. Therefore a reduction in cellular viability mediated by the compound *in vivo* (and 3D spheroid cultures) could appear more pronounced than in 2D assays. Such a response may be occurring with RNAi:MSC dual inhibition in the 2D HCT116 cell assay, raising the possibility that the effects of hits identified under 2D conditions may be amplified when transferred into 3D and *in vivo* systems.

In summary, the role of distinct CDK8 functions in HCT116 cellular responses is currently unclear. What is also unclear is whether any gene products (identified here) that mediate HCT116 viability in the presence of MSC (in 2D culture) are linked to Wnt or immediate CDK8 targets. Nonetheless, consideration of the biological function of two of the top esiRNA hits does raise possible mechanistic links. These gene products are HARS and BRAF.

Histidyl Aminoacyl tRNA Synthetase

The outstanding hit of the esiRNA chemical sensitisation screen was cytoplasmic Histidyl Aminoacyl tRNA Synthetase (HARS or HisRS; (Ibb, 2004)), whose endogenous expression in HCT116 cells conferred resistance to MSC. HARS's enzymatic activity is essential for protein translation, charging the cognate tRNA with histidine for its subsequent incorporation into proteins. Identification of this enzyme as the strongest hit in the esiRNA screen was surprising and equally very interesting, as few direct links have previously been described connecting it to either Wnt or CDK8 function. Interestingly, manual scrutiny of the interaction data also showed an RNAi:MSC combination-dependent with the inhibition of RARS (arginyl-tRNA synthetase), however this gene did not reach the stringent hit selection criteria.

A link of potential significance between HARS and Wnt is the observation that the kinase TNIK (TRAF2 and NCK-interacting protein kinase) was able to bind to HARS in a yeast-2-hybrid protein-protein interaction assay (Camargo et al., 2007). Although TNIK was shown to be required for Wnt signalling in the intestine this link has only been made in one report (Mahmoudi et al., 2009), and evidence has yet to been presented to validate its suggested binding to HARS. A second putative link may also exist between HARS and Wnt-driven hair biology. Despite its ubiquitous expression, a mutation in HARS causes its aminoacylation function to become defective resulting in Usher syndrome (Puffenberger et al., 2012). Patients with Usher syndrome experience progressive hearing loss (amongst other pathologies) resulting from mutations in HARS, which may be linked to damage or loss of cochlea hair cells (although the data is preliminary).

More generally, an emerging literature suggests that there is great potential in combining translational inhibitors including rapamycin analogues and other chemotherapeutic agents. The results presented here hint at a possible future combinatorial link between an inhibitor of transcription (MSC:CDK8) and inhibitors of translation, perhaps via pathways including HARS.

Interestingly recent evidence suggests that amino-acyl tRNA synthetases may be 'repurposed' for non-translational roles, as nuclear and extracellular roles have been uncovered; sites where translation does not occur. Eukaryotic amino-acyl transferases have been shown to be organised into multi-synthetase complexes that have roles in regulation (Yang, 2013) and non-translational functions for amino-acyl transferases have been demonstrated in roles including angiogenesis, mTOR signalling, inflammatory responses and tumour growth (Bonfils et al., 2012; Dorrell et al., 2007; Han et al., 2012; Park et al., 2012; Pierce et al., 2011; Xu et al., 2012). Of particular interest is the observation that leucine tRNA synthetase (LARS) is a key component of a regulatory complex that controls the activity of the mTORC1 complex since the AKT/mTOR pathway is required downstream of APC loss for tumourigenesis and can be blocked by treatment with the mTOR inhibitor, rapamycin (Ashton et al., 2010; Fujishita et al., 2008).

There are two key questions that must be addressed by further studies in order to determine the utility of HARS as a drug target:

1. How general is the requirement for HARS?
2. Is HARS enzymatic activity required for conditional lethality?

A panel of colorectal cancer cell lines could be probed to assess the breadth of the necessity of HARS inhibition to confer MSC sensitivity. This will help to ascertain HARS's role as a broadly-relevant 'druggable' target. Furthermore, 3D spheroid assays could identify whether the HARS RNAi:MSC combinatorial effect is amplified in 3D culture.

It is currently unclear whether either the structural or enzymatic properties of HARS are critical for HCT116 survival when treated with MSC. In order to understand the mechanism of synergy of MSC with the loss-of-function of HARS, HARS inducible shRNA knockout cell lines could be generated, and the ability of wild-type or mutant (e.g. kinase dead) HARS to rescue RNAi:MSC synthetic lethality elucidated. If HARS enzymatic activity were to be shown to be critical in maintaining cells viability in the presence of MSC, the rational design of HARS

inhibitors could be conducted (based on the knowledge of HARS's active site). Alternatively a high-throughput screen for HARS inhibitors could be carried out using compound libraries. It is predicted that any HARS inhibitors created/identified would improve the potency of MSC when used in combination, and may potentially broaden the panel of patients that would benefit from treatment with MSC.

Additionally, it would be useful to know what effects MSC has on HARS (if any), to determine how its function may be altered (and hence providing further information that may help understanding of the resulting biology, i.e. viability reduction). For example, determination of MSC-dependent changes in HARS phosphorylation by mass spectrometry may provide insights into the viability reduction mechanism.

Serine/threonine-protein kinase B-raf

A further significant hit was the serine/threonine protein kinase, BRAF. One of three Raf kinases, BRAF functions as part of the Ras/MAP (Mitogen-activated protein) kinase signalling pathway to phosphorylate MEK (MAP kinase kinase), thus it has a key role in the regulation of downstream Ras/MAPK target genes. RAF kinases are critical to cellular function, and defects in BRAF are found in a wide range of cancers, including colorectal cancer. Despite the Ras/MAPK activation process being tightly regulated by multiple phosphatases and kinases, an activation mutation of BRAF (V600E) is commonly seen in many cancer subtypes (Davies et al., 2002).

In the cDNA screen, the identification of Medaka HRAS and KRAS ability to super-activate TCF-dependent transcription complemented the previous identification of HRAS and KRAS in Jamie Freeman's *Xenopus tropicalis* cDNA screen (Freeman, 2008). The determination of synergistic interactions between Wnt and Ras/MAPK signalling was in line with studies showing that Ras/MAPK

signalling can modulate Wnt/β-catenin signalling, and may be essential for the expression of Wnt target genes and tumour progression in colorectal cancer (Kim et al., 2007; Phelps et al., 2009).

Of the three Raf kinases only BRAF was determined to have synergistic interaction with MSC, although a manual search of the esiRNA:MSC interaction dataset showed that ARAF also exhibited MSC dependent interaction (but this was not significant enough to pass the selection criteria; see Appendix 7). Despite BRAF RNAi:MSC only reducing HCT116 viability by ~10%, this result was highly reproducible and this clear evidence of synergy was mirrored in BRAF inhibitor investigations. Interactions were probed further using compound-compound assays, assessing the interaction of MSC with the highly selective BRAF inhibitor (against both wild-type and mutant), RAF265, in HCT116 cells. RAF265 (at 1μM) synergised reproducibly with MSC, albeit a relatively high concentration of 2.5μM MSC in HCT116 cells (Figure 29; 200 times the 7df3 TCF-reporter IC_{50}, but lower than RAF265 inhibitor cellular IC_{50} of 5 and 10μM in HT29 and MDAMB231 cells respectively (Mordant et al., 2010)), with synergy also evident in Ls174T cells (Figure 30). Interestingly, three other BRAF inhibitors and two MEK inhibitors (that act downstream of BRAF in the MAPK pathway) did not show synergy (data not shown). The reason for this is unclear but may be related to the specificity of RAF265, since it is postulated to be highly wild-type BRAF specific with lower mutant kinase specificity. Further studies are required to determine the biology of this response since RAF265 also targets VEGFR2 (and CRAF to a lesser extent), thus the 'pan-inhibitory' activity of the compound may be contributing to its combinatorial efficacy with MSC. The observation that some RAF inhibitors show a paradoxic activation of the Ras/MAPK, pathway particularly when Ras is mutant (as with HCT116 and Ls174T cells) due the ability of the inhibitors to induce BRAF-CRAF-dimer formation and MEK activation (Baljuls et al., 2013), is also an interesting one. Further studies will be required to investigate whether RAF265 actually activates

Raf-MAPK signalling as part of its ability to co-operate with MSC in reducing tumour cell viability.

Novel cDNA regulators of Wnt signalling

Fourteen cDNAs were shown to super-activate TCF-dependent transcription in the presence of Wnt signalling co-activation, of which SezL2 (seizure related 6 homolog (mouse)-like 2), IKZF1 (Ikaros family zinc finger 1) and TGIF1 (TGFB-induced factor homeobox 1) currently have no known links to Wnt signalling. Both TGIF1 and IKZF1 act at the transcriptional level, although their potential function in the context of Wnt signalling is unclear as TGIF1 is a transcriptional co-repressor (Bertolino et al., 1995), and IKZF1 both activates and inhibits transcription (Kim et al., 1999). Little is known about Sez6L2, other than it is likely to be expressed exclusively in the brain where it may contribute to a specialised endoplasmic reticulum function within neurons (by comparison with its murine homologue (Miyazaki et al., 2006)). One additional hit of interest was HMGXB4 (HMG box domain containing 4). This non-histone chromosomal protein is believed to negatively regulate Wnt/β-catenin signalling during development (by similarity to the *Xenopus laevis* homologue, (Yamada et al., 2003)), thus why its overexpression in the HEK-based context activates TCF-dependent transcription is unclear. Further work is required to determine the mechanism of action of these activators within the Wnt/β-catenin signalling context.

Of the fourteen cDNAs determined to super-activate TCF-dependent transcription in the presence of Wnt signalling co-activation, eight induced activity independently of pathway stimulation by ΔNLRP (including the putatively labelled 'HMGB2*' hit previously described). Four of the hits were known Wnt signalling activators (Wnt-1, β-catenin, KRAS and HRAS) with three, including the transcription factor DMRTA2, having little known association with Wnt signalling. It had been shown that Wnt/β-catenin signalling positively regulates the expression of DMRTA2 during the development of the cerebral cortex (Konno et

al., 2012), however whether DMRTA2 has any direct effect on Wnt signalling in other contexts is unknown. The work presented here would suggest that DMRTA2 might positively regulate TCF-dependent transcription by means of a feedback loop, however this would require further investigation.

The ability of MSC to disrupt the activating ability of the cDNA hits (both with and without ΔNLRP co-activation) was determined. As expected, all ΔNLRP-dependent interactions were inhibited by MSC since MSC is able to block transcription induced by ΔNLRP alone. Significantly, MSC was unable to disrupt GBX1 and HMGB2 induced ΔNLRP-*independent* TCF-dependent transcription. Overexpression of these transcription factors conferred resistance to the CDK8 inhibitor, suggesting that their transcriptional regulation functions may not require Mediator complex co-activation. Again, there is limited information describing the wider activity of these transcription factors; GBX1 has been shown to be essential for Wnt/β-catenin dependent regulation of neural patterning in zebrafish embryos (Rhinn et al., 2009), and HMGB2 enhances Wnt signalling in murine embryos and is essential for forelimb digit development (Itou et al., 2011). This study suggests that GBX1 and HMGB2 might have important roles in MSC resistance via the maintenance of Wnt signalling. For example, overexpression of either gene in a clinical context might be regarded as a contra-indication for MSC-class therapies. Further studies of these functions may identify the underlying mechanisms by which they induce TCF-dependent transcription.

Overall, novel Wnt pathway regulators and genes that co-operate with MSC were identified in two whole genome screens. The results point to a particularly novel area of biology in the role of aminoacyl tRNA synthetases that will be followed up in future studies. In addition, many future avenues of work have been raised that could be of benefit to patients in the long term. Of highest priority may be studies that translate the observations here into 3D culture where stem cell function can be analysed.

Bibliography

Adler, A.S., McCleland, M.L., Truong, T., Lau, S., Modrusan, Z., Soukup, T.M., Roose-Girma, M., Blackwood, E.M., and Firestein, R. (2012). CDK8 Maintains Tumor dedifferentiation and embryonic stem cell pluripotency. Cancer Res. *72*, 2129–2139.

Aguilera, O., Fraga, M.F., Ballestar, E., Paz, M.F., Herranz, M., Espada, J., García, J.M., Muñoz, A., Esteller, M., and Gonzalez-Sancho, J.M. (2006). Epigenetic inactivation of the Wnt antagonist Dickkopf-1 (Dkk-1) gene in human colorectal cancer. Oncogene *25*, 4116–4121.

Amado, N.G., Fonseca, B.F., Cerqueira, D.M., Neto, V.M., and Abreu, J.G. (2011). Flavonoids: potential Wnt/beta-catenin signaling modulators in cancer. Life. Sci. *89*, 545–554.

Amit, S. (2002). Axin-mediated CKI phosphorylation of beta-catenin at Ser 45: a molecular switch for the Wnt pathway. Genes Dev. *16*, 1066–1076.

Angers, S., and Moon, R.T. (2009). Proximal events in Wnt signal transduction. Nature Rev. Mol. Cell Biol. *10*, 468–477.

Ashton, G.H., Morton, J.P., Myant, K., Phesse, T.J., Ridgway, R.A., Marsh, V., Wilkins, J.A., Athineos, D., Muncan, V., Kemp, R., et al. (2010). Focal adhesion kinase is required for intestinal regeneration and tumorigenesis downstream of Wnt/c-Myc signaling. Dev. Cell *19*, 259–269.

Bafico, A., Gazit, A., Pramila, T., Finch, P.W., Yaniv, A., et al. (1999). Interaction of frizzled related protein (FRP) with Wnt ligands and the frizzled receptor suggests alternative mechanisms for FRP inhibition of Wnt signaling. J. Biol. Chem. *274*, 16180–16187.

Bafico, A., Liu, G., Goldin, L., Harris, V., and Aaronson, S.A. (2004). An autocrine mechanism for constitutive Wnt pathway activation in human cancer cells. Cancer Cell *6*, 497–506.

Baljuls, A., Kholodenko, B.N., and Kolch, W. (2013). It takes two to tango - signalling by dimeric Raf kinases. Mol. Biosyst. *9*, 551–558.

Bao, R., Christova, T., Song, S., Angers, S., Yan, X., and Attisano, L. (2012). Inhibition of tankyrases induces axin stabilization and blocks Wnt signalling in breast cancer cells. PLoS ONE *7*, e48670.

Barker, N., Ridgway, R.A., van Es, J.H., van de Wetering, M., Begthel, H., et al. (2009). Crypt stem cells as the cells-of-origin of intestinal cancer. Nature *457*, 608–611.

Barker, N., van Es, J.H., Kuipers, J., Kujala, P., van den Born, M., Cozijnsen, M., Haegebarth, A., Korving, J., Begthel, H., Peters, P.J., et al. (2007). Identification of stem cells in small intestine and colon by marker gene Lgr5. Nature *449*, 1003–1007.

Barolo, S., and Posakony, J.W. (2002). Three habits of highly effective signaling pathways: principles of transcriptional control by developmental cell signaling. Genes Dev. *16*, 1167–1181.

Basu, D., Reyes-Mugica, M., and Rebbaa, A. (2012). Role of the Beta catenin destruction complex in mediating chemotherapy-induced senescence-associated secretory phenotype. PLoS ONE *7*, e52188.

Batlle, E., Henderson, J.T., Beghtel, H., van den Born, M.M., Sancho, E., Huls, G., Meeldijk, J., Robertson, J., van de Wetering, M., Pawson, T., et al. (2002). beta-catenin and TCF mediate cell positioning in the intestinal epithelium by controlling the expression of EphrinB. Cell *111*, 251–263.

Bejsovec, A., and Arias, A.M. (1991). Roles of wingless in patterning the larval epidermis of Drosophila. Development *113*, 471–485.

Benhamouche, S., Decaens, T., Godard, C., Chambrey, R., Rickman, D.S., Moinard, C., Vasseur-Cognet, M., Kuo, C.J., Kahn, A., Perret, C., et al. (2006). Apc tumor suppressor gene is the “zonation-keeper” of mouse liver. Dev. Cell *10*, 759–770.

Bertolino, E., Reimund, B., Wildt-Perinic, D., and Clerc, R.G. (1995). A novel homeobox protein which recognizes a TGT core and functionally interferes with a retinoid-responsive motif. J. Biol. Chem. *270*, 31178–31188.

Bertrand, F.E., Angus, C.W., Partis, W.J., and Sigounas, G. (2012). Developmental pathways in colon cancer: Crosstalk between WNT, BMP, Hedgehog and Notch. Cell Cycle *11*, 4344–4351.

Bhat, R.A., Stauffer, B., Komm, B.S., and Bodine, P.V.N. (2007). Structure-function analysis of secreted frizzled-related protein-1 for its Wnt antagonist function. J. Cell. Biochem. *102*, 1519–1528.

Biechele, T.L., Camp, N.D., Fass, D.M., Kulikauskas, R.M., Robin, N.C., White, B.D., Taraska, C.M., Moore, E.C., Muster, J., Karmacharya, R., et al. (2010). Chemical-genetic screen identifies riluzole as an enhancer of Wnt/β-catenin signaling in melanoma. Chem. Biol. *17*, 1177–1182.

Bilic, J., Huang, Y.L., Davidson, G., Zimmermann, T., Cruciat, C.M., et al. (2007). Wnt induces LRP6 signalosomes and promotes dishevelled-dependent LRP6 phosphorylation. Science *316*, 1619–1622.

Birmingham, A., Selfors, L.M., Forster, T., Wrobel, D., Kennedy, C.J., Shanks, E., Santoyo-Lopez, J., Dunican, D.J., Long, A., Kelleher, D., et al. (2009). Statistical methods for analysis of high-throughput RNA interference screens. Nature Meth. *6*, 569–575.

Bishop-Bailey, D., and Warner, T.D. (2003). PPARγ ligands induce prostaglandin production in vascular smooth muscle cells: indomethacin acts as a peroxisome proliferator-activated receptor-γ antagonist. FASEB J.*17*, 1925–1927.

Bjerknes, M., and Cheng, H. (1981a). The stem-cell zone of the small intestinal epithelium. I. Evidence from Paneth cells in the adult mouse. American J. Anat. *160*, 51–63.

Bjerknes, M., and Cheng, H. (1981b). The stem-cell zone of the small intestinal epithelium. II. Evidence from paneth cells in the newborn mouse. American J. Anat. *160*, 65–75.

Blumenthal, A., Ehlers, S., Lauber, J., Buer, J., Lange, C., Goldmann, T., Heine, H., Brandt, E., and Reiling, N. (2006). The Wingless homolog WNT5A and its receptor Frizzled-5 regulate inflammatory responses of human mononuclear cells induced by microbial stimulation. Blood *108*, 965–973.

Bonfils, G., Jaquenoud, M., Bontron, S., Ostrowicz, C., Ungermann, C., and De Virgilio, C. (2012). Leucyl-tRNA synthetase controls TORC1 via the EGO complex. Mol. Cell *46*, 105–110.

Bourhis, E., Wang, W., Tam, C., Hwang, J., Zhang, Y., Spittler, D., Huang, O.W., Gong, Y., Estevez, A., Zilberleyb, I., et al. (2011). Wnt antagonists bind through a short peptide to the first β-propeller domain of LRP5/6. Structure *19*, 1433–1442.

Boutros, M., Brás, L.P., and Huber, W. (2006). Analysis of cell-based RNAi screens. Genome Biol. *7*, R66.

Brennan, K., Gonzalez-Sancho, J.M., Castelo-Soccio, L.A., Howe, L.R., and Brown, A.M. (2004). Truncated mutants of the putative Wnt receptor LRP6/Arrow can stabilize beta-catenin independently of Frizzled proteins. Oncogene *23*, 4873–4884.

Brideau, C., Gunter, B., Pikounis, B., and Liaw, A. (2003). Improved statistical methods for hit selection in high-throughput screening. J. Biomol. Screen. *8*, 634–647.

Brott, B.K., and Sokol, S.Y. (2002). Regulation of Wnt-LRP signaling by distinct domains. MCB *22*, 6100–6110.

Buchert, M., Athineos, D., Abud, H.E., Burke, Z.D., Faux, M.C., Samuel, M.S., Jarnicki, A.G., Winbanks, C.E., Newton, I.P., Meniel, V.S., et al. (2010). Genetic dissection of differential signaling threshold requirements for the Wnt/beta-catenin pathway in vivo. PLoS Genet. *6*, e1000816.

Buchholz, F., Kittler, R., Slabicki, M., and Theis, M. (2006). Enzymatically prepared RNAi libraries. Nature Methods *3*, 696–700.

Cadigan, K.M., and Waterman, M.L. (2013). TCF/LEFs and Wnt Signaling in the Nucleus. Cold Spring Harb. Perspect. Biol. Ed. Nusse, He, van Amerongen, 105–126.

Caldwell, G.M., Jones, C., Gensberg, K., Jan, S., Hardy, R.G., et al. (2004). The Wnt antagonist sFRP1 in colorectal tumorigenesis. Cancer Res. *64*, 883–888.

Camargo, L.M., Collura, V., Rain, J.C., Mizuguchi, K., Hermjakob, H., Kerrien, S., Bonnert, T.P., Whiting, P.J., and Brandon, N.J. (2007). Disrupted in Schizophrenia 1 Interactome: evidence for the close connectivity of risk genes and a potential synaptic basis for schizophrenia. Mol. Psychiatry *12*, 74–86.

Cancer Research UK. www.cancerresearchuk.org

Carmona-Saez, P., Chagoyen, M., Tirado, F., Carazo, J.M., and Pascual-Montano, A. (2007). GENECODIS: a web-based tool for finding significant concurrent annotations in gene lists. Genome Biol. *8*, R3.

Carrera, I., Janody, F., Leeds, N., Duveau, F., and Treisman, J.E. (2008). Pygopus activates Wingless target gene transcription through the mediator complex subunits Med12 and Med13. PNAS *105*, 6644–6649.

Carreras Puigvert, J., Stechow, von, L., Siddappa, R., Pines, A., Bahjat, M., Haazen, L.C.J.M., Olsen, J.V., Vrieling, H., Meerman, J.H.N., Mullenders, L.H.F., et al. (2013). Systems biology approach identifies the kinase csnk1a1 as a regulator of the DNA damage response in embryonic stem cells. Sci. Signal. *6*, 1–14.

Casas-Selves, M., Kim, J., Zhang, Z., Helfrich, B.A., Gao, D., Porter, C.C., Scarborough, H.A., Bunn, P.A., Chan, D.C., Tan, A.C., et al. (2012). Tankyrase and the canonical Wnt pathway protect lung cancer cells from EGFR inhibition. Cancer Res. *72*, 4154–4164.

Castellone, M.D., Teramoto, H., Williams, B.O., Druey, K.M., and Gutkind, J.S. (2005). Prostaglandin E2 promotes colon cancer cell growth through a novel Gs-Axin-{beta}-catenin signaling axis. Science 310, 1504–1510.

Cavallo, R.A., Cox, R.T., Moline, M.M., Roose, J., Polevoy, G.A., et al. (1998). Drosophila Tcf and Groucho interact to repress Wingless signalling activity. Nature *395*, 604–608.

Chen, G., Fernandez, J., Mische, S., and Courey, A.J. (1999). A functional interaction between the histone deacetylase Rpd3 and the corepressor groucho in Drosophila development. Genes Dev. *13*, 2218–2230.

Chen, S., Bubeck, D., MacDonald, B.T., Liang, W.X., Mao, J.H., Malinauskas, T., Llorca, O., Aricescu, A.R., Siebold, C., He, X., et al. (2011). Structural and functional studies of LRP6 ectodomain reveal a platform for Wnt signaling. Dev. Cell *21*, 848–861.

Chen, T., Li, M., Ding, Y., Zhang, L.S., Xi, Y., et al. (2009). Identification of zinc-finger BED domain-containing 3 (Zbed3) as a novel axin-interacting protein that activates Wnt/beta-catenin signaling. J. Biol. Chem. *284*, 6683–6689.

Clarke, M.F., and Fuller, M. (2006). Stem cells and cancer: two faces of eve. Cell *124*, 1111–1115.

Clevers, H. (2006). Wnt/beta-catenin signaling in development and disease. Cell *127*, 469–480.

Clevers, H., and Nusse, R. (2012). Wnt/beta-catenin signaling and disease. Cell *149*, 1192–1205.

Conaway, R.C., Sato, S., Tomomori-Sato, C., Yao, T., and Conaway, J.W. (2005). The mammalian Mediator complex and its role in transcriptional regulation. TIBS *30*, 250–255.

Cole, M.F., Johnstone, S.E., Newman, J.J., Kagey, M.H., and Young, R.A. (2008). Tcf3 is an integral component of the core regulatory circuitry of embryonic stem cells. Genes Dev. *22*, 746–755.

Collu, G.M., Meurette, O., and Brennan, K. (2009). Is there more to Wnt signalling in breast cancer than stabilisation of β-catenin? Breast Cancer Res. *11*, 105–106.

Coombs, G.S., Schmitt, A.A., Canning, C.A., Alok, A., Low, I.C.C., Banerjee, N., Kaur, S., Utomo, V., Jones, C.M., Pervaiz, S., et al. (2012). Modulation of Wnt/beta-catenin signaling and proliferation by a ferrous iron chelator with therapeutic efficacy in genetically engineered mouse models of cancer. Oncogene *31*, 213–225.

Cox, L.S., and Lane, D.P. (1995). Tumour suppressors, kinases and clamps: how p53 regulates the cell cycle in response to DNA damage. Bioessays *17*, 501–508.

Cruciat, C.M., and Niehrs, C. (2013). Secreted and Transmembrane Wnt Inhibitors and Activators. Cold Spring Harb. Perspect. Biol. Ed. Nusse, He, van Amerongen, 39-64.

Cselenyi, C.S., Jernigan, K.K., Tahinci, E., Thorne, C.A., Lee, L.A., and Lee, E. (2008). LRP6 transduces a canonical Wnt signal independently of Axin degradation by inhibiting GSK3's phosphorylation of beta-catenin. PNAS *105*, 8032–8037.

Curtin, J.C., and Lorenzi, M.V. (2010). Drug discovery approaches to target Wnt signaling in cancer stem cells. Oncotarget *1*, 563–577.

Dajani, R., Fraser, E., Roe, S.M., Yeo, M., Good, V.M., Thompson, V., Dale, T.C., and Pearl, L.H. (2003). Structural basis for recruitment of glycogen synthase kinase 3beta to the axin-APC scaffold complex. EMBO J. *22*, 494–501.

Daniels, D.L., and Weis, W.I. (2005). Beta-catenin directly displaces Groucho/TLE repressors from Tcf/Lef in Wnt-mediated transcription activation. Nature Struct. Mol. Biol. *12*, 364–371.

Dann, C.E., Hsieh, J.C., Rattner, A., Sharma, D., Nathans, J., and Leahy, D.J. (2001). Insights into Wnt binding and signalling from the structures of two Frizzled cysteine-rich domains. Nature *412*, 86–90.

DasGupta, R., Kaykas, A., Moon, R.T., and Perrimon, N. (2005). Functional genomic analysis of the Wnt-wingless signaling pathway. Science *308*, 826–833.

Davidson, G., Wu, W., Shen, J., Bilic, J., Fenger, U., Stannek, P., Glinka, A., and Niehrs, C. (2005). Casein kinase 1 gamma couples Wnt receptor activation to cytoplasmic signal transduction. Nature *438*, 867–872.

Davies, H., Bignell, G.R., Cox, C., Stephens, P., Edkins, S., Clegg, S., Teague, J., Woffendin, H., Garnett, M.J., Bottomley, W., et al. (2002). Mutations of the BRAF gene in human cancer. Nature *417*, 949–954.

De Ferrari, G.V., and Moon, R.T. (2006). The ups and downs of Wnt signaling in prevalent neurological disorders. Oncogene *25*, 7545–7553.

de Sousa, E.M.F., Vermeulen, L., Richel, D., and Medema, J.P. (2011). Targeting Wnt signaling in colon cancer stem cells. Clin. Cancer Res. *17*, 647–653.

De, A. (2011). Wnt/Ca^{2+} signaling pathway: a brief overview. Acta Biochim. Biophys. Sin. *43*, 745–756.

DeAlmeida, V.I., Miao, L., Ernst, J.A., Koeppen, H., Polakis, P., and Rubinfeld, B. (2007). The soluble wnt receptor Frizzled8CRD-hFc inhibits the growth of teratocarcinomas in vivo. Cancer Res. *67*, 5371–5379.

Devenport, D., and Fuchs, E. (2008). Planar polarization in embryonic epidermis orchestrates global asymmetric morphogenesis of hair follicles. Nature Cell Biol. *10*, 1257–1268.

Donner, A.J., Ebmeier, C.C., Taatjes, D.J., and Espinosa, J.M. (2010). CDK8 is a positive regulator of transcriptional elongation within the serum response network. Nature Struct. Mol. Biol. *17*, 194–201.

Dorrell, M.I., Aguilar, E., Scheppke, L., Barnett, F.H., and Friedlander, M. (2007). Combination angiostatic therapy completely inhibits ocular and tumor angiogenesis. PNAS *104*, 967–972.

Echeverri, C.J., Beachy, P.A., Baum, B., Boutros, M., Buchholz, F., Chanda, S.K., Downward, J., Ellenberg, J., Fraser, A.G., Hacohen, N., et al. (2006). Minimizing the risk of reporting false positives in large-scale RNAi screens. Nature Meth. *3*, 777–779.

Elder, D.J., and Paraskeva, C. (1998). COX-2 inhibitors for colorectal cancer. Nature Medicine *4*, 392–393.

Emami, K.H., Nguyen, C., Ma, H., Kim, D.H., Jeong, K.W., Eguchi, M., Moon, R.T., Teo, J.L., Oh, S.W., Kim, H.Y., et al. (2004). A small molecule inhibitor of beta-catenin/cyclic AMP response element-binding protein transcription. PNAS *101*, 12682–12687.

Ettarh, R., Cullen, A., and Calamai, A. (2010). NSAIDs and cell proliferation in colorectal cancer. Pharmaceuticals *3*, 2007–2021.

Ettenberg, S.A., Charlat, O., Daley, M.P., Liu, S., Vincent, K.J., Stuart, D.D., Schuller, A.G., Yuan, J., Ospina, B., and Green, J. (2010). Inhibition of tumorigenesis driven by different Wnt proteins requires blockade of distinct ligand-binding regions by LRP6 antibodies. PNAS *107*, 15473–15478.

Ewan, K.B., and Dale, T.C. (2008). The potential for targeting oncogenic Wnt/beta-catenin signaling in therapy. Curr. Drug Targets *9*, 532–547.

Ewan, K., Pajak, B., Stubbs, M., Todd, H., Barbeau, O., Quevedo, C., Botfield, H., Young, R., Ruddle, R., Samuel, L., et al. (2010). A useful approach to identify novel small-molecule inhibitors of Wnt-dependent transcription. Cancer Res. *70*, 5963–5973.

Fallahi-Sichani, M., Honarnejad, S., Heiser, L.M., Gray, J.W., and Sorger, P.K. (2013). Metrics other than potency reveal systematic variation in responses to cancer drugs. Nature Chem. Biol. Advance online publication 1-9

Fanto, M., and McNeill, H. (2004). Planar polarity from flies to vertebrates. J. of Cell Sci. *117*, 527–533.

Farmer, H., McCabe, N., Lord, C.J., Tutt, A.N.J., Johnson, D.A., Richardson, T.B., Santarosa, M., Dillon, K.J., Hickson, I., Knights, C., et al. (2005). Targeting the DNA repair defect in BRCA mutant cells as a therapeutic strategy. Nature *434*, 917–921.

Fiedler, M., Sanchez-Barrena, M.J., Nekrasov, M., Mieszczanek, J., Rybin, V., Muller, J., Evans, P., and Bienz, M. (2008). Decoding of methylated histone H3 tail by the Pygo-BCL9 Wnt signaling complex. Mol. Cell *30*, 507–518.

Firestein, R., Bass, A.J., Kim, S.Y., Dunn, I.F., Silver, S.J., Guney, I., Freed, E., Ligon, A.H., Vena, N., Ogino, S., et al. (2008). CDK8 is a colorectal cancer oncogene that regulates beta-catenin activity. Nature *455*, 547–551.

Firestein, R., and Hahn, W.C. (2009). Revving the Throttle on an oncogene: CDK8 takes the driver seat. Cancer Res. *69*, 7899–7901.

Fodde, R., Smits, R., and Clevers, H. (2001). APC, signal transduction and genetic instability in colorectal cancer. Nature Rev. Cancer *1*, 55–67.

Freeman, J. (2008) Identification of a network of functional interactions regulating Wnt signalling. Cardiff University.

Fujishita, T., Aoki, K., Lane, H., Aoki, M., and Taketo, M.M. (2008). Inhibition of the mTORC1 pathway suppresses intestinal polyp formation and reduces mortality in Apc716 mice. PNAS *105*, 13544–13549.

Furumoto, T., Tanaka, A., Ito, M., Malik, S., Hirose, Y., Hanaoka, F., and Ohkuma, Y. (2007). A kinase subunit of the human mediator complex, CDK8, positively regulates transcriptional activation. Genes Cells *12*, 119–132.

Galbraith, M.D., Donner, A.J., and Espinosa, J.M. (2010). CDK8: a positive regulator of transcription. Transcription *1*, 4–12.

Galceran, J., Farinas, I., Depew, M.J., Clevers, H., and Grosschedd, R. (1999). $Wnt3a^{(-/-)}$ - phenotype and limb deficiency in $Lef1^{(-/-)}Tcf1^{(-/-)}$mice. Genes Dev. *13*, 709–717.

Garber, K. (2009). Drugging the Wnt pathway: problems and progress. JNCI *101*, 548–550.

Gaulton, A., Bellis, L.J., Bento, A.P., Chambers, J., Davies, M., Hersey, A., Light, Y., McGlinchey, S., Michalovich, D., Al-Lazikani, B., et al. (2012). ChEMBL: a large-scale bioactivity database for drug discovery. Nucleic Acids Res. *40*, D1100–D1107.

Gerbe, F., van Es, J.H., Makrini, L., Brulin, B., Mellitzer, G., Robine, S., Romagnolo, B., Shroyer, N.F., Bourgaux, J.F., Pignodel, C., et al. (2011). Distinct ATOH1 and Neurog3 requirements define tuft cells as a new secretory cell type in the intestinal epithelium. J. of Cell Biol. *192*, 767–780.

Ghogomu, S.M., van Venrooy, S., Ritthaler, M., Wedlich, D., and Gradl, D. (2006). HIC-5 is a novel repressor of lymphoid enhancer factor/T-cell factor-driven transcription. J. Biol. Chem. *281*, 1755–1764.

Gong, Y., Bourhis, E., Chiu, C., Stawicki, S., DeAlmeida, V.I., Liu, B.Y., Phamluong, K., Cao, T.C., Carano, R.A.D., Ernst, J.A., et al. (2010). Wnt isoform-specific interactions with coreceptor specify inhibition or potentiation of signaling by LRP6 antibodies. PLoS ONE *5*, e12682.

Gonsalves, F.C., Klein, K., Carson, B.B., Katz, S., Ekas, L.A., Evans, S., Nagourney, R., Cardozo, T., Brown, A.M.C., and DasGupta, R. (2011). An RNAi-based chemical genetic screen identifies three small-molecule inhibitors of the Wnt/wingless signaling pathway. PNAS *108*, 5954–5963.

Groden, J., Thliveris, A., Samowitz, W., Carlson, M., Gelbert, L., Albertsen, H., Joslyn, G., Stevens, J., Spirio, L., Robertson, M., et al. (1991). Identification and characterization of the familial adenomatous polyposis coli gene. Cell *66*, 589–600.

Grosch, S., Tegeder, I., Niederberger, E., Bräutigam, L., and Geisslinger, G. (2001). COX-2 independent induction of cell cycle arrest and apoptosis in colon cancer cells by the selective COX-2 inhibitor celecoxib. Faseb J. *15*, 2742–2744.

Grossmann, T.N., Yeh, J.T.H., Bowman, B.R., Chu, Q., Moellering, R.E., and Verdine, G.L. (2012). Inhibition of oncogenic Wnt signaling through direct targeting of β-catenin. PNAS *109*, 17942–17947.

Gurney, A., Axelrod, F., Bond, C.J., Cain, J., Chartier, C., Donigan, L., Fischer, M., Chaudhari, A., Ji, M., Kapoun, A.M., et al. (2012). Wnt pathway inhibition via the targeting of Frizzled receptors results in decreased growth and tumorigenicity of human tumors. PNAS *109*, 11717–11722.

Ha, N.C., Tonozuka, T., Stamos, J.L., Choi, H.J., and Weis, W.I. (2004). Mechanism of phosphorylation-dependent binding of APC to β-catenin and its role in β-catenin degradation. Mol. Cell *15*, 511–521.

Hagen, T., Di Daniel, E., Culbert, A.A., and Reith, A.D. (2002). Expression and characterization of GSK-3 mutants and their effect on beta-catenin phosphorylation in intact cells. J. Biol. Chem. *277*, 23330–23335.

Hall, J.M., Lee, M.K., Newman, B., Morrow, J.E., Anderson, L.A., Huey, B., and King, M.C. (1990). Linkage of early-onset familial breast cancer to chromosome 17q21. Science *250*, 1684–1689.

Han, J.M., Jeong, S.J., Park, M.C., Kim, G., Kwon, N.H., Kim, H.K., Ha, S.H., Ryu, S.H., and Kim, S. (2012). Leucyl-tRNA synthetase is an intracellular leucine sensor for the mTORC1-signaling pathway. Cell *149*, 410–424.

Handeli, S., and Simon, J.A. (2008). A small-molecule inhibitor of Tcf/beta-catenin signaling down-regulates PPARgamma and PPARdelta activities. Mol. Cancer Ther. *7*, 521–529.

Harrison-Uy, S.J., and Pleasure, S.J. (2012). Wnt signaling and forebrain development. Cold Spring Harb. Perspect. Biol. Ed. Nusse, He, van Amerongen, 297-307.

Hart, M., Concordet, J.P., Lassot, I., Albert, I., del los Santos, R., Durand, H., Perret, C., Rubinfeld, B., Margottin, F., Benarous, R., et al. (1999). The F-box protein beta-TrCP associates with phosphorylated beta-catenin and regulates its activity in the cell. Curr. Biol. *9*, 207–10.

Havsteen, B.H. (2002). The biochemistry and medical significance of the flavonoids. Pharmacol. Ther. *96*, 67–202.

He, B., Reguart, N., You, L., Mazieres, J., Xu, Z., et al. (2005). Blockade of Wnt-1 signaling induces apoptosis in human colorectal cancer cells containing downstream mutations. Oncogene *24*, 3054–3058.

He, T.C., Sparks, A.B., Rago, C., Hermeking, H., Zawel, L., da Costa, L.T., Morin, P.J., Vogelstein, B., and Kinzler, K.W. (1998). Identification of c-MYC as a target of the APC pathway. Science *281*, 1509–1512.

He, X., He, X., Semenov, M., Semenov, M., Tamai, K., Tamai, K., Zeng, X., and Zeng, X. (2004). LDL receptor-related proteins 5 and 6 in Wnt/beta-catenin signaling: arrows point the way. Development *131*, 1663–1677.

He, X., Saint-Jeannet, J.P., Wang, Y., Nathans, J., Dawid, I., and Varmus, H. (1997). A member of the Frizzled protein family mediating axis induction by Wnt-5A. Science *275*, 1652–1654.

He, X.C., Yin, T., Grindley, J.C., Tian, Q., Sato, T., Tao, W.A., Dirisina, R., Porter-Westpfahl, K.S., Hembree, M., Johnson, T., et al. (2007). PTEN-deficient intestinal stem cells initiate intestinal polyposis. Nature Genet. *39*, 189–198.

Henderson, W.R., Chi, E.Y., Ye, X., Nguyen, C., Tien, Y.T., Zhou, B., Borok, Z., Knight, D.A., and Kahn, M. (2010). Inhibition of Wnt/β-catenin/CREB binding protein (CBP) signaling reverses pulmonary fibrosis. PNAS *107*, 14309–14314.

Hengartner, C.J., Myer, V.E., Liao, S.M., Wilson, C.J., Koh, S.S., and Young, R.A. (1998). Temporal regulation of RNA polymerase II by Srb10 and Kin28 cyclin-dependent kinases. Mol. Cell *2*, 43–53.

Hernando, E., Nahle, Z., Juan, G., Diaz-Rodriguez, E., Alaminos, M., et al. (2004). Rb inactivation promotes genomic instability by uncoupling cell cycle progression from mitotic control. Nature *430*, 797–802.

Hirata, A., Utikal, J., Yamashita, S., Aoki, H., Watanabe, A., Yamamoto, T., Okano, H., Bardeesy, N., Kunisada, T., Ushijima, T., et al. (2013). Dose-dependent roles for canonical Wnt signalling in de novo crypt formation and cell cycle properties of the colonic epithelium. Development *140*, 66–75.

Hoeppner, L.H., Secreto, F.J., and Westendorf, J.J. (2009). Wnt signaling as a therapeutic target for bone diseases. Expert Opin. Ther. Targets *13*, 485–496.

Hsieh, J.C., Kodjabachian, L., Rebbert, M.L., Rattner, A., Smallwood, P.M., Samos, C.H., Nusse, R., Dawid, I.B., and Nathans, J. (1999). A new secreted protein that binds to Wnt proteins and inhibits their activities. Nature *398*, 431–436.

Hu, T., and Li, C. (2010). Convergence between Wnt-β-catenin and EGFR signaling in cancer. Mol. Cancer *9*, 236.

Huang, D.W., Sherman, B.T., and Lempicki, R.A. (2009a). Systematic and integrative analysis of large gene lists using DAVID bioinformatics resources. Nature Protoc. *4*, 44–57.

Huang, S.M.A., Mishina, Y.M., Liu, S., Cheung, A., Stegmeier, F., Michaud, G.A., Charlat, O., Wiellette, E., Zhang, Y., Wiessner, S., et al. (2009b). Tankyrase inhibition stabilizes axin and antagonizes Wnt signalling. Nature *461*, 614–620.

Ibb, M. (2004). Aminoacyl-tRNAs: setting the limits of the genetic code. Genes Dev. *18*, 731–738.

Ingenuity Pathway Analysis. www.ingenuity.com

Ishitani, T., Kishida, S., Hyodo-Miura, J., Ueno, N., Yasuda, J., Waterman, M., Shibuya, H., Moon, R.T., Ninomiya-Tsuji, J., and Matsumoto, K. (2003). The TAK1-NLK mitogen-activated protein kinase cascade functions in the Wnt-5a/Ca(2+) pathway to antagonize Wnt/beta-catenin signaling. Mol. Cell. Biol. *23*, 131–139.

Itasaki, N., and Hoppler, S. (2009). Crosstalk between Wnt and bone morphogenic protein signaling: A turbulent relationship. Dev. Dyn. *239*, 16–33.

Itou, J., Taniguchi, N., Oishi, I., Kawakami, H., Lotz, M., and Kawakami, Y. (2011). HMGB factors are required for posterior digit development through integrating signaling pathway activities. Dev. Dyn. *240*, 1151–1162.

Janda, C.Y., Waghray, D., Levin, A.M., Thomas, C., and Garcia, K.C. (2012). Structural basis of Wnt recognition by Frizzled. Science. *337*, 259–263.

Janssen, K.P., Alberici, P., Fsihi, H., Gaspar, C., Breukel, C., Franken, P., Rosty, C., Abal, M., Marjou, El, F., Smits, R., et al. (2006). APC and oncogenic KRAS are synergistic in enhancing Wnt signaling in intestinal tumor formation and progression. Gastroent. *131*, 1096–1109.

Jarde, T., Evans, R.J., McQuillan, K.L., Parry, L., Feng, G.J., Alvares, B., Clarke, A.R., and Dale, T.C. (2013). In vivo and in vitro models for the therapeutic targeting of Wnt signaling using a Tet-OΔN89β-catenin system. Oncogene *32*, 883–893.

Johnson, E.B., Hammer, R.E., and Herz, J. (2005). Abnormal development of the apical ectodermal ridge and polysyndactyly in Megf7-deficient mice. Hum. Mol. Genet. *14*, 3523–3538.

Joslyn, G., Carlson, M., Thliveris, A., Albertsen, H., Gelbert, L., Samowitz, W., Groden, J., Stevens, J., Spirio, L., and Robertson, M. (1991). Identification of deletion mutations and three new genes at the familial polyposis locus. Cell *66*, 601–613.

Kapoor, A., Goldberg, M.S., Cumberland, L.K., Ratnakumar, K., Segura, M.F., Emanuel, P.O., Menendez, S., Vardabasso, C., Leroy, G., Vidal, C.I., et al. (2010). The histone variant macroH2A suppresses melanoma progression through regulation of CDK8. Nature *468*, 1105–1109.

Kawamoto, S.A., Coleska, A., Ran, X., Yi, H., Yang, C.Y., and Wang, S. (2012). Design of triazole-stapled BCL9 α-helical peptides to target the β-catenin/B-cell CLL/lymphoma 9 (BCL9) protein–protein interaction. J. Med. Chem. *55*, 1137–1146.

Kestler, H.A., and Kuhl, M. (2008). From individual Wnt pathways towards a Wnt signalling network. PTRSL *363*, 1333–1347.

Kikuchi, A., Yamamoto, H., and Sato, A. (2009). Selective activation mechanisms of Wnt signaling pathways. TICB *19*, 119–129.

Kim, C.H., Oda, T., Itoh, M., Jiang, D., Artinger, K.B., Chandrasekharappa, S.C., Driever, W., and Chitnis, A.B. (2000). Repressor activity of Headless/Tcf3 is essential for vertebrate head formation. Nature *407*, 913–6.

Kim, D., Kim, D., Rath, O., Rath, O., Kolch, W., Kolch, W., Cho, K.H., and Cho, K.H. (2007). A hidden oncogenic positive feedback loop caused by crosstalk between Wnt and ERK pathways. Oncogene *26*, 4571–4579.

Kim, J., Sif, S., Jones, B., Jackson, A., Koipally, J., Heller, E., Winandy, S., Viel, A., Sawyer, A., Ikeda, T., et al. (1999). Ikaros DNA-binding proteins direct formation of chromatin remodeling complexes in lymphocytes. Immunity *10*, 345–355.

Kim, S., Xu, X., Hecht, A., and Boyer, T.G. (2006). Mediator is a transducer of Wnt/beta-catenin signaling. J. Biol. Chem. *281*, 14066–14075.

Kimelman, D., and Xu, W. (2006). beta-catenin destruction complex: insights and questions from a structural perspective. Oncogene *25*, 7482–7491.

Kinzler, K.W., and Vogelstein, B. (1996). Lessons from hereditary colorectal cancer. Cell *87*, 159–170.

Kinzler, K.W., Nilbert, M.C., Su, L.K., Vogelstein, B., Bryan, T.M., Levy, D.B., Smith, K.J., Preisinger, A.C., Hedge, P., McKechnie, D., et al. (1991). Identification of FAP locus genes from chromosome 5q21. Science *253*, 661–665.

Kittler, R., Putz, G., Pelletier, L., Poser, I., Heninger, A.K., Drechsel, D., Fischer, S., Konstantinova, I., Habermann, B., Grabner, H., et al. (2004). An endoribonuclease-prepared siRNA screen in human cells identifies genes essential for cell division. Nature *432*, 1036–1040.

Klampfer, L. (2008). The role of signal transducers and activators of transcription in colon cancer. Front. Biosci. *13*, 2888–2899.

Klein, P.S. (2012). GSK-3 and Wnt signaling in neurogenesis and bipolar disorder. Front. Mol. Neurosci. *5*, 1–13.

Knox, C., Law, V., Jewison, T., Liu, P., Ly, S., Frolkis, A., Pon, A., Banco, K., Mak, C., Neveu, V., et al. (2011). DrugBank 3.0: a comprehensive resource for “omics” research on drugs. Nucleic Acids Res. *39*, D1035–D1041.

Knuesel, M.T., Meyer, K.D., Donner, A.J., Espinosa, J.M., and Taatjes, D.J. (2009). The human CDK8 subcomplex is a histone kinase that requires Med12 for activity and can function independently of mediator. Mol. Cell. Biol. *29*, 650–661.

Knuesel, M.T., Meyer, K.D., Bernecky, C., and Taatjes, D.J. (2009). The human CDK8 subcomplex is a molecular switch that controls Mediator coactivator function. Genes Dev. *23*, 439–451.

Koles, K., and Budnik, V. (2012). Wnt Signaling in neuromuscular junction development. Cold Spring Harb. Perspect. Biol. Ed. Nusse, He, van Amerongen, 373-394.

Kongkanuntn, R., Bubb, V.J., Sansom, O.J., Wyllie, A.H., Harrison, D.J., and Clarke, A.R. (1999). Dysregulated expression of beta-catenin marks early neoplastic change in Apc mutant mice, but not all lesions arising in Msh2 deficient mice. Oncogene *18*, 7219–7225.

Konno, D., Iwashita, M., Satoh, Y., Momiyama, A., Abe, T., Kiyonari, H., and Matsuzaki, F. (2012). The mammalian DM domain transcription factor Dmrta2 is required for early embryonic development of the cerebral cortex. PLoS ONE *7*, e46577.

Korinek, V., Barker, N., Moerer, P., van Donselaar, E., Huls, G., Peters, P.J., and Clevers, H. (1998). Depletion of epithelial stem-cell compartments in the small intestine of mice lacking Tcf-4. Nature Genet. *19*, 379–383.

Kosinski, C., Li, V.S.W., Chan, A.S.Y., Zhang, J., Ho, C., Tsui, W.Y., Chan, T.L., Mifflin, R.C., Powell, D.W., Yuen, S.T., et al. (2007). Gene expression patterns of human colon tops and basal crypts and BMP antagonists as intestinal stem cell niche factors. PNAS *104*, 15418–15423.

Kramps, T., Peter, O., Brunner, E., Nellen, D. and Froesch, B. (2002). Wnt/wingless signaling requires BCL9/legless-mediated recruitment of pygopus to the nuclear β-catenin-TCF complex. Cell. *109*, 47–60.

Kratochwil, K., Galceran, J., Tontsch, S., Roth, W., and Grosschedl, R. (2002). FGF4, a direct target of LEF1 and Wnt signaling, can rescue the arrest of tooth organogenesis in Lef1(-/-) mice. Genes Dev. *16*, 3173–3185.

Kuhl, M., Sheldahl, L.C., Malbon, C.C., and Moon, R.T. (2000). Ca(2+)/calmodulin-dependent protein kinase II is stimulated by Wnt and Frizzled homologs and promotes ventral cell fates in Xenopus. JBC *275*, 12701–12711.

Kühl, S.J., and Kühl, M. (2012). On the role of Wnt/β-catenin signaling in stem cells. BBA *1830*, 2297–2306.

la Roche, de, M., Rutherford, T.J., Gupta, D., Veprintsev, D.B., Saxty, B., et al. (2012). An intrinsically labile alpha-helix abutting the BCL9-binding site of beta-catenin is required for its inhibition by carnosic acid. Nature Comms. *3*, 680–10.

Lee, H.J., Wang, N.X., Shi, D.L., and Zheng, J.J. (2009). Sulindac inhibits canonical Wnt signaling by blocking the PDZ domain of the protein dishevelled. Angew. Chem. Int. Ed. *48*, 6448–6452.

Lee, S.B., Gong, Y.D., Park, Y.I., and Dong, M.S. (2013). 2,3,6-Trisubstituted quinoxaline derivative, a small molecule inhibitor of the Wnt/beta-catenin signaling pathway, suppresses cell proliferation and enhances radiosensitivity in A549/Wnt2 cells. Biochem. Biophys. Res. Commun. *431* 746–752.

Lepourcelet, M., Chen, Y.N., France, D.S., Wang, H., Crews, P., Petersen, F., Bruseo, C., Wood, A.W., and Shivdasani, R.A. (2004). Small-molecule antagonists of the oncogenic Tcf/beta-catenin protein complex. Cancer Cell *5*, 91–102.

Lian, X., Hsiao, C., Wilson, G., Zhu, K., Hazeltine, L.B., Azarin, S.M., Raval, K.K., Zhang, J., Kamp, T.J., and Palecek, S.P. (2012). Robust cardiomyocyte differentiation from human pluripotent stem cells via temporal modulation of canonical Wnt signaling. PNAS *109*, 10759–10760.

Lickert, H., Takeuchi, J.K., Both, Von, I., Walls, J.R., McAuliffe, F., Adamson, S.L., Henkelman, R.M., Wrana, J.L., Rossant, J., and Bruneau, B.G. (2004). Baf60c is essential for function of BAF chromatin remodelling complexes in heart development. Nature *432*, 107–112.

Lim, S., and Kaldis, P. (2013). Cdks, cyclins and CKIs: roles beyond cell cycle regulation. Development *140*, 3079–3093.

Lin, J., Wang, X., and Dorsky, R.I. (2011). Progenitor expansion in APC mutants is mediated by Jak/Stat signaling. BMC Dev. Biol. *11*, 73-81.

Lin, K., Wang, S., Julius, M.A., Kitajewski, J., Moos, M., and Luyten, F.P. (1997). The cysteine-rich frizzled domain of Frzb-1 is required and sufficient for modulation of Wnt signaling. PNAS *94*, 11196–11200.

Lin, X., and Perrimon, N. (1999). Dally cooperates with Drosophila Frizzled 2 to transduce Wingless signalling. Nature *400*, 281–284.

Liu, B.Y., Soloviev, I., Huang, X., Chang, P., Ernst, J.A., Polakis, P., and Sakanaka, C. (2012). Mammary Tumor Regression Elicited by Wnt Signaling Inhibitor Requires IGFBP5. Cancer Res. *72*, 1568–1578.

Liu, G., Bafico, A., and Aaronson, S.A. (2005). The mechanism of endogenous receptor activation functionally distinguishes prototype canonical and noncanonical Wnts. Mol. Cell. Biol. *25*, 3475–3482.

Liu, H., Fergusson, M.M., Wu, J.J., Rovira, I.I., Liu, J., Gavrilova, O., Lu, T., Bao, J., Han, D., Sack, M.N., et al. (2011). Wnt Signaling Regulates Hepatic Metabolism. Sci. Signal. *4*, ra6–ra6.

Liu, J., Xing, Y., Hinds, T.R., Zheng, J., and Xu, W. (2006). The Third 20 Amino Acid Repeat Is the Tightest Binding Site of APC for β-Catenin. JMB *360*, 133–144.

Liu, T., Lee, Y.N., Malbon, C.C., and Wang, H.Y. (2002). Activation of the beta-catenin/Lef-Tcf pathway is obligate for formation of primitive endoderm by mouse F9 totipotent teratocarcinoma cells in response to retinoic acid. J. Biol. Chem. *277*, 30887–30891.

Liu, W., Dong, X., Mai, M., Seelan, R.S., and Taniguchi, K. (2000). Mutations in AXIN2 cause colorectal cancer with defective mismatch repair by activating β-catenin/TCF signalling. Nature. *26*, 146–147.

Lloyd-Lewis, B. (2011) High-throughput screening for novel regulators of beta-catenin in Wnt signalling. Cardiff University.

Logan, C.Y., and Nusse, R. (2004). The Wnt signaling pathway in development and disease. Ann. Rev. Cell Dev. Biol. *20*, 781–810.

Lopez-Rios, J., Esteve, P., Ruiz, J.M., and Bovolenta, P. (2008). The Netrin-related domain of Sfrp1 interacts with Wnt ligands and antagonizes their activity in the anterior neural plate. Neural Dev. *3*, 19-37.

Lu, W., Lu, W., Yamamoto, V., Yamamoto, V., Ortega, B., Ortega, B., Baltimore, D., and Baltimore, D. (2004). Mammalian Ryk is a Wnt coreceptor required for stimulation of neurite outgrowth. Cell *119*, 97–108.

Lu, W., Lin, C., Roberts, M.J., Waud, W.R., Piazza, G.A., and Li, Y. (2011). Niclosamide suppresses cancer cell growth by inducing Wnt co-receptor LRP6 degradation and inhibiting the Wnt/β-catenin pathway. PLoS ONE *6*, e29290.

Lucero, O.M., Dawson, D.W., Moon, R.T., and Chien, A.J. (2010). A re-evaluation of the “oncogenic” nature of Wnt/beta-catenin signaling in melanoma and other cancers. Curr. Oncol. Rep. *12*, 314–318.

Luis, T.C., Naber, B., Roozen, P., and Brugman, M.H. (2011). Canonical Wnt signaling regulates hematopoiesis in a dosage-dependent fashion. Cell Stem Cell *9*, 345–356.

Lundholt, B.K., Scudder, K.M., and Pagliaro, L. (2003). A simple technique for reducing edge effect in cell-based assays. J. Biomol. Screen *8*, 566–570.

Macdonald, B.T., and He, X. (2012). Frizzled and LRP5/6 receptors for Wnt/β-catenin signaling. Cold Spring Harb. Perspect. Biol. Ed. Nusse, He, van Amerongen, 65-87.

MacDonald, B.T., Yokota, C., Tamai, K., Zeng, X., and He, X. (2008). Wnt signal amplification via activity, cooperativity, and regulation of multiple intracellular PPPSP motifs in the Wnt co-receptor LRP6. J. Bio. Chem. *283*, 16115–16123.

Mahmoudi, T., .Li, V.S., Li, .Ng, S.S., .Taouatas, N., .Vries, R.G., et al. (2009). The kinase TNIK is an essential activator of Wnt target genes. EMBO J. *28*, 3329–3340.

Major, M.B., Roberts, B.S., Berndt, J.D., Marine, S., Anastas, J., Chung, N., Ferrer, M., Yi, X., Stoick-Cooper, C.L., Haller, von, P.D., et al. (2008). New regulators of Wnt/beta-catenin signaling revealed by integrative molecular screening. Sci. Signal. *1*, ra12.

Malanchi, I., Santamaria-Martínez, A., Susanto, E., Peng, H., Lehr, H.A. et al. (2011). Interactions between cancer stem cells and their niche govern metastatic colonization. Nature *481*, 85–89.

Malik, S., and Roeder, R.G. (2005). Dynamic regulation of pol II transcription by the mammalian Mediator complex. TIBS *30*, 256–263.

Malik, S., and Roeder, R.G. (2010). The metazoan Mediator co-activator complex as an integrative hub for transcriptional regulation. Nature *11*, 761–772.

Malumbres, M., and Barbacid, M. (2005). Mammalian cyclin-dependent kinases. TIBS *30*, 630–641.

Malumbres, M., and Barbacid, M. (2009). Cell cycle, CDKs and cancer: a changing paradigm. Nature Rev. Cancer *9*, 153–166.

Malumbres, M., Harlow, E., Hunt, T., Hunter, T., Lahti, J.M., Manning, G., Morgan, D.O., Tsai, L.H., and Wolgemuth, D.J. (2009). Cyclin-dependent kinases: a family portrait. Nature Cell Biol. *11*, 1275–1276.

Mao, B., Wu, W., Davidson, G., Marhold, J., Li, M., Mechler, B.M., Delius, H., Hoppe, D., Stannek, P., Walter, C., et al. (2002). Kremen proteins are Dickkopf receptors that regulate Wnt/beta-catenin signalling. Nature *417*, 664–667.

Mao, B., Wu, W., Li, Y., Hoppe, D., Stannek, P., Glinka, A., and Niehrs, C. (2001a). LDL-receptor-related protein 6 is a receptor for Dickkopf proteins. Nature *411*, 321–325.

Mao, B., and Niehrs, C. (2003). Kremen2 modulates Dickkopf2 activity during Wnt/LRP6 signaling. Gene *302*, 179–183.

Mao, J., Wang, J., Liu, B., Pan, W., Farr, G.H. et al. (2001b). Low-density lipoprotein receptor-related protein-5 binds to Axin and regulates the canonical Wnt signaling pathway. Mol. Cell *7*, 801–9.

Mao, Y., Lin, N., Tian, W., Han, X., Han, X., Huang, Z., and An, J. (2012). Design, synthesis, and biological evaluation of new diaminoquinazolines as β-catenin/Tcf4 pathway inhibitors. J. Med. Chem. *55*, 1346–1359.

von Marschall, Z., and Fisher, L.W. (2010). Secreted Frizzled-related protein-2 (sFRP2) augments canonical Wnt3a-induced signaling. Biochem. Biophys. Res. *400*, 299–304.

Marsh, V., Winton, D.J., Williams, G.T., Dubois, N., Trumpp, A., Sansom, O.J., and Clarke, A.R. (2008). Epithelial Pten is dispensable for intestinal homeostasis but suppresses adenoma development and progression after Apc mutation. Nature Genet. *40*, 1436–1444.

McMahon, A.P., and Moon, R.T. (1989). Ectopic expression of the proto-oncogene int-1 in Xenopus embryos leads to duplication of the embryonic axis. Cell *58*, 1075–1084.

Merrill, B.J. (2012). Wnt pathway regulation of embryonic stem cell self-renewal. Cold Spring Harb. Perspect. Biol. Ed. Nusse, He, van Amerongen, 233-249.

Merrill, B.J., Pasolli, H.A., Polak, L., and Rendl, M. (2004). Tcf3: a transcriptional regulator of axis induction in the early embryo. Development *131*, 263–274.

Miki, T., Bottaro, D.P., Fleming, T.P., Smith, C.L., Burgess, W.H., Chan, A.M., and Aaronson, S.A. (1992). Determination of ligand-binding specificity by alternative splicing: two distinct growth factor receptors encoded by a single gene. PNAS *89*, 246–250.

Minami, I., Yamada, K., Otsuji, T.G., Yamamoto, T., Shen, Y., Otsuka, S., Kadota, S., Morone, N., Barve, M., Asai, Y., et al. (2012). A small molecule that promotes cardiac differentiation of human pluripotent stem cells under defined, cytokine- and xeno-free conditions. Cell Rep. *2*, 1448–1460.

Miyazaki, T., Hashimoto, K., Uda, A., Sakagami, H., Nakamura, Y., Saito, S.Y., Nishi, M., Kume, H., Tohgo, A., Kaneko, I., et al. (2006). Disturbance of cerebellar synaptic maturation in mutant mice lacking BSRPs, a novel brain-specific receptor-like protein family. FEBS Lett. *580*, 4057–4064.

Mologni, L., Brussolo, S., Ceccon, M., and Gambacorti-Passerini, C. (2012). Synergistic effects of combined Wnt/KRAS inhibition in colorectal cancer cells. PLoS ONE *7*, e51449.

Moore, A.C., Amann, J.M., Williams, C.S., Tahinci, E., Farmer, T.E., Martinez, J.A., Yang, G., Luce, K.S., Lee, E., and Hiebert, S.W. (2008). Myeloid translocation gene family members associate with T-cell factors (TCFs) and influence TCF-dependent transcription. Mol. Cell. Biol. *28*, 977–987.

Mordant, P., Loriot, Y., Leteur, C., Calderaro, J., Bourhis, J., Wislez, M., Soria, J.C. and Deutsch, E. (2010). Dependence on phosphoinositide 3-kinase and RAS-RAF pathways drive the activity of RAF265, a novel RAF/VEGFR2 inhibitor, and RAD001 (Everolimus) in combination. Mol. Cancer Ther. *9*, 358–368.

Morin, P.J., Sparks, A.B., Korinek, V., Barker, N., Clevers, H., Vogelstein, B., and Kinzler, K.W. (1997). Activation of beta-catenin-Tcf signaling in colon cancer by mutations in beta-catenin or APC. Science *275*, 1787–1790.

Morris, E.J., Ji, J.Y., Yang, F., Di Stefano, L., Herr, A., Moon, N.S., Kwon, E.J., Haigis, K.M., Naar, A.M., and Dyson, N.J. (2008). E2F1 represses beta-catenin transcription and is antagonized by both pRB and CDK8. Nature *455*, 552–556.

Moser, A.R., Pitot, H.C., and Dove, W.F. (1990). A dominant mutation that predisposes to multiple intestinal neoplasia in the mouse. Science *247*, 322–324.

Naito, A.T., Sumida, T., Nomura, S., Liu, M.L., Higo, T. et al. (2012). Complement C1q activates canonical Wnt signaling and promotes aging-related phenotypes. Cell *149*, 1298–1313.

Neumann, C.J., and Cohen, S.M. (1996). Distinct mitogenic and cell fate specification functions of wingless in different regions of the wing. Development *122*, 1781–1789.

Niehrs, C. (2012). The complex world of WNT receptor signalling. Nature Rev. Mol. Cell Biol. *13*, 767–779.

Nishisho, I., Nakamura, Y., Miyoshi, Y., Miki, Y. and Ando, H. (1991). Mutations of chromosome 5q21 genes in FAP and colorectal cancer patients. Science *251*, 1366–1370.

Nishita, M., Enomoto, M., Yamagata, K., and Minami, Y. (2010). Cell/tissue-tropic functions of Wnt5a signaling in normal and cancer cells. Trends in Cell Biology *20*, 346–354.

Nogales-Cadenas, R., Carmona-Saez, P., Vazquez, M., Vicente, C., Yang, X., Tirado, F., Carazo, J.M., and Pascual-Montano, A. (2009). GeneCodis: interpreting gene lists through enrichment analysis and integration of diverse biological information. Nucleic Acids Res. *37*, W317–W322.

Orford, K., Crockett, C., Jensen, J.P., Weissman, A.M. and Byers, S.W. (1997). Serine phosphorylation-regulated ubiquitination and degradation of beta-catenin. J. Biol. Chem. *272*, 24735–24738.

Osada, T., Chen, M., Yang, X.Y., Spasojevic, I., Vandeusen, J.B., Hsu, D., Clary, B.M., Clay, T.M., Chen, W., Morse, M.A., et al. (2011). Antihelminth compound niclosamide downregulates Wnt signaling and elicits antitumor responses in tumors with activating APC mutations. Cancer Res. *71*, 4172–4182.

Paganoni, S., Bernstein, J., and Ferreira, A. (2010). Ror1-Ror2 complexes modulate synapse formation in hippocampal neurons. Neuroscience *165*, 1261–1274.

Papkoff, J., Brown, A.M., and Varmus, H.E. (1987). The int-1 proto-oncogene products are glycoproteins that appear to enter the secretory pathway. Mol. Cell. Biol. *7*, 3978–3984.

Park, M.C., Kang, T., Han, J.M., Kim, S.B., Park, Y.J., Cho, K., Park, Y.W., Guo, M., Yang, X.L., Schimmel, P., et al. (2012). Secreted human glycyl-tRNA synthetase implicated in defense against ERK-activated tumorigenesis. PNAS e640–e647.

Park, S., Gwak, J., Cho, M., Song, T., Won, J., Kim, D.E., Shin, J.G., and Oh, S. (2006). Hexachlorophene inhibits Wnt/beta-catenin pathway by promoting Siah-mediated beta-catenin degradation. Mol. Pharmacol. *70*, 960–966.

Perrimon, N., and Bernfield, M. (2000). Specificities of heparan sulphate proteoglycans in developmental processes. Nature *404*, 725–728.

Phelps, R.A., Chidester, S., Dehghanizadeh, S., Phelps, J., Sandoval, I.T., Rai, K., Broadbent, T., Sarkar, S., Burt, R.W., and Jones, D.A. (2009). A two-step model for colon adenoma initiation and progression caused by APC loss. Cell *137*, 623–634.

Pierce, S.B., Chisholm, K.M., Lynch, E.D., Lee, M.K., Walsh, T., Opitz, J.M., Li, W., Klevit, R.E., and King, M.C. (2011). Mutations in mitochondrial histidyl tRNA synthetase HARS2 cause ovarian dysgenesis and sensorineural hearing loss of Perrault syndrome. PNAS *108*, 6543–6548.

Pinto, D., and Clevers, H. (2005a). Wnt control of stem cells and differentiation in the intestinal epithelium. Exp. Cell Res. *306*, 357–363.

Pinto, D., and Clevers, H. (2005b). Wnt, stem cells and cancer in the intestine. Biol. Cell *97*, 185–196.

Pires-daSilva, A., and Sommer, R.J. (2003). The evolution of signalling pathways in animal development. Nature Rev. Genet. *4*, 39–49.

Pitts, T.M., Davis, S.L., Eckhardt, S.G., and Bradshaw-Pierce, E.L. (2013). Targeting nuclear kinases in cancer: Development of cell cycle kinase inhibitors. Pharmacol. Ther. *(In press)*

Porter, D.C., Farmaki, E., and Altilia, S. (2012). Cyclin-dependent kinase 8 mediates chemotherapy-induced tumor-promoting paracrine activities. PNAS *109*, 13799–13804.

Puffenberger, E.G., Jinks, R.N., Sougnez, C., Cibulskis, K., Willert, R.A., Achilly, N.P., Cassidy, R.P., Fiorentini, C.J., Heiken, K.F., Lawrence, J.J., et al. (2012). Genetic mapping and exome sequencing identify variants associated with five novel diseases. PLoS ONE *7*, e28936.

Radtke, F., and Clevers, H. (2005). Self-renewal and cancer of the gut: two sides of a coin. Science *307*, 1904–1909.

Radulescu, S., Brookes, M.J., Salgueiro, P., Ridgway, R.A., McGhee, E., Anderson, K., Ford, S.J., Stones, D.H., Iqbal, T.H., Tselepis, C., et al. (2012). Luminal iron levels govern intestinal tumorigenesis after Apc loss in vivo. Cell Rep. *2*, 270–282.

Ramanathan, Y., Rajpara, S.M., Reza, S.M., Lees, E., Shuman, S., Mathews, M.B., and Pe'ery, T. (2001). Three RNA polymerase II carboxyl-terminal domain kinases display distinct substrate preferences. J. Biol. Chem. *276*, 10913–10920.

Reya, T., O'Riordan, M., Okamura, R., Devaney, E., Willert, K., Nusse, R., and Grosschedl, R. (2000). Wnt signaling regulates B lymphocyte proliferation through a LEF-1 dependent mechanism. Immunity *13*, 15–24.

Rhinn, M., Lun, K., Ahrendt, R., Geffarth, M., and Brand, M. (2009). Zebrafish gbx1 refines the midbrain-hindbrain boundary border and mediates the Wnt8 posteriorization signal. Neural Dev. *4*, 12.

Riffell, J.L., Lord, C.J., and Ashworth, A. (2012). Tankyrase-targeted therapeutics: expanding opportunities in the PARP family. Nature Rev. Drug Discov. *11*, 923–936.

Rodriguez, J., Esteve, P., Weinl, C., Ruiz, J.M., Fermin, Y., Trousse, F., Dwivedy, A., Holt, C., and Bovolenta, P. (2005). SFRP1 regulates the growth of retinal ganglion cell axons through the Fz2 receptor. Nature Neurosci. *8*, 1301–1309.

Roose, J., Huls, G., van Beest, M., Moerer, P., van der Horn, K., Goldschmeding, R., Logtenberg, T., and Clevers, H. (1999). Synergy between tumor suppressor APC and the beta-catenin-tcf4 target tcf1. Science *285*, 1923–1926.

Roose, J., Molenaar, M., Peterson, J., Hurenkamp, J., Brantjes, H., Moerer, P., van de Wetering, M., Destree, O., and Clevers, H. (1998). The Xenopus Wnt effector XTcf-3 interacts with Groucho-related transcriptional repressors. Nature *395*, 608–612.

Rubinfeld, B., Souza, B., Albert, I., Muller, O., Chamberlain, S.H., Masiarz, F.R., Munemitsu, S., and Polakis, P. (1993). Association of the APC gene product with ß-catenin. Science *262*, 1731–1733.

Rudloff, S., and Kemler, R. (2012). Differential requirements for β-catenin during mouse development. Development *139*, 3711–3721.

Saneyoshi, T., Kume, S., Amasaki, Y., and Mikoshiba, K. (2002). The Wnt/calcium pathway activates NF-AT and promotes ventral cell fate in Xenopus embryos. Nature *417*, 295–299.

Sansom, O.J., Reed, K.R., Hayes, A.J., and Ireland, H. (2004). Loss of Apc in vivo immediately perturbs Wnt signaling, differentiation, and migration. Genes & Dev. *18*, 1385–1390.

Sansom, O.J., Meniel, V., Wilkins, J.A., Cole, A.M., Oien, K.A. et al. (2006). Loss of Apc allows phenotypic manifestation of the transforming properties of an endogenous K-ras oncogene in vivo. PNAS *103*, 14122–14127.

Sansom, O.J., Meniel, V.S., Muncan, V., Phesse, T.J., Wilkins, J.A., Reed, K.R., Vass, J.K., Athineos, D., Clevers, H., and Clarke, A.R. (2007). Myc deletion rescues Apc deficiency in the small intestine. Nature *446*, 676–679.

Saraswati, S., Alfaro, M.P., Thorne, C.A., Atkinson, J., Lee, E., and Young, P.P. (2010). Pyrvinium, a potent small molecule Wnt inhibitor, promotes wound repair and post-MI cardiac remodeling. PLoS ONE *5*, e15521.

Sato, A., Yamamoto, H., Sakane, H., Koyama, H., and Kikuchi, A. (2010). Wnt5a regulates distinct signalling pathways by binding to Frizzled2. EMBO J. *29*, 41–54.

Schepers, A., and Clevers, H. (2012). Wnt Signaling, Stem Cells, and Cancer of the Gastrointestinal Tract. Cold Spring Harb. Perspect. Biol. Ed. Nusse, He, van Amerongen, 251-264.

Schuijers, J., and Clevers, H. (2012). Adult mammalian stem cells: the role of Wnt, Lgr5 and R-spondins. EMBO J. *31*, 2685–2696.

Schwarz-Romond, T., Metcalfe, C., and Bienz, M. (2007). Dynamic recruitment of axin by Dishevelled protein assemblies. J. Cell Sci. *120*, 2402–2412.

Shibata, H., Toyama, K., Shioya, H., Ito, M., and Hirota, M. (1997). Rapid colorectal adenoma formation initiated by conditional targeting of the Apc gene. Science *278*, 120–123.

Shimizu, H., Julius, M.A., Giarre, M., Zheng, Z., Brown, A.M., and Kitajewski, J. (1997). Transformation by Wnt family proteins correlates with regulation of beta-catenin. Cell Growth Differ. *8*, 1349–1358.

Simons, M., Gault, W.J., Gotthardt, D., Rohatgi, R., Klein, T.J. et al. (2009). Electrochemical cues regulate assembly of the Frizzled/Dishevelled complex at the plasma membrane during planar epithelial polarization. Nature Cell Biol. *11*, 286–294.

Sinnberg, T., Menzel, M., Ewerth, D., Sauer, B., Schwarz, M., Schaller, M., Garbe, C., and Schittek, B. (2011). β-Catenin signaling increases during melanoma progression and promotes tumor cell survival and chemoresistance. PLoS ONE *6*, e23429.

Smalley, W.E., and DuBois, R.N. (1997). Colorectal cancer and nonsteroidal anti-inflammatory drugs. Advances in Pharmacology *39*, 1–20.

Spemann, H., and Mangold, H. (1924). über Induktion von Embryonalanlagen durch Implantation artfremder Organisatoren. Roux' Arch. Entw. Mech. *100*, 599–638.

Spemann, H., and Mangold, H. (2001). Induction of embryonic primordia by implantation of organizers from a different species. Translation of original text, Int. J. Dev. Biol. *45*, 13–38.

Stamos, J.L., and Weis, W.I. (2013). The beta-catenin destruction complex. Cold Spring Harb. Perspect. Biol. Ed. Nusse, He, van Amerongen, 89-104.

Su, L.K., Vogelstein, B., and Kinzler, K.W. (1993). Association of the APC tumor suppressor protein with catenins. Science *262*, 1734–1737.

Su, Y.Y., Fu, C., Ishikawa, S., Stella, A., Kojima, M., and Shitoh, K. (2008). APC is essential for targeting phosphorylated β-catenin to the SCF β-TrCP ubiquitin ligase. Mol. Cell *32*, 652–661.

Sun, Y., Campisi, J., Higano, C., Beer, T.M., Porter, P., Coleman, I., True, L., and Nelson, P.S. (2012). Treatment-induced damage to the tumor microenvironment promotes prostate cancer therapy resistance through WNT16B. Nature Medicine *18*, 1359–1368.

Swiatek, W., Kang, H., Garcia, B.A., Shabanowitz, J., Coombs, G.S., Hunt, D.F., and Virshup, D.M. (2006). Negative regulation of LRP6 function by casein kinase I epsilon phosphorylation. J. Biol. Chem. *281*, 12233–12241.

Taatjes, D.J. (2010). The human Mediator complex: a versatile, genome-wide regulator of transcription. TIBS *35*, 315–322.

Tabas-Madrid, D., Nogales-Cadenas, R., and Pascual-Montano, A. (2012). GeneCodis3: a non-redundant and modular enrichment analysis tool for functional genomics. Nucleic Acids Res. *40*, W478–W483.

Takagi, Y., Calero, G., Komori, H., Brown, J.A., Ehrensberger, A.H., Hudmon, A., Asturias, F., and Kornberg, R.D. (2006). Head module control of mediator interactions. Mol. Cell *23*, 355–364.

Takahashi-Yanaga, F., Yoshihara, T., Jingushi, K., Miwa, Y., Morimoto, S., Hirata, M., and Sasaguri, T. (2008). Celecoxib-induced degradation of T-cell factors-1 and -4 in human colon cancer cells. Biochem. Biophys. Res. Commun. *377*, 1185–1190.

Tamai, K., Semenov, M., Kato, Y., Spokony, R., Liu, C., Katsuyama, Y., Hess, F., Saint-Jeannet, J. P., and He, X. (2000). LDL-receptor-related proteins in Wnt signal transduction. Nature *407*, 530–535.

Tamai, K., Zeng, X., Liu, C., Zhang, X., Harada, Y., Chang, Z., and He, X. (2004). A mechanism for Wnt coreceptor activation. Mol. Cell *13*, 149–156.

Tang, W., Dodge, M., Gundapaneni, D., Michnoff, C., Roth, M., and Lum, L. (2008). A genome-wide RNAi screen for Wnt/beta-catenin pathway components identifies unexpected roles for TCF transcription factors in cancer. PNAS *105*, 9697–9702.

Tauriello, D.V.F., Jordens, I., Kirchner, K., Slootstra, J.W., Kruitwagen, T., et al. (2012). Wnt/β-catenin signaling requires interaction of the Dishevelled DEP domain and C terminus with a discontinuous motif in Frizzled. PNAS *109*, e812–e820.

Tenbaum, S.P., Puig, I., Chicote, I., Landolfi, S., Herance, J. Gispert, J.D., Mendizabal, L., et al. (2012). Beta-catenin confers resistance to PI3K and AKT inhibitors and subverts FOXO3a to promote metastasis in colon cancer. Nature Med. *18*, 892–901.

Theis, M., and Buchholz, F. (2011). High-throughput RNAi screening in mammalian cells with esiRNAs. Methods *53*, 424–429.

Thorne, C.A., Hanson, A.J., Schneider, J., Tahinci, E., Orton, D., Cselenyi, C.S., Jernigan, K.K., Meyers, K.C., Hang, B.I., Waterson, A.G., et al. (2010). Small-molecule inhibition of Wnt signaling through activation of casein kinase 1α. Nature Chem. Biol. *6*, 829–836.

Tian, W., Han, X., Yan, M., Xu, Y., Duggineni, S., Lin, N., Luo, G., Li, Y.M., Han, X., Huang, Z., et al. (2012). Structure-based discovery of a novel inhibitor targeting the β-Catenin/Tcf4 interaction. Biochemistry *51*, 724–731.

Tol, J., Nagtegaal, I.D., and Punt, C.J.A. (2009). BRAF mutation in metastatic colorectal cancer. N. Engl. J. Med. *361*, 98–99.

Tolwinski, N.S., Wehrli, M., Rives, A., Erdeniz, N., DiNardo, S., et al. (2003). Wg/Wnt signal can be transmitted through Arrow/LRP5,6 and Axin independently of Zw3/Gsk3beta Activity. Dev. Cell *4*, 407–418.

Trosset, J.Y., Dalvit, C., Knapp, S., Fasolini, M., Veronesi, M., Mantegani, S., Gianellini, L.M., Catana, C., Sundström, M., Stouten, P.F.W., et al. (2006). Inhibition of protein-protein interactions: The discovery of druglike β-catenin inhibitors by combining virtual and biophysical screening. Proteins *64*, 60–67.

Tsutsui, T., Umemura, H., Tanaka, A., Mizuki, F., Hirose, Y., and Ohkuma, Y. (2008). Human mediator kinase subunit CDK11 plays a negative role in viral activator VP16-dependent transcriptional regulation. Genes Cells *13*, 817–826.

Valvezan, A.J., Zhang, F., Diehl, J.A., and Klein, P.S. (2012). Adenomatous Polyposis Coli (APC) Regulates Multiple Signaling Pathways by Enhancing Glycogen Synthase Kinase-3 (GSK-3) Activity. J. Bio. Chem. *287*, 3823–3832.

van Amerongen, R. (2012). Alternative Wnt Pathways and Receptors. Cold Spring Harb. Perspect. Biol. Ed. Nusse, He, van Amerongen, 127-145.

van Amerongen, R., and Nusse, R. (2009). Towards an integrated view of Wnt signaling in development. Development *136*, 3205–3214.

van Amerongen, R., Mikels, A., and Nusse, R. (2008). Alternative wnt signaling is initiated by distinct receptors. Sci. Signal. *1*, re9–re9.

van Beest, M., Dooijes, D., and van de Wetering, M. (2000). Sequence-specific high mobility group box factors recognize 10–12-base pair minor groove motifs. JBC *275*, 27266–27273.

van de Wetering, M., and Clevers, H. (1992). Sequence-specific interaction of the HMG box proteins TCF-1 and SRY occurs within the minor groove of a Watson-Crick double helix. EMBO J. *11*, 3039–3044.

van de Wetering, M., Sancho, E., Verweij, C., de Lau, W., Oving, I., et al. (2002). The beta-catenin/TCF-4 complex imposes a crypt progenitor phenotype on colorectal cancer cells. Cell *111*, 241–250.

Veeman, M.T., Slusarski, D.C., Kaykas, A., Louie, S.H., and Moon, R.T. (2003). Zebrafish prickle, a modulator of noncanonical Wnt/Fz signaling, regulates gastrulation movements. Curr. Biology *13*, 680–685.

Venerando, A., Girardi, C., Ruzzene, M., and Pinna, L.A. (2013). Pyrvinium pamoate does not activate protein kinase CK1, but promotes Akt/PKB down-regulation and GSK3 activation. Biochem. J. *452*, 131–137.

Voronkov, A., and Krauss, S. (2012). Wnt/beta-catenin signaling and small molecule inhibitors. Curr. Pharm. Des. *19*, 634–664.

Wang, J., Sinha, T., and Wynshaw-Boris, A. (2012). Wnt signaling in mammalian development: lessons from mouse genetics. Cold Spring Harb. Perspect. Biol. Ed. Nusse, He, van Amerongen, 217-232.

Wang, W., Liu, H., Wang, S., Hao, X., and Li, L. (2011). A diterpenoid derivative 15-oxospiramilactone inhibits Wnt/β-catenin signaling and colon cancer cell tumorigenesis. Cell Res. *21*, 730–740.

Wend, P., Holland, J.D., Ziebold, U., and Birchmeier, W. (2010). Wnt signaling in stem and cancer stem cells. Semin. Cell Dev. Biol. *21*, 855–863.

Westerling, T., Kuuluvainen, E., and Mäkelä, T.P. (2007). Cdk8 is essential for preimplantation mouse development. Mol. Cell. Biol. *27*, 6177–6182.

Willert, K., Shibamoto, S., and Nusse, R. (1999). Wnt-induced dephosphorylation of axin releases beta-catenin from the axin complex. Genes Dev. *13*, 1768–73.

Wong, G.T., Gavin, B.J., and McMahon, A.P. (1994). Differential transformation of mammary epithelial cells by Wnt genes. Mol. Cell. Biol. *14*, 6278–6286.

Wong, H.C., Bourdelas, A., Krauss, A., Lee, H.J., Shao, Y., Wu, D., Mlodzik, M., Shi, D.L., and Zheng, J. (2003). Direct binding of the PDZ domain of Dishevelled to a conserved internal sequence in the C-terminal region of Frizzled. Mol. Cell. *12*, 1251–1260.

Wright, K.J., and Tjian, R. (2009). Wnt signaling targets ETO coactivation domain of TAF4/TFIID in vivo. PNAS *106*, 55–60.

Wu, G., Huang, H., Garcia Abreu, J., and He, X. (2009). Inhibition of GSK3 phosphorylation of beta-catenin via phosphorylated PPPSPXS motifs of Wnt coreceptor LRP6. PLoS ONE *4*, e4926.

Wu, W., Glinka, A., Delius, H., and Niehrs, C. (2000). Mutual antagonism between dickkopf1 and dickkopf2 regulates Wnt/beta-catenin signalling. Curr. Biology *10*, 1611–1614.

Xavier, C.P.R., Lima, C.F., Rohde, M., and Pereira-Wilson, C. (2011). Quercetin enhances 5-fluorouracil-induced apoptosis in MSI colorectal cancer cells through p53 modulation. Cancer Chemother. Pharmacol. *68*, 1449–1457.

Xu, W., and Ji, J.Y. (2011). Dysregulation of CDK8 and Cyclin C in tumorigenesis. J. Genetics and Genomics *38*, 439–452.

Xu, Z., Wei, Z., Zhou, J.J., Ye, F., Lo, W.S., Wang, F., Lau, C.F., Wu, J., Nangle, L.A., Chiang, K.P., et al. (2012). Internally Deleted Human tRNA Synthetase Suggests Evolutionary Pressure for Repurposing. Structure/Folding and Design *20*, 1470–1477.

Yamada, M., Ohkawara, B., Ichimura, N., Hyodo-Miura, J., Urushiyama, S., Shirakabe, K., and Shibuya, H. (2003). Negative regulation of Wnt signalling by HMG2L1, a novel NLK-binding protein. Genes Cells *8*, 677–684.

Yamamoto, H. (1999). Phosphorylation of Axin, a Wnt signal negative regulator, by Glycogen Synthase Kinase-3beta regulates its stability. J. Bio. Chem. *274*, 10681–10684.

Yamamoto, H., Komekado, H., and Kikuchi, A. (2006). Caveolin is necessary for Wnt-3a-dependent internalization of LRP6 and accumulation of beta-catenin. Dev. Cell *11*, 213–223.

Yang, W., Xia, Y., Ji, H., Zheng, Y., Liang, J., Huang, W., Gao, X., Aldape, K., and Lu, Z. (2011). Nuclear PKM2 regulates β-catenin transactivation upon EGFR activation. Nature *480*, 118–122.

Yang, X.L. (2013). Structural disorder in expanding the functionome of Aminoacyl-tRNA synthetases. Chem. Biol. *20*, 1093–1099.

Yang, Y., Mallampati, S., Sun, B., Zhang, J., Kim, S., Lee, J.S., Gong, Y., Cai, Z., and Sun, X. (2013). Wnt pathway contributes to the protection by bone marrow stromal cells of acute lymphoblastic leukemia cells and is a potential therapeutic target. Cancer Lett. *333*, 9–17.

Yashiroda, Y., Okamoto, R., Hatsugai, K., Takemoto, Y., Goshima, N., Saito, T.,

Hamamoto, M., Sugimoto, Y., Osada, H., Seimiya, H., et al. (2010). A novel yeast cell-based screen identifies flavone as a tankyrase inhibitor. Biochem. Biophys. Res. Commun. *394*, 569–573.

Ying, Y., and Tao, Q. (2009). Epigenetic disruption of the Wnt/beta-catenin signaling pathway in human cancers. Epigenetics *4*, 307–312.

Yo, Y.T., Lin, Y. W., Wang, Y.C., Balch, C., Huang, R.L., Chan, M., Sytwu, H.K., Chen, C.K., Chang, C.C., Nephew, K.P., et al. (2012). Growth inhibition of ovarian tumor-initiating cells by niclosamide. Mol. Cancer Ther. *11*, 1703–1712.

Yu, D.H., Macdonald, J., Liu, G., Lee, A.S., Ly, M., et al. (2008). Pyrvinium targets the unfolded protein response to hypoglycemia and its anti-tumor activity is enhanced by combination therapy. PLoS ONE *3*, e3951.

Zarnescu, D.C., and Zinsmaier, K.E. (2009). Ferrying Wingless across the Synaptic Cleft. Cell *139*, 229–231.

Zecca, M., Basler, K., and Struhl, G. (1996). Direct and long-range action of a Wingless morphogen gradient. Cell *87*, 833–844.

Zeng, X., Tamai, K., Doble, B., Li, S., Huang, H., Habas, R., Okamura, H., Woodgett, J., and He, X. (2005). A dual-kinase mechanism for Wnt co-receptor phosphorylation and activation. Nature *438*, 873–877.

Zeng, X., Huang, H., Tamai, K., Zhang, X., Harada, Y., Yokota, C., Almeida, K., Wang, J., Doble, B., Woodgett, J., et al. (2008). Initiation of Wnt signaling: control of Wnt coreceptor Lrp6 phosphorylation/activation via frizzled, dishevelled and axin functions. Development *135*, 367–375.

Zhang, G. N., Liang, Y., Zhou, L. J., Chen, S. P., Chen, G., Zhang, T. P., Kang, T., and Zhao, Y. P. (2011). Combination of salinomycin and gemcitabine eliminates pancreatic cancer cells. Cancer Lett. *313*, 137–144.

Zhang, J., Chung, T., and Oldenburg, K. (1999). A Simple Statistical Parameter for Use in Evaluation and Validation of High Throughput Screening Assays. J. Biomol. Screen *4*, 67–73.

Zhao, J., Ramos, R., and Demma, M. (2012). CDK8 regulates E2F1 transcriptional activity through S375 phosphorylation. Oncogene *32*, 3520–3530.

Zimmerman, Z.F., Moon, R.T., and Chien, A.J. (2012). Targeting Wnt Pathways in Disease. Cold Spring Harb. Perspect. Biol. Ed. Nusse, He, van Amerongen, 423-446.

Appendices

Appendix 1: Wnt 'canonical pathway' therapeutics

Appendix 2: Colorectal cancer cell line mutation status

Appendix 3: cDNA library IDs (on CD)

Appendix 4: esiRNA primary screen well identities (on CD)

Appendix 5: esiRNA primary screen sequences (on CD)

Appendix 6: Non-overlapping esiRNA sequences (on CD)

Appendix 7: esiRNA primary screen master results (on CD)

Appendix 8: Small molecule:MSC chequerboard compound combination studies in HCT116 cells

Loc[n]	Target	Therapeutic	Effect	Type	Disease	Stage	Supplier	Reference
Ex	PORCN	**LGK-974 (C57)**	I	SM	Melanoma, breast, pancreatic cancer	P I	Miltenyl, Novartis, Cellagen,Biovision	(Proffitt et al., 2012) NCT01351103
Ex	PORCN	3 IWP series I, II, III	I	SM	Developmental system tests	P I	(Dodge et al., 2012)	(Dodge et al., 2012)
Ex	PORCN	IWP-2	I	SM	Developmental system tests	P I	Multiple	(Chen et al., 2009a)
Ex	Wnt-1	**Wnt-1 Ab.**	I	B	Lung, breast cancer	D	(He et al., 2004)	(He et al., 2004; Wei et al., 2009)
Ex	Wnt-1	WIF-1	I	B	Bladder, osteosarcoma, prostate	T	(Tang et al., 2009)	(Tang et al., 2009)
Ex	Wnt-2	**Wnt-2 Ab**.	I	B	Melanoma	D	(You et al., 2004)	(You et al., 2004)
Ex	Soluble Wnt-3A	Ant1.4Br, Ant1.4Cl	I	SM	Not tested	T	(Morrell et al., 2008)	(Morrell et al., 2008)
Ex	Wnt-3	**sFZD7**	I	B	HCC	D	(Wei et al., 2011)	(Wei et al., 2011)

Ex	Wnt	**sFRP-4**	I	B	Renal fibrosis	Pre	(Surendran et al., 2005)	(Surendran et al., 2005)
Ex	sFRP-1	WAY-316606	A	SM	Osteoporosis	T	Multiple	(Bodine et al., 2009; Moore et al., 2009)
Ex	sFRP-1	Iminooxothiazolidines No.5	A	SM	Osteoporosis	D	Wyeth Research	(Shi et al., 2009)
Ex	Fzd-1,2 -*Wnt3,5A*	**Wnt peptide UM206**	I	P	Myocardial infarction	D	(Laeremans et al., 2011)	(Laeremans et al., 2011)
Ex	Fzd-5 - *Wnt5A*	**Wnt peptide Foxy-5**	I	P	Prostate cancer	Pre	WntResearch	(Säfholm et al., 2008)
Ex	Fzd7	Fzd7 Ab.	I	B	Wilm's tumour	D	(Pode-Shakked et al., 2011)	(Pode-Shakked et al., 2011)
Ex	Fzd-1,2,5,7,8	**Fzd Ab OMP-18R5 Vantictumab**	I	B	Breast, pancreatic, colon, lung cancer	P I	OncoMed	(Gurney et al., 2012)
Ex	Wnt-1	**F8CRDhFc OMP-54F28**	I	B	Teratocarcinoma, breast, solid tumours	P I	OncoMed	(DeAlmeida et al., 2007; Liu et al., 2012)
Ex	Fzd-10	**Fzd10 Ab. (^{90}Y)-MAb 92-13**	I	B	Synovial sarcoma	D	(Fukukawa et al.,	(Fukukawa et al.,

							2008)	2008)
Ex	SOST	**Sclerostin Ab. AMG-785**	A	B	Osteoporosis	P III	Amgen	(Padhi et al., 2010)
Ex	SOST	**Sclerostin Ab.**	A	B	Osteoporosis	Pre	Novartis	US Patent 7879322
Ex	SOST	**Sclerostin Ab.**	A	B	Osteoporosis, osteopenia, osteoarthritis	Pre	Eli Lilly	US Patent 20100221263
Ex	Dkk1	**Dkk1 Ab. BHQ880, RH2-18LC01**	A	B	MM	P II	Novartis, Merck	(Fulciniti et al., 2009; Glantschnig et al., 2010)
Ex	LRP5/6	**IIIC3**	A	SM	Diabetes	D	Enzo Life Sciences	(Li et al., 2012)
Ex	ZNFR3 + Lgr5	**R-spondin1 Nu206**	A	B	Inflammatory colitis	P I	Nuvelo	(Zhao et al., 2007)
Ex	LRP6 - *Dkk1*	**Mesd peptide**	I	P	Breast cancer	Pre	Abgent	(Liu et al., 2010)
Ex	LRP6- *Wnt3/3A*	**LRP6 Ab, mAb. A7-IgG**	I	B	Breast Cancer	Pre	Novartis	(Ettenberg et al., 2010)
Ex	LRP6 - *Wnt1,2,6,7a,7b,9a,10a,10b*	**LRP6 Ab, mAb. B2 -IgG**	I	B	Breast Cancer	Pre	Novartis	(Ettenberg et al., 2010)

Ex	LRP6 -*Wnt3/3A*	**LRP6 Ab. YW211.31**	I	B	Teratocarcinoma	Pre	Genentech	(Gong et al., 2010)
Ex	LRP6 -*Wnt1, 2, 2b, 6, 8a, 9a, 9b, 10b*	**LRP6 Ab. YW210.09**	A	B	Breast cancer	Pre	Genentech	(Gong et al., 2010)
Ex	LRP6 -*Dkk1*	LRP6 Ab. MAb135	A	B	Osteolysis in MM	D	Nuvelo	(Binnerts et al., 2009)
Cy	LRP6/Fzd1	**Niclosamide**	I	SM	Colon, ovarian cancer	Pre	Multiple	(Chen et al., 2009b; Osada et al., 2011; Lu et al., 2011b; Fonseca et al., 2012; Yo et al., 2012)
Cy	LRP6	**Salinomycin**	I	SM	CLL, breast, MM, prostate cancer	Pre	Multiple	(Gupta et al., 2009; Lu et al., 2011a)
Cy	Dvl *Fzd7*	**Fzd Peptide RHPD**	I	P	HCC	D	(Nambotin et al., 2011)	(Nambotin et al., 2011)
Cy	Gαo	BIM-46174	I	SM	Lung prostate cancer	D	(Prevost, 2006)	(Prevost, 2006)
Cy	ARFGAP1	QS11	A	SM	Breast cancer cell migration	T	Multiple	(Zhang et al.,

								2007)
Cy	Dvl -*Fzd*	3289-8625	I	SM	Prostate cancer	T	Multiple	(Grandy et al., 2009)
Cy	Dvl -*Fzd7*	**FJ9**	I	SM	Lung cancer, melanoma	D	{Fujii:2007wz}	(Fujii et al., 2007)
Cy	Dvl -*Fzd*	NSC668036, J01-017a	I	SM	Cancer	T, D	Multiple	(Shan et al., 2012)
Cy	CK1δ/ε	PF670462	I	SM	Breast cancer, fibrosarcoma cells	T	Multiple	(Cheong et al., 2011)
Cy	CK1α activator	**Pyrvinium**	I	SM	Colon cancer, cardiomyogenesis	Pre	Multiple	(Saraswati et al., 2010; Thorne et al., 2010; Basu et al., 2012; Saraswati et al., 2012)
Cy	PKCα activator	**CGK062**	I	SM	Prostate tumours	Pre	Glixx Labs	(Gwak et al., 2012)
Cy	TNKS1/2	**XAV-939**	I	SM	Colon cancer, fibrosis, cardimyogenesis, multiple sclerosis	T	Novartis, Multiple	(Huang et al., 2009; Fancy et al., 2011; Wang et al., 2011a; Distler et

								al., 2012; Ulsamer et al., 2012)
Cy	TNKS1/2	IWR-1	I	SM	Colon, prostate cancer	T	Multiple	(Chen et al., 2009a)
Cy	TNKS1/2	JW67, **JW74** & **JW55**	I	SM	Colon cancer	Pre	ChemBioNet	(Waaler et al., 2011; Shultz et al., 2012; Waaler et al., 2012)
Cy	TNKS2	WIKI4	I	SM	Colon cancer	D	Chembridge	(James et al., 2012)
Cy	GSK-3	**AZD2858**	A	SM	Osteoporosis	T	Astra Zeneca	(Marsell et al., 2012)
Cy	GSK-3	**SB-216763**	A	SM	Type 2 diabetes, colon cancer	T	Multiple	(Coghlan et al., 2000)
Cy	GSK-3	**Tideglusib (NP031112)**	A	SM	Alzheimer's, progressive supranuclear palsy	P II	Multiple	(Luna-Medina et al., 2007), NCT01049399, NCT01350362

Cy	Axin/β-catenin	SKL2001	A	SM	Osteoporosis	T	Merck/Millipore	(Gwak et al., 2011)
Cy	(β-catenin)	**AV-65**	I	SM	MM	D	(Yao et al., 2011)	(Yao et al., 2011)
Cy	(β-catenin)	CCT031374	I	SM	Colon cancer	T	Multiple	(Ewan et al., 2010)
Cy	(β-catenin)	Hexachlorophene	I	SM	Colon cancer	T	Multiple	(Park et al., 2006)
Cy	(β-catenin)	DCA Bile Acid	A	SM	Colon cancer (diet mechanism)	T	Multiple	(Pai et al., 2004)
N	β-catenin -*TCF4*	iCRT3,-5,-14	I	SM	Breast, colon cancer, MM	D	Sigma Aldrich	(Gonsalves et al., 2011; Narayanan et al., 2012)
N	β-catenin -*TCF4*	BC21	I	SM	Colon cancer	D	Calbiochem	(Tian et al., 2012)
N	β-catenin -*TCF4*	PNU-74654	I	SM	None tested	T	Multiple	(Trosset et al., 2006)
N	β-catenin -*TCF4*	fStAx-35	I	P	Colon cancer	D	(Grossmann and Yeh, 2012)	(Grossmann and Yeh, 2012)
N	β-catenin -*TCF4*	Stapled Bcl9 peptide	I	P	None tested	D	(Kawamoto et al.,	(Kawamoto et al.,

							2012)	2012)
N	TCF4 - β-catenin	**PKF115-584 (Calphostin), CGP049090, PKF118-310, PKF118-774 (haloquinone)**	I	SM	Colon cancer HCC, CLL, melanoma	T	Multiple	(Chen et al., 2000; Lepourcelet et al., 2004; Minke et al., 2009; Gandhirajan et al., 2010; Wei et al., 2010; Sinnberg et al., 2011; Halbedl et al., 2013)
N	(TCF4 - β-catenin)	**NC043**	I	SM	Colon cancer	Pre	(Wang et al., 2011b)	(Wang et al., 2011b)
N	(TCF4 - β-catenin)	**HQBA**	I	SM	Colon cancer	Pre	(Coombs et al., 2011)	(Coombs et al., 2011)
N	PP2A	**IQ-1**	I	SM	Inflammatory lung disease	T	Calbiochem	(Miyabayashi et al., 2007; Zemans et al., 2011)
N	CBP -*β-catenin*	**ICG-001**	I	SM	Colon cancer, pulmonary fibrosis	T	Multiple	(Emami et al., 2004; Henderson et al., 2010)

N	CBP -*β-catenin*	**PRI-724**	I	SM	Advanced solid tumours	P I	Prism Pharma Co.	(Garber, 2009)
N	CBP -*β-catenin*	**CWP232291**	I	SM	AML	P I	JW Pharma.	(Garber, 2009)
N	β-catenin -*Bcl9*	Carnosic acid	I	SM	Colon cancer	D	Multiple	(Barni et al., 2012; la Roche et al., 2012)
N	LEF-1	**Ethacrynic acid**	I	SM	CLL, MM	Pre	Multiple	(Lu et al., 2009; Kim et al., 2012b)
N	CDK8	**Senexin A**	I	SM	Lung cancer stroma	D	Senex Biotech.	(Porter et al., 2012)
MU								
MU	Unknown	KY02111	I	SM	Cardiomyocyte differentiation	T	Glixx Labs	(Minami et al., 2012)
MU	Unknown	GDK-100017	I	SM	NSCLC, Colon	D	(Lee et al., 2013)	(Lee et al., 2013)
MU	Unknown	WAY-262611	A	SM	Osteoporosis	D	Wyeth, Calbiochem	(Pelletier et al., 2009)
MU	Unknown	3,3'-Bisindoles	I	SM	Not tested	D	(Arai et al., 2013)	(Arai et al., 2013)
MU	Unknown	Cpd1, Cpd2	A	SM	Not tested	T	Merck	(Verkaar et al.,

								2011)
MU	Unknown	2-amino-4-[3,4-(methylenedioxy)benzyl-amino]-6-(3-methoxyphenyl)pyrimidine	A	SM	Not tested	T	(Liu et al., 2005)	(Liu et al., 2005)
MU	Unknown	Trifluridine, Kaempferol, FG7142, Eseroline, Ethyl 9H-pyrido[3,4-b]indole-3-carboxylate	A	SM	Not tested	D	Multiple	(Zhao et al., 2012b)
MU	Unknown	quinoxaline derivatives	I	SM	NSLC	D	(Gong et al., 2011)	(Gong et al., 2011)
MU	Unknown	diaminoquinazolines	I	SM	Colorectal cancer	D	Pfizer	(Chen et al., 2009c; Dehnhardt et al., 2010; Mao et al., 2012)
MU	Various	**NSAIDS Eg. Sulindac, celecoxib**	I		Colon	N/A	N/A	(Lee et al., 2009; Takahashi-Yanaga et al., 2008; Grosch et al., 2001)

MU	Various	Flavonoids Eg. Quercetin, curcumin, flavone, dihydroxy flavone	I	Various	N/A	N/A	(Amado et al., 2011; Thorne et al., 2011)
MU	RAR, RXR, PPARγ, AR, GR, VDR	NHRs Eg. FH535	I	Various	N/A	N/A	(Beildeck et al., 2010; Handeli and Simon, 2008; Wang et al., 2009)
MU	Various	**GPCR agonist/antagonists. Eg. Clozapine**	A	Eg. Schizophrenia	N/A	N/A	(Kang et al., 2004; Roh et al., 2007)

Appendix 1. Wnt 'canonical pathway' therapeutics

Wnt therapeutics are listed according to their approximate order of action from the extracellular space (Ex) via the cytoplasm (Cy) to the nucleus (N). MU; molecules with multi-level or undefined action. Targets are indicated together with specific interactions, in italics, that are blocked if known. Therapeutics in bold have been demonstrated to have action in mammalian systems *in vivo*. Inhibitory (I) or activating (A) effects are noted by Small Molecule (SM), Peptide (P) or Biological agents (B). Stage of development of the therapeutic is noted or estimated (Preclinical, Pre; Phase I, P I; Tool compound, T; Discovery phase, D).

Cell Line	Type	Wnt/β-catenin pathway alteration	Fold Reporter Induction: Topflash/Fopflash	Reference	Biomarkers	Minus	Confirmed mutations	Notes	Sanger CGP cell line DB
HCT116	colon carcinoma	oncogenic β-catenin, ↑ Wnt1, ↑ Wnt7b	6 fold	PNAS 2002: 99, 8265-70	Biomarkers available: Axin2, Bmp4, Emp1, FGF9 (CE)	Relatively low reporter induction	CDKN2A p.R24fs*20; CTNNB1 p.S45del; KRAS p.G13D; MLH1 p.S252*; PIK3CA p.H1047R c.3140A>G Reported in another cancer sample as somatic Heterozygous Verified		http://www.sanger.ac.uk/perl/genetics/CGP/core_line_viewer?action=sample&id=905936
SW480	colon carcinoma	APC inactivation, (C terminal trunc.) ↑ Wnt1	4-6 fold	Oncogene 2008: 27, 966-75.	Axin2, cMyc		905962 APC p.Q1338*; KRAS p.G12V; MAP2K4 p.? ; SMAD4 p.? ; TP53 p.R273H; TP53 p.P309S	check if same applies to SW620 (APC mutant, same patient, better xenograft	
SW620	colon carcinoma	APC inactivation, (C terminal trunc.) ↑ Wnt2	good in Merck Serono model	also PNAS 2004: 101, 12682-87			905962 APC p.Q1338*; KRAS p.G12V; MAP2K4 p.? ; SMAD4 p.? ; TP53 p.R273H; TP53 p.P309S	Isolated from lymph node metastases 1 year after SW480 isolated from primary. In house SNP profiling confirmed SW480 and SW620 from same patient	http://www.sanger.ac.uk/perl/genetics/CGP/core_line_viewer?action=sample&id=905962
Ls174T	colon carcinoma	oncogenic b-catenin	10 fold	Cell 2002: 111, 241-50	Lots of biomarkers available, Cell 2002: 111, 241-50	Relatively low reporter induction	CTNNB1 p.S45F; KDM6A p.E1316fs*17; KRAS p.G12D; PIK3CA p.H1047R	Beta-catenin shRNA reporter line available	http://www.sanger.ac.uk/perl/genetics/CGP/core_line_viewer?action=sample&id=907793
DLD-1	colon carcinoma	APC inactivation	4 fold	Cell 2002: 111, 241-50	Lots of biomarkers available, Cell 2002: 111, 241-50	Relatively low reporter induction	KRAS G13D; PIK3CA E545K; also APC, BRCA2, p53		
COLO 205	colon carcinoma	APC mutant					APC p.T1556fs*3; BRAF p.V600E; SMAD4 p.?; TP53 p.Y103_L111>L	highly amplified CDK8; shCDK8 and CDK19 underway	http://www.sanger.ac.uk/perl/genetics/CGP/core_line_viewer?action=sample&id=905961
COLO320	colon carcinoma	APC mutant					APC p.S811*; TP53 p.R248W	Amplified CDK8 - line is distinct from colo205	http://www.sanger.ac.uk/perl/genetics/CGP/core_line_viewer?action=sample&id=910569

Appendix 2. Colorectal cancer cell line mutation status

The mutation status of each of the cell lines used for further compound combination studies.

Appendix 8. Small molecule:MSC chequerboard compound combination studies in HCT116 cells

The dose response curves for RAF265, BIO, BX-795 (labelled as MSC2119074A), Senexin A (labelled as MSC2501503A) and Salinomycin (labelled as MSC1913177A) are shown with and without MSC titration (labelled as MSC2316900).

RAF265

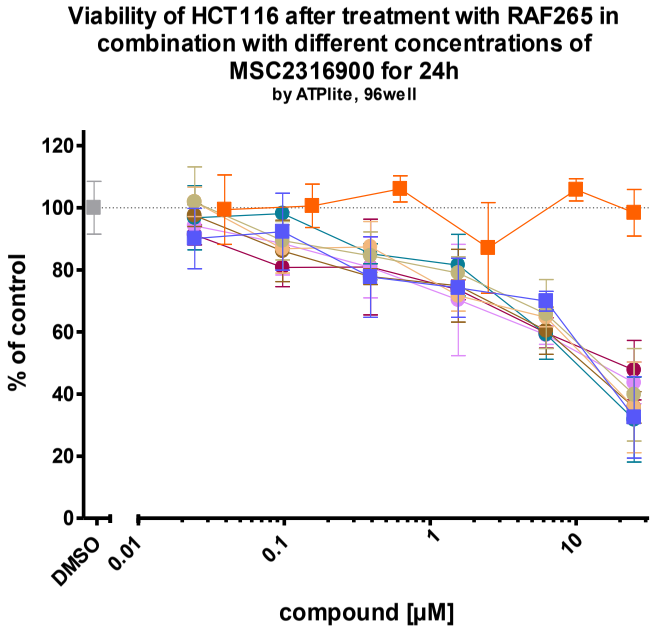
Viability of HCT116 after treatment with RAF265 in combination with different concentrations of MSC2316900 for 24h
by ATPlite, 96well
% of control
compound [µM]
DMSO
0.01
0.1
1
10
single treatment
control
RAF265
MSC2316900
combination treatment
RAF265/MSC2316900 [0,04µM]
RAF265/MSC2316900 [0,16µM]
RAF265/MSC2316900 [0,63µM]
RAF265/MSC2316900 [2,5µM]
RAF265/MSC2316900 [10µM]
RAF265/MSC2316900 [25µM]

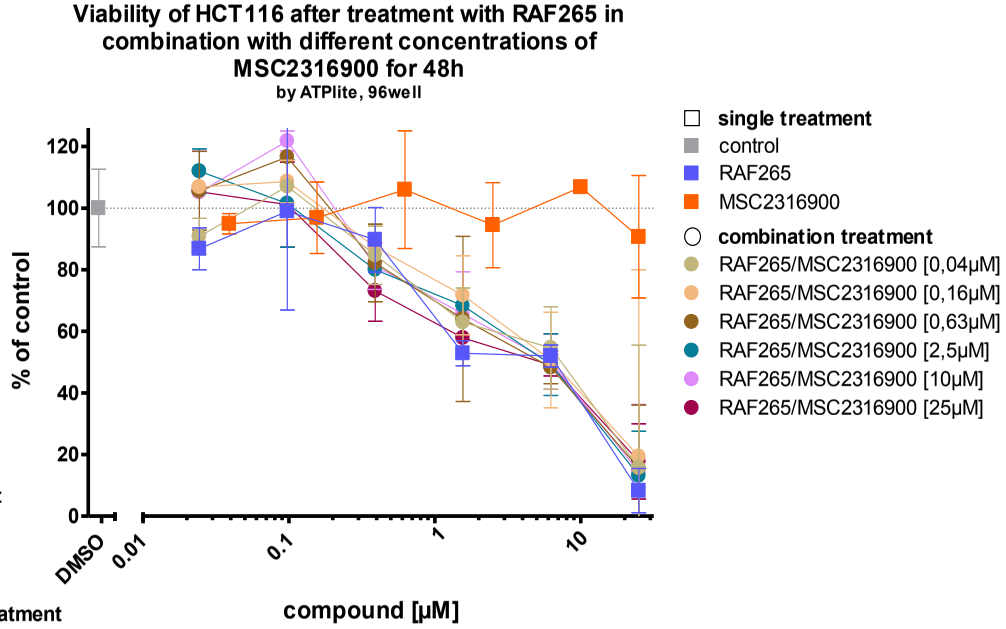
Viability of HCT116 after treatment with RAF265 in combination with different concentrations of MSC2316900 for 48h
by ATPlite, 96well
% of control
compound [µM]
DMSO
0.01
0.1
1
10
single treatment
control
RAF265
MSC2316900
combination treatment
RAF265/MSC2316900 [0,04µM]
RAF265/MSC2316900 [0,16µM]
RAF265/MSC2316900 [0,63µM]
RAF265/MSC2316900 [2,5µM]
RAF265/MSC2316900 [10µM]
RAF265/MSC2316900 [25µM]

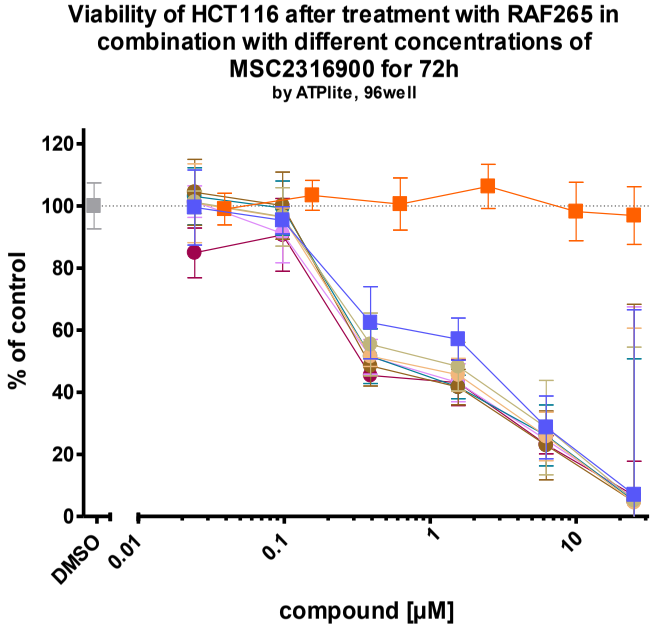
Viability of HCT116 after treatment with RAF265 in combination with different concentrations of MSC2316900 for 72h
by ATPlite, 96well
% of control
compound [µM]
DMSO
0.01
0.1
1
10
single treatment
control
RAF265
MSC2316900
combination treatment
RAF265/MSC2316900 [0,04µM]
RAF265/MSC2316900 [0,16µM]
RAF265/MSC2316900 [0,63µM]
RAF265/MSC2316900 [2,5µM]
RAF265/MSC2316900 [10µM]
RAF265/MSC2316900 [25µM]

BIO

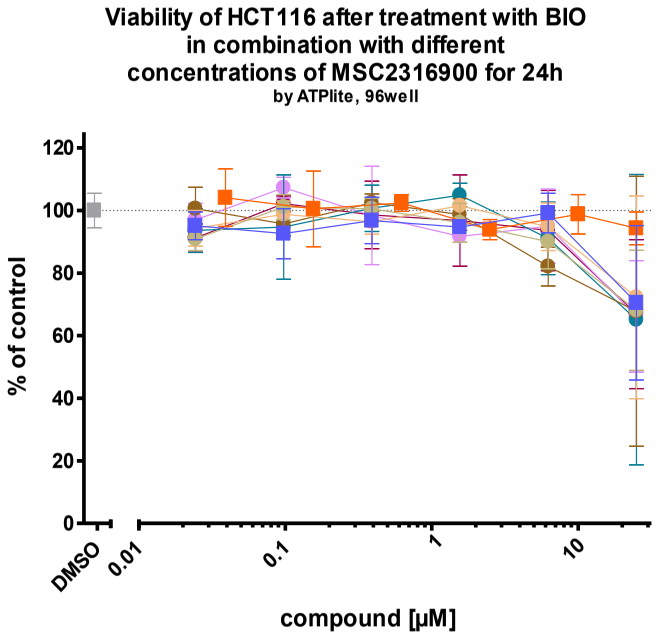
Viability of HCT116 after treatment with BIO
in combination with different
concentrations of MSC2316900 for 24h
by ATPlite, 96well
% of control
compound [µM]
DMSO
0.01
0.1
1
10
single treatment
control
BIO
MSC2316900
combination treatment
BIO/MSC2316900[0,04µM]
BIO/MSC2316900[0,16µM]
BIO/MSC2316900[0,63µM]
BIO/MSC2316900[2,5µM]
BIO/MSC2316900[10µM]
BIO/MSC2316900[25µM]

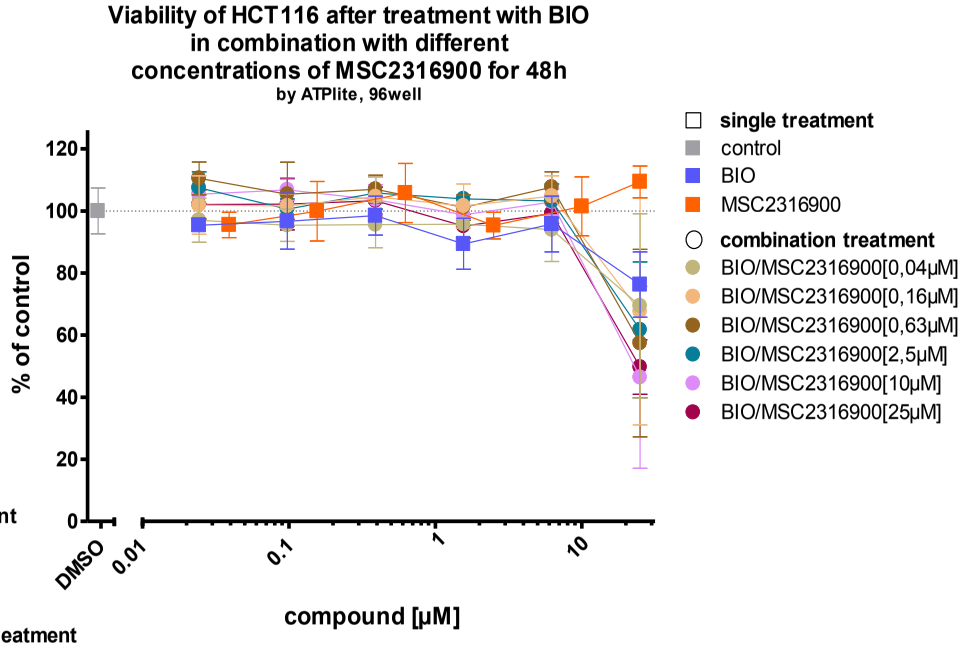
Viability of HCT116 after treatment with BIO
in combination with different
concentrations of MSC2316900 for 48h
by ATPlite, 96well
% of control
compound [µM]
DMSO
0.01
0.1
1
10
single treatment
control
BIO
MSC2316900
combination treatment
BIO/MSC2316900[0,04µM]
BIO/MSC2316900[0,16µM]
BIO/MSC2316900[0,63µM]
BIO/MSC2316900[2,5µM]
BIO/MSC2316900[10µM]
BIO/MSC2316900[25µM]

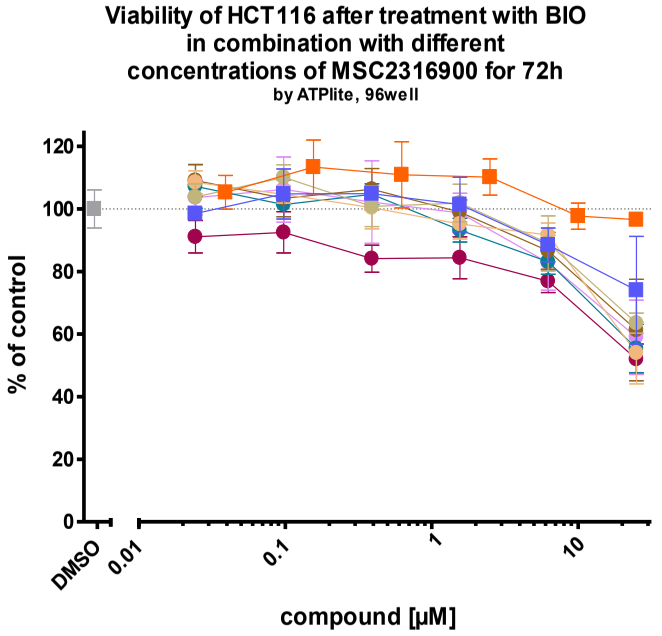
Viability of HCT116 after treatment with BIO
in combination with different
concentrations of MSC2316900 for 72h
by ATPlite, 96well
% of control
compound [µM]
DMSO
0.01
0.1
1
10
single treatment
control
BIO
MSC2316900
combination treatment
BIO/MSC2316900[0,04µM]
BIO/MSC2316900[0,16µM]
BIO/MSC2316900[0,63µM]
BIO/MSC2316900[2,5µM]
BIO/MSC2316900[10µM]
BIO/MSC2316900[25µM]

BX-795

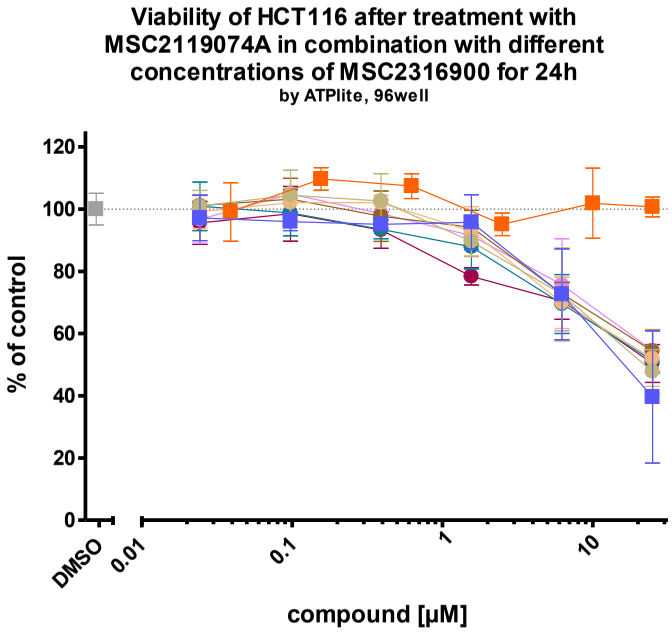
Viability of HCT116 after treatment with MSC2119074A in combination with different concentrations of MSC2316900 for 24h
by ATPlite, 96well
% of control
compound [µM]
DMSO
0.01
0.1
1
10
0
20
40
60
80
100
120

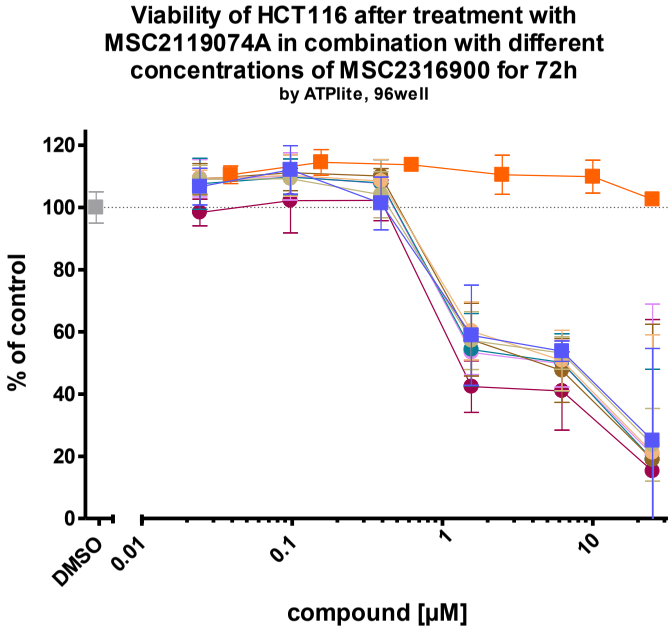
Viability of HCT116 after treatment with MSC2119074A in combination with different concentrations of MSC2316900 for 72h
by ATPlite, 96well
% of control
compound [µM]
DMSO
0.01
0.1
1
10
0
20
40
60
80
100
120

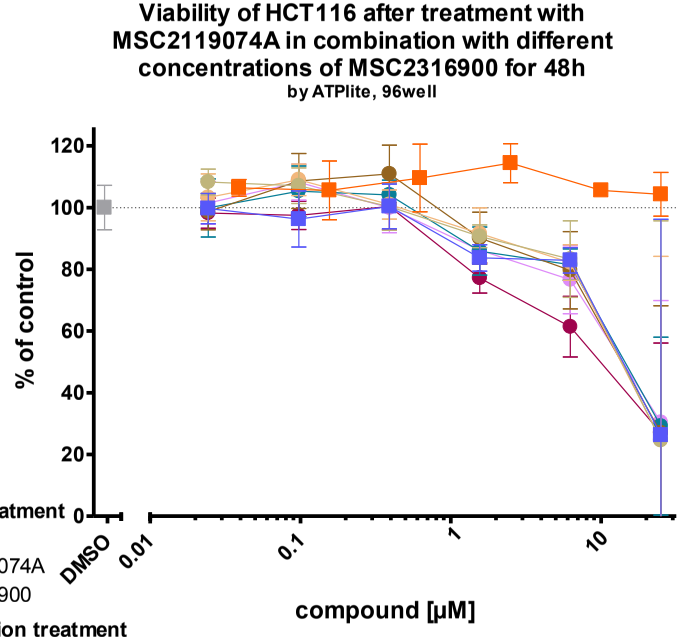
Viability of HCT116 after treatment with MSC2119074A in combination with different concentrations of MSC2316900 for 48h
by ATPlite, 96well
% of control
compound [µM]
DMSO
0.01
0.1
1
10
0
20
40
60
80
100
120

Senexin A

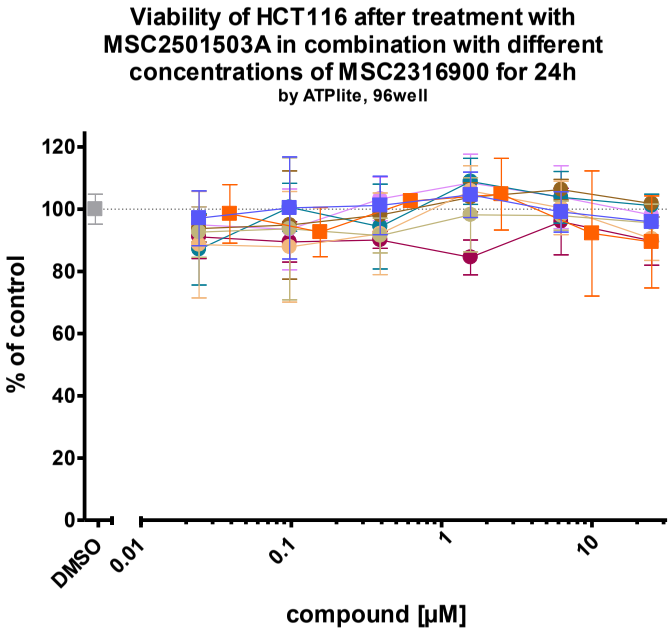
Viability of HCT116 after treatment with MSC2501503A in combination with different concentrations of MSC2316900 for 24h
by ATPlite, 96well
% of control
compound [µM]
DMSO
0.01
0.1
1
10
0
20
40
60
80
100
120

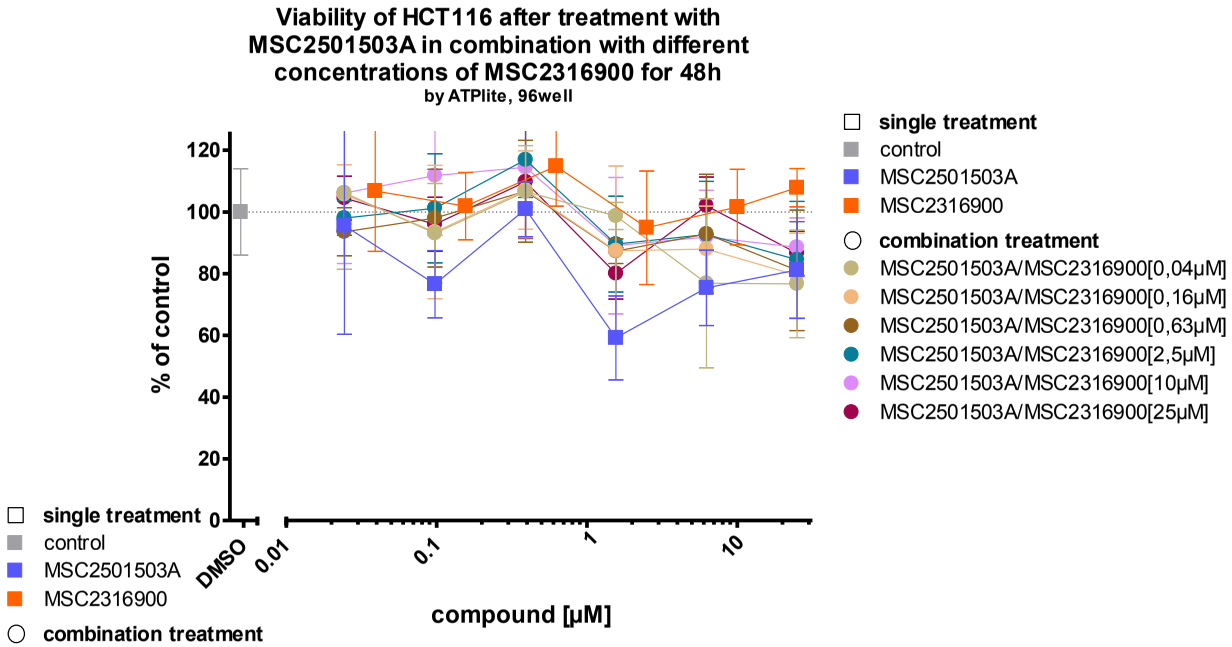
Viability of HCT116 after treatment with MSC2501503A in combination with different concentrations of MSC2316900 for 48h
by ATPlite, 96well
% of control
compound [µM]
DMSO
0.01
0.1
1
10
0
20
40
60
80
100
120
single treatment
control
MSC2501503A
MSC2316900
combination treatment
MSC2501503A/MSC2316900[0,04µM]
MSC2501503A/MSC2316900[0,16µM]
MSC2501503A/MSC2316900[0,63µM]
MSC2501503A/MSC2316900[2,5µM]
MSC2501503A/MSC2316900[10µM]
MSC2501503A/MSC2316900[25µM]

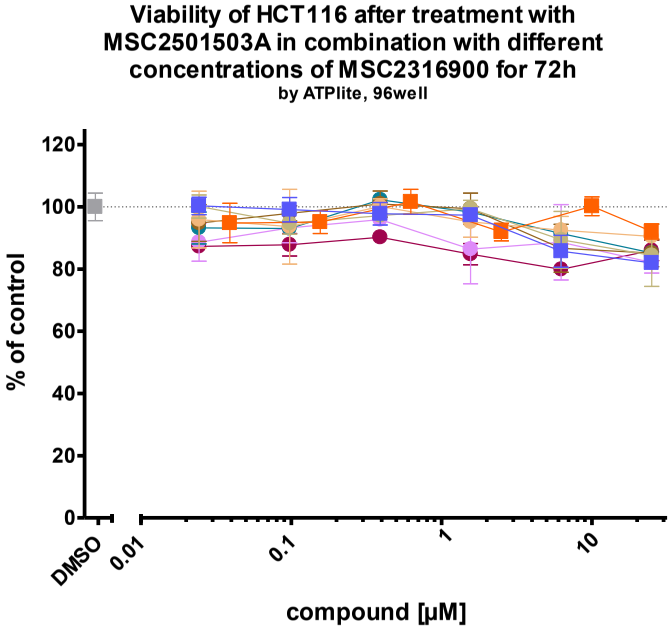
Viability of HCT116 after treatment with MSC2501503A in combination with different concentrations of MSC2316900 for 72h
by ATPlite, 96well
% of control
compound [µM]
DMSO
0.01
0.1
1
10
0
20
40
60
80
100
120
single treatment
control
MSC2501503A
MSC2316900
combination treatment
MSC2501503A/MSC2316900[0,04µM]
MSC2501503A/MSC2316900[0,16µM]
MSC2501503A/MSC2316900[0,63µM]
MSC2501503A/MSC2316900[2,5µM]
MSC2501503A/MSC2316900[10µM]
MSC2501503A/MSC2316900[25µM]

Salinomycin

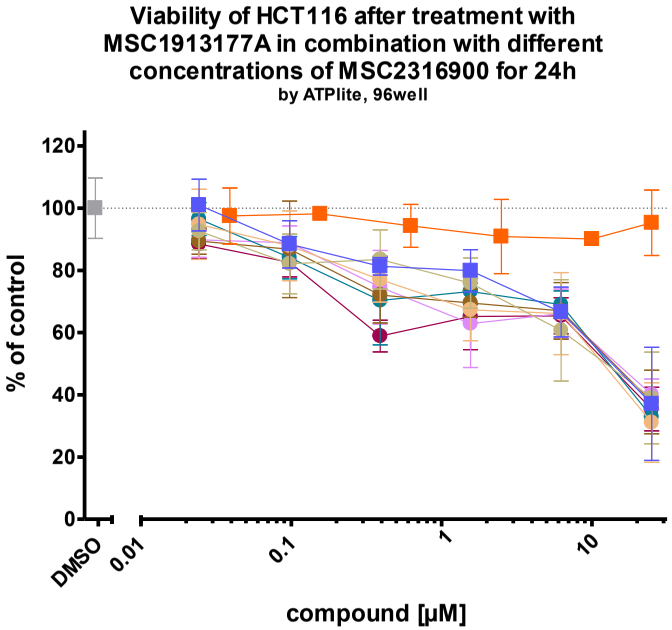

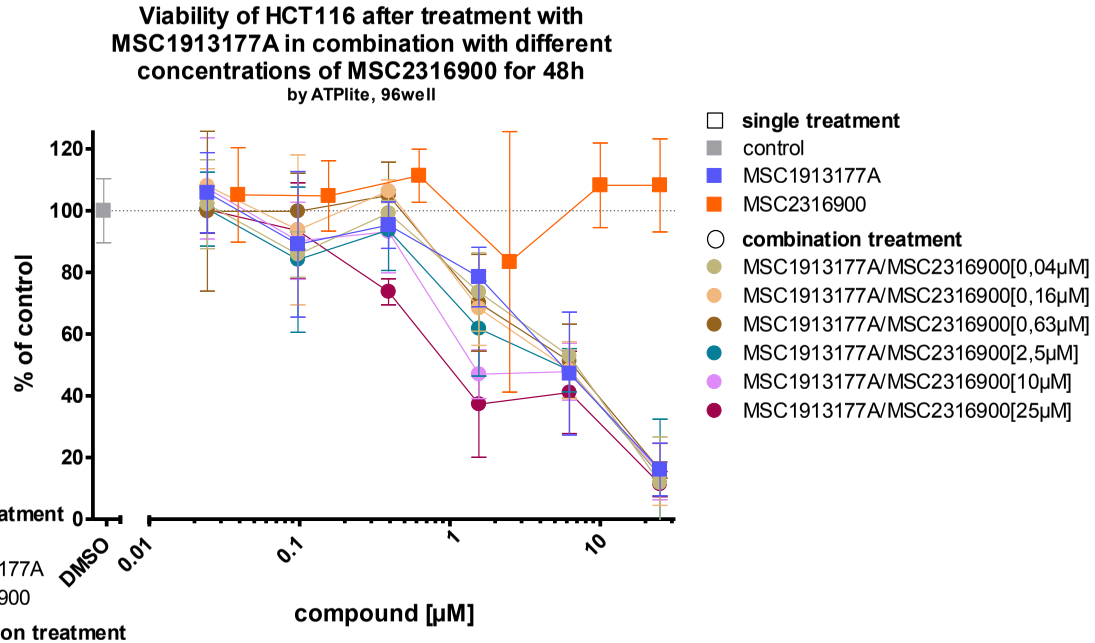

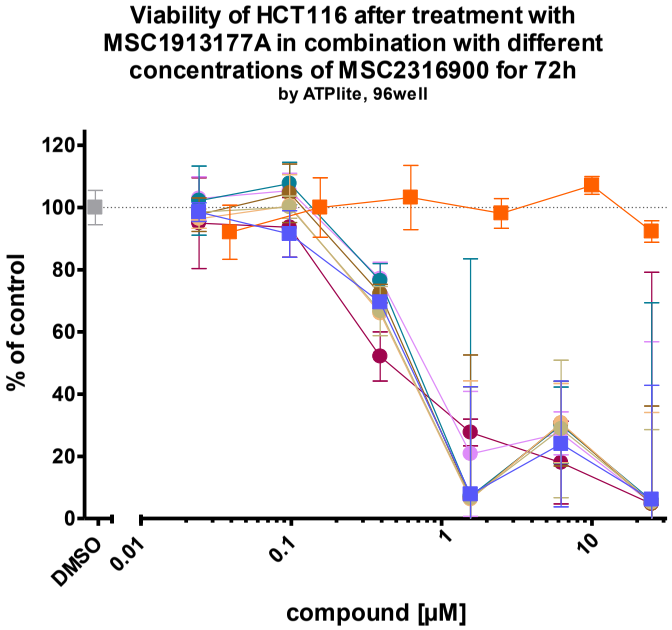

Appendix 1 Bibliography

Amado, N.G., Fonseca, B.F., Cerqueira, D.M., Neto, V.M., and Abreu, J.G. (2011). Flavonoids: potential Wnt/beta-catenin signaling modulators in cancer. Life Sci. *89*, 545–554.

Arai, T., Yamamoto, Y., Awata, A., Kamiya, K., Ishibashi, M., and Arai, M.A. (2013). Catalytic asymmetric synthesis of mixed 3,3′-bisindoles and their evaluation as Wnt signaling inhibitors. Angew. Chem. Int. Ed. *52*, 2486–2490.

Barni, M.V., Carlini, M.J., Cafferata, E.G., Puricelli, L., and Moreno, S. (2012). Carnosic acid inhibits the proliferation and migration capacity of human colorectal cancer cells. Oncol. Rep *27*, 1041–1048.

Basu, D., Reyes-Mugica, M., and Rebbaa, A. (2012). Role of the Beta catenin destruction complex in mediating chemotherapy-induced senescence-associated secretory phenotype. PLoS ONE *7*, e52188.

Beildeck, M.E., Gelmann, E.P., and Stephen, W.B. (2010). Cross-regulation of signaling pathways: An example of nuclear hormone receptors and the canonical Wnt pathway. Exp. Cell Res. *316*, 1763–1772.

Binnerts, M.E., Tomasevic, N., Bright, J.M., Leung, J., Ahn, V.E., Kim, K.A., Zhan, X., Liu, S., Yonkovich, S., Williams, J., et al. (2009). The first propeller domain of LRP6 regulates sensitivity to DKK1. Mol. Biol. Cell *20*, 3552–3560.

Bodine, P.V.N., Stauffer, B., Ponce-de-Leon, H., Bhat, R.A., Mangine, A., Seestaller-Wehr, L.M., Moran, R.A., Billiard, J., Fukayama, S., Komm, B.S., et al. (2009). A small molecule inhibitor of the Wnt antagonist secreted frizzled-related protein-1 stimulates bone formation. Bone *44*, 1063–1068.

Chen, B., Dodge, M.E., Tang, W., Lu, J., Ma, Z., Fan, C.W., Wei, S., Hao, W., Kilgore, J., Williams, N.S., et al. (2009a). Small molecule-mediated disruption of Wnt-dependent signaling in tissue regeneration and cancer. Nat. Chem. Biol. *5* 100-107.

Chen, M., Wang, J., Lu, J., Bond, M.C., Ren, X.R., Lyerly, H.K., Barak, L.S., and Chen, W. (2009b). The anti-helminthic niclosamide inhibits Wnt/Frizzled1 signaling. Biochemistry *48*, 10267–10274.

Chen, R.H., Ding, W.V., and McCormick, F. (2000). Wnt signaling to β-Catenin involves two interactive components. J. Biol. Chem. *275*, 17894–17899.

Chen, Z., Venkatesan, A.M., Dehnhardt, C.M., Santos, O.D., Santos, E.D., Ayral-Kaloustian, S., Chen, L., Geng, Y., Arndt, K.T., Lucas, J., et al. (2009c). 2,4-Diamino-quinazolines as inhibitors of β-catenin/Tcf-4 pathway: Potential treatment for colorectal cancer. Bioorg. Med. Chem. Lett. *19*, 4980–4983.

Cheong, J.K., Hung, N.T., Wang, H., Tan, P., Voorhoeve, P.M., Lee, S.H., and Virshup, D.M. (2011). IC261 induces cell cycle arrest and apoptosis of human cancer cells via CK1δ/ε and Wnt/β-catenin independent inhibition of mitotic spindle formation. Oncogene *30*, 2558–2569.

Coghlan, M.P., Culbert, A.A., Cross, D.A., Corcoran, S.L., Yates, J.W., Pearce, N.J., Rausch, O.L., Murphy, G.J., Carter, P.S., Roxbee Cox, L., et al. (2000). Selective small molecule inhibitors of glycogen synthase kinase-3 modulate glycogen metabolism and gene transcription. Chem. Biol. *7*, 793–803.

Coombs, G.S., Schmitt, A.A., Canning, C.A., Alok, A., Low, I.C.C., Banerjee, N., Kaur, S., Utomo, V., Jones, C.M., Pervaiz, S., et al. (2011). Modulation of Wnt and beta-catenin signaling and proliferation by a ferrous iron chelator with therapeutic efficacy in genetically engineered mouse models of cancer. Oncogene *31*, 213–225.

DeAlmeida, V.I., Miao, L., Ernst, J.A., Koeppen, H., Polakis, P., and Rubinfeld, B. (2007). The soluble wnt receptor Frizzled8CRD-hFc inhibits the growth of teratocarcinomas *in vivo*. Cancer Res. *67*, 5371–5379.

Dehnhardt, C.M., Venkatesan, A.M., Chen, Z., Ayral-Kaloustian, S., Santos, Dos, O., Delos Santos, E., Curran, K., Follettie, M.T., Diesl, V., Lucas, J., et al. (2010). Design and synthesis of novel diaminoquinazolines with *in vivo* efficacy for β-catenin/T-cell transcriptional factor 4 pathway inhibition. J. Med. Chem. *53*, 897–910.

Distler, A., Deloch, L., Huang, J., Dees, C., Lin, N.Y., Palumbo-Zerr, K., Beyer, C., Weidemann, A., Distler, O., Schett, G., et al. (2012). Inactivation of tankyrases reduces experimental fibrosis by inhibiting canonical Wnt signalling. Ann. Rheum. Dis. *0*, 1-6

Dodge, M.E., Moon, J., Tuladhar, R., Lu, J., Jacob, L.S., Zhang, L.S., Shi, H., Wang, X., Moro, E., Mongera, A., et al. (2012). Diverse chemical scaffolds support direct inhibition of the membrane-bound O-acyltransferase Porcupine. J. Biol. Chem. *287*, 23246–23254.

Emami, K.H., Nguyen, C., Ma, H., Kim, D.H., Jeong, K.W., Eguchi, M., Moon, R.T., Teo, J.L., Oh, S.W., Kim, H.Y., et al. (2004). A small molecule inhibitor of beta-catenin/cyclic AMP response element-binding protein transcription. PNAS *101*, 12682–12687.

Ettenberg, S.A., Charlat, O., Daley, M.P., Liu, S., Vincent, K.J., Stuart, D.D., Schuller, A.G., Yuan, J., Ospina, B., and Green, J. (2010). Inhibition of tumorigenesis driven by different Wnt proteins requires blockade of distinct ligand-binding regions by LRP6 antibodies. PNAS *107*, 15473–15478.

Ewan, K., Pajak, B., Stubbs, M., Todd, H., Barbeau, O., Quevedo, C., Botfield, H., Young, R., Ruddle, R., Samuel, L., et al. (2010). A useful approach to identify novel small-molecule inhibitors of Wnt-dependent transcription. Cancer Res. *70*, 5963–5973.

Fancy, S.P.J., Harrington, E.P., Yuen, T.J., Silbereis, J.C., Zhao, C., Baranzini, S.E., Bruce, C.C., Otero, J.J., Huang, E.J., Nusse, R., et al. (2011). Axin2 as regulatory and therapeutic target in newborn brain injury and remyelination. Nat. Neurosci. *14*, 1009–1016.

Fonseca, B.D., Diering, G.H., Bidinosti, M.A., Dalal, K., Alain, T., Balgi, A.D., Forestieri, R., Nodwell, M., Rajadurai, C.V., Gunaratnam, C., et al. (2012). Structure-activity analysis of niclosamide reveals potential role for cytoplasmic pH in control of mammalian target of rapamycin complex 1 (mTORC1) signaling. J. Biol. Chem. *287*, 17530–17545.

Fujii, N., You, L., Xu, Z., Uematsu, K., Shan, J., He, B., Mikami, I., Edmondson, L.R., Neale, G., Zheng, J., et al. (2007). An antagonist of dishevelled protein-protein interaction suppresses beta-catenin-dependent tumor cell growth. Cancer Res. *67*, 573–579.

Fukukawa, C., Hanaoka, H., Nagayama, S., Tsunoda, T., Toguchida, J., Endo, K., Nakamura, Y., and Katagiri, T. (2008). Radioimmunotherapy of human synovial sarcoma using a monoclonal antibody against FZD10. Cancer Sci. *99*, 432–440.

Fulciniti, M., Tassone, P., Hideshima, T., Vallet, S., Nanjappa, P., Ettenberg, S.A., Shen, Z., Patel, N., Tai, Y.T., Chauhan, D., et al. (2009). Anti-DKK1 mAb (BHQ880) as a potential therapeutic agent for multiple myeloma. Blood *114*, 371–379.

Gandhirajan, R.K., Staib, P.A., Minke, K., Gehrke, I., Plickert, G., Schlosser, A., Schmitt, E.K., Hallek, M., and Kreuzer, K.A. (2010). Small molecule inhibitors of Wnt/beta-catenin/lef-1 signaling induces apoptosis in chronic lymphocytic leukemia cells *in vitro* and *in vivo*. Neoplasia *12*, 326–335.

Garber, K. (2009). Drugging the Wnt pathway: problems and progress. J. Natl. Cancer Inst. *101*, 548–550.

Glantschnig, H., Hampton, R.A., Lu, P., Zhao, J.Z., Vitelli, S., Huang, L., Haytko, P., Cusick, T., Ireland, C., Jarantow, S.W., et al. (2010). Generation and selection of novel fully human monoclonal antibodies that neutralize Dickkopf-1 (DKK1) inhibitory function in vitro and increase bone mass in vivo. J. Biol. Chem. *285*, 40135–40147.

Gong, Y., Bourhis, E., Chiu, C., Stawicki, S., DeAlmeida, V.I., Liu, B.Y., Phamluong, K., Cao, T.C., Carano, R.A.D., Ernst, J.A., et al. (2010). Wnt isoform-specific interactions with coreceptor specify inhibition or potentiation of signaling by LRP6 antibodies. PLoS ONE *5*, e12682.

Gong, Y.D., Dong, M.S., Lee, S.B., Kim, N., Bae, M.S., and Kang, N.S. (2011). A novel 3-arylethynyl-substituted pyrido[2,3,-b]pyrazine derivatives and pharmacophore model as Wnt2/β-catenin pathway inhibitors in non-small-cell lung cancer cell lines. Bioorg. Med. Chem. *19*, 5639–5647.

Gonsalves, F.C., Klein, K., Carson, B.B., Katz, S., Ekas, L.A., Evans, S., Nagourney, R., Cardozo, T., Brown, A.M.C., and DasGupta, R. (2011). An RNAi-based chemical genetic screen identifies three small-molecule inhibitors of the Wnt/wingless signaling pathway. PNAS *108*, 5954–5963.

Grandy, D., Shan, J., Zhang, X., Rao, S., Akunuru, S., Li, H., Zhang, Y., Alpatov, I., Zhang, X.A., and Lang, R.A. (2009). Discovery and characterization of a small molecule inhibitor of the PDZ domain of dishevelled. J. Biol. Chem. *284*, 16256–16263.

Grosch, S., Tegeder, I., Niederberger, E., Bräutigam, L., and Geisslinger, G. (2001). COX-2 independent induction of cell cycle arrest and apoptosis in colon cancer cells by the selective COX-2 inhibitor celecoxib. FASEB J. *15*, 2742–2744.

Grossmann, T.N., and Yeh, J. (2012). Inhibition of oncogenic Wnt signaling through direct targeting of β-catenin. PNAS *109*, 17942-17947.

Gupta, P.B., Onder, T.T., Jiang, G., Tao, K., Kuperwasser, C., Weinberg, R.A., and Lander, E.S. (2009). Identification of selective inhibitors of cancer stem cells by high-throughput screening. Cell *138*, 645–659.

Gurney, A., Axelrod, F., Bond, C.J., Cain, J., Chartier, C., Donigan, L., Fischer, M., Chaudhari, A., Ji, M., Kapoun, A.M., et al. (2012). Wnt pathway inhibition via the targeting of Frizzled receptors results in decreased growth and tumorigenicity of human tumors. PNAS *109*, 11717-11722.

Gwak, J., Hwang, S.G., Park, H.S., Choi, S.R., Park, S.H., Kim, H., Ha, N.C., Bae, S.J., Han, J.K., Kim, D.E., et al. (2011). Small molecule-based disruption of the Axin/β-catenin protein complex regulates mesenchymal stem cell differentiation. Cell Res. *22*, 237–247.

Gwak, J., Lee, J.H., Chung, Y.H., Song, G.Y., and Oh, S. (2012). Small molecule-based promotion of PKCα-mediated β-Catenin degradation suppresses the proliferation of CRT-positive cancer cells. PLoS ONE *7*, e46697.

Halbedl, S., Kratzer, M.C., Rahm, K., Crosta, N., Masters, K.S., Zippert, J., Bräse, S., and Gradl, D. (2013). Synthesis of novel inhibitors blocking Wnt signaling downstream of beta-catenin. FEBS Lett. *586*, 522–527.

Handeli, S., and Simon, J.A. (2008). A small-molecule inhibitor of Tcf/beta-catenin signaling down-regulates PPARgamma and PPARdelta activities. Mol. Cancer Ther. *7*, 521–529.

He, B., You, L., Uematsu, K., Xu, Z., Lee, A.Y., Matsangou, M., McCormick, F., and Jablons, D.M. (2004). A monoclonal antibody against Wnt-1 induces apoptosis in human cancer cells. Neoplasia *6*, 7–14.

Henderson, W.R., Chi, E.Y., Ye, X., Nguyen, C., Tien, Y.T., Zhou, B., Borok, Z., Knight, D.A., and Kahn, M. (2010). Inhibition of Wnt/β-catenin/CREB binding protein (CBP) signaling reverses pulmonary fibrosis. PNAS *107*, 14309-14314.

Huang, S.M., Mishina, Y.M., Liu, S., Cheung, A., Stegmeier, F., Michaud, G.A., Charlat, O., Wiellette, E., Zhang, Y., Wiessner, S., et al. (2009). Tankyrase inhibition stabilizes axin and antagonizes Wnt signalling. Nature *461*, 614-620.

James, R.G., Davidson, K.C., Bosch, K.A., Biechele, T.L., Robin, N.C., Taylor, R.J., Major, M.B., Camp, N.D., Fowler, K., Martins, T.J., et al. (2012). WIKI4, a novel inhibitor of tankyrase and Wnt/ß-catenin signaling. PLoS ONE *7*, e50457.

Kang, U.G., Seo, M.S., Roh, M.S., Kim, Y., Yoon, S.C., and Kim, Y.S. (2004). The effects of clozapine on the GSK-3-mediated signaling pathway. FEBS Lett. *560*, 115–119.

Kawamoto, S.A., Coleska, A., Ran, X., Yi, H., Yang, C.Y., and Wang, S. (2012). Design of triazole-stapled BCL9 α-helical peptides to target the β-Catenin/B-cell CLL/lymphoma 9 (BCL9) protein–protein interaction. J. Med. Chem. *55*, 1137–1146.

Kim, Y., Gast, S.M., Endo, T., Lu, D., Carson, D., and Schmidt-Wolf, I.G.H. (2012b). In vivo efficacy of the diuretic agent ethacrynic acid against multiple myeloma. Leuk. Res. *36*, 598–600.

la Roche, de, M., Rutherford, T.J., Gupta, D., Veprintsev, D.B., Saxty, B., Freund, S.M., and Bienz, M. (2012). An intrinsically labile α-helix abutting the BCL9-binding site of β-catenin is required for its inhibition by carnosic acid. Nat. Commun. *3*, 680–10.

Laeremans, H., Hackeng, T.M., van Zandvoort, M.A.M.J., Thijssen, V.L.J.L., Janssen, B.J.A., Ottenheijm, H.C.J., Smits, J.F.M., and Blankesteijn, W.M. (2011). Blocking of Frizzled signaling with a homologous peptide fragment of Wnt3a/Wnt5a reduces infarct expansion and prevents the development of heart failure after myocardial infarction. Circulation *124*, 1626–1635.

Lee, H.J., Wang, N.X., Shi, D.L., and Zheng, J.J. (2009). Sulindac inhibits canonical Wnt signaling by blocking the PDZ domain of the protein Dishevelled. Angew. Chem. Int. Ed. Engl. *48*, 6448–6452.

Lee, S.B., Gong, Y.D., Park, Y.I., and Dong, M.S. (2013). 2,3,6-Trisubstituted quinoxaline derivative, a small molecule inhibitor of the Wnt/beta-catenin signaling pathway, suppresses cell proliferation and enhances radiosensitivity in A549/Wnt2 cells. Biochem. Biophys. Res. Commun. *431*, 746-752.

Lepourcelet, M., Chen, Y.N., France, D.S., Wang, H., Crews, P., Petersen, F., Bruseo, C., Wood, A.W., and Shivdasani, R.A. (2004). Small-molecule antagonists of the oncogenic Tcf/beta-catenin protein complex. Cancer Cell *5*, 91–102.

Li, X., Shan, J., Chang, W., Kim, I., Bao, J., Lee, H.J., Zhang, X., Samuel, V.T., Shulman, G.I., and Liu, D. (2012). Chemical and genetic evidence for the involvement of Wnt antagonist Dickkopf2 in regulation of glucose metabolism. PNAS *109*, 11402–11407.

Liu, B.Y., Soloviev, I., Huang, X., Chang, P., Ernst, J.A., Polakis, P., and Sakanaka, C. (2012). Mammary tumor regression elicited by Wnt signaling inhibitor requires IGFBP5. Cancer Res. *72*, 1568–1578.

Liu, C.C., Prior, J., Piwnica-Worms, D., and Bu, G. (2010). LRP6 overexpression defines a class of breast cancer subtype and is a target for therapy. PNAS *107*, 5136–5141.

Liu, J., Wu, X., Mitchell, B., Kintner, C., Ding, S., and Schultz, P.G. (2005). A small-molecule agonist of the Wnt signaling pathway. Angew. Chem. Int. Ed. Engl. *44*, 1987–1990.

Lu, D., Choi, M.Y., Yu, J., Castro, J.E., Kipps, T.J., and Carson, D.A. (2011a). Salinomycin inhibits Wnt signaling and selectively induces apoptosis in chronic lymphocytic leukemia cells. PNAS *108*, 13253–13257.

Lu, D., Liu, J.X., Endo, T., Zhou, H., Yao, S., and Willert, K. (2009). Ethacrynic acid exhibits selective toxicity to chronic lymphocytic leukemia cells by inhibition of the Wnt/β-Catenin pathway. PLoS ONE *4*, e8294.

Lu, W., Lin, C., Roberts, M.J., Waud, W.R., Piazza, G.A., and Li, Y. (2011b). Niclosamide suppresses cancer cell growth by inducing Wnt co-receptor LRP6 degradation and inhibiting the Wnt/β-catenin pathway. PLoS ONE *6*, e29290.

Luna-Medina, R., Cortes-Canteli, M., Sanchez-Galiano, S., Morales-Garcia, J.A., Martinez, A., Santos, A., and Perez-Castillo, A. (2007). NP031112, a thiadiazolidinone compound, prevents inflammation and neurodegeneration under excitotoxic conditions: potential therapeutic role in brain disorders. J. Neurosci. *27*, 5766–5776.

Mao, Y., Lin, N., Tian, W., Han, X., Han, X., Huang, Z., and An, J. (2012). Design, synthesis, and biological evaluation of new diaminoquinazolines as β-catenin/Tcf4 pathway inhibitors. J. Med. Chem. *55*, 1346–1359.

Marsell, R., Sisask, G., Nilsson, Y., Sundgren-Andersson, A.K., Andersson, U., Larsson, S., Nilsson, O., Ljunggren, Ö., and Jonsson, K.B. (2012). GSK-3 inhibition by an orally active small molecule increases bone mass in rats. Bone *50*, 619–627.

Minami, I., Yamada, K., Otsuji, T.G., Yamamoto, T., Shen, Y., Otsuka, S., Kadota, S., Morone, N., Barve, M., Asai, Y., et al. (2012). A small molecule that promotes cardiac differentiation of human pluripotent stem cells under defined, cytokine- and xeno-free conditions. Cell Reports *2*, 1448–1460.

Minke, K.S., Staib, P., Puetter, A., Gehrke, I., Gandhirajan, R.K., Schlosser, A., Schmitt, E.K., Hallek, M., and Kreuzer, K.A. (2009). Small molecule inhibitors of WNT signaling effectively induce apoptosis in acute myeloid leukemia cells. Eur. J. Haematol. *82*, 165–175.

Miyabayashi, T., Teo, J.L., Yamamoto, M., McMillan, M., Nguyen, C., and Kahn, M. (2007). Wnt/beta-catenin/CBP signaling maintains long-term murine embryonic stem cell pluripotency. PNAS *104*, 5668–5673.

Moore, W.J., Kern, J.C., Bhat, R., Commons, T.J., Fukayama, S., Goljer, I., Krishnamurthy, G., Magolda, R.L., Nogle, L., Pitts, K., et al. (2009). Modulation of Wnt signaling through inhibition of secreted frizzled-related protein I (sFRP-1) with N-substituted piperidinyl diphenylsulfonyl sulfonamides. J. Med. Chem. *52*, 105–116.

Morrell, N.T., Leucht, P., Zhao, L., Kim, J.B., ten Berge, D., Ponnusamy, K., Carre, A.L., Dudek, H., Zachlederova, M., McElhaney, M., et al. (2008). Liposomal packaging generates Wnt protein with *in vivo* biological activity. PLoS ONE *3*, e2930.

Nambotin, S.B., Lefrancois, L., Sainsily, X., Berthillon, P., Kim, M., Wands, J.R., Chevallier, M., Jalinot, P., Scoazec, J.Y., Trepo, C., et al. (2011). Pharmacological inhibition of Frizzled-7 displays anti-tumor properties in hepatocellular carcinoma. J. Hepat.*54*, 288–299.

Narayanan, B.A., Doudican, N.A., Park, J., Xu, D., Narayanan, N.K., DasGupta, R., and Mazumder, A. (2012). Antagonistic effect of small-molecule inhibitors of Wnt/β-catenin in multiple myeloma. Anticancer Res. *32*, 4697–4707.

Osada, T., Chen, M., Yang, X.Y., Spasojevic, I., Vandeusen, J.B., Hsu, D., Clary, B.M., Clay, T.M., Chen, W., Morse, M.A., et al. (2011). Antihelminth compound niclosamide downregulates Wnt signaling and elicits antitumor responses in tumors with activating APC mutations. Cancer Res. *71*, 4172–4182.

Padhi, D., Jang, G., Stouch, B., Fang, L., and Posvar, E. (2010). Single-dose, placebo-controlled, randomized study of AMG 785, a sclerostin monoclonal antibody. J. Bone Miner. Res. *26*, 19–26.

Pai, R., Tarnawski, A.S., and Tran, T. (2004). Deoxycholic acid activates β-catenin signaling pathway and increases colon cell cancer growth and invasiveness. Mol. Biol. Cell *15*, 2156–2163.

Park, S., Gwak, J., Cho, M., Song, T., Won, J., Kim, D.E., Shin, J.G., and Oh, S. (2006). Hexachlorophene inhibits Wnt/beta-catenin pathway by promoting Siah-mediated beta-catenin degradation. Mol. Pharmacol. *70*, 960–966.

Pelletier, J.C., Lundquist, J.T., Gilbert, A.M., Alon, N., Bex, F.J., Bhat, B.M., Bursavich, M.G., Coleburn, V.E., Felix, L.A., Green, D.M., et al. (2009). (1-(4-(Naphthalen-2-yl)pyrimidin-2-yl)piperidin-4-yl)methanamine: a wingless beta-catenin agonist that increases bone formation rate. J. Med. Chem. *52*, 6962–6965.

Pode-Shakked, N., Harari-Steinberg, O., Haberman-Ziv, Y., Rom-Gross, E., Bahar, S., Omer, D., Metsuyanim, S., Buzhor, E., Jacob-Hirsch, J., Goldstein, R.S., et al. (2011). Resistance or sensitivity of Wilms' tumor to anti-FZD7 antibody highlights the Wnt pathway as a possible therapeutic target. Oncogene *30*, 1664–1680.

Porter, D.C., Farmaki, E., and Altilia, S. (2012). Cyclin-dependent kinase 8 mediates chemotherapy- induced tumor-promoting paracrine activities. PNAS 109, 13799-13804.

Prevost, G.P. (2006). Anticancer activity of BIM-46174, a new inhibitor of the heterotrimeric Gα/Gβ protein complex. Cancer. Res. *66*, 9227–9234.

Proffitt, K.D., Madan, B., Ke, Z., Pendharkar, V., Ding, L., Lee, M.A., Hannoush, R.N., and Virshup, D.M. (2012). Pharmacological inhibition of the Wnt acyltransferase PORCN prevents growth of Wnt-driven mammary cancer. Cancer Res. *73*, 502–507.

Roh, M.S., Seo, M.S., Kim, Y., Kim, S.H., Jeon, W.J., Ahn, Y.M., Kang, U.G., Juhnn, Y.S., and Kim, Y.S. (2007). Haloperidol and clozapine differentially regulate signals upstream of glycogen synthase kinase 3 in the rat frontal cortex. Exp. Mol. Med. *39*, 353–360.

Säfholm, A., Tuomela, J., Rosenkvist, J., Dejmek, J., Härkönen, P., and Andersson, T. (2008). The Wnt-5a-derived hexapeptide Foxy-5 inhibits breast cancer metastasis in vivo by targeting cell motility. Clin. Cancer Res. *14*, 6556–6563.

Saraswati, S., Alfaro, M.P., Thorne, C.A., Atkinson, J., Lee, E., and Young, P.P. (2010). Pyrvinium, a potent small molecule Wnt inhibitor, promotes wound repair and post-MI cardiac remodeling. PLoS ONE *5*, e15521.

Saraswati, S., Deskins, D.L., Holt, G.E., and Young, P.P. (2012). Pyrvinium, a potent small molecule Wnt inhibitor, increases engraftment and inhibits lineage commitment of mesenchymal stem cells (MSCs). Wound Repair Regen. *20*, 185–193.

Shan, J., Zhang, X., Bao, J., Cassell, R., and Zheng, J.J. (2012). Synthesis of potent dishevelled PDZ domain inhibitors guided by virtual screening and NMR studies. Chemical Biology & Drug Design *79*, 376–383.

Shi, M., Stauffer, B., Bhat, R., and Billiard, J. (2009). Identification of iminooxothiazolidines as secreted frizzled related protein-1 inhibitors. Bioorg. Med, Chem. Lett. *19*, 6337-6339.

Shultz, M.D., Kirby, C.A., Stams, T., Chin, D.N., Blank, J., Charlat, O., Cheng, H., Cheung, A., Cong, F., Feng, Y., et al. (2012). [1,2,4]Triazol-3-ylsulfanylmethyl)-3-phenyl-[1,2,4]oxadiazoles: Antagonists of the Wnt pathway that inhibit tankyrases 1 and 2 via novel adenosine pocket binding. J. Med. Chem. *55*, 1127–1136.

Sinnberg, T., Menzel, M., Ewerth, D., Sauer, B., Schwarz, M., Schaller, M., Garbe, C., and Schittek, B. (2011). β-catenin signaling increases during melanoma progression and promotes tumor cell survival and chemoresistance. PLoS ONE *6*, e23429.

Surendran, K., Schiavi, S., and Hruska, K.A. (2005). Wnt-dependent beta-catenin signaling is activated after unilateral ureteral obstruction, and recombinant secreted frizzled-related protein 4 alters the progression of renal fibrosis. J. Am. Soc. Nephrol. *16*, 2373–2384.

Takahashi-Yanaga, F., Yoshihara, T., and Jingushi, K. (2008). Celecoxib-induced degradation of T-cell factors-1 and -4 in human colon cancer cells. Biochem. Biophys. Res. Commun. *377*, 1185-1190.

Tang, Y., Simoneau, A.R., Liao, W.X., Yi, G., Hope, C., Liu, F., Li, S., Xie, J., Holcombe, R.F., Jurnak, F.A., et al. (2009). WIF1, a Wnt pathway inhibitor, regulates SKP2 and c-myc expression leading to G1 arrest and growth inhibition of human invasive urinary bladder cancer cells. Mol. Cancer Ther. *8*, 458–468.

Thorne, C.A., Hanson, A.J., Schneider, J., Tahinci, E., Orton, D., Cselenyi, C.S., Jernigan, K.K., Meyers, K.C., Hang, B.I., Waterson, A.G., et al. (2010). Small-molecule inhibition of Wnt signaling through activation of casein kinase 1α. Nat. Chem. Biol. *6*, 829–836.

Thorne, C.A., Lafleur, B., Lewis, M., Hanson, A.J., Jernigan, K.K., Weaver, D.C., Huppert, K.A., Chen, T.W., Wichaidit, C., Cselenyi, C.S., et al. (2011). A biochemical screen for identification of small-molecule regulators of the Wnt pathway using Xenopus egg extracts. J. Biomol. Screen. *16*, 995–1006.

Tian, W., Han, X., Yan, M., Xu, Y., Duggineni, S., Lin, N., Luo, G., Li, Y.M., Han, X., Huang, Z., et al. (2012). Structure-based discovery of a novel inhibitor targeting the β-catenin/Tcf4 interaction. Biochemistry *51*, 724–731.

Trosset, J.Y., Dalvit, C., Knapp, S., Fasolini, M., Veronesi, M., Mantegani, S., Gianellini, L.M., Catana, C., Sundström, M., Stouten, P.F.W., et al. (2006). Inhibition of protein-protein interactions: The discovery of druglike β-catenin inhibitors by combining virtual and biophysical screening. Proteins *64*, 60–67.

Ulsamer, A., Wei, Y., Kim, K.K., Tan, K., Wheeler, S., Xi, Y., Thies, R.S., and Chapman, H.A. (2012). Axin pathway activity regulates *in vivo* pY654-β-catenin accumulation and pulmonary fibrosis. J. Biol. Chem. *287*, 5164–5172.

Verkaar, F., van der Stelt, M., Blankesteijn, W.M., van der Doelen, A.A., and Zaman, G.J.R. (2011). Discovery of novel small molecule activators of β-catenin signaling. PLoS ONE *6*, e19185.

Waaler, J., Machon, O., Kries, von, J.P., Wilson, S.R., Lundenes, E., Wedlich, D., Gradl, D., Paulsen, J.E., Machonova, O., Dembinski, J.L., et al. (2011). Novel synthetic antagonists of canonical Wnt signaling inhibit colorectal cancer cell growth. Cancer Res. *71*, 197–205.

Waaler, J., Machon, O., Tumova, L., Dinh, H., Korinek, V., Wilson, S.R., Paulsen, J.E., Pedersen, N.M., Eide, T.J., Machonova, O., et al. (2012). A novel tankyrase inhibitor decreases canonical Wnt signaling in colon carcinoma cells and reduces tumor growth in conditional APC mutant mice. Cancer Res. *72*, 2822–2832.

Wang, H., Hao, J., and Hong, C.C. (2011a). Cardiac Induction of Embryonic Stem Cells by a Small Molecule Inhibitor of Wnt/β-Catenin Signaling. ACS Chem. Biol. *6*, 192–197.

Wang, P.S., Chou, F.S., Bloomston, M., Vonau, M.S., Saji, M., Espinosa, A., and Pinzone, J.J. (2009). Thiazolidinediones downregulate Wnt/beta-catenin signaling via multiple mechanisms in breast cancer cells. J. Surg. Res. *153*, 210–216.

Wang, W., Liu, H., Wang, S., Hao, X., and Li, L. (2011b). A diterpenoid derivative 15-oxospiramilactone inhibits Wnt/β-catenin signaling and colon cancer cell tumorigenesis. Cell Res. *21*, 730–740.

Wei, W., Chua, M.S., Grepper, S., and So, S.K. (2009). Blockade of Wnt-1 signaling leads to anti-tumor effects in hepatocellular carcinoma cells. Mol. Cancer *8*, 76.

Wei, W., Chua, M.S., Grepper, S., and So, S. (2010). Small molecule antagonists of Tcf4/β-catenin complex inhibit the growth of HCC cells *in vitro* and *in vivo*. Int. J. Cancer *126*, 2426-2436.

Wei, W., Chua, M.S., Grepper, S., and So, S.K. (2011). Soluble Frizzled-7 receptor inhibits Wnt signaling and sensitizes hepatocellular carcinoma cells towards doxorubicin. Mol. Cancer *10*, 1-12.

Yao, H., Ashihara, E., Strovel, J.W., Nakagawa, Y., Kuroda, J., Nagao, R., Tanaka, R., Yokota, A., Takeuchi, M., Hayashi, Y., et al. (2011). AV-65, a novel Wnt/β-catenin signal inhibitor, successfully suppresses progression of multiple myeloma in a mouse model. Blood Cancer J. *1*, e43.

Yo, Y.T., Lin, Y.W., Wang, Y.C., Balch, C., Huang, R.L., Chan, M.W.Y., Sytwu, H.K., Chen, C.K., Chang, C.C., Nephew, K.P., et al. (2012). Growth inhibition of ovarian tumor-initiating cells by niclosamide. Mol. Cancer. Ther. *11*, 1703–1712.

You, L., He, B., Xu, Z., Uematsu, K., Mazieres, J., Fujii, N., Mikami, I., Reguart, N., McIntosh, J.K., Kashani-Sabet, M., et al. (2004). An anti-Wnt-2 monoclonal antibody induces apoptosis in malignant melanoma cells and inhibits tumor growth. Cancer Res. *64*, 5385–5389.

Zemans, R.L., Briones, N., Campbell, M., McClendon, J., Young, S.K., Suzuki, T., Yang, I.V., De Langhe, S., Reynolds, S.D., and Mason, R.J. (2011). Neutrophil transmigration triggers repair of the lung epithelium via β-catenin signaling. PNAS *108*, 15990–15995.

Zhang, Q., Major, M.B., Takanashi, S., Camp, N.D., Nishiya, N., Peters, E.C., Ginsberg, M.H., Jian, X., Randazzo, P.A., Schultz, P.G., et al. (2007). Small-molecule synergist of the Wnt/beta-catenin signaling pathway. PNAS*104*, 7444–7448.

Zhao, J., de Vera, J., Narushima, S., Beck, E.X., Palencia, S., Shinkawa, P., Kim, K.A., Liu, Y., Levy, M.D., Berg, D.J., et al. (2007). R-spondin1, a novel intestinotrophic mitogen, ameliorates experimental colitis in mice. Gastroenterology *132*, 1331–1343.

Zhao, W.N., Cheng, C., Theriault, K.M., Sheridan, S.D., Tsai, L.H., and Haggarty, S.J. (2012b). A high-throughput screen for Wnt/β-catenin signaling pathway modulators in human iPSC-derived neural progenitors. J. Biomol. Screen. *17*, 1252–1263.